Degradation of α-Hexachlorocyclohexane and Organochlorine Contaminant Fate in High Arctic Lakes

by

Paul Anthony Helm

A thesis submitted in conformity with the requirements
for the degree of Master of Applied Science
Graduate Department of Chemical Engineering and Applied Chemistry
University of Toronto

0-612-45581-5

Degradation of α-Hexachlorocyclohexane and Organochlorine Contaminant Fate in High Arctic Lakes

Master of Applied Science, 1999

Paul Anthony Helm

Graduate Department of Chemical Engineering and Applied Chemistry
University of Toronto

α-hexachlorocyclohexane (α-HCH) degradation was investigated in Amituk, Char and Meretta lakes on Cornwallis Is., NT, to determine its importance as a loss pathway and to identify influential factors. Enantiomeric degradation was related to stream temperatures and contact time with substrates. Approximately 7% of α-HCH was enantioselectively degraded in streams. The total Amituk Lake α-HCH inventory declined by 50% annually leading to an estimated degradation rate of 0.80 y^{-1}. However, lake degradation was primarily non-enantioselective, although ERs observed in each of the lakes may reflect water residence times.

Contaminant fate modeling predicted lake organochlorine concentrations to within 1 to 1.5 standard deviations of measured values. Meltwater import and export were the dominant chemical processes, followed by chemical-specific degradation that accounted for 10-90% of lake losses, and air-water exchange. Degradation half-lives of 50 000 h for heptachlor epoxide and 11 000 h for γ-HCH simulated annual changes in concentrations in Amituk Lake.

ACKNOWLEDGEMENTS

I am very grateful for the support of many individuals throughout my Masters program. Particular thanks to:

Dr. Miriam Diamond, my supervisor and colleague, for welcoming me as her graduate student, and for providing me with unexpected research opportunities and continued guidance. She has inspired me to continue working in this exciting field.

Ray Semkin, for sharing data and insights from the Amituk Lake Study and for logistical support for my summer excursions to the Arctic. Thanks also to his field crew in 1994: Peter Amarualik, Jill Franklyn, Bruce Gray, Pat Healey, Brenda Koenig, Sean Kinney, John Kraft, Mike Mawhinney, Roy Neureuther and Camilla Teixeira.

Dr. Terry Bidleman, and particularly Liisa Jantunen, of the Atmospheric Environment Service, for analytical and logistical support, for helpful discussions of results, and for the opportunities that have presented themselves.

Dr. C. Jia and Dr. Bidleman for constructive comments as members of my defense committee.

Polar Continental Shelf Project and staff, for two smooth field seasons logistically, and a lot of fun.

John Roppa for field assistance and friendship this past summer.

Dr. L. Barrie and C. Halsall, for organochlorine air concentrations at Alert.

NSERC, the Northern Student Training Program, and Indian and Northern Affairs, for funding my graduate studies and research trips to the North.

Diamonds in the Rough, past and present, especially Mehran, Sarah, Murali and Neely.

Family and friends, for support and breaks when needed most.

Corey, my wife and friend, for patience and support through summer field trips abroad, and particularly during thesis preparation. I would not have succeeded without you.

TABLE OF CONTENTS

LIST OF TABLES

Chapter 2

Chapter 3

Chapter 4

Chapter 5

LIST OF FIGURES

Chapter 1

Chapter 2

Chapter 3

Chapter 4

Chapter 5

1. Introduction

1.1 Contaminants in the Arctic

To many, the Canadian Arctic is a remote and pristine environment, virtually untouched by humans. However, since 'Arctic Haze' was first noted by Mitchell (1956), research efforts have documented the presence of anthropogenic contaminants throughout all components of arctic ecosystems.

Arctic pollution research intensified in the 1970s and 1980s with investigations into atmospheric turbidity and aerosol particles (e.g. Shaw, 1975, 1982; Rahn and McCaffrey, 1979). The origin of aerosol pollution in the North American Arctic was thought to be distant Eurasian and mid-latitudinal North American sources (e.g. Rahn and McCaffrey, 1980; Rahn and Heidam, 1981; Barrie et al., 1981; Barrie, 1986). Highly persistent industrial organic and halogenated organic compounds (Khalil and Rasmussen, 1983; Hov et al., 1984) and potentially toxic pesticides (Oehme and Ottar, 1984; Hoff and Chan, 1986) were also detected in arctic air. Muir et al. (1986) suggested long-range atmospheric transport as an important pathway for accumulation of these compounds in arctic marine wildlife. More recent research has demonstrated that such compounds are found throughout arctic air, seawater, suspended sediments, and snow (e.g. Barrie et al., 1992, 1997; Hargrave et al., 1988; Gregor et al., 1995), in marine mammals, fish, and birds (e.g. Muir et al., 1992, 1996a), and in terrestrial wildlife (e.g. Thomas et al., 1992, Muir et al., 1996a).

Concerns of Canadian aboriginal peoples regarding health risks of contaminated traditional diets led to the establishment of the Technical Committee on Contaminants in Northern Ecosystems and Native Diets in 1985. In 1991 the Northern Contaminants Program, part of the Arctic Environmental Strategy, was established to reduce or eliminate contaminants in traditional foods, and to provide information to individuals and communities for food-related decisions (Shearer and Murray, 1997). This research was undertaken as part of the Northern Contaminants Program.

1.2 Contaminant Fate

Migration into, accumulation within, and loss of chemical from various environmental media are aspects of contaminant fate. A chemical's fate depends upon physico-chemical properties like water solubility and vapour pressure, while reactivity in the environment and solubility in organic media govern its persistence and accumulation potential.

Organochlorines are among the most commonly detected group of contaminants in the Arctic (e.g. Oehme and Ottar, 1984; Hargrave et al., 1988). The presence of chlorine atoms in their structure renders them relatively unreactive and increases their hydrophobicity. They are generally sparingly soluble in water. These traits allow organochlorine compounds to exist in the environment long enough to be transported to remote regions like the Arctic, and to accumulate in organic compartments such as sediments and biota. Vapour pressures in part determine which compounds are more abundant in arctic air and water (Wania and Mackay, 1993). Compounds with higher vapour pressures, like hexachlorocyclohexanes and di- and trichlorobiphenyls, are present at greater concentrations than hexa- and heptachlorobiphenyls and DDT (Patton et al., 1991; Iwata et al., 1993).

Understanding contaminant fate helps explain how contaminants reach the arctic, and can also improve our understanding of what happens to these chemicals once they have entered the arctic environment. Knowledge of the characteristics of arctic snowpacks, lakes, and streams can be combined with the physico-chemical properties and measured loadings of particular compounds to estimate chemical fate. Modeling of contaminant fate in environmental media can identify important loss mechanisms for chemicals, focus sampling efforts, and provide the ability to predict contaminant levels given such scenarios as loading reductions.

In this study, a model developed by Freitas et al. (1994, 1997), based on the QWASI (Quantitative Water Air Sediment Interaction) fugacity-type mass balance model (Mackay and Paterson, 1981; Mackay et al., 1983; Mackay and Diamond, 1989), was modified and used to investigate contaminant fate in small arctic lakes. One aspect of chemical fate, biodegradation, was studied further for α-hexachlorocyclohexane (α-HCH), since initial evidence suggests the importance of such degradation in the arctic may be greater than expected (Falconer et al., 1995a). α-HCH is the most abundant organochlorine compound in arctic air and surface waters. It is also a chiral compound, having two enantiomers that can be separated analytically, thereby providing a measure of enantioselective biodegradation processes.

1.3 Study Area

This study focuses on contaminant fate within watersheds of small freshwater lakes in the Canadian high Arctic. Amituk Lake, Char Lake, and Meretta Lake were included in the study, all of which are located on Cornwallis Island, NT.

Amituk Lake (75° 02' N, 93° 45' W) (Figure 1.1 (a)), located on the east side of the island, has an area of 0.38 km^2, mean depth of 19.4 m, maximum depth of 43.0 m, and a drainage area of 26.5 km^2 consisting of 6 subcatchments. Gorge, Mud and Cave Creek basins account for 76% of this area and in 1994 accounted for 92.7% of stream discharge into the lake (Kinney, 1997).

Char (74°42' N, 94°56' W) and Meretta Lakes (74°41' N, 95°02' W) (Figure 1.1 (b)), located near the village of Resolute on the south side of Cornwallis Island, have been well characterized limnologically (e.g. Schindler et al., 1974a,b). Char Lake has an area of 0.53 km^2, mean depth of 10.2 m, maximum depth of 27.5 m, and a drainage area of 4.35 km^2. Char Lake supplies drinking water to the village of Resolute. Meretta Lake has an area of 0.26 km^2, maximum depths of 12 m and 9 m in the lower and upper basins, respectively, and a mean depth of 3.25 m in the upper basin. Meretta Lake has received sewage effluent from the Department of Transport base north of the lake (Schindler et al., 1974b).

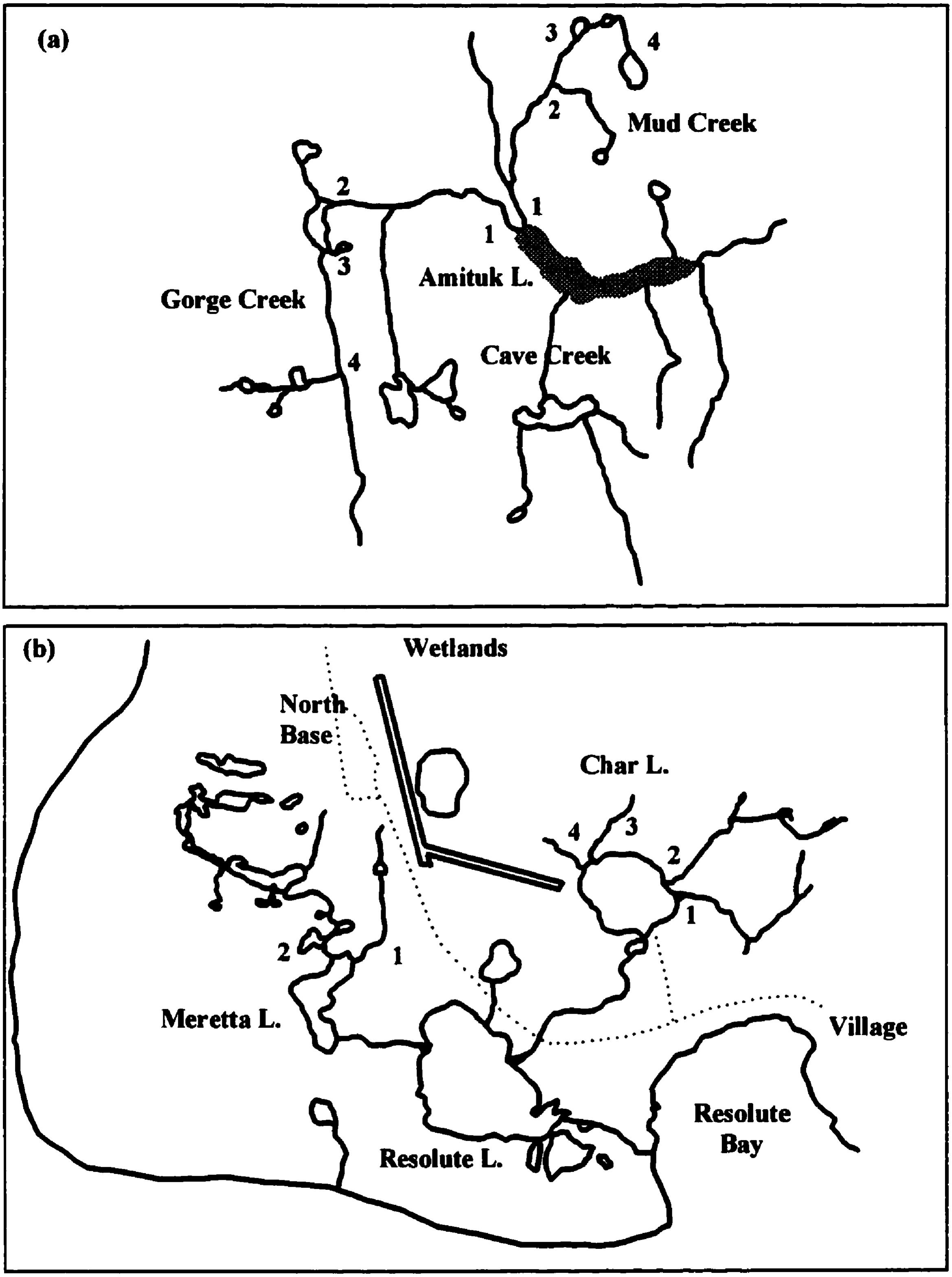

Figure 1.1: (a) Amituk Lake (75°02' N, 93°45' W) and its basin with 1997 sampling sites numbered and (b) Resolute area with Char Lake (74°42' N, 94°56' W) and Meretta Lake (74°41 N, 94°56' W) basins and numbered inlet streams

1.4 Research Objectives and Thesis Outline

The specific objectives of the investigation into biological degradation of α-HCH were:

- to determine the importance of enantioselective degradation as a loss pathway of α-HCH from the arctic environment;
- to identify factors that influence degradation of α-HCH.

The objectives of the modeling component of this study were:

- to understand, qualitatively and quantitatively, the fate of organochlorine contaminants in arctic freshwater lakes;
- to identify possible sinks for organic contaminants;
- to estimate the time response of arctic lakes to changes in contaminant loadings.

Chapter 2 provides information describing the occurrence and extent of contamination of the Arctic by organochlorine compounds. The physical and limnological characteristics of arctic watersheds that influence contaminant dynamics are presented. Degradation of α-HCH, specifically enantioselective degradation, is also discussed.

Chapter 3 investigates the importance of enantioselective degradation as a loss mechanism for α-HCH. Results from sampling at Amituk Lake in 1994 and from Char, Meretta, and Amituk Lakes in 1997 are presented. The extent of degradation of α-HCH is estimated and factors influencing enantioselective degradation are identified.

Chapter 4 presents background on fugacity- and aquivalence-type multimedia models and describes the application of a QWASI-based mass balance model to organochlorine contaminant fate in arctic freshwater systems. Chemical loadings to, and characteristics of, Amituk Lake used to obtain model results, and 1993 and 1994 measured concentrations for comparisons, are listed in Chapter 4. Steady- and unsteady-state model results are presented and interpreted to explain overall contaminant fate in the Amituk Lake basin in Chapter 5.

Chapter 6 summarizes study results into conclusions regarding contaminant fate in arctic freshwater lakes and the role of biological degradation. In addition, recommendations for further study are presented.

2. Background

Intensive arctic pollution research has been conducted over the last decade as part of the Canadian Arctic Environmental Strategy - Northern Contaminants Program and the international Arctic Monitoring and Assessment Program. This literature review will begin by summarizing the occurrence and fate of organic contaminants in the arctic environment. It will then focus on the hydrological and limnological characteristics of arctic lakes that are critical in understanding chemical fate within these systems. Finally, the degradation and transformation mechanisms of α-hexachlorocyclohexane (α-HCH) will be discussed, and studies of its enantioselective behaviour reviewed.

2.1 Organochlorine Contaminants in the Arctic Environment

The occurrence of organochlorine contaminants (OCs) in the Arctic was first documented in Arctic marine mammals (e.g. Holden, 1970; Addison and Brodie, 1973; Addison and Smith, 1974; Clausen et al., 1974; Bowes and Jonkel, 1975). Since then, the state of knowledge of Arctic contamination has been reviewed for air (Barrie et al., 1992, 1997), marine (Muir et al., 1992, 1996a; Norstrom and Muir, 1994), and terrestrial environments (Thomas et al., 1992; Muir et al., 1996a). The pesticide DDT and polychlorinated biphenyls (PCBs) were the primary OC contaminants found in early studies while improved analytical techniques allowed for detection and quantification of other OC compounds like CHB (chlorinated bornanes or toxaphene), HCHs, and chlordane-related compounds. Many of these compounds are persistent and bioaccumulate up the arctic food chain such that organisms at higher trophic levels, like polar bears, seals, and whales, have significant OC body burdens (Muir et al., 1992, 1996a; Norstrom and Muir, 1994). Of particular concern is the possibility that traditional native diets could lead to daily OC intake that exceed standards (Muir et al., 1989; Kinloch et al., 1992) and result in high levels within the human population (Dewailly et al., 1989,1994). Although there have been local sources of DDT (Brown and Brown, 1970), PCBs (Bright et al., 1995), and toxaphene in the Arctic and sub-Arctic, these are of minor importance relative to contributions of these contaminants through long-range atmospheric transport (Barrie et al., 1992).

Pollution concerns in the Arctic began in the 1950s with the observation of atmospheric pollution or 'Arctic Haze' (Mitchell, 1956). Since then, considerable research into the occurrence, levels, pathways, and sources of pollution has been undertaken and has been the subject of several reviews (e.g. Rahn and Heidam, 1981; Barrie, 1986; Barrie et al., 1992). Aerosol studies concluded that arctic air pollution had distant sources in more southerly latitudes (e.g. Rahn and McCaffrey, 1980; Barrie et al, 1981). In the 1980s, anthropogenic organic compounds were detected in Alaskan Arctic air (Khalil and Rasmussen, 1983; Rasmussen and Khalil, 1984) and in Norwegian Arctic air (Hov et al., 1984). Detected compounds included halogenated hydrocarbons like chlorinated solvents, chlorofluorocarbons, and brominated compounds, industrial and agricultural chemicals like HCHs, chlordanes, hexachlorobenzene (HCB), pentachlorobenzene, PCBs, and combustion-related polycyclic aromatic hydrocarbons (PAHs) like fluoranthene (Oehme and Ottar, 1984; Pacyna and Oehme, 1988).

OCs have been measured in Canadian Arctic air at Mould Bay, N.W.T. (Hoff and Chan, 1986), at the Ice Island in the Arctic Ocean near Ellesmere Island, N.W.T. (Hargrave et al., 1988; Patton et al., 1989), at Resolute Bay, N.W.T. (Bidleman et al., 1995a), and at Alert, N.W.T. (Patton et al., 1991; Fellin et al., 1996; Hargrave et al., 1997; Halsall et al., 1998). Table 2.1 summarizes average air concentrations from these studies. α-HCH is the most abundant OC in arctic air followed by HCB and γ-HCH. Concentrations of α- and γ-HCH and PCC declined between the mid-1980s and mid-1990s, likely resulting from bans on the use of these products in several countries, particularly for α-HCH (Li et al., 1998).

Many OCs found in arctic air are also found in northern waters. Reported average concentrations from several studies are summarized in Table 2.2. As was the case for air, α-HCH is the most abundant in marine surface waters followed by γ-HCH and CHB (toxaphene), while compounds with lower solubilities, such as chlordanes and DDT, had low concentrations. Concentrations of α-HCH and γ-HCH in surface seawater have shown little change over the same time that air concentrations have declined, causing a reversal in the direction of air-water gas exchange for these compounds (Jantunen and Bidleman, 1995, 1996, 1997; Bidleman et al., 1995b). Air-water exchange has been hypothesized to drive contaminant levels in the surface layer. Net deposition of CHB, chlordanes, and endosulfan-I accounted for 50-100% of open water surface inventories while volatilization of HCHs and HCB may lower surface inventories by 4-20% (Hargrave et al., 1997). Limited exchange

Table 2.1: Average air concentrations (pg/m^3) of organochlorine compounds in the Canadian Arctic

	α-HCH	γ-HCH	HCB	CC	TC	CN	TN	ΣChlord.	ΣDDT	ΣPCB	PCC	Reference
Mould Bay												
June 1984	-	-	-	1.1-1.8	0.45-1.7	nd-0.4	1.0-1.5	-	-	-	-	Hoff & Chan, 1986
Ice Island												
May-June 1986	425	70	73	-	-	-	-	3.6	< 1	-	-	Hargrave et al., 1988
Aug.-Sept. 1986	253	17	63	-	-	-	-	1.9	< 1	-	-	
Ice Island												
Aug.-Sept. 1986	546	31	189	2.8	1.1	0.40	1.5	5.8	1.0	15.1	44	Patton et al., 1989
June 1987	340	45	147	4.0	2.3	0.67	3.7	10.7	5.2	17.6	36	
Alert												
Feb.-Apr. 1988	165	23	153	1.3	1.2	0.03	1.4	-	1.44	49	17	Patton et al., 1991
Alert												
May-Sept. 1992	57.0	15.4	55.8	1.4	1.0	-	-	-	1.2	-	10.0	Fellin et al., 1996
Oct.-Apr. 1992	61.7	10.4	62.3	1.6	1.8	-	-	-	2.9	-	5.2	
Resolute Bay												
August 1992	114	9.8	-	1.4	0.51	0.12	0.77	-	< 0.3	-	6.9	Bidleman et al., 1995a
Alert												
Jan.-Dec. 1993	59.9	9.76	56.7	1.01	0.47	0.12	0.88	-	0.79	-	-	Halsall et al., 1998
Jan.-Dec. 1994	60.8	11.5	55.6	1.34	0.63	0.15	1.16	-	1.28	-	-	

Table 2.2: Average seawater concentrations (pg/L) of organochlorine compounds in Northern waters

	α-HCH	γ-HCH	HCB	CC	TC	CN	TN	ΣDDT	ΣPCB	PCC	Reference
Bering-Chukchi Seas											
1981 (Bering Sea & N. Pac.)	2750	650	-	4.7	4.3	< 0.2	1.4	2.1	-	-	Kawano et al., 1988
1988	2350	590	60	50	-	30	-	-	-	-	Hinckley et al., 1991
1990 (Chukchi Sea)	1400	180	-	2.6	0.9	-	0.6	0.3	8.4	-	Iwata et al., 1993
1990 (Bering Sea)	1500	190	-	1.9	1.5	-	0.5	1.0	12	-	Iwata et al., 1993
1993	2000	450	-	-	-	-	-	-	-	-	Jantunen & Bidleman, 1995
1994	1820	330	-	1.2*	1.8*	0.33*	0.76*	-	-	19*	Jantunen & Bidleman, 1997; 1998*
Resolute Bay											
1992	4700	440	-	4.5	7.3	0.4	1.5	< 5	-	48	Bidleman et al., 1995a
1993	3640	520	15	1.3	0.5	-	-	-	-	85	Hargrave et al., 1997
Canada Basin											
1986	4470	610	-	-	-	-	-	-	-	-	Hargrave et al., 1988
1987	7100	810	-	-	-	-	-	-	-	-	Patton et al., 1989
1994	2310	490	-	1.2*	1.3*	0.33*	0.80*	-	-	58*	Jantunen & Bidleman, 1997; 1998*

Values with (*) from corresponding reference across stratified layers and low sedimentation rates result in minimal losses (Hargrave et al., 1997).

The contribution of distant sources to arctic ecosystem contamination has been well established (e.g. Barrie et al., 1981; Rahn and Heidam, 1981; Oehme and Ottar, 1984). Evidence to support long-range transport and its pathways has been documented and includes use of air mass back trajectories, source tracing compounds and mixture compositions, concentration trends of various compounds, and concentration responses to use trends. Two main mechanisms or pathways of pollution movement to northern regions have been proposed: air mass movement from source regions and the global condensation process.

To explain the first process, Iverson (1984) and Joranger and Ottar (1984) have suggested that ground level air pollution moving into the Arctic can only originate in regions with similar air temperatures. In winter, the polar front moves south into Eurasia and central North America (Joranger and Ottar, 1984; Oehme and Ottar, 1984) allowing greater inputs of contaminants to arctic air masses from lower latitudes. Thus, arctic air pollution levels are higher in winter than in summer for aerosols and some organic compounds (Rahn and McCaffrey, 1980; Barrie et al., 1981; Khalil and Rasmussen, 1983).

Using air mass back trajectories, Barrie et al. (1981) found that air masses entering the Canadian Arctic during winter often originated in Siberia; however, North American air masses were common, and occasional pulses from Europe also occurred. Pacyna and Ottar (1988) associated events of increased levels of several OCs with air mass trajectories that passed over the former Soviet Union. However, the use of air mass trajectories limits identification of sources to regions along its path and may not account for contaminants collected in the air mass outside the range of back-calculations.

Contaminant composition can also provide indicators of source regions. Aerosols with higher levels of metals and soot relative to vanadium, typical of regions with coal-burning and metal-finishing industries, were associated with air masses from Siberia (Barrie et al., 1981). Knowledge of the use patterns of particular pesticides in countries along air mass trajectories may also aid in identifying sources (Pacyna and Oehme, 1988). Many OCs are mixtures of compounds with several isomers or congeners, or have characteristic metabolites. Isomer ratios and congener signatures can be used as tracers of source regions.

Pacyna and Oehme (1988) found α-HCH to γ-HCH ratios vary according to source region. European sources gave ratios of 4:1 to 1:1, North American sources had ratios from 10:1 to 7:1, while higher ratios were associated with long-range transport. The use of α-/γ-HCH ratios as indicators is complicated by the use of different HCH formulations (Voldner and Li, 1995), isomerization in the environment (Benezet and Matsumura, 1973; Malaiyandi and Shah, 1984), and solubility differences between the isomers. Ratios of *p,p*'-DDT to *p,p*'-DDE can also be indicators of air mass origin (Atlas and Giam, 1988; Iwata et al., 1993). High DDT/DDE ratios indicate close proximity to local sources, while remote locations exhibit low ratios. Near India, ratios were high where DDT is still used, but in the North Pacific and North Atlantic, DDT/DDE ratios were low (Iwata et al., 1993). The change in ratios may result from UV exposure during long-range transport or the greater mobility of DDE relative to DDT, which is a function of their physico-chemical properties (Iwata et al., 1993).

The second transport mechanism that has been hypothesized involves temperature-dependent partitioning of low-volatility contaminants and fractionation by latitude by condensing according to their vapour pressures at ambient temperatures (Wania and Mackay, 1993, 1995, 1996). The systematic movement of persistent compounds from warmer to colder regions by re-emission from soils was suggested by Ottar (1981) and the possibility of transport regulated by physico-chemical properties was raised by Iwata et al. (1993). Evidence to support the global fractionation hypothesis includes observations that the more volatile congeners of PCBs (Patton et al., 1991) and CHBs (Bidleman et al., 1989) are found in arctic air, that deposition of OCs on plants (Calamari et al., 1991; Ockenden et al., 1998a) and semipermeable membrane devices (Ockenden et al., 1998b) increases as temperature decreases, and that trichlorobiphenyl concentrations in burbot tissues increase with latitude while heavier PCBs decrease (Muir et al., 1990). Sediment cores from lakes at varying latitudes show a decline in concentrations of total DDT with latitude while the more volatile HCB increased (Muir et al., 1995). The total PCB composition in lake sediments also changed with latitude. Tetra- to octachlorobiphenyls decreased while di- and trichlorobiphenyl concentrations remained relatively constant and the percentage of di- and trichlorobiphenyls of total PCBs increased (Muir et al., 1996b). Iwata et al. (1993) found that α-HCH air concentrations decreased with latitude from India to the Bering and Chukchi

Seas, whereas seawater concentrations increased. DDT water concentrations were high in the source regions of India and Southeast Asia but dropped rapidly and exhibited limited spatial variation otherwise (Iwata et al., 1993).

Upon reaching the Arctic, many of these compounds condense into the marine and terrestrial environment where they bioaccumulate up the food chain. Native peoples can be exposed to higher levels of these compounds through traditional diets causing concern over possible health consequences (Jensen et al., 1997). Understanding the fate of OCs in the Arctic environment will allow the development of predictive models that can aid in assessing the risks of exposure for years to come as sources of these compounds and levels in the environment change.

2.2 Physical and Limnological Characteristics of Arctic Lakes

Knowledge of physical and limnological characteristics of arctic watersheds is essential in understanding chemical fate as they drive contaminant dynamics (Schindler et al., 1995; Freitas et al., 1997). Arctic systems differ from those of lower latitude watersheds in that they are less productive, have low temperatures, and are ice-covered for much of the year. This section reviews characteristics of arctic freshwater lakes and their watersheds in general, and on Cornwallis Island in particular.

The Arctic is classified as a desert because of its arid conditions. Annual average precipitation at Resolute on Cornwallis Island is 131.4 mm, of which approximately 40% falls as rain from June to August (Environment Canada, 1990). The remainder falls as snow during two peak periods in late spring and early fall (Schindler et al., 1974a; Environment Canada, 1990). Average daily temperatures range from -33.2°C in February to 4.1°C in July, while temperatures above 0°C occur from late June to August. Winters are long and dark, lasting from early September to early June with polar night from November through January. Summers are short with an average of 9 frost-free days but have twenty-four hour daylight from May to mid-August. Winds average 21.5 km/h and are primarily from the NNW, except for July and August when they are predominantly from the west and southeast (Environment Canada, 1990).

Lake hydrology is defined by these climatic conditions. Snow accumulates in depressions, valleys, and sheltered areas during the winter, while exposed surfaces tend to be bare or thinly covered. Winds redistribute fallen snow and can result in higher accumulations in lake basins than predicted by measured precipitation at weather stations (Woo et al., 1983). Snowmelt begins in June when temperatures rise above 0°C and is rapid and intense, with most of the annual inflow entering the lakes within the first few weeks (Woo, 1976, 1980; Woo et al., 1981; Schindler et al., 1974a). After the peak melt, the influence of snowmelt on basin hydrology is diminished and streams are maintained by subsurface flow and suprapermafrost meltwater (Woo and Steer, 1983).

Lakes remain ice covered until mid- to late July, although a moat of open water forms around the ice sheet along the shoreline during the melt period in June (Schindler et al., 1974a; Bergmann and Welch, 1985; Heron, 1985). Cold ice-melt water with few solutes, which is less dense than the water column, forms a layer under the ice (Welch and Bergmann, 1985). Inflowing waters pass over the ice during peak melt, or enter the lake and move towards the outlet atop the water column but below the ice-melt layer. This plume of water becomes wider as it travels through the lake, mixing only to a limited extent with the deeper water (Bergmann and Welch, 1985; Semkin, 1996). Mixing occurs with higher inflowing water velocities (Bergmann and Welch, 1985), or temperature- or solute-driven density currents (Hobbie, 1984; Hambrey, 1994). Complete mixing only occurs at ice-off and lasts from 0-6 weeks (Schindler et al., 1974a).

In August, winds and colder temperatures cool lake waters to near 0°C and by late-September ice crystals form and accumulate at the windward shore (Schindler et al., 1974a; Welch and Bergmann, 1985). Once formed, ice sheet thickness increases linearly, reaching maximum thickness of 2.2 to 2.4 m in May then maintaining this thickness for a few weeks until melt begins in June (Schindler et al., 1974a; Heron, 1985). Ice can account from 18% of lake volume for deeper lakes, up to 100% for small shallow lakes and ponds (Schindler et al., 1974a). As the ice forms and thickens, freeze-out or cryoconcentration of solutes leads to density currents and increased salt concentrations in the remaining water (Schindler et al., 1974a; Welch and Bergmann, 1985). This phenomenon could potentially lead to higher contaminant concentrations in the lake over winter (Freitas et al., 1994, 1997).

Slow lake mixing may occur over winter resulting from density differences due to freeze-out and from heat transfer from lake sediments to overlying water (Welch and Bergmann, 1985). Heat absorbed by the sediments over the summer is transferred to the colder winter waters, thereby increasing the density of overlying water and causing it to move downslope towards the deepest part of the lake. Meanwhile, waters just below the ice which have higher solute concentrations and greater densities, move shoreward and sink. This circulation pattern has been confirmed with dye experiments (Welch and Bergmann, 1985).

Knowledge of high Arctic lake limnology comes largely from studies conducted in the 1960s and 1970s and has been reviewed by Hobbie (1973, 1984). Studies at Char and Meretta Lakes near Resolute, Cornwallis Island, N.W.T. (e.g. Morgan and Kalff, 1972; Schindler et al., 1974a,b; Welch and Kalff, 1974; de March, 1975, 1978; Rigler, 1975) have contributed to this understanding.

Arctic lakes are generally low in nutrients, have fewer species at limited trophic levels, and are cold throughout the year. Low productivity rates result in oligotrophic conditions (< 100 g·C/m^2/yr) for most lakes (Hobbie, 1973). Low nutrient concentrations due to naturally low inputs from precipitation may limit production in arctic lakes more than low temperatures (Schindler et al., 1974a; de March, 1975). Nitrogen and phosphorus inputs are lower than in temperate lakes, with phosphorus the limiting nutrient (Schindler et al., 1974b; de March, 1975). Benthic primary production is often many times higher than phytoplankton production (Hobbie, 1973), as it is at Char Lake where benthic production accounted for 80% of the 21.1 g·C/m^2/yr total primary production (Welch and Kalff, 1974). Light penetration through the ice also impacts photosynthetic production. In the high Arctic, ice is transparent while snow cover is thin, compared to subarctic and temperate lake ice, making light conditions under the ice more favourable for algal production (Hobbie, 1973). Phytoplankton biomass begins to increase in February, after polar night, and reaches its maximum while ice still covers the lake (Hobbie, 1973). Organic carbon inputs are also low in arctic lakes and, combined with low productivity, result in sediments with very low organic carbon fractions relative to temperate lakes. The organic carbon fraction was found to be 3% or less in four lakes > 75°N latitude in the Canadian Arctic (Muir et al., 1995) and ranged from 0.3-2.4% in Char Lake (de March, 1978).

Trophic structures in arctic systems are thought to be simpler than temperate systems, although Hobbie (1973) suggests the number of interactions, and not their complexity, are diminished. There are fewer planktonic, benthic, and fish species present in arctic systems than in temperate systems. Although fewer phytoplankton species are present, from 9 to 147 species have been identified in arctic lakes (Hobbie, 1973). Arctic lakes can have more algae, usually present just under the ice for maximum irradiation, than sub-arctic and alpine lakes (Hobbie, 1973). The bacterial community in Char and Meretta Lakes was dominated by 1-2 x 0.5 μm rods with 2-80 x 10^8 bacteria L^{-1} in Meretta Lake and 0.1-2 x 10^8 bacteria L^{-1} in Char Lake, the value for Char being among the lowest ever reported (Morgan and Kalff, 1972). Zooplankton biomass is low in arctic lakes but similar to temperate lakes in winter (Hobbie, 1973). Up to 10 invertebrate species have been found in arctic lakes and are mainly rotifers and copepods (Hobbie, 1973). Reproduction cycles vary from a few months to two years and are limited by ice cover and temperature (Hobbie, 1973). Benthic animals, dominated by chironomid larvae, are a food source for shorebirds and fish (Hobbie, 1973). Arctic char, the only fish found in more oligotrophic waters, feed on chironomid larvae and zooplankton, can reach ages of 40 years (Hobbie, 1973), and have slow growth rates due to cold temperatures (Rigler, 1975).

These physical, chemical, and biological characteristics of arctic lakes combine to have important effects on contaminant movement and accumulation in lake water, sediments, and the food chain.

2.3 Degradation of α-Hexachlorocyclohexane

α-Hexachlorocyclohexane (α-HCH) has been established as the most abundant OC in arctic air and water. Although it is not as toxic and bioaccumulative as many of the OCs present in the Arctic, its abundance allows for a better understanding of the pathways of more toxic compounds. This section reviews the production and use of α-HCH, its degradation mechanisms, and evidence of its biological degradation in the environment, particularly in the Arctic. A more comprehensive review of toxicity and environmental fate of the HCH isomers has been compiled by Willett et al. (1998).

HCH is an insecticide produced by the chlorination of benzene in the presence of ultraviolet light (IPCS, 1992; Deo et al., 1994). First used in 1943 (Li et al., 1998), the product has two forms, technical HCH and lindane, of which technical HCH usage has been banned or restricted in many countries and most developed nations (Voldner and Li, 1995). Technical HCH consists of 60-70% α-HCH, 5-12% β-HCH, 10-15% γ-HCH, and small percentages of δ-HCH and ε-HCH (IPCS, 1992). Lindane is > 90% γ-HCH (IPCS, 1992) and is still in use in North American and European countries (Voldner and Li, 1995).

The α-HCH isomer is unique relative to the other predominant HCH isomers in that it is chiral, with two enantiomers (Figure 2.1). Each enantiomer is the non-superimposable mirror image of the other and shares the same physico-chemical properties, except they rotate the plane of polarized light in opposite directions. Development of novel analytical techniques in the early 1990s allowed for separation of α-HCH enantiomers by gas chromatography (Faller et al., 1991a; Müller et al., 1992). Separation of the (+)-α-HCH and (-)-α-HCH enantiomers allows differentiation between biotic, enantioselective processes like enzymatic interactions or microbial degradation, and abiotic, non-enantiospecific chemical and photochemical processes. Differences in the (+)-α-HCH/(-)-α-HCH enantiomer ratio (ER) from the racemic value of 1.0 found in the technical HCH product are indicative of the presence of enantioselective processes.

Abiotic transformation processes that influence the fate of α-HCH include hydrolysis and photolysis in the aquatic environment, and photooxidation in the atmosphere. In basic aqueous solutions, dehydrochlorination of HCHs occurs producing pentachlorocyclohexenes (PCCHs) and trichlorobenzenes (Ngabe et al., 1993). A hydrolysis half-life of 26 years was calculated for α-HCH in water at pH 8 and 5°C (Ngabe et al., 1993), conditions similar to those in the Arctic. Photolysis rates of α-HCH are unknown.

Atmospheric reactions are expected to be important in pollutant removal from the environment (Schroeder and Lane, 1988). Estimates of atmospheric half-lives for α-HCH range from 2.3 d, calculated from structure-activity relationships (Atkinson, 1987; quoted in

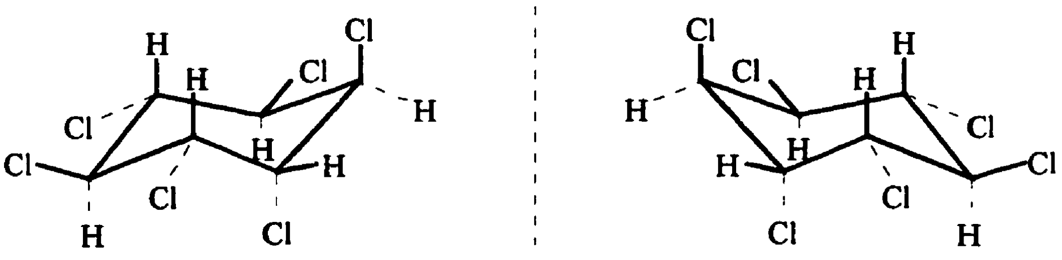

(+)-α-HCH (-)-α-HCH

Figure 2.1: Structures of α-HCH enantiomers, non-superimposable mirror images.

Mackay et al., 1997), to 120 d from extrapolation of laboratory rate constants (Brubaker and Hites, 1998). The expected reaction mechanism of OH radicals with α-HCH is H-atom abstraction (Kwok and Atkinson, 1995), but reaction rates found by Brubaker and Hites (1998) suggest this photooxidation reaction may not be an important loss mechanism of α-HCH.

Interconversion may play a significant role in the fate and persistence of certain HCH isomers in the environment. Isomerization of γ-HCH and the other isomers to α-HCH has been reported under environmental and extreme conditions, through chemical, photochemical, and biological interactions. Heating HCH isomers to 140°C in the presence of anhydrous $FeCl_3$ caused interconversion (Whetstone et al., 1953). α-HCH was the most stable, slowly converting to a mixture of the other isomers, while β-HCH mainly converted to α-HCH, and γ-HCH to δ-HCH, which then converted to α-HCH. Transformation of γ-HCH to α-HCH by microbial populations can result in levels higher than those expected by selective accumulation of impurities in the applied pesticide (Benezet and Matsumura, 1973; Vonk and Quirijns, 1979). Isomerization is also possible under sunlight (Steinwandter, 1976, 1978a,b) and UV radiation (Malaiyandi and Shah, 1984).

The importance of biotic degradation and uptake of OC compounds is evident in the practice of bioremediation and the high levels found in higher organisms, respectively. Studies on the occurrence, significance and mechanisms of biological degradation, conversion, and uptake of HCH isomers have been thoroughly reviewed (Deo et al., 1994; Johri et al., 1996).

Besides isomerization, microorganisms can transform HCH isomers by reductive dechlorination, dehydrochlorination, dehydrogenation, and oxidation (Deo et al., 1994; Johri et al., 1996). Reductive dechlorination, which involves the substitution of a hydrogen atom for a chlorine atom, usually in an anaerobic environment, was found to be important in the degradation of organochlorine pesticides (Deo et al., 1994). Recent studies have reconsidered the relative importance of anaerobic and aerobic HCH degradation. Bachmann et al. (1988a,b) demonstrated that mineralization of α-HCH was faster and more complete under aerobic than anaerobic conditions and proposed that the mechanism proceeded via dehydrochlorination of α-HCH to pentachlorocyclohexene (PCCH). Several other studies have identified PCCH as an HCH metabolite and suggest dehydrochlorination as the degradation mechanism (e.g. Ludwig et al., 1992; Sahu et al., 1995; Buser and Müller, 1995). Oxidative mechanisms such as oxygenation and dehydrogenation are more common in higher organisms (Deo et al., 1994; Johri et al., 1996).

Most α-HCH degradation studies make no distinction between its enantiomers. More recent studies have been undertaken using chiral techniques to detect enantioselective microbial degradation and uptake, to revisit reaction mechanisms, and to determine degradation rates. Analysis of seawater from the North Sea found that the α-HCH enantiomer ratio (ER) averaged 0.88 (Faller et al., 1991a). Differences from the racemic value of 1.0 were attributed to enantioselective microbial degradation and possible enantioselective isomerization from γ-HCH to α-HCH. Further investigations found ERs varied from region to region within the North Sea with values >1.0, < 1.0, and near 1.0 (Faller et al., 1991b). Different microbial populations were thought to account for the variation. Controlled experiments monitored formation of chiral metabolites β-PCCH and γ-PCCH from α-HCH and γ-HCH, respectively (Hühnerfuss et al., 1992; Ludwig et al., 1992). The (+)-β-PCCH / (-)-β-PCCH ER changed over the experimental period reflecting enantioselective degradation of β-PCCH, while the γ-PCCH ER remained at ~1.0, suggesting that a chiral substrate is a requirement for enantioselectivity. The (+) enantiomers of α-HCH and β-PCCH, which correspond with each other, degraded more quickly than the (-) enantiomers. Although isomerization of γ-HCH to α-HCH was noted, it did not proceed enantioselectively (Hühnerfuss et al., 1992). Rate constants for the degradation of HCH isomers and enantiomers in sewage sludge were in the order γ- > (+)-α- > (-)-α- > δ- > β-HCH, and rates for (+)-α-HCH and (-)-α-HCH differed by a factor of 2-3 (Buser and Müller, 1995). Enantioselective degradation was not found to occur in a pond water sample or in sterilized sludge. Results were found to be consistent with anti-periplanar dehydrochlorination of Cl and H atoms in axial positions (Buser and Müller, 1995).

Enantioselective uptake and degradation of α-HCH by higher marine and terrestrial organisms have also been investigated. ERs in mussels (0.89) and flounder livers (0.80-0.94) from the North Sea were similar to that of the water (0.84), while ducks that feed on mussels had ERs ranging from 1.4 - 2.8 in ill ducks, to near complete degradation of (-)-α-HCH in healthy ducks (Pfaffenberger et al., 1992). ER values > 1 in ducks suggest different enzymatic pathways may be responsible for degradation in higher trophic levels (Möller and Hühnerfuss, 1993). ERs in marine mammals vary among species and tissues within particular animals. ERs were > 1.0 in the blubber of hooded seals and harbour porpoises but < 1.0 in the blubber of harp seals (Hummert et al., 1995). Tanabe et al. (1996) found ERs of 1.6-2.8 in the blubber of small cetaceans that varied between animals from different locations, attributing the differences to population feeding habits and species-specific metabolism. Feeding habits were found to partially explain ERs in northern fur seals and double-breasted cormorants (Iwata et al., 1998). In fur seals, ERs in blubber, milk, lung, and liver ranged between 1.2 and 1.9, while ERs of 28 and 32 were found in brain tissues (Mössner et al., 1992). The high brain values were thought to result from enantioselective transport of (+)-α-HCH across the blood-brain barrier. ERs in terrestrial roe-deer livers ranged from 0.03-0.40 with (+)-α-HCH being selectively degraded (Pfaffenberger et al., 1994), differing from values found in livers of many marine organisms. Research to date has demonstrated the complexity of pathways involved in the degradation of α-HCH among all levels of organisms.

In the Arctic, enantiomeric analyses have provided evidence for the occurrence of enantioselective degradation. In the Bering and Chukchi Seas, α-HCH ERs in seawater ranged from 1.05 to 1.14 in surface waters (1-40 m) and as low as 0.76 in deeper (133-298 m) water (Jantunen and Bidleman, 1996, 1997). In the Canadian Basin and Greenland Sea ERs were < 1.0 and also decreased with depth (Jantunen and Bidleman, 1996, 1997, 1998). In boundary layer air, the ERs were also > 1.0 in the Bering and Chukchi Seas and < 1.0 in the Canada Basin and Greenland Sea, providing evidence of out-gassing of α-HCH in northern waters (Jantunen and Bidleman, 1996, 1997). ERs for particulate phase α-HCH in northern waters were similar to water values with a few exceptions where degradation was either more enhanced on the particles or the ER was reversed relative to that in the water (Jantunen and Bidleman, 1998). The authors suggested that this may indicate a decoupling of degradation between phases and the actions of different microbial communities. Degradation rates of 0.117 y^{-1} for (+)-α-HCH and 0.030 y^{-1} for (-)-α-HCH were determined for the Eastern Arctic Ocean from estimates of the age of the water mass at depth and from measured ERs and concentrations (Harner et al., in press). In the Canadian Arctic archipelago, the α-HCH ER was 1.00 in air and 0.93 in Resolute Bay seawater (Falconer et al., 1995b). At Amituk Lake on Cornwallis Island, N.W.T., ERs ranged from 0.65 to 0.99 in stream meltwater and was 0.77 in the lake (Falconer et al., 1995a). In the lower Canadian Arctic, (+)-α-HCH depletion was reported in the lakes and rivers of the Yukon River and Mackenzie River basins and in Great Slave Lake (Alaee et al., 1995, 1997a,b). These studies provide clear evidence that low-productivity arctic ecosystems are able to degrade α-HCH.

The ER has been discussed as an indicator of biotic, enantioselective degradation or uptake of chiral pollutants. However, the ER also has application as a possible tracer of contaminant sources and of air-water gas exchange. The air above soils was shown to have α-HCH ERs characteristic of the soil close to the ground and approach more racemic values with increased height, likely from mixing with racemic α-HCH from long-range transport (Finizio et al., 1998). ERs of heptachlor-*exo*-epoxide in Great Lakes air were similar to values found in soils in possible source regions (Bidleman et al., 1998). The ER ratio above water bodies in the boundary layer can provide an indication of whether out-gassing of the compound of interest from the water might be occurring. This was shown for arctic marine waters (Jantunen and Bidleman, 1996) and Lake Ontario. For the latter, the air above the lake had minimum ER values during the summer months when volatilization from the lake was at its peak and was racemic during winter when regional air masses predominate (Ridal et al., 1997).

The following chapter estimates the importance of microbial degradation of α-HCH using ERs for the Amituk basin on Cornwallis Island, N.W.T., and identifies some of the factors that influence microbial degradation in high Arctic watersheds.

3. Enantioselective Degradation α-Hexachlorocyclohexane in Arctic Watersheds

The occurrence and fate of α-hexachlorocyclohexane (α-HCH) has received considerable attention in the Arctic as discussed in the previous chapter, particularly air and water concentrations and air-water gas exchange. However, the importance of possible α-HCH loss mechanisms from the arctic environment are not well understood. Degradation, sedimentation and air-water exchange are the expected removal processes. Sedimentation was found to be negligible (<4%) relative to air-water exchange in controlling contaminant levels in the water column in the Canadian Arctic archipelago (Hargrave et al., 1997). Although found to occur in the Arctic, the importance of degradation in removal of α-HCH remains unknown. Only recently has quantification of α-HCH loss from the Arctic Ocean by degradation been attempted (Harner et al., in press).

Arctic freshwater contaminant processes and fluxes were studied from 1992-1994 at Amituk Lake on Cornwallis Island, N.W.T. in the Canadian Arctic (Semkin, 1996; Barrie et al., 1997). Selected samples from 1992 were analyzed for α-HCH enantiomer ratios (ERs) (Falconer et al., 1995a) and results suggested ER values were inversely related to stream temperatures. This chapter presents α-HCH ER and concentration results from the final year of the Amituk Lake study and from recent field investigations. The importance of enantioselective degradation as a loss mechanism for α-HCH in high arctic watersheds is estimated, and factors affecting this process are identified.

3.1 Methods

3.1.1 Sampling Sites

Sampling was conducted over several field seasons at Amituk Lake, and in July 1997 at Char and Meretta Lakes. At Amituk Lake (Figure 1.1 (a), Ch. 1), water chemistry, stream discharge, and contaminant levels were measured over the summer in each of 1992, 1993, and 1994 by a project team directed by Ray Semkin of the National Water Research Institute of Environment Canada. The project, entitled "Processes and fluxes of contaminants in aquatic systems," was conducted under the Northern Contaminants Program. During the final year of the Amituk Lake Project, water samples were collected from each of the five major inlet streams, the outflow, and lake depths of 3, 20, and 40 m over June, July and August.

In July 1997, water samples were collected from four locations, indicated in Figure 1.1 (a) (Ch. 1), along each of Mud and Gorge Creeks at Amituk Lake. At Char Lake, samples were collected from four inlet streams, the outflow and the lake at 10 m depth. Finally, at Meretta Lake, two inlet streams, the outlet, and the lake at 5 m were sampled (Figure 1.1 (b)).

3.1.2 Sample Collection and Extraction

Sample collection, extraction, and cleanup procedures for 1994 samples were as described by Falconer et al. (1995a). In 1997, water samples were collected from stream surfaces with a stainless steel bucket and from lake depths with a submersible pump, then transferred to stainless steel cannisters. Each sample received 1.0 mL of d_6-α-HCH in acetone as a surrogate standard. Approximately 18 L of water was passed through glass fibre filters to remove particles, then through 1 g, 6 mL Isolute ENV+ cartridges (Jones Chromatography, Lakewood, Colorado) to extract dissolved HCHs. Filters and cartridges were wrapped in aluminum foil, sealed in plastic bags, and stored at ~5°C until returning to the laboratory. Cartridges were conditioned with 5 mL methanol then 5 mL deionized water before the samples were processed. Blanks were prepared by passing chromatographic-pure water through the extraction apparatus.

HCHs were eluted from extraction cartridges with 20 mL dichloromethane, exchanged into to isooctane, and reduced in volume to ~1 mL. Samples were cleaned up by column chromatography with 0.5 g neutral alumina (6% water) topped with sodium sulfate, and eluted with 10 mL of 10% DCM-petroleum ether, and transferred to isooctane. Mirex (10 μL) was added as an internal standard and then extracts were shaken with concentrated sulfuric acid for final cleanup.

Other water quality and chemistry data were collected according to standard methods of the National Water Research Institute (Inland Waters Directorate, 1979). These included measurements of: stream discharge, Ca^{2+}, Mg^{2+}, alkalinity, pH, water temperature, conductivity, dissolved and particulate organic carbon, Na^{+}, and Cl^{-}, among other parameters.

3.1.3 Quantitative Analysis

Quantification of HCHs in 1994 samples used procedures described by Falconer et al. (1995a). HCHs in 1997 samples were determined using a Hewlett Packard 5890 GC with ^{63}Ni electron capture detector (ECD). Samples (2 μL) were injected splitless (split opened after 30 s) onto a DB-5 column (60 m length, 0.25 mm i.d., 0.25 μm film thickness, J&W Scientific) using hydrogen carrier gas at 60 cm s^{-1} and nitrogen at 50 mL min^{-1} as the make-up gas. The injector and detector temperatures were each 250°C. The temperature program was as follows: initial temperature, 90°C; 10°C min^{-1} to 160°C; 2°C min^{-1} to 200°C; 20°C min^{-1} to 270°C; 15 min hold. Data were collected and quantified against five standards using an HP Chemstation.

3.1.4 Chiral Analysis

Separation of the α-HCH enantiomers was performed by gas chromatography-negative ion mass spectroscopy (GC-NIMS) using a HP 5890 GC-5989B MS. The primary separation column was BGB-172 (20% *tert*-butyldimethylsilylated β-cyclodextrin in OV-1701, BGB Analytik AG, Switzerland) with results confirmed using a Beta-DEX 120 column (20% permethylated β-cyclodextrin in SPB-35, Supelco) Each column was 30 m in length with a 0.25 mm i.d. and 0.25 μm film thickness. (+)-α-HCH eluted first on the Beta-DEX column (Falconer et al., 1995a) while (-)-α-HCH eluted first on the BGB-172 (Jantunen and Bidleman, 1998). Temperature conditions were: initial temperature, 90°C; 10°C min^{-1} to 140°C; 1°C min^{-1} to 180°C; 10 min. hold; 10°C min^{-1} to 220°C; 10 min. hold. Other GC-NIMS instrument conditions were: injector temperature, 220°C; transfer line temperature, 220°C; helium carrier gas at 40 cm s^{-1}; quadrupole temperature, 100°C; source temperature, 150°C; and methane at a nominal pressure of 1.0 Torr. Ions 255 and 257 were monitored, with target ion 255 used in calculations and ion 257 used as a qualifier.

3.2 Results and Discussion

3.2.1 Quality Control

Analytical blank procedures and typical blank and recovery values are described by Falconer et al. (1995a). α-HCH concentrations for 1994 samples were blank and recovery corrected.

Detectable amounts of α-HCH were not found in 1997 water sample blanks (n=9), thus a blank correction was not applied. Recoveries of the d_6-α-HCH surrogate averaged 81 ± 7% (range 58-93%, n=59). Additional samples were spiked with 231 ng α-HCH and average recovery was 90 ± 5% (n=6, corrected for native amounts in water samples). Reported concentrations were corrected according to individual d_6-α-HCH recoveries.

ERs of selected 1994 and 1997 samples were confirmed by comparing results obtained on the BGB-172 column and Beta-DEX 120 columns. The average percent difference was 2.5 ± 3.0% between the two columns (n=50). Standard α-HCH ERs were 0.99 ± 0.01 (n=8) for the Beta-DEX 120 column and 1.01 ± 0.01 (n=9) on the BGB-172 column. Sample 255/257 ion ratios were within ± 5% of standard ion ratios.

Sampling variation was estimated by taking samples in triplicate on one occasion. The average α-HCH concentration and ER for these samples had relative standard deviations of 1.4% and 2.2%, respectively.

3.2.2 Enantiomeric Degradation in Arctic Streams

Table 3.1 and Figure 3.1 summarize ERs in Amituk Lake and the streams which were compared with water chemistry, temperature, discharges and α-HCH concentrations to determine where in the watershed degradation was occurring, the amount degraded, and factors affecting degradation. Complete data are included in Appendix A1.

ERs in Amituk Lake streams decreased from a racemic value of 1.01 ± 0.01 (n = 4) in snow to as low as 0.36 and 0.65 in Gorge and Cave Creeks, respectively, in August (Figure 3.1, series A), indicating that (+)-α-HCH is preferentially degraded. Similar values and trends were found by Falconer et al. (1995a) for the same streams but sampled over a shorter time in 1992. Concentrations of α-HCH peaked at 2330, 307, and 958 pg L^{-1} for Gorge, Mud, and Cave Creeks, respectively, at the beginning of snowmelt or during peak

Table 3.1: Median and range α-HCH concentrations and ERs, stream temperatures and discharge, and water chemistry parameters measured at Amituk Lake June to August, 1994.

Measured Parameter	Creeks			Lake			
	Gorge	Mud	Cave	3 m	20 m	40 m	Outflow
Enantiomer Ratio	0.72 0.36-1.00	0.71 0.64-0.88	0.74 0.60-0.92	0.76 0.73-0.90	0.74 0.73-0.77	0.72 0.66-0.74	0.81 0.75-0.90
α-HCH Conc. (pg L^{-1})	419 89-2330	119 20-307	529 293-958	644 583-944	520 469-598	688 342-727	851 514-1069
Temperature (°C)	3.0 0.0-4.0	6.8 2.0-10.0	1.5 0.0-2.0	2.4 1.7-3.7	2.7 2.4-3.7	2.8 2.4-3.7	-
Discharge (x 10^{-3} m^3 s^{-1})	177 24-2453	75 7-536	226 18-573	- -	- -	- -	961 284-3525
Ca^{2+} (mg L^{-1})	19.0 9.8-21.1	26.1 19.5-31.1	19.4 14.4-21.8	20.6 15.4-26.0	22.9 20.2-25.2	24.3 21.1-25.9	-
Mg^{2+} (mg L^{-1})	4.21 2.52-7.60	3.35 2.32-5.90	3.11 1.69-3.37	3.98 2.75-4.58	4.19 3.92-4.70	4.47 3.94-5.03	-
Conductivity (μS cm^{-1})	126 70-166	152 117-200	126 86-141	137 104-161	157 137-158	157 136-170	-
Alkalinity (meq L^{-1})	1.20 0.65-1.66	1.51 1.16-1.91	1.19 0.82-1.38	1.30 0.96-1.51	1.50 1.30-1.51	1.51 1.32-1.62	-
pH	8.18 7.81-8.27	8.20 8.04-8.44	8.12 8.02-8.28	8.24 8.16-8.33	8.25 8.20-8.34	8.21 8.09-8.32	-
DOC (mg L^{-1})	0.61 0.19-1.17	0.78 0.33-1.14	0.59 0.34-0.89	0.59 0.46-0.76	0.55 0.38-0.61	0.59 0.48-0.77	-
SS (mg L^{-1})	0.26 0.11-17.76	0.51 0.20-6.86	5.15 1.10-18.10	1.14 0.15-2.22	1.11 0.25-1.19	1.11 0.43-2.06	-
$N\text{-}NO_3$ (x 10^{-2} mg L^{-1})	4.1 0.8-8.0	2.4 1.2-12.8	2.2 1.8-3.1	2.1 1.4-2.8	2.2 1.6-2.8	2.1 0.8-8.4	-

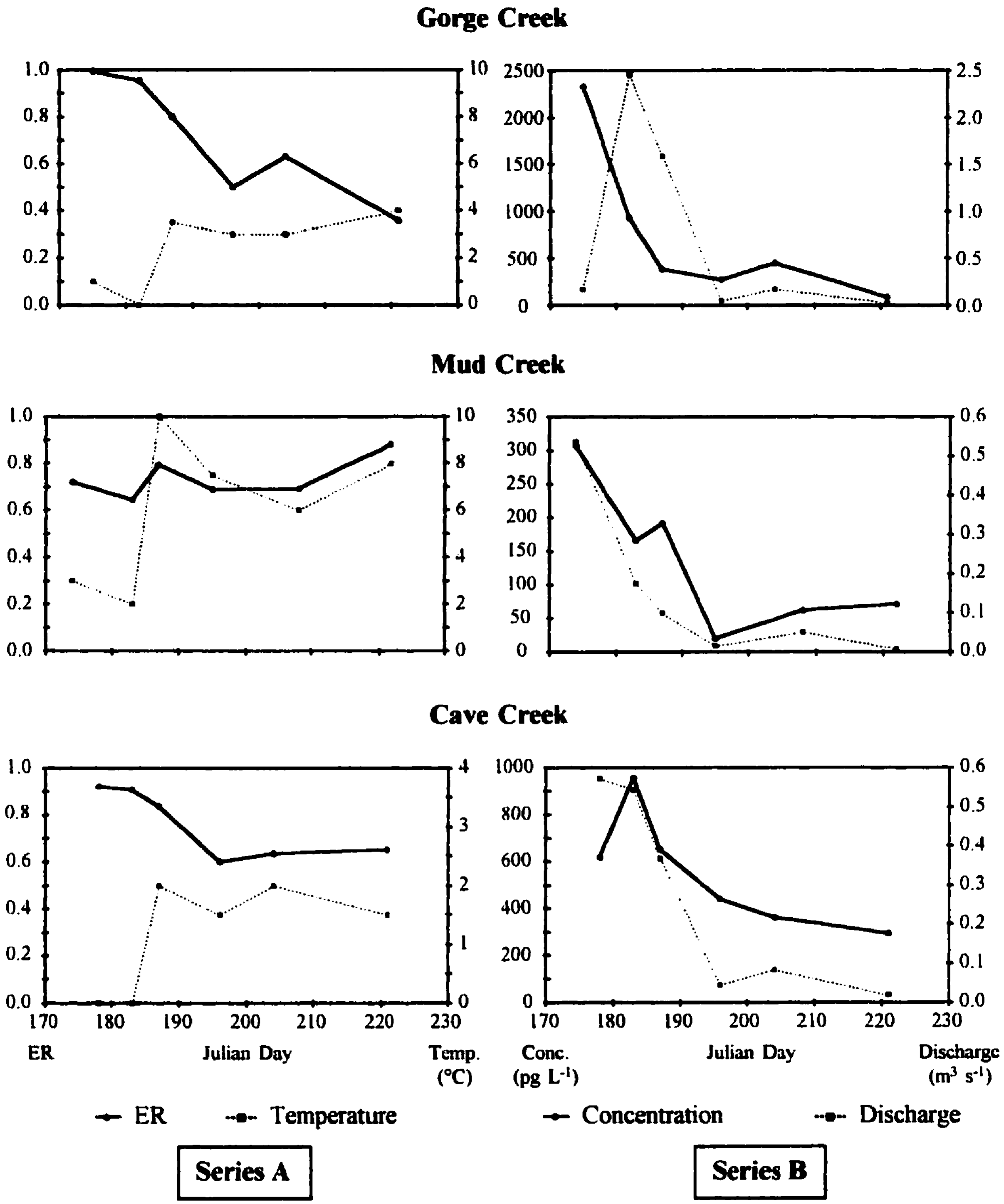

Figure 3.1: Summer 1994 trends of α-HCH ERs and stream temperatures (Series A) and α-HCH concentrations and stream discharges (Series B) for streams flowing into Amituk Lake

meltwater runoff and then declined to as low as 89, 20, and 293 pg L^{-1} in late summer (Figure 3.1, series B). Preferential elution of α-HCH from the snowpack has been reported (Semkin, 1996; Barrie et al., 1997) and is expected from model calculations (Wania, 1997). These concentrations are lower than 1992 values (Falconer et al., 1995a), reflecting declines in basin snowpack α-HCH burdens (Barrie et al., 1997), likely resulting from lower atmospheric concentrations (Li et al., 1998).

Stream discharges were highest in late June to early July and then rapidly declined to a level that was maintained through August (Figure 3.1, series B). This is typical of arctic hydrology in which snowmelt occurs rapidly (Woo et al., 1981) and stream flow is diminished in late summer but maintained by subsurface flow (Woo and Steer, 1983).

ERs were negatively correlated with stream temperature in Gorge and Cave Creeks (Figure 3.1, series A). Decreasing ERs with increasing temperatures were reported by Falconer et al. (1995a), and are consistent with enantioselective degradation by enzymatic pathways which are highly temperature sensitive. According to the "Q_{10} Rule", the rate of a biological reaction doubles for every 10 degree rise in temperature. The temperature increase in Gorge Creek was 3-4°C which might lead to a 24-33% increase in biodegradation rates. If only the (+)-α-HCH enantiomer degrades, an ER of 0.6-0.7 might be expected relative to those at lower temperatures, but the ER in Gorge Creek declined to 0.36. The increased rate of biodegradation associated with the 2°C temperature increase in Cave Creek also could not account for the ER decline. However, in Mud Creek, the ER changed less than expected by the 8°C increase. In addition, both the (+) and (-) enantiomers degrade but at different rates (Buser and Müller, 1995; Harner et al., in press), implying that changes in ERs expected from rate changes will be less than assumed here. Clearly, other factors in addition to stream temperature influence the rate of biodegradation and the use of the ER as a reliable indicator of the rate.

Since enantioselective degradation of α-HCH is biologically mediated (Buser and Müller, 1995; Faller et al., 1991a), ERs will be influenced by factors that favour microbial activity, such as nutrient availability and contaminant exposure to microbial populations. A linear correlation analysis between ERs and several water chemistry parameters that are indicators of such conditions showed statistically significant ($p < 0.05$) negative correlations with temperature, conductivity, Mg^{2+} and alkalinity for Gorge Creek (Table 3.2). Results for Cave and Mud Creeks are listed in Appendix A2. Chemical weathering parameters like conductivity, Ca^{2+}, Mg^{2+}, and alkalinity increase as stream flows decline (Semkin, 1996; unpubl.), as do stream volume to surface area ratios, thereby allowing greater contact between water and bed surfaces. Increasing temperatures throughout summer also deepen the active layer of basin slopes (Woo and Steer, 1982) and stream beds (Kinney, 1997), leading to greater contact between meltwater and stream substrates. In addition, after peak snowmelt, water from snowbanks typically flows over or through depressions and rills (Woo and Steer, 1982) that support the limited vegetation in the catchment, and likely provide substrates for microbial activity. Thus, the results suggest that enantioselective degradation is enhanced by the greater contact time between the chemical in the water and stream or slope substrates, the presumed site of microbial communities. Although changes in nutrient parameters such as dissolved organic carbon (DOC) and nitrate-nitrogen may be expected to impact enantioselective degradation, correlation coefficients between these and ERs were low since these parameters did not exhibit a summer trend.

To explore where along the streams degradation was occurring, Mud and Gorge Creeks were sampled at several sites on two dates in 1997 (Figure 3.2). Temperature differences, both between sites and between sampling dates, did not account for ER differences according to the "Q_{10} rule". Again, enhanced contact with substrates due to lower discharges may explain ER differences which are not accounted for by temperature effects. Although ERs may be expected to decline as stream waters approach the lake, this was not the case for Gorge Creek. ERs and concentrations were higher at the downstream sites (1 and 2) while stream temperatures were lower, suggesting that local site conditions control the observed ER. In the Gorge Creek basin there was a snow and ice-filled gorge near the downstream sites while upstream sites were devoid of snow and subject to groundwater flow entering the stream.

Declines of α-HCH ERs and concentrations with stream discharges indicate that stream hydrology is a major factor controlling the extent of α-HCH degradation in stream watersheds. To illustrate this, the amounts of α-HCH enantioselectively degraded in Mud, Gorge, and Cave Creek basins were estimated using ER measurements and frequent concentration measurements (Semkin, unpubl.). Daily concentrations and ERs were estimated by fitting polynomial curves to measured data, then daily α-HCH loadings (mg)

Table 3.2: Correlation coefficients (r^2) for α-HCH ERs and concentrations, and stream discharge, temperature, and water chemistry parameters for Gorge Creek in 1994.

Parameter	ER	Conc.	Discharge	Temp.	SS	Cond.	Ca^{2+}	Mg^{2+}	Alkal.	NO_3-N	DOC
ER	1.00										
Concentration	0.61	1.00									
Discharge	0.35	0.00	1.00								
Temperature	***0.67***	0.50	0.29	1.00							
Suspend. Sed.	0.32	***0.90***	0.07	0.21	1.00						
Conductivity	***0.73***	0.16	***0.79***	0.44	0.02	1.00					
Ca^{2+}	0.51	0.03	***0.95***	0.32	0.01	***0.92***	1.00				
Mg^{2+}	***0.84***	0.32	0.53	0.50	0.12	***0.92***	***0.71***	1.00			
Alkalinity	***0.80***	0.23	***0.72***	0.50	0.06	***0.99***	***0.88***	***0.94***	1.00		
NO_3-N	0.41	0.06	0.56	0.25	0.00	***0.79***	***0.69***	***0.80***	***0.76***	1.00	
DOC	0.22	0.59	0.02	0.11	***0.65***	0.01	0.00	0.02	0.03	0.04	1.00

Bold italicized type - significant to $p < 0.05$

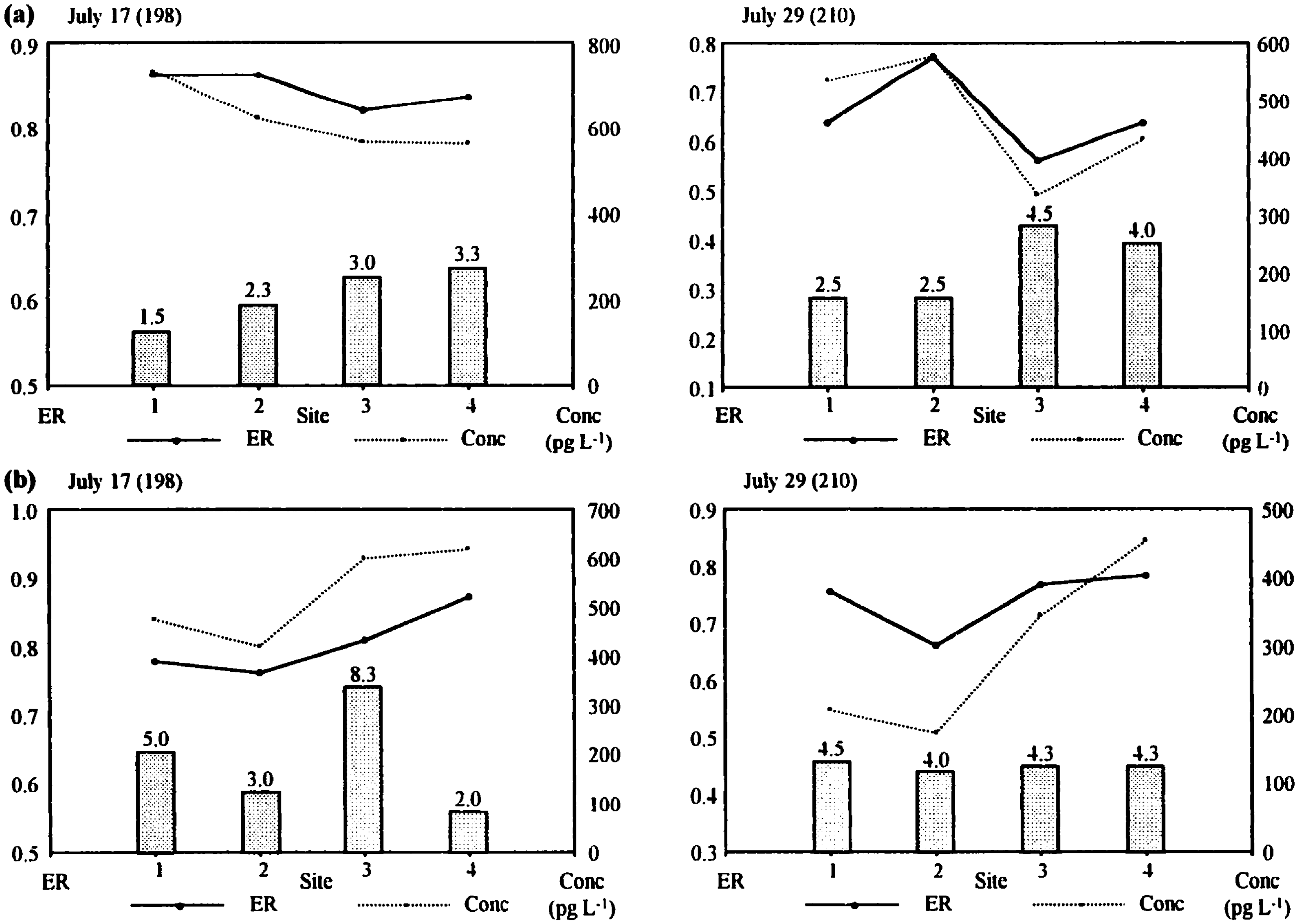

Figure 3.2: 1997 α-HCH ERs, concentrations and stream temperatures (bars) for (a) Gorge and (b) Mud Creeks (Site 1 is downstream, Site 4 is upstream; see Fig. 1.1(a) (p. 4) for site locations)

were calculated using measured daily stream discharges and the estimated concentrations. α-HCH concentration prediction equations are discussed further in Chapter 4. ER prediction equations are listed in Appendix A3. The amount enantioselectively degraded (N_{deg}) was estimated by:

$$N_{\mathrm{deg}} = [\ X_{\alpha\text{-HCH}} / (\mathrm{ER} + 1)\ ] - [\ \mathrm{ER} \cdot X_{\alpha\text{-HCH}} / (\mathrm{ER} + 1)\ ] \qquad (1)$$

where $X_{\alpha\text{-HCH}}$ is total α-HCH loadings (mg) and ER is the (+)/(-)-α-HCH enantiomer ratio. The derivation of equation (1) is detailed in Appendix A3 and assumes that only the (+) enantiomer degrades. This calculation represents a minimum estimate since it does not account for enantioselective degradation which may affect both enantiomers but at different rates (Buser and Müller, 1995; Harner et al., in press), or possible non-enantioselective microbial degradation. Measured stream discharges and predicted and measured α-HCH ERs and concentrations, along with estimated amounts degraded, are presented in Appendix A3. For Gorge Creek, enantioselective degradation was estimated at 164 mg, representing a loss of 6% of total α-HCH entering the lake. Only 38 mg or 23% of this amount was degraded after mid-July when ERs were much lower. The amounts enantioselectively degraded in Mud and Cave creeks were 25 mg (13%) and 52 mg (8%), respectively, and of these amounts, 2% and 26% were degraded after mid-July. Combined, approximately 7% of total α-HCH was enantioselectively degraded prior to entering Amituk Lake. Thus, although ERs and α-HCH loadings are high during peak melt, the relative amount of α-HCH enantioselectively degraded during this period is greater than later in summer when ERs are lower. In comparison, rates of base hydrolysis of α-HCH (Ngabe et al., 1993) calculated using extreme pH and temperature values for Gorge, Mud, and Cave Creeks (Table 3.1) could account for < 1% of α-HCH degradation in Gorge and Cave creeks, and ~2% in Mud Creek where temperatures reached 10°C.

To extend these observations and to further examine factors affecting enantioselective degradation in streams, the inlet streams of Char and Meretta Lakes were sampled (Figure 1.1 (b), Ch. 1). Char and Amituk Lakes are oligotrophic, similar to Amituk Lake, while Meretta Lake is nutrient-enriched due to past sewage inputs. ERs in streams entering Char Lake (Figure 3.3) were similar to those of Amituk Lake, decreasing with increasing stream temperatures and over time as stream discharges declined. ERs of streams 1 and 2 of Meretta Lake (Figure 3.4) ranged from 0.42 to 0.54 versus 0.73 to 0.81, respectively, despite no differences in stream temperatures. The stream 1 basin contains an abandoned sewage lagoon and has moss and algae laden stream beds that likely support an abundant microbial community.

The influence of microbially-rich substrates was further investigated by sampling a wetland near the North Base on July 26, 1997. Wetlands are fed by surface and subsurface flows and are biologically productive areas supporting mosses and vascular plants (Woo and Young, 1998). α-HCH ERs were 0.85 in the wetland inflow, 0.69 in a standing pool within the wetland, and 0.63 in the outflow. Concentrations at each of these locations were 433, 285 and 175 pg L^{-1}, respectively. Both ERs and concentrations declined while passing through the wetland, although water temperatures increased only slightly from 10.0 to 11.8°C, confirming the importance of biologically productive substrates and sufficient contact time between substrate and chemical. The effect of the temperature increase on enantioselective degradation rates would not account for the ER decline, and the decrease in α-HCH concentrations are greater than would be expected from the ER alone. Other processes such as volatilization, uptake or sorption by mosses and/or sediments, hydrolysis and non-enantioselective microbial degradation will affect the α-HCH concentration along the ~300 m flowpath of the wetland.

3.2.3 α-HCH Enantiomers in Arctic Lakes

The results presented above clearly demonstrate that enantioselective degradation occurs in small streams and wetlands within arctic watersheds. However, it is unclear whether enantioselective degradation occurs within lakes and if so, what its importance might be relative to that in streams. To examine within-lake degradation, ERs were measured at three depths and the outflow of Amituk Lake throughout summer 1994, and from Char and Meretta Lakes in 1997. An understanding of arctic lake hydrology and limnology, discussed in the previous chapter (S. 2.2), is important as such factors influence contaminant fate and dynamics (Schindler et al., 1995; Freitas et al., 1997).

The range and median values of α-HCH ERs and concentrations for three depths and the outflow of Amituk Lake are listed in Table 3.1. Figure 3.5 illustrates ERs at 3, 20 and

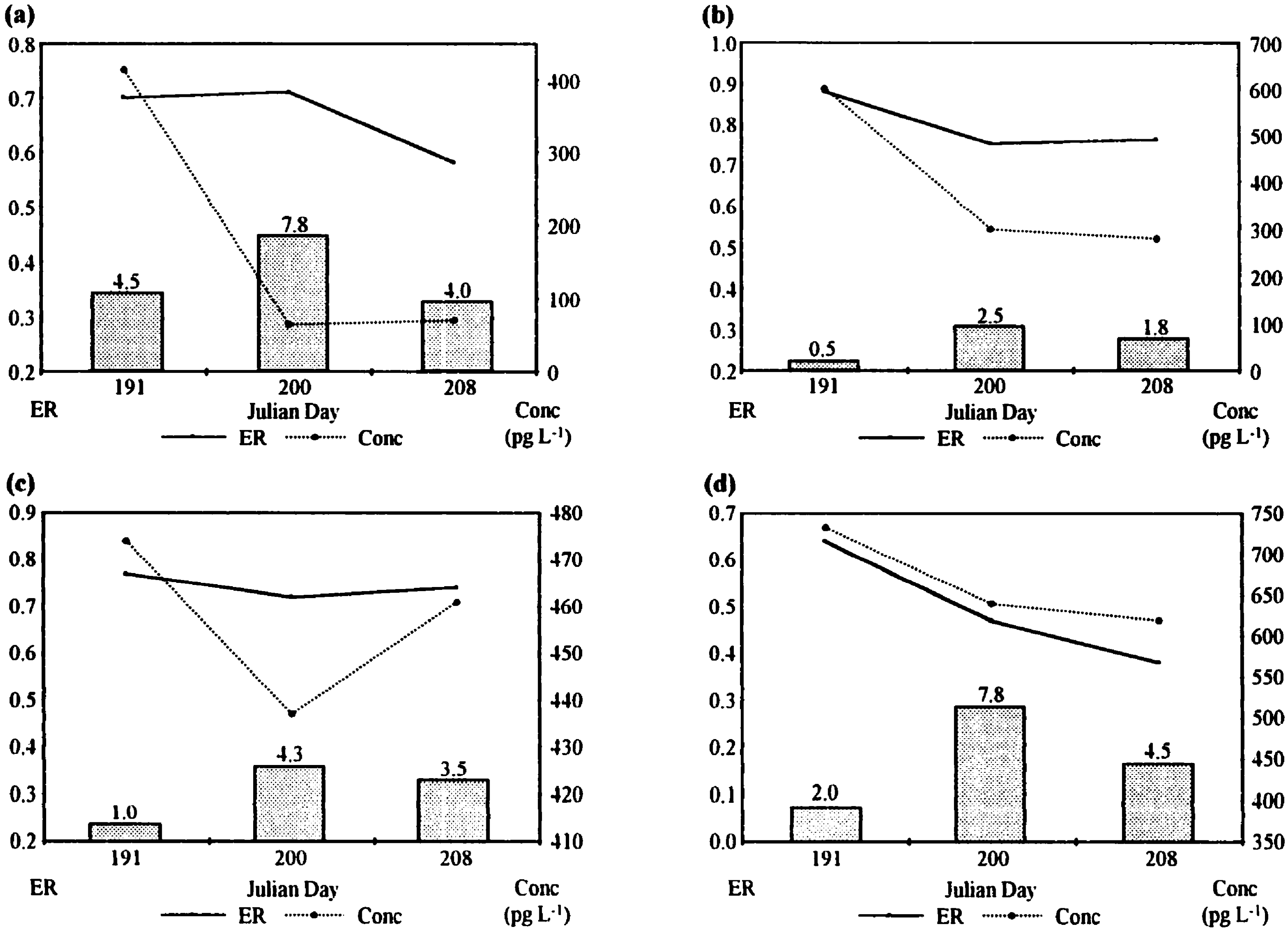

Figure 3.3: 1997 α-HCH ERs, concentrations and stream temperatures (bars) for (a) Inlet 1, (b) Inlet 2, (c) Inlet 3, and (d) Inlet 4 of Char Lake (see Fig. 1.1(b) (p. 4) for sampling locations)

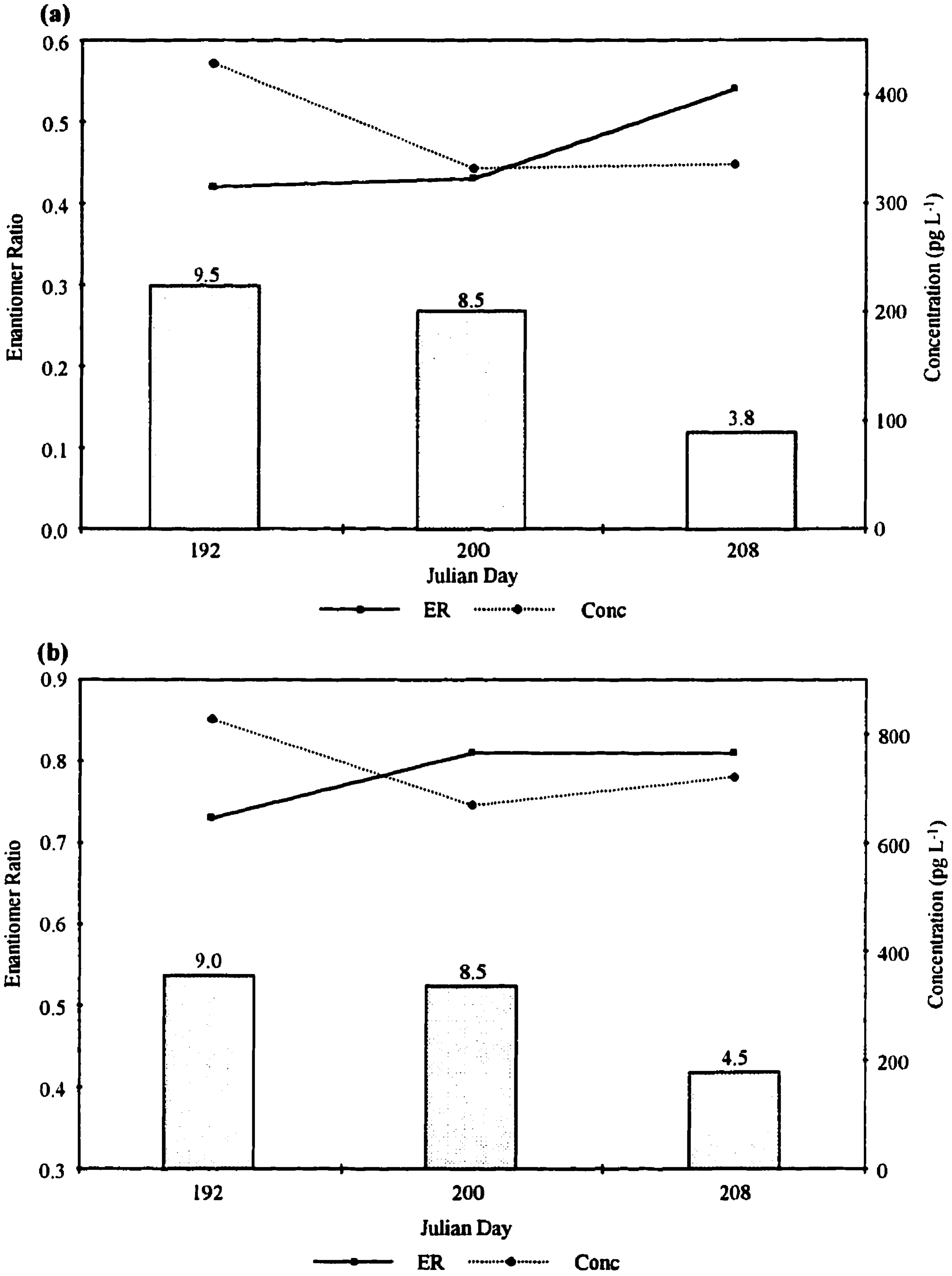

Figure 3.4: 1997 α-HCH ERs and concentrations and stream temperatures (bars) for (a) Inlet 1 and (b) Inlet 2 of Meretta Lake (see Fig. 1.1(b) (p. 4) for sampling locations)

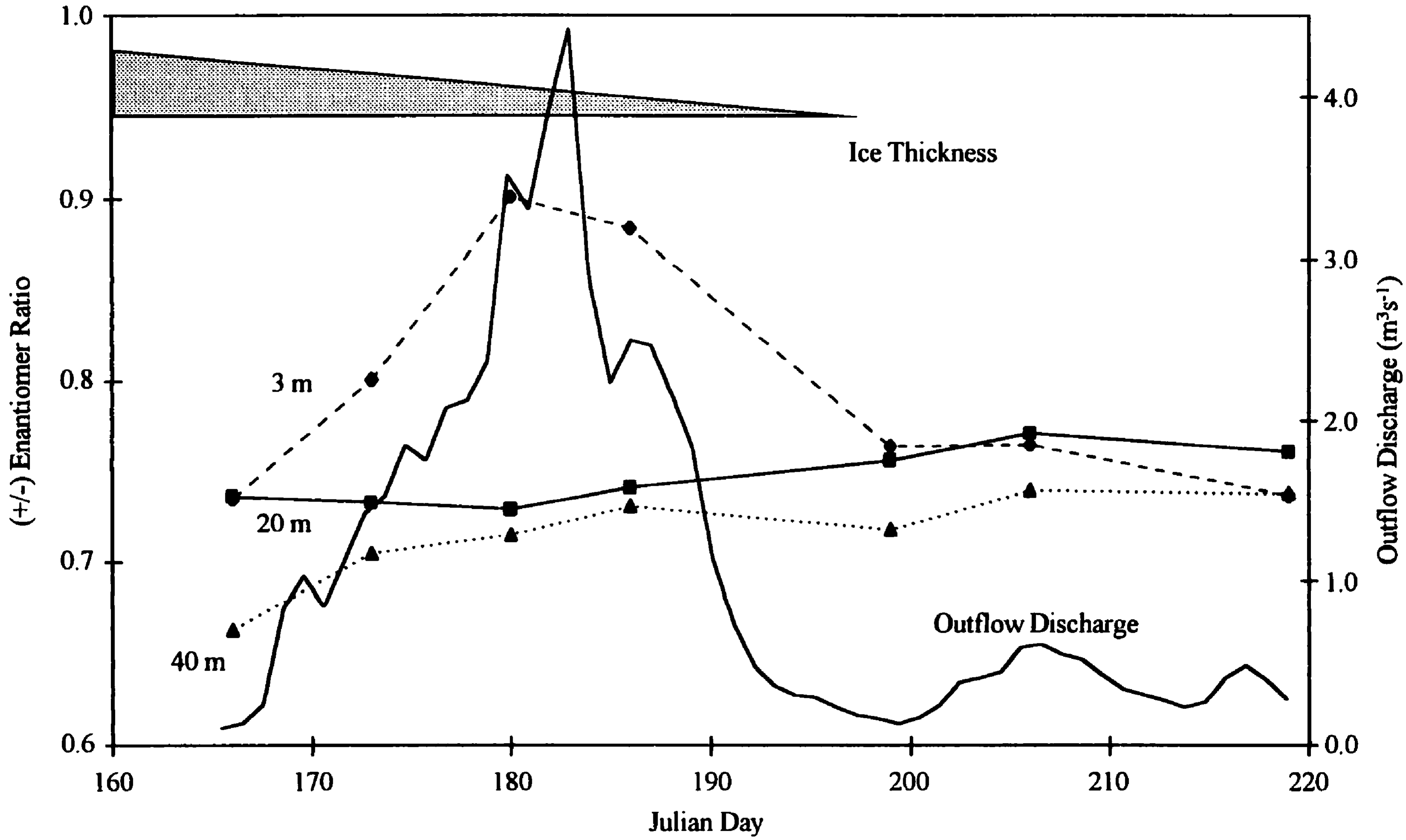

Figure 3.5: Summer 1994 trends for α-HCH ERs at 3, 20 and 40 m depths of Amituk Lake, representative ice thickness from 2.2 m on day 166 to ice-off on or about day 199, and lake outflow discharge over the sampling period

40 m depths from June 15 to August 7, 1994 (Julian Day 166 to 219), along with the outflow daily discharge hydrograph and a graphical representation of ice cover varying from 2.2 m thickness on June 15 to ice-off on ~July 18.

The ERs measured at 3 m reflect hydrological events occurring in the lake. Prior to snowmelt the ER was 0.73, the same as in the bulk water column represented by the 20 m measurement. ERs quickly increased to 0.80-0.90 as stream inputs peaked, then declined to 0.76 in mid-July, similar to values found at other depths following lake turnover. α-HCH concentrations followed an identical trend, increasing from 644 to 944 pg L^{-1} before declining to near 600 pg L^{-1} by mid-July, which again was representative of the bulk water column.

ERs at 20 m increased from 0.73 to 0.77 over June to late July while concentrations increased from 469-499 to 598 pg L^{-1} from June to early August. These increases coincided with lake turnover after ice-off when water from the upper layer, having elevated α-HCH concentrations and ERs, mixed with deeper waters.

A similar trend occurred at 40 m, with ERs increasing from 0.66 to 0.74 between June and early August, while α-HCH concentrations increased from 342 to near 700 pg L^{-1}. The lowest ER and concentration was recorded on June 15 and reflects over-winter lake conditions when water at 40 m remains in close proximity to the sediments due to limited mixing under the ice (Welch and Bergmann, 1985; Welch, 1991). The sediments are a likely substrate for microbial activity, and the lower ER and α-HCH concentration at this depth may reflect α-HCH depletion by microbial degradation.

The outflow integrates runoff and within-lake processes, similarly to waters at 3 m depth, and thus their ER and concentration trends were virtually identical. The slightly higher outflow concentrations may reflect snowmelt loadings, whereas the 3 m depth is more influenced by water free of α-HCH (Bergmann and Welch, 1985). ERs were highest during peak discharge when the lake was still ice covered and most of the inflowing water passed over or around the ice sheet. Comparison of volume-weighted ERs in the inflow with those at 3 m depth and in the outflow, indicated that 80-100% of outflow and 3 m waters was comprised of inflow water during peak snowmelt, with lake water comprising the remainder. At ice-off in mid-July, the water column mixed, and ERs and concentrations at all depths and in the outflow approached similar values.

The occurrence of enantioselective degradation within Amituk Lake itself is difficult to determine since patterns in the lake reflect both within-lake and watershed processes. Measured ERs (0.73-0.77) indicate that approximately 25% of (+)-α-HCH is depleted relative to (-)-α-HCH in the lake. To examine the relative importance of within-lake versus watershed processes, within-lake degradation was estimated and comparisons were made of year-to-year ERs in Amituk Lake and ERs in nearby Char and Meretta Lakes.

The lower ERs at 20 and 40 m before ice-off than after summer suggest that degradation occurs within the lake over the long winter when there are no inputs of α-HCH. Fresh spring inputs then cause ERs and concentrations to increase over the summer. An upper limit may be placed on the extent of over-winter degradation by considering the α-HCH inventory in Amituk Lake in 1993 and at the beginning of the 1994 melt. The estimated 1993 inventory was 6977 mg based on average concentrations at 3 and 20 m for the last four summer measurements and lake volumes of 1.74×10^6 m^3 for 0-5 m depth and 5.60×10^6 m^3 for 5-41 m depth (Semkin et al., unpubl.). The inventory on June 15, 1994 was estimated to be 3346 mg using measured concentrations (Figure 3.5) and water volumes of 9.74×10^5 m^3, 5.13×10^6 m^3, and 4.68×10^5 m^3 at 3, 20, and 40 m depths, respectively. Assuming no atmospheric inputs or volatilization losses during ice cover and minimal sedimentation (Freitas et al., 1997), degradation within the lake could account for the change in lake inventory from August 1993 to June 1994. Degradation was assumed to be first order such that:

$$C = C_o \exp[-(k_\alpha + k_h)t] \qquad (2)$$

where C and C_o are the lake α-HCH inventories on June 15, 1994 and end of summer, 1993, respectively, t is the over-winter time of 308 days from August 10, 1993 to June 15, 1993, k_α is the rate of microbial degradation and k_h is the rate of hydrolysis. The hydrolysis rate in the lake at pH 8.2 and 2°C would be 0.022 y^{-1} ($t_{1/2}$=32 y) (Ngabe et al., 1993) and could account for approximately 128 mg or 2% of α-HCH loss. The remaining loss of 3500 mg or 50% would then be attributable to microbial degradation with a first order rate constant of 0.85 y^{-1} ($t_{1/2}$=0.82 y). This value is approximately a factor of six greater than the combined microbial degradation rates for (+)- and (-)-α-HCH ($k_{m+} + k_{m-}$) of 0.147 y^{-1} reported for the

Eastern Arctic Ocean (Harner et al., in press). Using the 1992 lake α-HCH inventory of 14 401 mg calculated from a summer average of 1963 pg L^{-1} and a June 1993 inventory of 8315 mg (Semkin et al., unpubl.), the microbial degradation rate (k_α) was estimated to be 0.67 y^{-1} or $t_{1/2}$=1.0 y. Depending upon the average concentrations chosen to calculate α-HCH inventories in 1992 and 1993, the estimated microbial degradation rate may vary between 0.67 y^{-1} and 0.85 y^{-1}. Considerable variation in lake concentration measurements result in wide variation in estimated degradation rates.

Although ER values from 1993 were not measured, it is possible to estimate the extent of enantioselective degradation within the lake over winter by assuming the 1992 average lake ER of 0.77 (Falconer et al., 1995a). In addition, assuming that the sum of the microbial degradation rates of (+)-α-HCH ($k_{\alpha+}$) and (-)-α-HCH ($k_{\alpha-}$) totals the overall estimated degradation rate of 0.85 y^{-1}, and that $k_{\alpha+}$ is three times greater than $k_{\alpha-}$ as found by Buser and Müller (1995), then the expected ER in 1994 should be 0.54 (calculation in Appendix A3). An even lower ER would be expected if $k_{\alpha+}$ was four times greater than $k_{\alpha-}$ as found in the Eastern Arctic Ocean (Harner et al., in press). However, such low ERs were not observed in Amituk Lake, indicating that the loss of 50% of the lake's inventory of α-HCH is not due solely to enantioselective degradation but largely influenced by non-enantioselective microbial degradation. Alternatively, the relative rates of (+)-α-HCH and (-)-α-HCH may differ only slightly.

Concentrations of (+)-α-HCH and (-)-α-HCH predicted from the ERs for each stream as described above were incorporated into an unsteady-state mass balance model for Amituk Lake (Ch. 5, S. 5.2). Figure 3.6 shows predicted and measured lake ERs and combined inflow ERs for summer 1994. The model, which accounts for mixing, ice cover, precipitation and inflow loading changes over the summer months, demonstrates that inflowing α-HCH with high ERs during peak melt result in a slight increase in lake ERs near ice-off. (+)-α-HCH and (-)-α-HCH degradation rates were estimated from 1993 and 1994 inventories described previously and assuming a 1993 lake ER of 0.77. Including these values and extending the model over winter 1994-95 revealed only a small ER decline to 0.75 by the following June, again suggesting that within-lake degradation occurs mostly by non-enantioselective microbial degradation.

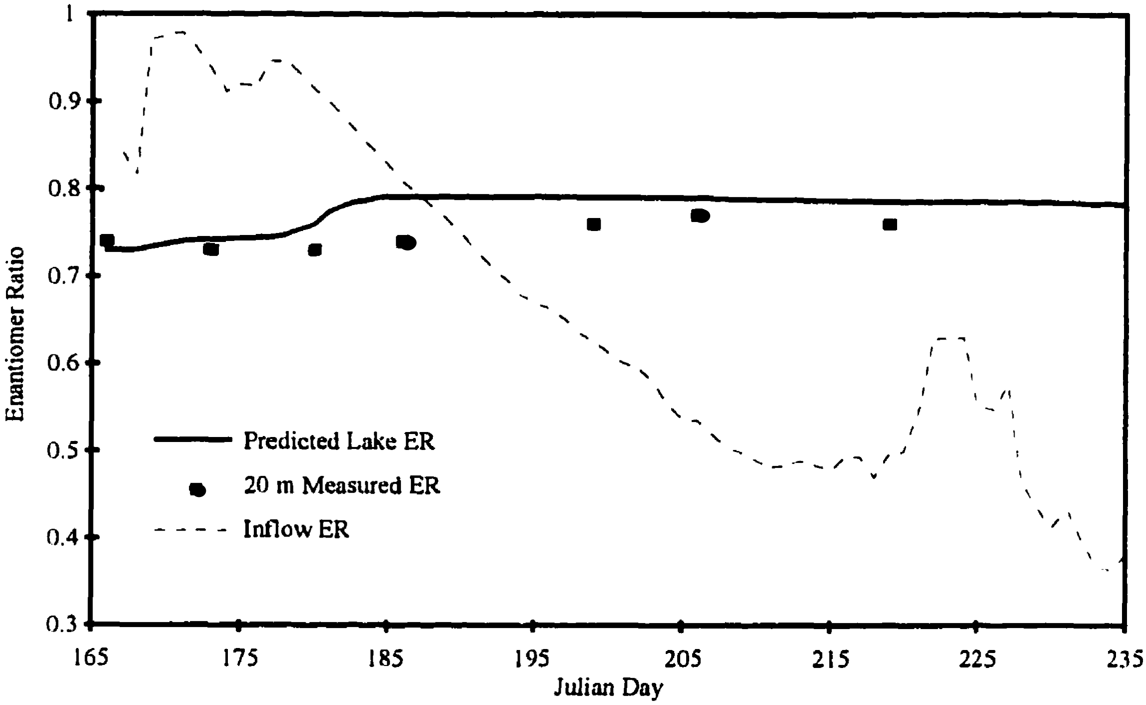

Figure 3.6: Measured and predicted a-HCH enantiomer ratios from the unsteady-state Amituk Lake mass balance model

Comparison of 1992 and 1994 Amituk Lake ERs provides further evidence of within-lake degradation. ERs of samples taken at 15-21 m prior to ice-off in 1992 averaged 0.77 ± 0.01 (n=4, Falconer et al., 1995a) and were found to be significantly higher ($p < 0.001$) than the 1994 average of 0.73 ± 0.01 (n=4) at 20 m in late June and early July. Concentrations at this depth averaged 2100 ± 800 pg L^{-1} in 1992 (Falconer et al., 1995a), which were 3-4 times higher than 1994 values. The lower 1994 average ER may indicate slow microbial enantioselective degradation of α-HCH within the lake as α-HCH loadings decline over time and contribute less undegraded α-HCH to the lake.

Samples were collected from Char and Meretta Lakes near Resolute to provide ERs from lakes of contrasting characteristics (Table 3.3). Phytoplankton production (Kalff and Welch, 1974) and bacterial numbers (Morgan and Kalff, 1972) have been much greater in Meretta Lake than in Char Lake due to past nutrient inputs. Such differences in biological activity may be expected to affect ERs. Char Lake ERs at 10 m depth ranged from 0.62 to 0.69 while Meretta Lake ERs at 5 m ranged from 0.84 to 0.89, and α-HCH concentrations in

Table 3.3: α-HCH ERs and concentrations and water temperatures measured in Char and Meretta Lakes, 1997

Site / Date	ER	Concentration (pg L^{-1})	Temperature (°C)
Char Lake			
July 10	0.65	1021	2.5
July 19	0.62	977	3.5
July 27	0.69	839	-
Meretta Lake			
July 11	0.84	1264	3.5
July 19	0.90	1205	-
July 27	-	-	-

the two lakes were similar. Enhanced enantioselective degradation was not found in the more productive lake, probably because of differences in water residence times between Char and Meretta Lakes.

Char Lake has a water renewal time of 9-14 years (Schindler et al., 1974a), while the estimated water residence time in Amituk Lake is ~3 years assuming half the inflow water mixes with the water column (Freitas et al., 1997). Meretta Lake water residence time is likely shorter than 3 years due to its relatively small volume and shallow bathymetry. Average ERs are 0.65, 0.75, and 0.88 for Char, Amituk, and Meretta Lakes, respectively. Alaee (1997b) found that Atlin Lake in the Yukon River Basin, with a water residence time of 18.3 years, had ERs ranging from 0.24-0.37. Alaee suggested that longer residence times allow greater within-lake enantioselective degradation and the hypothesis is supported by the observed ERs for lakes on Cornwallis Island.

3.3 Summary

The extent of degradation of α-HCH in arctic watersheds was estimated from ER and concentration measurements in Amituk Lake and its associated streams. Approximately 7% of the total α-HCH entering the lake via inlet streams was degraded enantioselectively. This value represents the lower limit of the total amount of α-HCH which is microbially degraded. Degradation within streams was influenced by contact time with substrates supporting microbial populations, stream temperature, and biological activity. Within

Amituk Lake, the variation of ERs at different depths throughout the summer reflect basin hydrology, particularly at 3 m depth which largely consisted of inflow water. Depleted α-HCH concentrations and ERs at 40 m depth prior to snowmelt indicates limited mixing and over-winter degradation at the sediment-water interface. The α-HCH inventory in the lake declined over-winter from 1993 to 1994. Approximately 2% of this loss was attributed to hydrolysis, while the remainder resulted largely by non-enantioselective microbial degradation or by enantioselective degradation with similar rate constants for each of the enantiomers. An overall degradation rate of 0.80 y^{-1} was estimated for α-HCH in Amituk Lake. Although ERs in Amituk Lake were largely due to input of degraded α-HCH from the watershed, in general, observed ERs in arctic lakes may be influenced by lake residence times.

4. Multimedia Modeling of Contaminant Fate

Discussions of contaminant fate in the environment examine the behaviour of chemicals within various environmental compartments or media. Concentrations, persistence, accumulation and reactivity within these compartments, and the partitioning behaviour between compartments for particular compounds constitute their multimedia environmental fate. The concept of a multimedia environment has been popularized in books by Cohen (1986) and Mackay (1991).

Multimedia modeling can be a qualitative and quantitative exercise, describing the behaviour of chemicals and their levels, respectively, in the environment. The models developed and applied to arctic lakes are based on the fugacity approach to multimedia modeling (Mackay, 1991).

4.1 Fugacity Approach

The use of the thermodynamic concept of fugacity in environmental modeling was developed by Mackay and coworkers (1981, 1982; Paterson and Mackay, 1985; Mackay, 1991). Descriptions of contaminant fate involve the movement of chemicals among phases or environmental compartments. This movement is governed by the second law of thermodynamics which states that entropy of the system always increases. Between phases, entropy is maximized at equilibrium, or when the chemical potential of a compound in one phase is equal to the chemical potential of that compound in an adjoining phase. The use of chemical potential as an equilibrium criterion is inconvenient since it is logarithmically related to concentration and difficult to determine as it can only be measured relative to a reference compound.

Fugacity was introduced in 1901 by G.N. Lewis as an equilibrium criterion that was easier to use than chemical potential. Fugacity is related logarithmically to chemical potential but linearly to concentration, and is defined as the "escaping tendency" of a compound from a particular phase or environmental compartment. It has dimensions of pressure and is related to partial pressure by a fugacity coefficient that approaches 1 under ideal conditions for ideal gases. Equilibrium between phases occurs when the fugacities of each phase are identical.

Fugacity (f) is related to a chemical concentration (C) within a phase by the expression:

$C = Z \cdot f$ (1)

where C is in mol/m^3, f is in Pa, and Z is the “fugacity capacity”, a proportionality constant, with dimensions of mol/m$^3 \cdot$Pa. The modeling approach uses calulated values of Z for various compartments, along with system-specific properties, to determine rates of chemical movement, or D values, by advective flows, diffusion, or transformation mechanisms. These values are then used in mass balance equations to determine fugacities for each compartment (f_i), from which chemical concentrations in phase i (C_i) are calculated (Mackay, 1991).

4.1.1 Z-values

The Z-value is a measure of the capacity of a phase for a particular chemical. Environmental media with high Z-values for a particular chemical have a greater capacity to absorb that compound, and chemical will have a tendency to partition into such a phase. Temperature-specific Z-values are calculated from the phsyico-chemical properties of the compound of interest, or partition coefficients, and from phase characteristics. Equations for calculating Z-values for organic compounds in the following compartments are:

Air: $Z_A = 1 / RT$ (2)

Water: $Z_W = 1 / H$ or C^S / P^S (3)

Sediment: $Z_S = f_{OC} \cdot 0.41 \cdot K_{OW} \cdot \rho_S / H$ (4)

where R is the gas constant (8.314 Pa$\cdot$m^3/mol$\cdot$K), T is ambient phase temperature (K), H is Henry’s law constant (Pa$\cdot$m^3/mol), and C^S, P^S and K_{OW} are the solubility in water, vapour pressure, and octanol-water partition coefficient of the chemical, respectively. f_{OC} is the fraction of organic carbon in the phase and $\breve{r}_S$ is the density of the phase (Mackay, 1991).

4.1.2 Aquivalence

The aquivalence approach (Mackay and Diamond, 1989) to environmental modeling was developed for chemicals with low or zero vapour pressures such as metal ions, inorganic minerals, or polymers. Calculating Z-values for compartments other than air using negligible vapour pressures would result in phase capacities approaching infinity, or fugacities approaching zero.

The aquivalence approach compensates for this problem by dividing the fugacity expressions for each phase by P^S/C^S:

$$f = C_A / Z_A = C_W / Z_W = C_S / Z_S \tag{5}$$

giving:

$$f \cdot C^S / P^S = Q = C_A RT \cdot C^S / P^S = C_W = C_S \cdot K_{SW} \tag{6}$$

where Q is a new equilibrium criterion equal to the water concentration, or aquivalence, with units of mol/m^3 (Mackay and Diamond, 1989). The Z-values listed in equations 2 to 4 now become dimensionless and are redefined as:

Air: $\underline{Z}_A = H / RT$ (7)

Water: $\underline{Z}_W = 1.0$ (8)

Sediment: $\underline{Z}_S = f_{OC} \cdot 0.41 \cdot K_{OW} \cdot \rho_S$ (9)

Concentrations are calculated as the product of Q_i and $\underline{Z}_i$.

4.1.3 D-values

In environmental systems, there are numerous processes at work that usually prevent compartments from attaining equilibrium with each other. Chemicals may move into and out of defined systems by advective processes like river flow or with air currents. Bidirectional diffusive exchange of chemicals across compartment interfaces usually occurs, e.g. between air and water, and sediment and water. Degradation processes may also reduce or transform the chemical in air, water, sediment, or soil.

These processes can be parameterized as rates or fluxes using either the fugacity (Mackay, 1991) or the aquivalence (Mackay and Diamond, 1989) approach. In the fugacity approach, the flux, R is given as:

$$R = Df \tag{10}$$

and has units of mol/h. In the aquivalence format, R is defined as:

$$R = DQ \tag{11}$$

while the units for D change from mol/h·Pa in fugacity form to m^3/h in aquivalence form.

Using either fugacity or aquivalence approaches, D-values can be defined for each of advective, diffusive, and transformation processes. Advective processes include sediment deposition or resuspension, wet and dry atmospheric deposition, and movement according to current velocities. D-values for these processes have the form:

$$D = GZ \qquad (12)$$

where G is the flow or deposition rate for the particular medium in m^3/h. The Z-value used is for the phase of origin; Z_S for sediment resuspension and Z_W for river inputs are examples.

Diffusive transport of chemicals across compartment interfaces is expressed by:

$$D = KAZ \qquad (13)$$

where K is the mass transfer coefficient for the compound of interest with units of m/h and A is the interfacial area of the adjoining compartments in m^2.

Chemical compounds may undergo degradative processes such as microbial or hydrolytic transformation in lake water or sediments. First order rate kinetics are assumed and the D-value is defined as:

$$D = kVZ \qquad (14)$$

where k is the reaction rate constant in h^{-1}, V is the compartment volume in m^3, and the Z-value is for the compartment in which the transformation occurs.

Calculating fluxes for each process using equation 10 or 11 provides an estimate of the amount of contaminant moving into or out of a particular compartment. Individual D-values may be compared to determine the relative importance of removal mechanisms within a particular compartment.

4.1.4 QWASI Model

The Quantitative Water Air Sediment Interaction (QWASI) model was developed by Mackay et al., (1983) and is detailed in Mackay (1991). The model combines transport processes into and out of the air, water, and soil compartments of water bodies that are parameterized by D-values as described above and listed in Mackay (1991). Equilibrium within compartments is assumed, that is, contaminants associated with suspended particles in the water column or with aerosols in the air are in equilibrium with contaminants in the surrounding water or air, respectively.

Parameters are assembled into mass balance expressions for the water (w) and sediment (s) compartments which are listed in aquivalence form using D-values as defined in Mackay (1991):

$$\partial V_W \underline{Z}_{BW} Q_W / \partial t = Q_A (D_M + D_Q + D_C + D_V) + Q_I(D_I + D_X) + Q_S(D_R + D_T) - Q_W(D_V + D_J + D_Y + D_D + D_T + D_W) \qquad (15)$$

$$\partial V_S \underline{Z}_{BS} Q_S / \partial t = Q_W(D_D + D_T) - Q_S(D_R + D_T + D_B + D_S) \qquad (16)$$

where $\underline{Z}_{BW}$ and $\underline{Z}_{BS}$ are the fugacity capacities of the bulk water and sediment phases, and inflow (Q_I) and air (Q_A) aquivalences are calculated from measurements and transport D-values are determined as described by Mackay (1991). Under steady-state conditions water (Q_W) and sediment (Q_S) aquivalences are obtained by setting the derivatives equal to zero, while the derivatives are solved for unsteady-state, time dependent circumstances.

4.2 Amituk Lake Models

Mass balance models using the aquivalence form have been developed for high arctic lakes by Freitas and co-workers (1994, 1997) and applied to Amituk and Char Lakes on Cornwallis Island, NT. Aquivalence-based models may be extended to include inorganic compounds and are thus more flexible than fugacity-based models. Contaminant loadings data were obtained for Amituk Lake in 1992 in the first year of a three year study of contaminant processes and fluxes in arctic aquatic systems (Semkin and Gregor, 1993; Semkin, 1996; Barrie et al., 1997). In the current study, this model was updated and modified and applied to Amituk Lake using contaminant loadings from the successive years of the Amituk Lake study, 1993 and 1994. The following sections briefly describes the steady-state and time-dependent versions of the model and lists the lake characteristics, chemical loadings and physico-chemical properties incorporated into the model.

4.2.1 Model Description

A mass balance aquivalence-based QWASI model developed and described by Freitas et al. (1994, 1997) for arctic lakes was modified and updated to consider contaminant fate processes and multi-year contaminant trends in Amituk Lake. Table 4.1 lists process, rate and concentration expressions used in the Amituk Lake model. Transport parameters (D-values) were calculated as described by Mackay (1991) from chemical- and lake-specific information presented in following sections. Air (Q_A) and inflow (Q_{IN}) aquivalences were calculated from measured concentrations. Water (Q_W) and sediment (Q_S) aquivalences were solved by substituting the calculated D-values and specified aquivalences into equations 15 and 16 presented above. Steady-state and unsteady-state, time-dependent solutions were obtained for a suite of organochlorine contaminants present in the Canadian Arctic. Concentrations in the water column and sediment bed were then calculated from their respective Z-values and Q_W and Q_S aquivalences. Model calculations were carried out using programs written in C++ (Borland, v. 4.5).

Table 4.1: Process, rate and concentration parameters and expressions incorporated into the Amituk Lake models

Process	D-values (m^3 h^{-1})	Rates (mol h^{-1})
Volatilization	Dwa = kow * Aw * Zw	Rwa = Dwa * Q_A
Adsorption	Daw = kow * Aw * Zw	Raw = Daw * Q_A
Wet Deposition	Dwd = Gwd * Zq	Rwd = Dwd * Q_A
Dry Deposition	Ddd = Gdd * Zq	Rdd = Ddd * Q_A
Rain Dissolution	Drn = Grn * Zw	Rrn = Drn * Q_A
Water Inflow	Dwi = Gawi * Zw	Rwi = Dwi * Q_{IN}
Particle Inflow	Dpi = Gip * Zip	Rpi = Dpi * Q_{IN}
Water Outflow	Dwo = Gawo * Zw	Rwo = Dwo * Q_W
Particle Outflow	Dpo = Gop * Zwcp	Rpo = Dpo * Q_W
Water Transformation	Dwt = Vw * ZwB * 0.693 / tw	Rwt = Dwt * Q_W
Sediment Burial	Dbr = Gbr * Zsed	Rbr = Dbr * Q_S
Sediment Transformation	Dst = Vs * ZsB * 0.693 / ts	Rst = Dst * Q_S
Sediment Resuspension	Drsp = Grsp * Zrsp	Rrsp = Drsp * Q_S
Sediment Deposition	Ddep = Gsed * Zwcp	Rdep = Ddep * Q_W
Sediment-Water Diffusion	Dsw = As * Zw * ks	Rsw = Dsw * Q_S
Water-Sediment Diffusion	Dws = As * Zw * ks	Rws = Dws * Q_W
	Concentrations (mol m^{-3})	
Water Column	Cwc = Q_W * Zw	
Water Outflow	Co = Q_{IN} * Zw * TFfrac + Q_W * Zw * (1 - TFfrac)	
Sediment	Csed = Q_S * Zsed	

Notes: kow - overall water-side mass transfer coefficient
TFfrac - fraction of water that flows through lake without mixing

4.2.1.1 Steady-state Model

The steady-state model considers the summer season at Amituk Lake. Contaminants enter the lake from inflowing meltwater streams from June through August and atmospheric exchange during the short ice-free period from July to September. Rates for inputs and internal processes such as sediment deposition and diffusion, and sediment and water transformation, are assumed constant and representative of summer conditions.

Due to density differences between inflowing meltwater and the lake water column, a substantial portion of inflowing meltwater passed over the lake without mixing with the bulk water column (Bergmann and Welch, 1985). Freitas et al. (1994, 1997) used measured 1992 DDT concentrations to calibrate a mixing parameter or throughflow fraction for the model, finding a value of 0.5 to provide good model results. This value was retained for the steady-state portion of the current study, but is best treated as a time-dependent variable.

Steady-state solutions for Q_W and Q_S are obtained by substituting the above transport parameters into eqs. 15 and 16, setting the time-derivative equal to zero, and rearranging:

$$Q_W = \frac{Q_A(Drn + Ddd + Dwd + Daw) + Q_{IN}(Dwi + Dpi)}{(Dwt + Dwa + Dwo + Ddep + Dws - \dfrac{(Ddep + Dws)(Drsp + Dsw)}{(Dsw + Dbr + Drsp + Dst)}} \qquad (17)$$

$$Q_S = \frac{Q_W(Ddep + Dws)}{(Drsp + Dsw + Dbr + Dst)} \qquad (18)$$

The program code for the steady-state model is listed in Appendix B1 and the input files are listed in Appendix B2. The remaining sections of this chapter list the lake characteristics, chemical loadings and physico-chemical properties incorporated into the steady-state model. Results for the suite of organochlorine compounds and PCB homolog groups are presented and discussed in the following chapter.

4.2.1.2 Unsteady-state Model

The variability of year-round processes were incorporated into an unsteady-state or time-dependent model. Processes included in this model were changes in ice cover, precipitation, stream discharge, and proportion of meltwater that mixes with the water column. The model assumed constant, annual values for sediment-water diffusion and transformation processes.

Treatment of variation in ice cover and precipitation has been described by Freitas and co-workers (1994, 1997). Annual ice growth and decay processes in high arctic lakes have been studied by Schindler and co-workers (1974a) and Heron (1985). Ice decay begins in mid-June and continues to mid-July. A linear decline in ice sheet area (parameterized as radius) from the shoreline and ice thickness (from 2.2 to 0 m (Semkin, unpubl.)) occurs over this period. June 15 is designated as the beginning of an annual cycle that starts ice decay and is assigned Adjusted Julian Day (AJD) 1. Decay continues to July 15 (AJD 31) then the lake is ice-free until September 14 (AJD 92). At this time, ice cover reappears and increases in thickness at a constant rate to a maximum thickness of 2.2 m on May 6 (AJD 326). The ice sheet is considered to completely cover the lake over this entire period. The maximum ice thickness is maintained until mid-June when the next annual cycle begins. The volume of unfrozen lake water is adjusted accordingly throughout the year. Ice cover is assumed to occupy 10% of lake volume at maximal thickness.

Exchange processes between the lake and the atmosphere vary throughout the year as a result of changes in ice cover. Air-water gas exchange, wet and dry aerosol deposition, and rain dissolution only occur when water is exposed to the atmosphere. The open water surface area increases from mid-June to mid-July and the entire surface is exposed from mid-July to mid-September.

Rain dissolution and wet deposition also vary with precipitation patterns. In the Resolute area, 40-50% of annual precipitation falls as rain from August to September (Environment Canada, 1990; Schindler et al., 1974a). Freitas and co-workers (1994, 1997) parameterized this via a normal distribution density function. In the current model, daily rainfall begins on June 15, peaks on August 3 (AJD 50), and ends on September 23 (AJD 101).

Constant daily rates for sedimentation processes such as deposition, resuspension and burial, were used from mid-June to late-September when inflowing waters carry particulate matter to the lake and wind-circulation resuspends sediments. During ice cover these processes are negligible and set to zero. Sediment-water diffusion and chemical transformation in water and sediment continue throughout the year.

The proportion of inflowing meltwater that mixes with the water column (parameterized by the throughflow fraction) was identified as an important factor in contaminant dynamics in Amituk Lake by Freitas and co-workers (1994, 1997). The parameter is difficult to evaluate although an estimated value of 0.5 was determined by Freitas (1994) by comparing modeled and measured DDT concentrations for varying throughflow fractions. This parameter is constant in the steady-state model. However, results presented in Chapter 3 of 1994 α-HCH enantiomer ratios (ERs) and concentrations in Amituk Lake at 3, 20 and 40 m depths and inflow and outflow streams reveal that the throughflow fraction varies over the summer. The highest stream discharges and α-HCH concentrations occurred when the lake was ice covered. Consequently, much of the contaminant load exited the lake without mixing with the water column. High ERs at 3 m depth and in the outflow but constant and much lower values at 20 m depth during this period support this. At ice-off, ERs at 20 m increase slightly while those at 3 m and in the outflow assume values similar to those at 20 m, suggesting complete mixing. This information was used to parameterize the throughflow fraction over the summer for the unsteady-state model and results are presented in the following chapter.

Daily discharge measurements were recorded throughout the summers of 1993 and 1994 for streams flowing into Amituk Lake and for the outflow, beginning in mid-June. Daily measurements for Gorge, Mud, Cave and East Creeks were incorporated into the unsteady-state model. Combined, these streams account for ~95% of the 1994 gauged stream discharge into Amituk Lake (Semkin, unpubl.). Discharge characteristics are illustrated in the following section. Loading contributions from direct runoff (10.6% of 1994 gauged inflow, Semkin, unpubl.) was incorporated into the model. Subsurface flow (~5% of gauged discharge, Kinney, 1997) was not included.

At Amituk Lake, 1993 stream organochlorine concentrations were found to vary temporally (Semkin, 1996; Barrie et al., 1997). Compounds with higher water solubilities such as α- and γ-HCH had high concentrations at the beginning of melt due to freezeout from ice crystals and preferential elution from the snowpack (Barrie et al., 1997). Less soluble compounds like PCBs and DDT did not exhibit the same trend, but instead increased slightly over the summer. Similar temporal trends were observed in Amituk Lake streams in 1994 (Semkin, unpubl.). Temporal variations in concentration were incorporated into the model using non-linear and linear regression techniques to generate equations from the measured concentrations for each stream. This is described in detail section 4.2.3.

The unsteady-state model calculates transport D-values and numerically solves the differential mass balance equations using initial sediment (Q_S^o) and water column (Q_W^o) aquivalences obtained from Amituk Lake concentrations from the summer of 1992 and June 1993 (Semkin, unpubl.) and reported sediment concentrations (Muir et al., 1995, 1996b). These values were substituted into the following time-dependent aquivalence equations:

$$Q_S = \frac{Q_W^o * \Sigma D_{WS} - Q_S^o * \Sigma D_{OS}}{Z_{SED} * V_S} + Q_S^o \tag{19}$$

$$Q_W = \frac{Q_A * \Sigma D_A + Q_{IN} * \Sigma D_I + Q_S^o * \Sigma D_S - Q_W^o * \Sigma D_W}{Z_W * V_W} + \frac{Q_W^o * V_W^o}{V_W} \tag{20}$$

where:

$\Sigma D_{WS} = Ddep + Dws$

$\Sigma D_I = Dwi + Dpi$

$\Sigma D_A = Drn + Ddd + Dwd + Daw$

$\Sigma D_W = Dwa + Dws + Dwt + Ddep + Dpo + Dwo$

$\Sigma D_{OS} = Dst + Dsw + Dbr + Drsp$

$\Sigma D_S = Dsw + Drsp$

and Z_W and Z_{SED} are the fugacity capacities of the water and sediment compartments, respectively, V_W is the calculated water volume, V_W^o is the initial water volume, and V_S is the active sediment volume. Appendices B3 and B4 list the unsteady-state model code and input files, respectively.

4.2.2 Lake Characteristics

Amituk Lake and its watershed are depicted and described in Chapter 1 (Figure 1.1(a), S. 1.3). The steady- and unsteady-state models include lake-specific characteristics that are listed in Table 4.2, in addition to the watershed's physical dimensions and climatology already discussed. The parameters used are the same as those used by Freitas and co-workers (1994; 1997) with the following exceptions. Updated sedimentation (burial)

Table 4.2: Physical and limnological characteristics of Amituk Lake used in the steady- and unsteady-state models

Characteristic	Value
Summer Air Temperature (July) (°C)	4 [A]
Summer Water Temperature (°C)	2 [C]
Annual Precipitation ($m\ yr^{-1}$)	0.1314 [A]
Water Surface Area (m^2)	3.78×10^5 [B]
Mean Depth (m)	19.4 [B]
Active Sediment Depth (m)	0.03
Active Sediment Area (m^2)	1.42×10^5
Sediment Deposition Rate ($g\ m^{-2}\ yr^{-1}$)	45.4 [C,D]
Sediment Resuspension Rate ($g\ m^{-2}\ yr^{-1}$)	0 [C]
Sediment Burial Rate ($g\ m^{-2}\ yr^{-1}$)	121 [E]
Inflow Particle Concentration ($mg\ L^{-1}$)	7.4 [C]
Water Column Particle Concentration ($mg\ L^{-1}$)	1.5 [C]
Water Inflow/Outflow Rate ($m^3\ yr^{-1}$)	
1993	5.34×10^6 [C]
1994	5.32×10^6 [C]
Aerosol Concentration ($\mu g\ m^{-3}$)	0.2 [F]
Aerosol Deposition Velocity ($m\ h^{-1}$)	1.8 [G]
Organic Carbon Fractions:	
Water Column Particles	0.05 [C]
Inflow Suspended Particles	0.05 [C]
Sediment Solids	0.012 [H]
Densities ($kg\ m^{-3}$):	
Aerosol Particles	2 000
Suspended Particles	1 500
Sediment Solids	2 000

A. Environment Canada (1990)
B. Semkin and Gregor (1993)
C. Semkin et al. (unpubl.)
D. Calculated in Freitas (1994)
E. Semkin (unpubl., avg. of 3 cores)
F. Barrie (1986)
G. Barrie et al. (1992)
H. Muir et al. (1995)

rates for 3 cores taken in 1993 were obtained and averaged (Semkin et al., unpubl.). The active sediment surface area was determined from the burial rate and from 1992 sediment trap data (Semkin, unpubl.) as per Freitas (1994). Aerosol particle concentrations vary over the year in the Canadian Arctic, reaching a peak during winter and early spring. During the summer when atmosphere-water exchange processes occur, aerosol concentrations are at a minimum, with values of ~0.2 mg m^{-3} of sulfate reported in the early 1980's at three locations (Barrie, 1986). A dry particle deposition velocity for arctic aerosols of 0.05 cm s^{-1} (1.8 m s^{-1}) has been reported (Barrie et al., 1992).

Inflowing stream discharges are an essential component for estimating contaminant loadings to Amituk Lake and are parameterized as follows. In the steady-state model, the gauged outflow value was assumed to equal meltwater inflow, thus accounting for ungauged inputs. Annual discharge was calculated from the sum of daily measurements for 1993 and 1994 (Semkin, 1996; unpubl.) and the values listed in Table 4.2. For the unsteady-state case, daily discharge measurements (m^3 s^{-1}, Semkin, 1996, unpubl.) for Gorge, Mud, Cave and East Creeks, and the outflow, were used as inputs to the model and a total inflow rate was calculated each day. This total rate was multiplied by 10.6% to account for ungauged inputs (Semkin, unpubl.). Missing values were estimated by averaging discharges on the preceding and following days. If multiple recordings were made on a particular day, the average was taken. Stream discharges for 1993 and 1994 are listed in Appendices B5 and B6, respectively. Discharges for the outflow and Gorge, Mud and Cave Creeks are illustrated in Figures 4.1 and 4.2 for 1993 and 1994, respectively.

4.2.3 Chemical Specific Properties and Loadings

Stream and lake waters from Amituk Lake were analyzed for a broad range of organochlorine (OC) contaminants from the summers of 1992 to 1994. Freitas and co-workers (1994, 1997) developed the mass balance models using 1992 concentrations and loadings for several of these compounds. However, sampling frequency increased in subsequent field seasons providing more extensive data sets for 1993 and 1994. For this study, these data sets were inspected for extent of censored data then several compounds were selected for model application. Selected compounds include OC pesticides, PCB

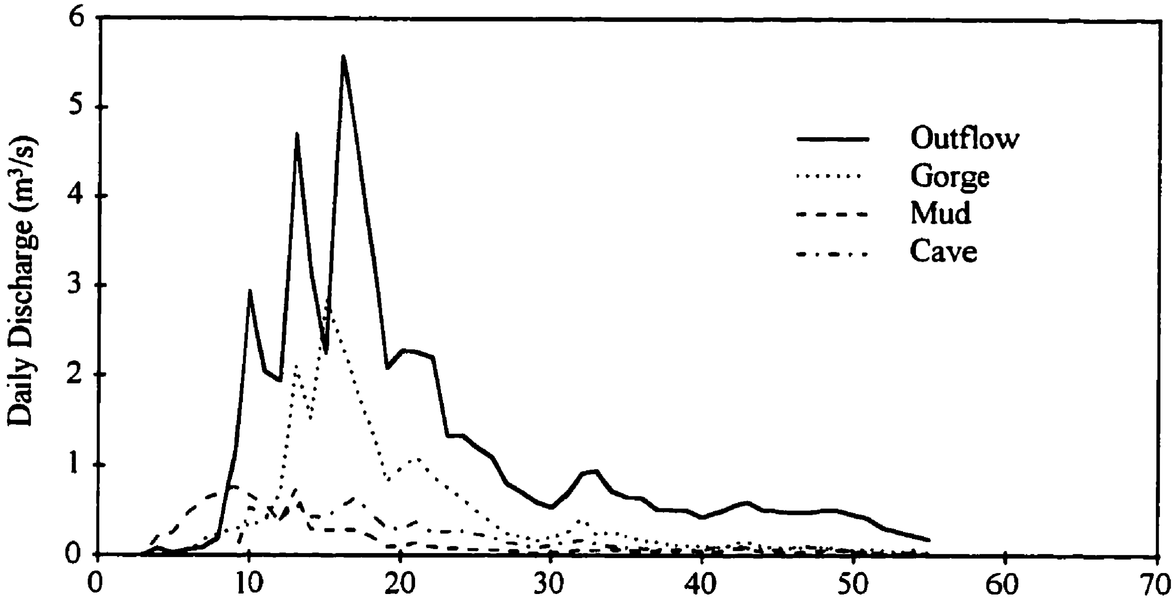

Figure 4.1: 1993 inflow stream discharges (Gorge, Mud and Cave Creeks) and outflow discharge by Adjusted Julian Day (Day 1 = June 15)

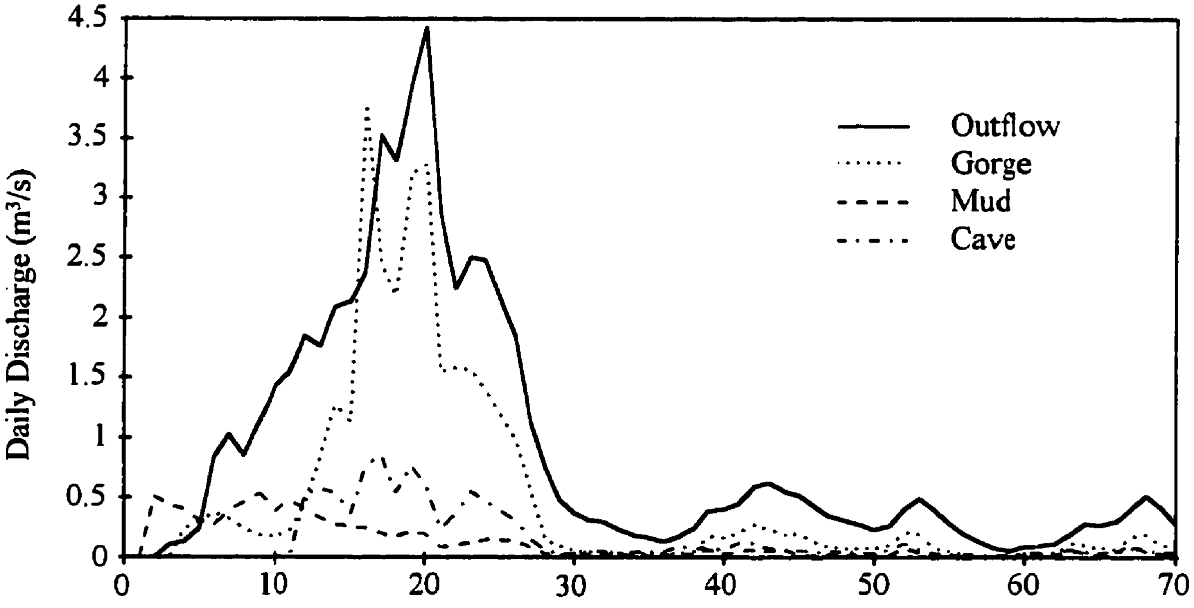

Figure 4.2: 1994 inflow stream discharges (Gorge, Mud and Cave Creeks) and outflow discharge by Adjusted Julian Day (Day 1 = June 15)

homologs, and hexachlorobenzene. Representative physico-chemical properties are listed in Tables 4.3 and 4.4.

Obtaining representative physico-chemical properties for these compounds under arctic conditions presents a significant challenge. Most properties have been measured at 20 or 25°C but vary with temperature. Only a few studies have determined the temperature dependence of properties like vapour pressure, solubility and Henry's Law constant at ambient arctic temperatures. Low temperature values for the chemicals of interest were selected where possible, otherwise values from the reference handbooks of Mackay et al. (1992, 1997) were chosen. Inspection of listed values in such compendiums reveals wide variations in reported properties, often by more than 1 or 2 orders of magnitude. The implications of this uncertainty on model predictions is examined in Chapter 5.

Incorporated into the model are the Henry's Law constant, log K_{OW}, and degradation rates. The Henry's Law constant (H) was calculated from the listed (Table 4.3) supercooled liquid solubilities (C_L) and vapour pressures (P_L), and from temperature-dependent measurements of H (Kucklick et al., 1991). Although vapour pressures of many of the compounds have been determined at low temperatures (e.g. Hinckley et al., 1990; Falconer and Bidleman, 1994), this is not the case for C_L. However, the temperature variation in P_L largely controls that of H, rather than variability in C_L (Schwarzenbach et al., 1993). As a result, H was calculated for the compounds of interest using temperature-adjusted P_L and C_L determined at 25°C, except for hexachlorobenzene where cold temperature C_L was reported (Shiu et al., 1997).

Rates of environmental degradation for the chosen chemicals have not been determined under arctic conditions. Thus environmental half-lives for the compounds in temperate regions, where water temperatures of 10-15°C were assumed, or class averages as assigned by Mackay et al. (1992, 1997) were selected. These half-lives were then doubled to account for the temperature-related decrease in biological degradation rates under arctic conditions (approx. 0-5°C) according to the 'Q-10 rule', that rates of enzymatic activity double for every 10°C increase in temperature. This was considered reasonable since biological mechanisms were assumed to dominate degradation losses. For α- and γ-HCH, degradation rates have been estimated in the water column of the Eastern Arctic Ocean

Table 4.3: Selected OC physico-chemical properties for initial model calculations

Compound	MW ($g\ mol^{-1}$)	Solubility ^{C} C_L ($mg\ L^{-1}$)	Vapour ^{D} Pressure, P_L (Pa)	Henry's Law ^{E} Constant, H ($Pa\ m^3\ mol^{-1}$)	log K_{OW} ^{C}	Degradation $t_{1/2}$ ^{F} Water (h)	Sediment (h)
α-HCH	290.85	33.3	0.02188	0.1235 ^{K}	3.81	41 160 ^{L}	41 160
β-HCH	290.85	66.0	0.0264 ^{I}	0.116	3.8	110 000 ^{O}	110 000
γ-HCH	290.85	53.5	0.005864	0.07554 ^{K}	3.7	148 000 ^{L}	148 000
Hexachlorobenzene	284.79	0.53 ^{G}	0.01215	6.53	5.5	110 000 ^{N}	110 000
Dieldrin	380.93	6.5	0.0006127	0.036	5.2	192 720 ^{M}	192 720
Endosulfan I	406.95	0.68	0.0003923	0.23	3.62	440 ^{M}	440
Heptachlor Epoxide	389.2	7.4	0.054 ^{I}	2.8	5.0	1 680 ^{M}	1 680
Σ-Chlordanes ^{A}	409.8	0.36	0.000307 ^{I}	0.35	6.0	70 000 ^{M}	70 000
Σ-DDT ^{B}	330.2	0.49	0.0000779	0.02	6.05	175 200 ^{M}	175 200
Σ-PCB ^{B}	302.3	0.479 ^{H}	0.00985 ^{J}	1.26	6.1 ^{H}	110 000 ^{N}	110 000

A. Σ-Chlordane = *cis* -chlordane, *trans* -chlordane, *trans* -nonachlor, properties are averages for these 3 compounds

B. Properties for Σ-DDT and Σ-PCB are averages weighted according to distribution of DDT, DDE, DDD and PCB homologs measured in 1994 in Amituk Lake and streams for Σ-DDT and in Amituk Lake for Σ-PCB (except for degradation).

C. Selected from Mackay et al. (1997), unless noted.

D. Calculated from Hinckley et al. (1990) @ 275 K, unless noted.

E. Calculated from selected P_L/C_L, unless noted.

F. Selected rates doubled to account for "Q-10 rule". Sediment values assumed to be equal to water half-lives.

G. C_S calculated by regression from Shui et al. (1997) @ 275 K, converted to C_L by $C_L=C_S(6.79*(1-T_m/T))$.

H. Average of selected values for eight homolog groups, weighted (note B).

I. Selected from Mackay et al. (1997).

J. Weighted homolog average, calculated from Falconer & Bidleman (1994) @ 275 K.

K. Calculated from Kucklick et al. (1991) @ 275 K.

L. Harner et al. (in press).

M. Quoted in Mackay et al. (1997).

N. Selected, Mackay et al. (1992), Class 9.

O. Assigned Class 9 of Mackay et al. (1997).

Table 4.4: Selected PCB homolog physico-chemical properties for initial model calculations

Compound	MW (g mol^{-1})	Solubility ^{A} C_L (mg L^{-1})	Vapour ^{B} Pressure, P_L (Pa)	Henry's Law ^{C} Constant, H (Pa m^3 mol^{-1})	log K_{OW} ^{A}	Degradation $t_{1/2}$ ^{D} Water (h)	Sediment (h)
Monochlorobiphenyl	188.7	4.41	0.128	5.50	4.5	11 000	34 000
Dichlorobiphenyl	223.1	1.45	0.012	1.84	5.1	11 000	34 000
Trichlorobiphenyl	257.5	0.354	2.84E-03	2.06	5.7	34 000	110 000
Tetrachlorobiphenyl	292	0.196	5.93E-04	0.88	5.9	110 000	110 000
Pentachlorobiphenyl	326.4	0.0693	1.23E-04	0.58	6.3	110 000	110 000
Hexachlorobiphenyl	360.9	0.00695	3.38E-05	1.75	7	110 000	110 000
Hepthachlorobiphenyl	395.3	0.0129	9.19E-06	0.28	6.9	110 000	110 000
Octachlorobiphenyl	429.8	0.0055	2.93E-06	0.23	7.3	110 000	110 000

A. Homolog average of selected values from Mackay et al. (1992).

B. Homolog average calculated Falconer and Bidleman (1994) @ 275 K.

C. Calculated from selected P_L/C_L.

D. Average values from assigned classes from Mackay et al. (1992), doubled to account for the "Q-10 rule".

(Harner et al., in press) and these rates were used in preliminary model runs. The model was used to examine the particular degradation behaviour of these two compounds in Amituk Lake.

Diffusion mass transfer coefficients (MTCs) were assumed to be constant with time and the same values were applied to each compound. Order of magnitude values selected and applied to polar regions by Wania and Mackay (1995) were used here.

Due to a higher occurrence of censored measurements than for more soluble compounds, sums of compounds were used for chlordane, DDT, and PCBs. For chlordane, the sum includes trans-nonachlor and cis- and trans-chlordane, and thus their averaged properties were used. For Σ-DDT and Σ-PCB, weighted averages were taken of individual compounds (DDT, DDE, DDD) and PCB homologs according to their observed occurrence.

Chemical-specific air and inflow concentrations were incorporated into the model to determine lake loadings. Air concentrations reported at Alert, NT were used in the both the steady- and unsteady-state models and are presented in Table 4.5 (Halsall and Barrie, unpubl., seasonal summaries in Halsall et al., 1998). Average values from June to August for 1993 and 1994 were considered as it is during this time that air-water exchange occurs in the lake. Although Cornwallis Island is some distance from Alert, the arctic air mass has been found to be quite homogeneous over large regions of the Canadian Arctic (Hoff and Chan. 1986) and thus these values were assumed for the air over Amituk Lake. Inflowing stream concentrations were treated separately for the two models in the following sections.

4.2.3.1 Inflow Chemical Concentrations and the Steady-state Model

Inflow discharge rates and concentrations were considered constant for the steady-state model. Chemical concentration measurements (Semkin, unpubl.) were averaged for each stream and an overall weighted average was calculated according to the contribution of total stream discharge to total inflow discharge. Annual chemical loadings were calculated as the product of daily discharges and concentrations (Table 4.6). Individual stream concentrations and discharges are presented in Appendices B5 (1993) and B6 (1994). Average chemical concentrations in Amituk Lake at 20 m depth and in the outflow are also listed with their standard deviations (Semkin, unpubl.). There is significant variation

Table 4.5: 1993 and 1994 summer OC air concentrations at Alert, NT [A]

	Air Concentrations (pg m^{-3})	
Compound	Jun.-Aug. 1993	Jun.-Aug. 1994
α-HCH	49.9	41.8
β-HCH	0.4	0.1
γ-HCH	6.3	7.0
Hexachlorobenzene	44.5	39.8
Dieldrin	1.7	1.4
Endosulfan I	4.4	4.4
Heptachlor Epoxide	1.6	1.5
Σ-Chlordanes	3.7	3.3
Σ-DDT	0.4	0.8
Σ-PCB	39.5	32.1
PCB Homologs		
MonoCB	3.7	3.3
DiCB	1.3	1.1
TriCB	15.4	12.3
TetraCB	6.3	4.8
PentaCB	5.9	3.9
HexaCB	3.4	2.9
HeptaCB	2.9	3.2
OctaCB	0.4	0.6

A. Calculated from data of C. Halsall and L. Barrie (unpubl.) which is summarized in Halsall et al., 1998.

among these measurements which may result in part from the time-dependence of chemical concentrations discussed in the next section. Steady-state model predictions were compared to these values. Sediment concentration from Amituk Lake are also listed (Muir et al., 1995; 1996b). Note that in 1994 more PCB congeners were analyzed than in 1993 resulting in an increase in concentrations relative to 1993.

Table 4.6: Mean OC concentrations in Amituk Lake, inflows, and outflow for 1993 and 1994 ^{A}, and reported lake sediments.

	1993 Concentrations (pg L^{-1}) ^{B}			1994 Concentrations (pg L^{-1}) ^{D}			
Compound	Inflow	Lake @ 20 m	Outflow	Inflow	Lake @ 20 m	Outflow	Sediment (ng g^{-1})
α-HCH	1470	1090 ± 261	1383 ± 424	602	564 ± 86	854 ± 313	0.35 ^{E}
β-HCH	39	41 ± 39	63 ± 33	29	30 ± 12	27 ± 11	0.01 ^{E}
γ-HCH	376	193 ± 120	194 ± 111	212	153 ± 29	255 ± 111	0.55 ^{E}
Hexachlorobenzene	32	21 ± 22	50 ± 45	6.8	7.5 ± 12	6.5 ± 8.5	1.14 ^{E}
Dieldrin	71	56 ± 22	33 ± 33	95	80 ± 27	111 ± 35	1.18 ^{E}
Endosulfan I	137	3.9 ± 5.4	69 ± 46	87	20 ± 11	71 ± 62	-
Heptachlor Epoxide	61	63 ± 27	63 ± 15	47	38 ± 19	51 ± 19	0.10 ^{E}
Σ-Chlordanes	90	30 ± 36	52 ± 25	5.5	0.5 ± 1.3	0.5 ± 2.7	1.65 ^{E}
Σ-DDT	44	40 ± 37	40 ± 28	19	36 ± 16	9 ± 4	1.67 ^{E}
Σ-PCB ^{C}	576	305 ± 115	462 ± 266	899	400 ± 190	487 ± 142	12.2 ^{F}
PCB Homologs ^{C}							
MonoCB	164	0 ± 0	70 ± 172	590	35 ± 65	126 ± 61	-
DiCB	110	28 ± 44	138 ± 144	12	16 ± 22	18 ± 12	-
TriCB	102	87 ± 43	66 ± 58	29	33 ± 30	21 ± 16	5.74 ^{F}
TetraCB	137	106 ± 53	123 ± 87	134	151 ± 86	147 ± 76	1.89 ^{F}
PentaCB	28	39 ± 30	35 ± 28	74	97 ± 29	93 ± 21	1.47 ^{F}
HexaCB	15	28 ± 17	25 ± 10	30	29 ± 13	34 ± 15	1.52 ^{F}
HeptaCB	1.7	0 ± 0	0 ± 0	22	24 ± 12	33 ± 10	0.28 ^{F}
OctaCB	2.4	6 ± 19	0 ± 0	2	10 ± 22	7 ± 9	0.03 ^{F}

A. Semkin et al. (unpubl.)

B. Mean concentrations • standard deviation; n = 9 for lake @ 20 m, n = 7 for outflow.

C. Excludes outlier from Lake @ 20 m on June 16, 1993.

D. Mean concentration ± standard deviation; n = 11 for lake @ 20 m, n = 17 for outflow.

E. Muir et al. (1995).

F. Muir et al. (1996b)

4.2.3.2 Inflow Chemical Concentrations and the Unsteady-state Model

Inflowing OC water concentrations vary as the melt season progresses at Amituk Lake (Semkin, 1996; Barrie et al., 1997). Concentrations for more soluble compounds decreased over the summer as meltwater flows decreased. Preferential elution from the snowpack due to freezeout from snow crystals explains this behaviour (Semkin, 1996; Barrie et al., 1997) which is predicted from snowpack and chemical properties (Wania, 1997).

Temporal variation in chemical concentrations were incorporated into the unsteady-state model by obtaining equations from linear and non-linear regression methods for concentration measurements in each inflowing stream. Equations for 1993 data were generally less complex and less accurate than those for 1994 data because of fewer measurements. Outlier points were discarded in some cases to improve fit. Fitted equations used in the model are listed in Appendix B7 while individual stream concentration measurements are listed in Appendices B5 and B6. To illustrate, Figures 4.3 and 4.4 show measured and fitted stream concentrations for 1993 and 1994.

Chemical loadings by stream inflows were assumed to end when measurements ended on AJD 55 and 70 for 1993 and 1994, respectively. Negative values calculated from the equations occurred later in the summer and were set to zero. Predicted lake concentrations calculated by the model from time-dependent loadings were compared to weekly measurements from Amituk Lake (Semkin, unpubl.). These are tabulated in Appendix B8.

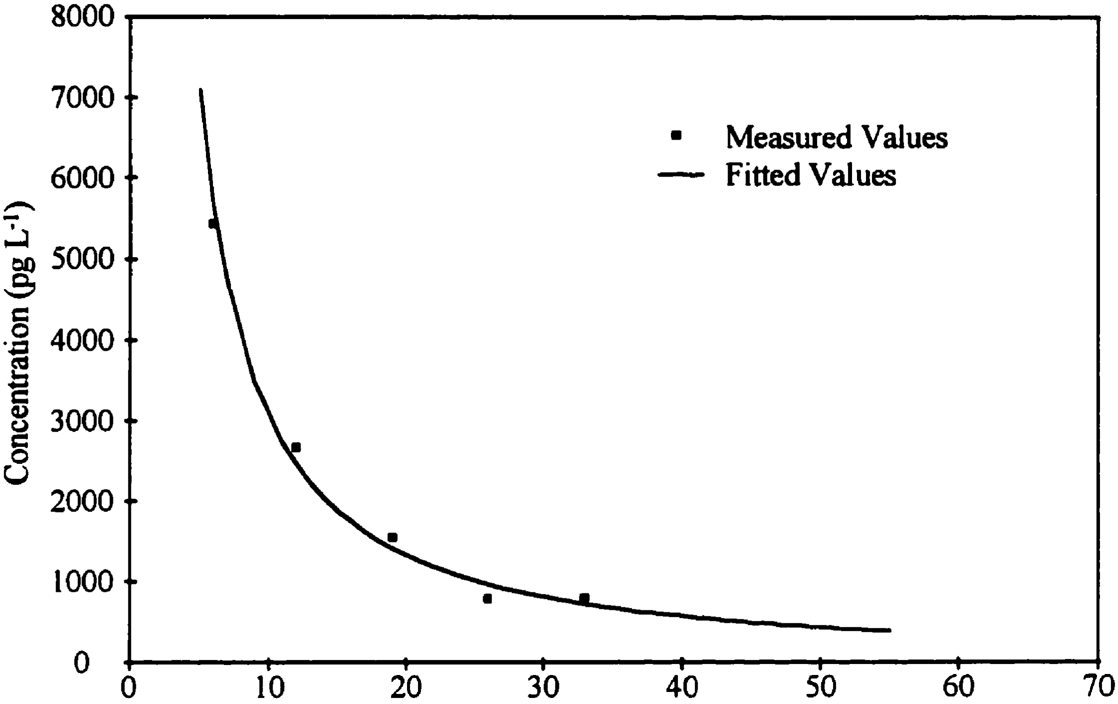

Figure 4.3: 1993 measured and fitted α-HCH concentrations in Gorge Creek by Adjusted Julian Day

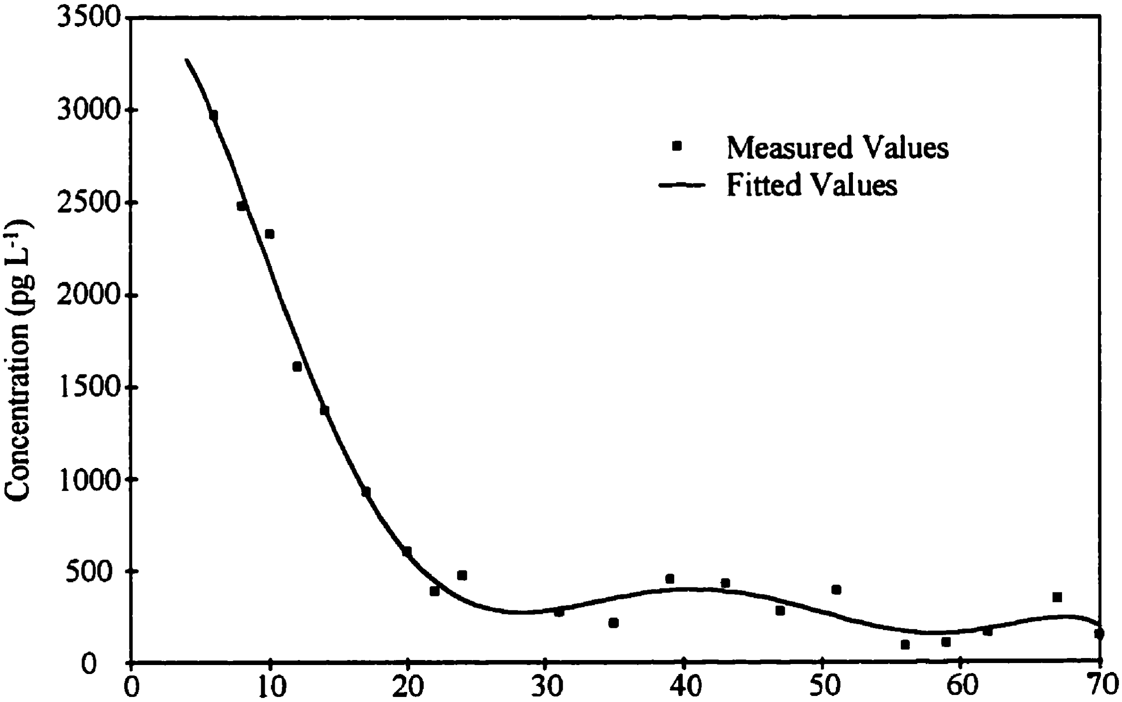

Figure 4.4: 1994 measured and fitted α-HCH concentrations in Gorge Creek by Adjusted Julian Day

5. Model Application to Amituk Lake

The steady- and unsteady-state models were applied to Amituk Lake to gain insight into important processes governing chemical movement in high arctic lakes and to predict the likely behaviour of the lake in response to changes in loadings.

Field work from the summers of 1993 and 1994 at Amituk Lake provided the most complete data set for basin hydrology and contaminant loadings to the lake and thus will be the focus of this chapter. Of particular interest is the response of the lake to changes in annual loadings and the importance of degradation in the fate of α-HCH. Steady-state model results are presented and discussed first, followed by the time-dependent analysis.

5.1 Amituk Lake Steady-state Model Results and Discussion

The steady-state model is a useful tool for investigating and identifying important processes and parameters. Although several factors exhibited temporal variation, the model simplifies the system by assuming average parameter values over the 3 month summer. This discussion expands on the steady-state modeling of work of Freitas (1994, 1997) who relied on only 1992 data for Amituk Lake.

In this research, the mixing parameter determined by Freitas and co-workers (1994, 1997) was re-evaluated for 1993 and 1994 loadings of several compounds then the modeled lake and outflow concentrations were compared to measured values for 10 organochlorine compounds. Model estimates of contaminant dynamics are presented and important processes identified. Differences in year-to-year loadings are discussed and a preliminary investigation of α-HCH degradation undertaken. Finally, the sensitivity of the model to parameter variation was examined to identify the most influential parameters and evaluate the impact of uncertainty.

5.1.1 Parameterization of Lake Mixing

The fraction of inflowing meltwater that passes through or over the lake was identified as a key factor by Freitas and co-workers (1994, 1997). Using their approach, the throughflow fraction was varied and the resulting predicted lake concentration was compared to the average measured values for α-HCH, HCB, Σ-DDT, Dieldrin, and Σ-PCB.

Fitted throughflow fractions are presented in Table 5.1. Substantial variation was found both between chemicals and between years for the same chemical. For Σ-DDT in 1994 the throughflow fraction was unable to account for differences in modeled and predicted lake concentrations. For all chemicals the standard deviation of average measured lake concentrations was broad, allowing predicted concentrations for some chemicals to fall within the average ± standard deviation regardless of value of the throughflow parameter.

Table 5.1: Fitted throughflow parameter for selected compounds

	Fitted Throughflow Fraction	
Compound	1993	1994
α-HCH	0.8	0.4
HCB	0.2	<0.1
Dieldrin	>0.9	0.9
Σ-DDT	0.2	(0)
Σ-PCB	0.8	0.8

It is not surprising that the optimal throughflow fraction varies by year and chemical. The throughflow fraction depends on the timing of loadings vis-à-vis streamflow which is chemical specific according to the nature of preferential elution from the snowpack (Semkin, 1996; Wania, 1997). The throughflow fraction also depends on yearly climatic influences of ice melt on the lake. Melt conditions influence the amount of water entering and mixing with the lake. Larger stream flows may cause the stable upper layer to reach greater depths in the lake (Bergmann and Welch, 1985; Semkin, 1996). As upper layer water passes over the lake, the depth it reaches increases (Bergmann and Welch, 1985; Semkin, 1996). The moat at the ice edge consists of well-mixed water (Bergmann and Welch, 1985) and the volume of moat water increases as ice cover declines, while complete stream and lake water mixing occurs upon ice-off. For the purposes of the steady-state model, the median throughflow fraction value of 0.5 determined by Freitas et al. (1994, 1997) was retained for all chemicals and years. The temporal dependence of the throughflow fraction, or mixing parameter, is discussed further for the unsteady-state model.

5.1.2 Contaminant Concentrations and Dynamics in Amituk Lake

Predicted 1993 and 1994 steady-state water column concentrations are summarized in Figure 5.1 for 10 organochlorine compounds (OCs), and in Figure 5.2 for eight PCB homologs. Modeled concentrations are compared to mean (± standard deviation) measured lake concentrations (Semkin, unpubl.). The model estimated lake concentrations to within, or nearly within, one standard deviation of measured values. Exceptions to this were heptachlor epoxide in both 1993 and 1994, and Σ-chlordane and mono-, penta-, and hexachlorobiphenyl in 1994. Predicted and measured outflow concentrations display similar agreement (not shown).

Modeled fluxes of selected OCs are depicted in Figures 5.3 to 5.6 for α-HCH, γ-HCH, dieldrin and Σ-PCB for each of 1993 and 1994. Estimated contaminant fluxes for all 10 OCs and the PCB homologs are listed in appendix C1. Inflowing snowmelt is by far the largest contributor to the contaminant burden of the lake, while only small amounts enter from direct atmospheric deposition to the lake itself (Figure 5.7). Contaminants in air are scavenged by falling snow and deposited to the snowpack that accumulates throughout the winter months (Gregor, 1990). The contaminant burden of the snowpack in part volatilizes or is released into streams during snowmelt that then enters the lake (Wania, 1997). HCB and Σ-chlordane were exceptions to this high relative importance of loadings from snowmelt with absorption from the atmosphere also of importance. For HCB, the relative importance of the loading processes reversed from 1993 to 1994 with absorption dominating. HCB has a high Henry's Law constant relative to the other compounds investigated, resulting in the greater importance of atmospheric exchange processes. For Σ-chlordane, a dramatic decline in 1994 loadings in snowmelt while air concentration remained constant contributed to the shift to net absorption.

Contaminant loss processes are compared in Figure 5.8 for 1994. Relative export rates were similar from 1993 to 1994. Chemical export is the dominant loss process, although degradation and volatilization have significant roles for several compounds. Losses to the sediments accounts for 0 to 10% of total losses. This percentage is small as the particulate load that is able to convey chemicals to the sediments is low. Only for the higher K_{OW} compounds Σ-DDT and Σ-PCB are sediment losses more important. Also, the

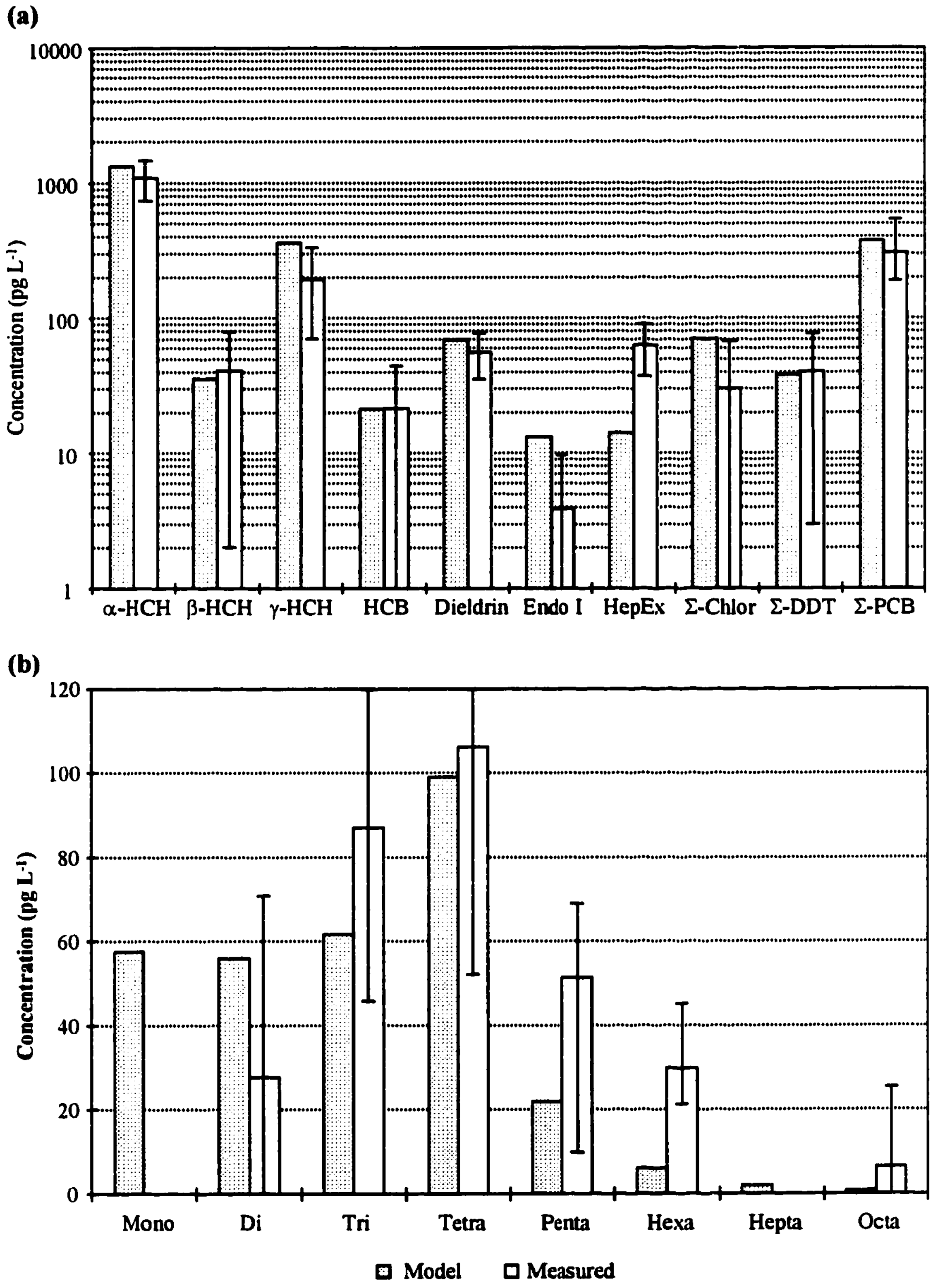

Figure 5.1: (a) Organochlorine and (b) PCB homolog modeled and measured concentrations in Amituk Lake for 1993
]]>

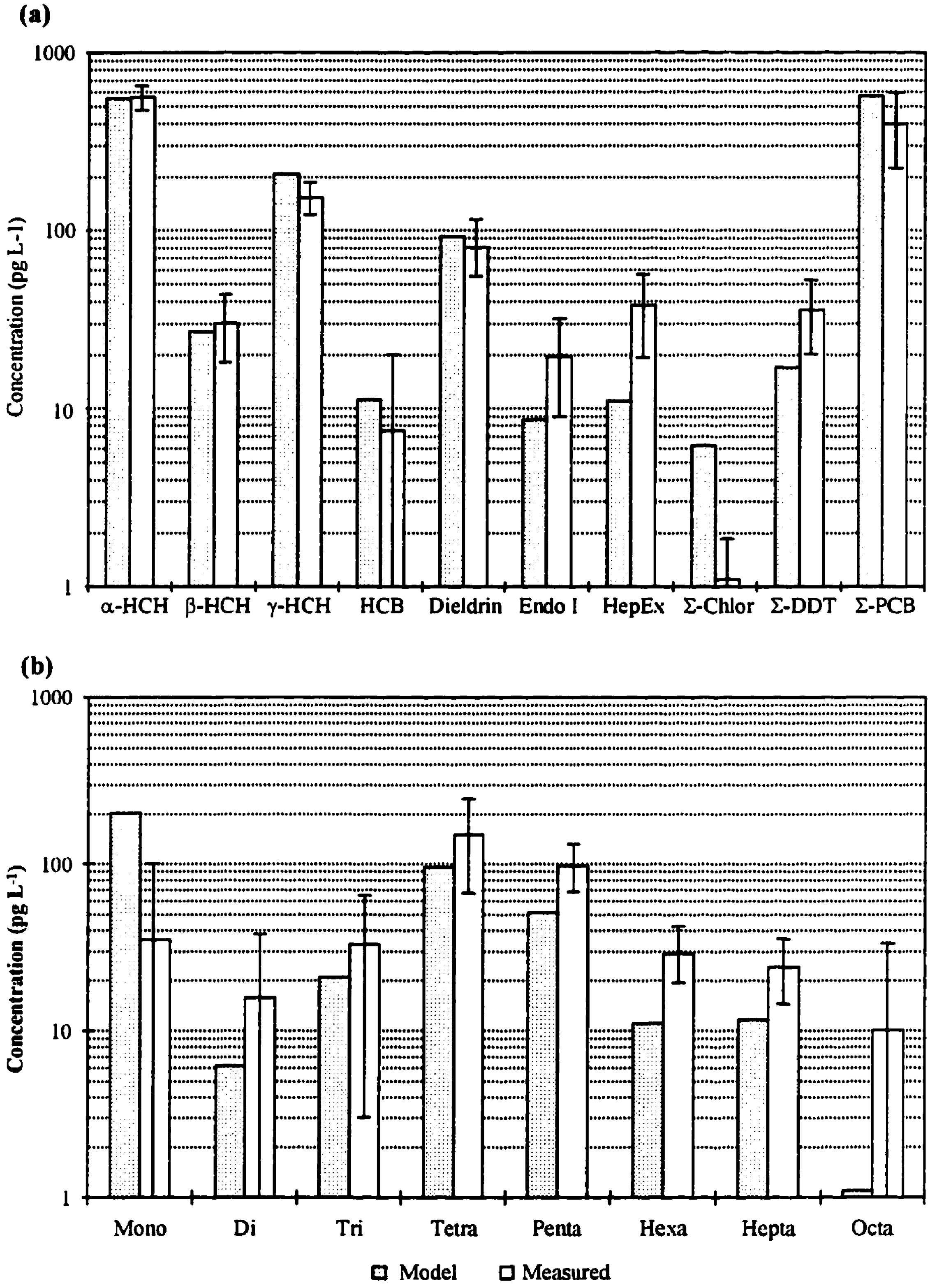

Figure 5.2: (a) Organochlorine and (b) PCB homolog modeled and measured concentrations in Amituk Lake for 1994

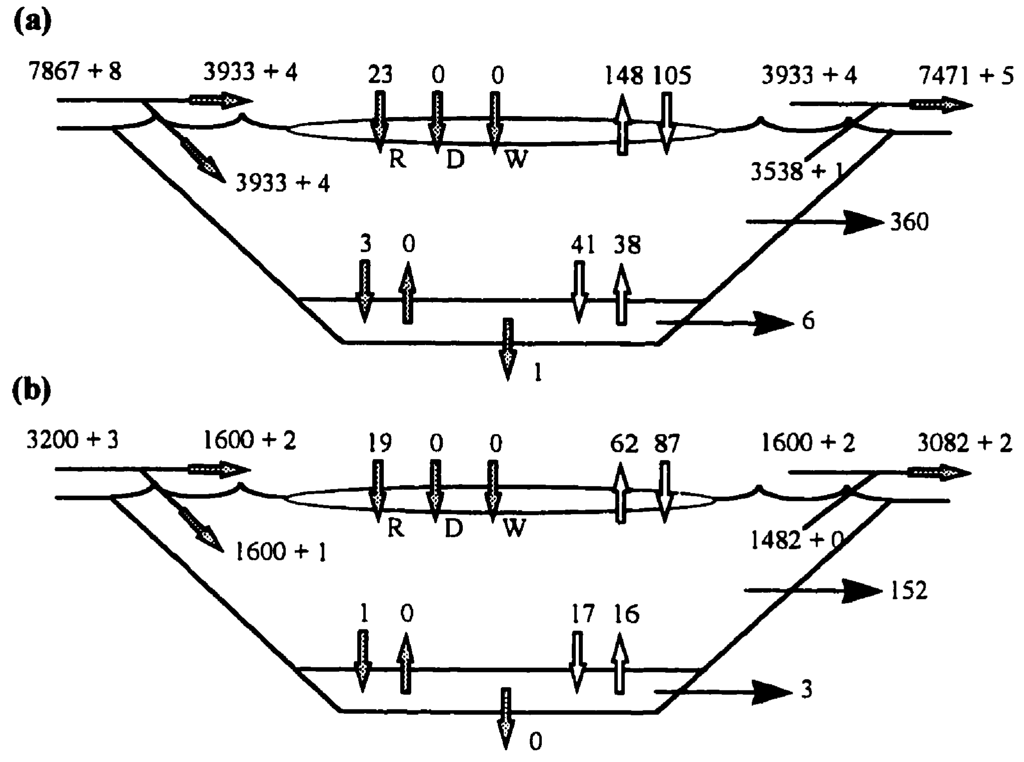

Figure 5.3: Fluxes (mg/year) of α-HCH in Amituk Lake in (a) 1993 and (b) 1994 (dissolved + particle phase, ➡ advection, ⇨ diffusion)

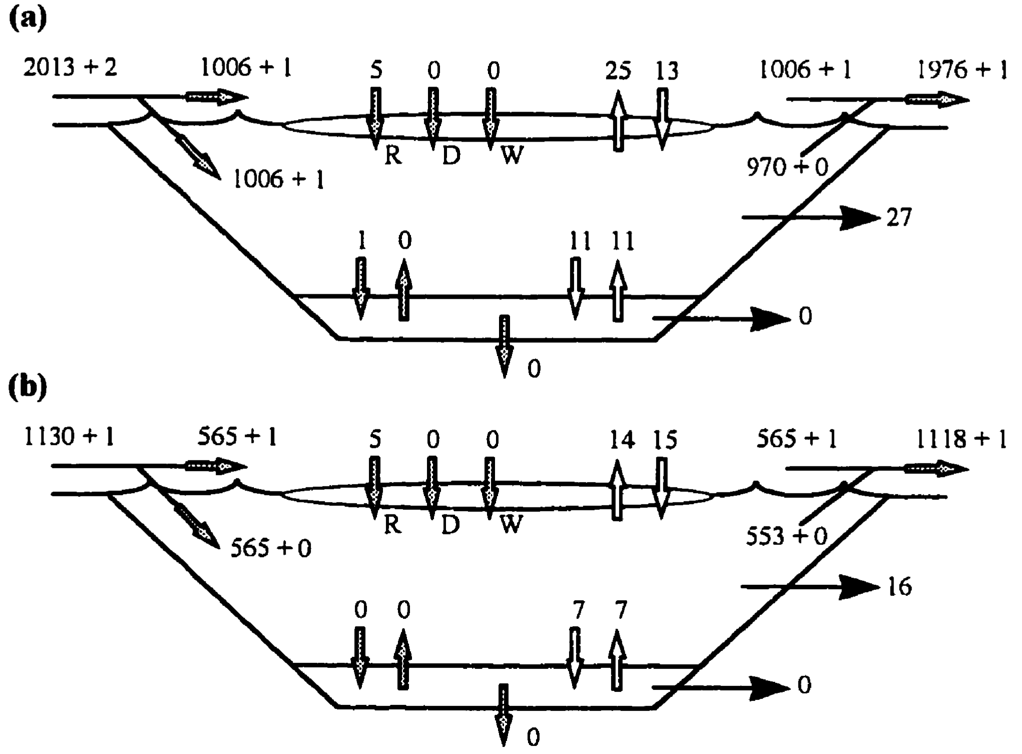

Figure 5.4: Fluxes (mg/year) of γ-HCH in Amituk Lake in (a) 1993 and (b) 1994 (dissolved + particle phases, ➡ advection, ⇨ diffusion)

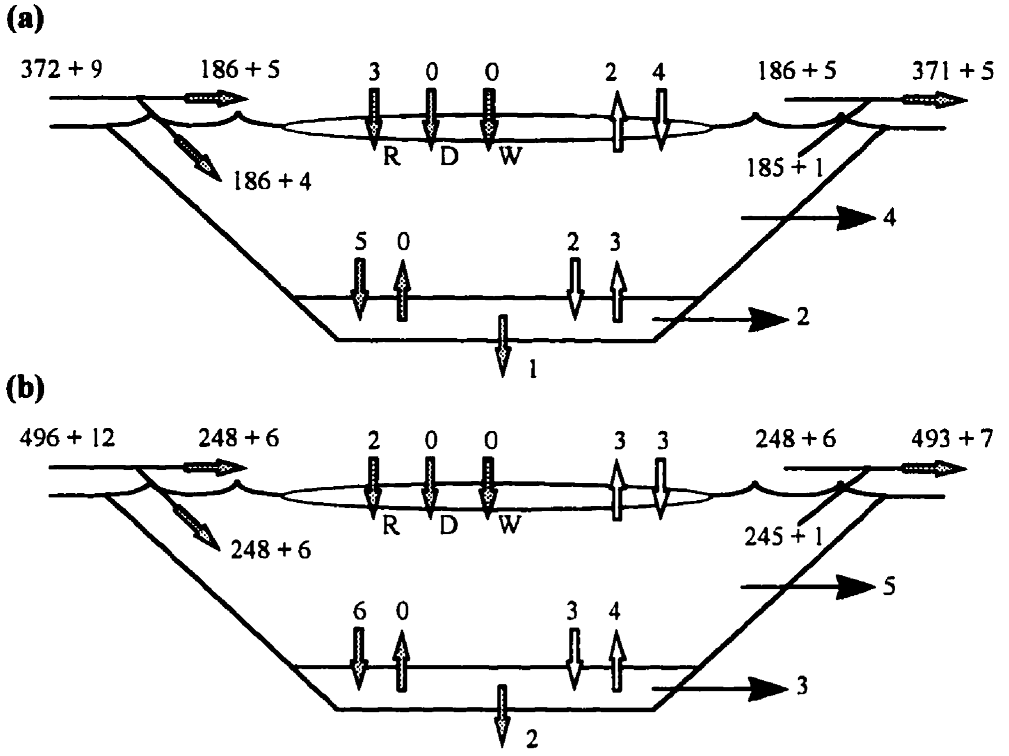

Figure 5.5: Fluxes (mg/year) of Dieldrin in Amituk Lake in (a) 1993 and (b) 1994 (dissolved + particle phase, ➡ advection, ⇨ diffusion)

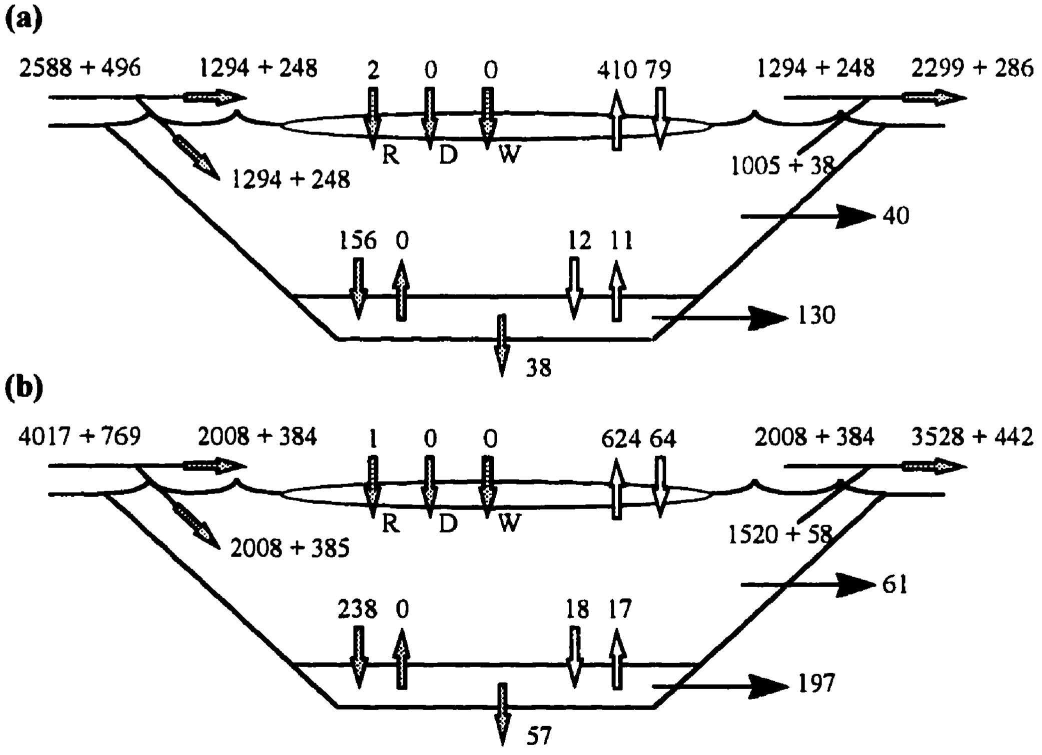

Figure 5.6: Fluxes (mg/year) of ΣPCB in Amituk Lake in (a) 1993 and (b) 1994 (dissolved + particle phase, ➡ advection, ⇨ diffusion)

fraction of organic carbon in the sediments (1.2%, Muir et al., 1995) is low which, in part, dictates the capacity of the sediments to retain contaminants.

The model indicates that degradation accounts for approximately 9% of total losses for α-HCH, 10% for Σ-DDT and Σ-PCB, 13% for Σ-chlordane, 58% for heptachlor epoxide and 90% for endosulfan I. Reported environmental and degradation half-lives were limited for heptachlor epoxide (Mackay et al., 1997) from which a value of 1680 h was used initially. However, model estimates improved when a degradation half-life of 50 000 h was used. Similarly, a degradation half-life of 11000 h (S. 5.2.2) for γ-HCH obtained from unsteady-state model results improved steady-state lake concentration estimates to within the measured average ● standard deviation in 1993 and 1994. Relative losses by degradation increased to 27% from 3% for γ-HCH while decreasing to 5% from 58% for heptachlor epoxide using these rates over literature values.

Volatilization losses are important for HCB, heptachlor epoxide, Σ-chlordane, and Σ-PCB accounting for 61, 19, 9 and 25%, respectively, of total losses because of the high Henry's Law constants for these compounds (Table 4.3). This increased to 44% for heptachlor epoxide with reduced degradation. The importance of volatilization and degradation to PCB losses results from relatively high Henry's Law constants and shorter degradation half-lives for the mono- to trichlorobiphenyl homologs, which contribute a greater proportion to total PCB levels than the tetra- to octachlorobiphenyl homologs.

The flux diagrams (Figures 5.3 to 5.6) also show chemical loading changes from 1993 to 1994 in the inflow. The amounts of α-HCH (Figure 5.3) and γ-HCH (Figure 5.4) entering the lake in 1994 decreased by 60% and 46%, respectively, relative to 1993, while dieldrin and Σ-PCB loadings increased. In turn, decreased α- and γ-HCH loadings changed modeled lake-atmospheric exchange rates. In 1993 the lake degassed α- and γ-HCH, however with decreased loadings in 1994, net air-water exchange approached zero for γ-HCH while net absorption occurred for α-HCH. Atmospheric concentrations of α-HCH have declined dramatically over the past two decades (Li et al., 1998). For example, a 50% decline in α-HCH concentrations from 1991 to 1995 was observed in Norway but γ-HCH concentrations remained constant over that time (Haugen et al., 1998). As a result northern water bodies have become a source of α-HCH, i.e. volatilization of α-HCH has been observed in the

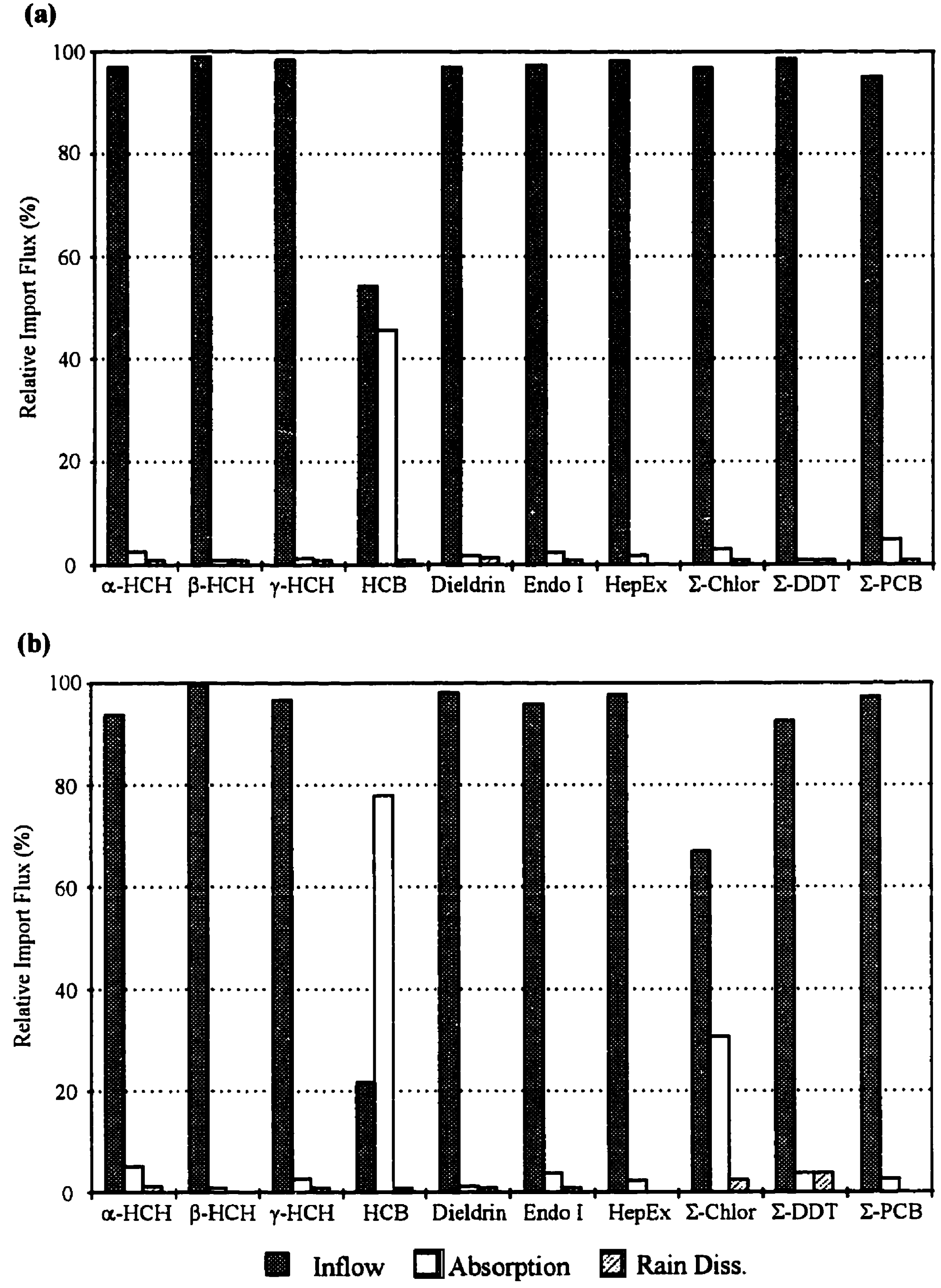

Figure 5.7: Relative organochlorine contaminant import fluxes for (a) 1993 and (b) 1994

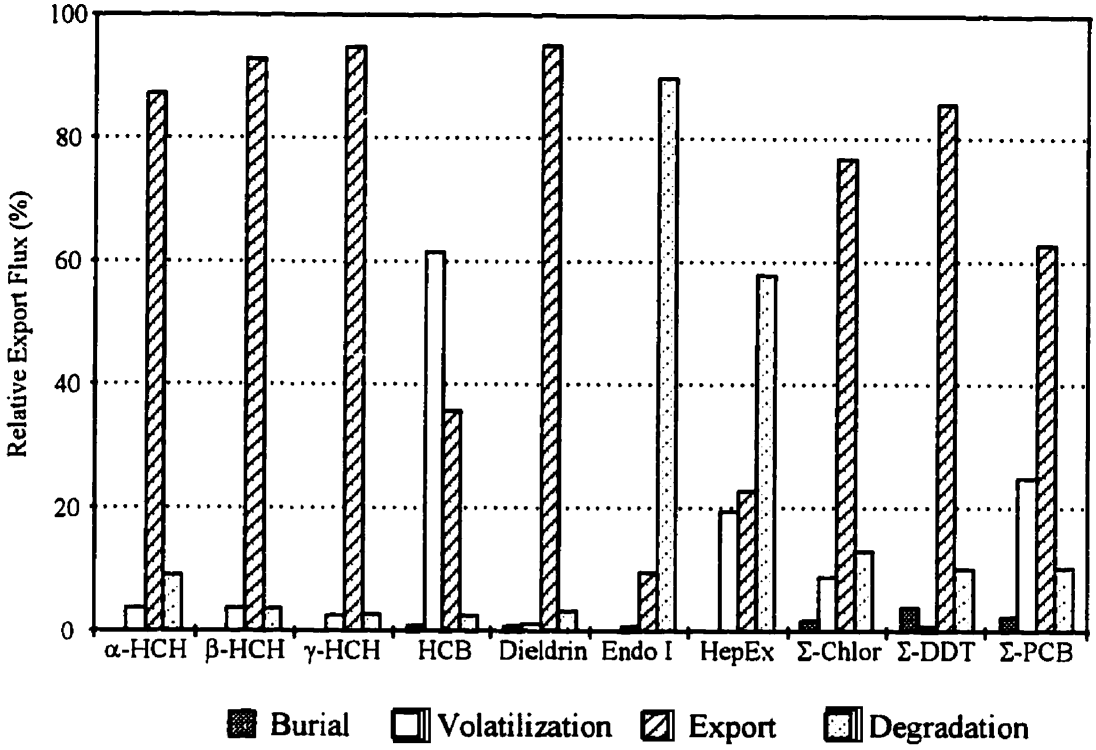

Figure 5.8: Relative organochlorine export fluxes for 1994 from Amituk Lake

Bering and Chukchi Seas (Jantunen and Bidleman, 1995), the Arctic Ocean (Jantunen and Bidleman, 1996, 1997; Harner et al., in press), Resolute Bay (Falconer et al., 1995b), and seasonally in Lake Ontario (Ridal et al., 1997). However, atmospheric concentrations of α- and γ-HCH were relatively constant at Alert (Table 4.5, Ch. 4) and at Tagish between 1993 and 1994 (Halsall et al., 1998). Thus the reason for the sharp decline in loadings to Amituk Lake is not apparent but may be due to geographical variation and inconsistencies in the arctic air mass. Higher HCH concentrations at the Tagish site in 1993 and 1994 (Halsall et al., 1998) and higher α-HCH concentrations at Resolute in 1992 (Bidleman et al., 1995a) than recorded at Alert support this possibility. Alternatively, variations influencing volatilization from the snowpack may change loadings to the lake (Wania, 1997).

The apparent increase in PCB loadings from 1993 to 1994 (Figure 5.6) likely result from analytical changes in 1994 when more PCB congeners were quantified in water. Arctic air concentrations remained constant from 1993 to 1994 (Stern et al., 1997), suggesting loading changes in the snowpack were not source driven. The 33% increase in dieldrin loadings at Amituk corresponds well with increases of approximately 22% and 37% at Alert and Tagish, respectively, from 1993 to 1994 (Halsall et al., 1998).

The response of lake concentrations to annual loading changes is shown in Figure 5.9 for selected compounds. Estimated lake concentrations respond quickly to changes in loadings. The model accurately predicts the effect of loading changes for α-HCH (Fig. 5.9 (a)), HCB (Fig. 5.9 (b)) and dieldrin (Fig. 5.9 (d)). The model underestimates lake concentration for Σ-DDT (Fig. 5.9 (c)) when loadings decline to much lower levels in 1994 than 1992, which may be due to internal loadings from sediments which is not considered by the steady-state model. For HCB, reduced inflow loadings in 1994 resulted in net absorption and higher modeled and measured lake than inflow concentrations.

Although measured organochlorine concentrations are available for Amituk Lake sediments, these were not used in model calibration. The steady-state model treats chemical that enters in a particular year and does not reflect historical loadings. The chemical inventory is less important in the water column where chemical persistences are short, varying from 1-3 years (Figure 5.14, S. 5.2.3; Freitas, 1994, 1997). However, historical contaminant burden is important for sediments in which the chemical persistence is very long in these ultra-oligotrophic lakes, e.g. approximately 20 years for Σ-PCB, 30 years for dieldrin (Figure 5.14, S. 5.2.3) and up to 74 years for *p,p'*-DDT (Muir et al., 1995). Sediment contributions are considered in the unsteady-state case as the model is initialized by the measured value.

Overall, the steady-state model reveals that contaminant inflow and export in streams dominate chemical transport processes. However, air-water gas exchange for HCB, heptachlor epoxide, Σ-chlordane and Σ-PCBs, and degradation for γ-HCH, Σ-chlordane and endosulfan I are also important loss mechanisms. Loading changes from 1993 to 1994 resulted in lake concentration differences that are adequately predicted by the model. The model indicates that loading changes affect the relative importance of absorption and volatilization for HCB and α- and γ-HCH, resulting in reversals in net flux directions for α-HCH and HCB.

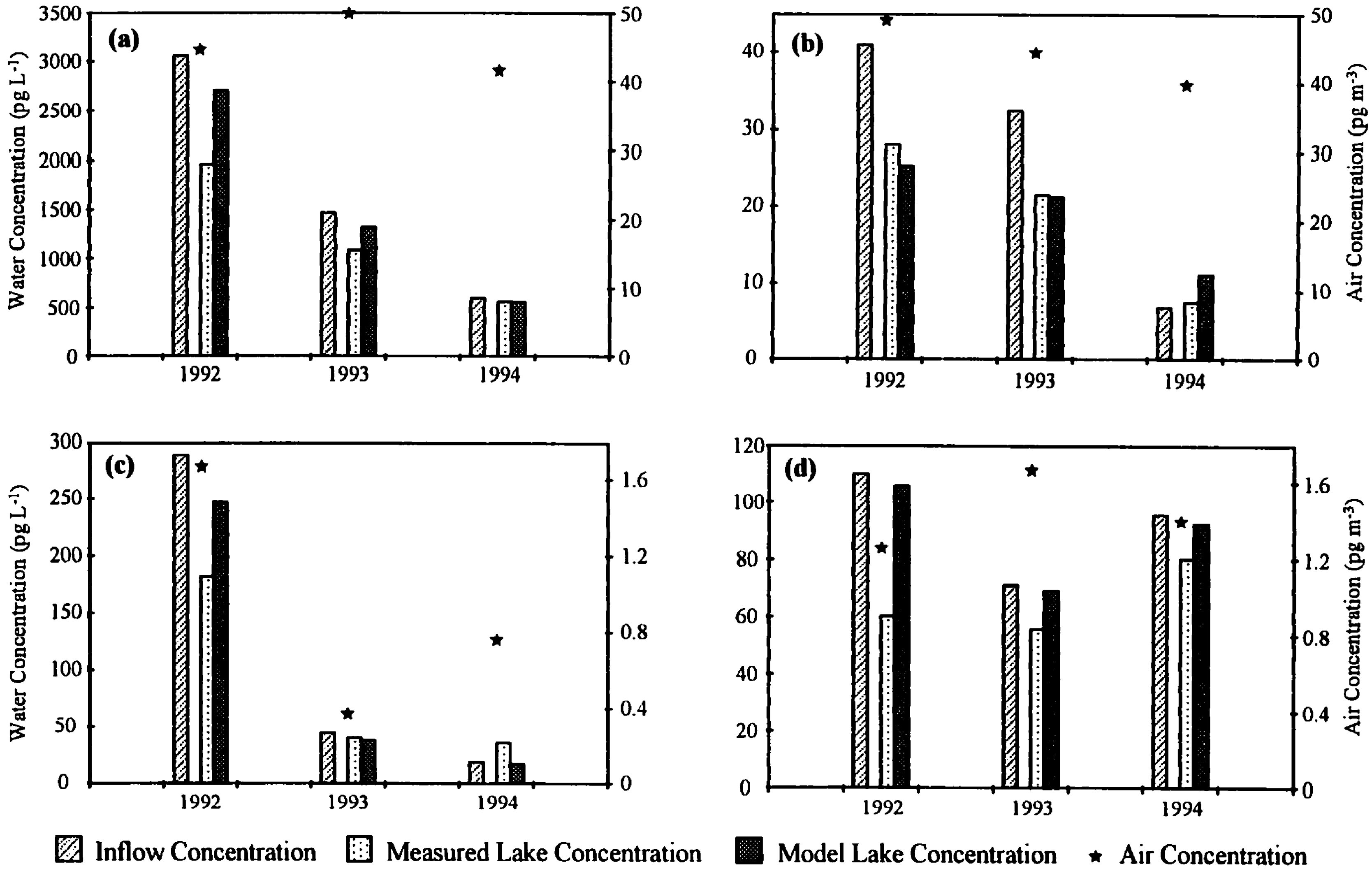

Figure 5.9: Annual variation of inflow, measured and modeled lake and air concentrations for (a) α-HCH, (b) HCB, (c) Σ-DDT and (d) Dieldrin

5.1.3 α-HCH Degradation

The steady-state model was applied to α-HCH in Amituk Lake first using a microbial degradation rate of 0.147 y^{-1} estimated for the Eastern Arctic Ocean (Harner et al., in press). However, from Chapter 3, the estimated degradation rate calculated from the reduction in α-HCH inventory within the lake from late-July/early-August 1993 to June 1994 was 0.796 y^{-1} or a half-life of 6960 h.

Using this faster rate the predicted concentration for 1993 remained within one standard deviation of the measured mean, while the 1994 estimated value was within a factor of 1.5 of the measured mean. Degradation losses from the water column became more important, accounting for approximately 37% of α-HCH loss compared to 9% in the previous case. In addition, the concentration change resulted in air-water exchange approaching equilibrium in 1993 and net absorption in 1994.

Degradation of α-HCH was also investigated in the sensitivity analysis (S. 5.1.4). Due to its solubility, the bulk of α-HCH transformation occurs in the water column. Predictably, parameters that influence its water column concentration also impact degradation. Varying each of the listed parameters revealed that inflow concentration, degradation half-life and ice-free days had the greatest influence on the magnitude of α-HCH transformation. A higher inflow concentration loads more chemical into the lake, thus more is degraded, while increasing the number of ice-free days in the steady-state model extends the period for which degradation occurs and increases the amount degraded. The effect of varying the half-life is explicit.

Enantiomer ratio results and concentration measurements near lake bottom in June 1994 suggest that enhanced degradation occurs in or near the sediments (Ch. 3, S. 3.2.3). The surface sediments are likely the most active site for microbial activity and thus chemical transformation, similarly to the case of mercury methylation (e.g. Verta et al., 1994). Transformation of the chemical by the microbes occurs in the aqueous phase rather than the pore water of the sediments (e.g. Rittman, 1994). Accordingly, the model results are sensitive to changes in the degradation rate in water but not sediment. The steady-state model does not account for degradation beyond the 3 month spring melt and summer ice-free period which, as discussed in Section 5.2.3, is critical to accurately estimating HCH behaviour.

5.1.4 Parameter Analysis

Model sensitivity to variations in parameter values was examined to identify the most influential parameters for each chemical and to evaluate the impact of uncertainty in parameters used in model formulation. To accomplish this, the values of several physico-chemical, lake characteristic, and chemical loading parameters were doubled individually for 1994 data, except sediment volume fraction and throughflow fraction which were changed by 50%. The percentage change in predicted lake (Tables 5.2 and 5.3) and sediment (Appendix C2) concentrations was then calculated.

Analysis results were similar to those of Freitas (1994) but include a broader set of chemicals. Model results were most sensitive to only about 7 out of 19 parameters tested and sensitivity was chemical-specific in most cases. Lake concentrations declined with an increase in the Henry's Law constant (H) for HCB (38%), heptachlor epoxide (14%), Σ-chlordane (9%) and Σ-PCB (19%), all of which have relatively high H values. These high H values account for sensitivity to doubling the air-side mass transfer coefficient. Both the solubility (C^S) and vapour pressure (P) terms of H are temperature sensitive, although P is likely the controlling factor (Schwarzenbach et al., 1993). Literature compilations of C^S and P vary considerably (e.g. Mackay et al., 1997) and most reported values were determined at temperatures above those typical of arctic conditions. However, the C^S (Shiu et al., 1997), P (Hinckley et al., 1990; Falconer and Bidleman, 1994) and H (Kucklick et al., 1991) values used in the model were corrected for temperature effects where possible. K_{OW} is relatively unimportant to model results, e.g. doubling K_{OW} decreased lake concentrations of only Σ-chlordane, Σ-DDT and Σ-PCB by 9, 11 and 9%, respectively. Doubling the water column degradation half-lives resulted in lake concentration increases for α-HCH (5%), heptachlor epoxide (40%) and endosulfan I (81%). However, the longer half-life found for heptachlor epoxide was much less sensitive to variation. Degradation rates are perhaps more poorly known than other physico-chemical properties.

Chemical loadings were dependent on inflowing water and secondarily, atmospheric concentrations. Lake concentrations increased by >90% due to doubling inflow

Table 5.2: Percent difference in lake water OC concentrations resulting from variation of physico-chemical and lake characteristic parameters listed in Tables 4.2 and 4.3

	Percentage Change from Base Case									
Parameter	α-HCH	β-HCH	γ-HCH	HCB	Dieldrin	Endo I	HepEx	Σ-Chlor	Σ-DDT	Σ-PCB
Henry's Law constant	-3.8	-3.5	-2.6	-38.5	-1.4	-0.9	-13.7	-9.0	-1.6	-18.7
Octanol-water Partition Coeff.	-0.1	-0.1	-0.1	-1.5	-1.9	0	-0.5	-9.2	-11.2	-9.4
Water MTC	0	0	0	1.9	0	0	-1	0.2	0	-0.6
Air MTC	1.4	-3.3	0.1	7.5	0	2.9	-12	19.9	2.4	-16.7
Sediment MTC	0	0	0	0	0.1	-0.1	-0.2	-0.3	0.2	0
Water Half-life	4.7	1.8	1.4	0.7	1.1	81.5	40.1	2.4	1.1	1.2
Sediment Half-life	0.1	0	0	0.2	0.3	0	0	0.4	0.6	0.4
Air Concentration	5.7	0.3	3	78.3	1.6	4	2.2	32.6	5.1	2.6
Inflow Water Concentration	94.3	99.7	97	21.7	98.4	96	97.8	67.4	94.9	97.4
Active Sediment Depth	-0.1	-0.1	0	-0.2	-0.4	0	0	-0.3	-0.5	-0.3
Water Inflow Rate	3.7	3.7	1.1	-10.1	1.8	79.3	61.2	-4.9	5.4	22
Annual Precipitation	0	0	0.5	0.2	0.4	0.2	0	1.3	2.1	0
Sediment Deposition	0	0	0	-1.2	-1.1	0	-0.3	-8.7	-10.3	-8.8
Sediment Burial	0	0	0	-0.1	-0.2	0	0	-0.1	-0.3	-0.1
Sediment/Lake Area Ratio	-0.1	-0.1	-0.1	-0.3	-0.6	-0.1	-0.3	-0.8	-0.9	-0.7
Sediment Organic Carbon Fraction	-0.1	-0.1	0	-0.2	-0.5	0	0	-0.3	-0.6	-0.3
Ice-free Days	-9.2	-6.6	-2.5	9	-2.5	-45.6	-42.3	14.6	-0.3	-20.1
Sediment Volume Fraction	0.1	0	0	0.2	0.3	0	0	0.4	0.6	0.4
Throughflow Fraction	-6.6	-6.6	-2.5	8.2	-3.7	-45.6	-42.4	5.8	-10.5	-25.7

Note: Each parameter was increased by 100% except for Sediment Volume Fraction (50% decrease) and Throughflow Fraction (50% increase).

concentrations for all compounds except HCB and Σ-chlordane, which increased by only 22 and 67%, respectively. However, only HCB and Σ-chlordane lake concentrations were affected by increasing air concentrations which is consistent with the importance of air-water exchange for these chemicals.

The throughflow fraction, inflow rate, and number of ice-free days influenced the lake concentrations of all chemicals. An increase in the sediment deposition rate only affected Σ-chlordane, Σ-DDT and Σ-PCB due to their affinity for particles. The number of ice-free days affects the duration for which air-water exchange and transformation processes occur. Thus more time for degradation and volatilization losses for α-HCH, heptachlor epoxide, endosulfan I and Σ-PCB resulted in significant declines in lake concentrations, while the HCB and Σ-chlordane concentrations increased because of the longer absorption period. Loadings to the lake were affected by the water inflow rate and the throughflow fraction. Higher inflow rates delivered more chemical to the lake resulting in concentration increases. A higher throughflow fraction resulted in less chemical laden water mixing with the lake and thus reduced lake concentrations. In both cases, HCB and Σ-chlordane were the exceptions because of how the relative importance of absorption fluxes were affected by these parameters. The higher throughflow reduced the effect of low inflow concentrations, increasing contributions from absorption, while the greater inflow rate reduced absorption effects. The effects of changes to throughflow and inflow rate were reversed when higher loadings from 1993 were considered.

The same parameters discussed above affected PCB homologs (Table 5.3) with several of the parameters exhibiting trends across the homolog groups. Less air-water exchange resulted from a decline in the influence of H for the more chlorinated homologs. Increasing K_{OW} and the sediment deposition rate decreased lake concentrations with increasing chlorine number, which is consistent with their particle reactivity and hence ability of suspended particles to remove chemicals from the water column. Doubling the air-side mass transfer coefficient resulted in lower lake concentrations for the mono- to hexachlorobiphenyls, which exhibit net volatilization. However, hepta- and octachlorobiphenyl exhibited net absorption resulting in higher lake concentrations due to

Table 5.3: Percent difference in lake water PCB concentrations resulting from variation of physico-chemical and lake characteristic parameters listed in Tables 4.2 and 4.4

	Percentage Change from Base Case							
Parameter	Mono	Di	Tri	Tetra	Penta	Hexa	Hepta	Octa
Henry's Law constant	-26.1	-20.6	-24.4	-16	-11.1	-14.6	-4.4	-2.7
Octanol-water Partition Coeff.	-0.2	-0.9	-3.6	-6.8	-15	-31.2	-32.5	-41.2
Water MTC	0	0	0	0	0	0	0	0
Air MTC	-25.9	-15.7	-7.9	-13.8	-7.6	-9.3	5.2	14.6
Sediment MTC	0	-0.2	0	0	0	0	0	0
Water Half-life	7.1	10.7	3.5	1.4	1.4	0.9	1.1	0.8
Sediment Half-life	0.1	0.2	0.3	0.4	0.4	0.2	0.3	0.2
Air Concentration	0.4	6.6	23.4	2.7	4	6.8	11.8	25.6
Inflow Water Concentration	99.6	93.4	76.6	97.3	96	93.2	88.2	74.4
Active Sediment Depth	-0.1	-0.1	-0.2	-0.3	-0.3	-0.2	-0.2	-0.1
Water Inflow Rate	48.6	28.8	14.4	16.3	17.6	44.1	29.3	37.9
Annual Precipitation	0	0.1	0.2	0	0.1	0.3	1.5	6.6
Sediment Deposition	-0.1	-0.7	-3	-6.2	-14.5	-30.9	-32.2	-41
Sediment Burial	0	0	-0.1	-0.1	-0.1	-0.1	-0.1	-0.1
Sediment/Lake Area Ratio	-0.2	-0.5	-0.5	-0.7	-0.7	-0.4	-0.5	-0.3
Sediment Organic Carbon Fraction	-0.1	-0.1	-0.3	-0.4	-0.4	-0.2	-0.2	-0.1
Ice-free Days	-39.4	-28.6	-13.6	-17	-10.7	-12	3	14.4
Sediment Volume Fraction	0.1	0.2	0.3	0.4	0.4	0.2	0.3	0.2
Throughflow Fraction	-39.4	-28.9	-15.4	-21.3	-22.1	-35.8	-28.8	-32.5

Note: Each parameter was increased by 100% except for Sediment Volume Fraction (50% decrease) and Throughflow Fraction (50% increase) increased absorption. A similar trend was observed for ice-free days. Degradation half-life affected only mono- and dichlorobiphenyl which are more readily degraded.

Sediment concentrations were affected similarly to water concentrations by the Henry's Law constant, air-side mass transfer coefficient, water half-lives, air and inflow concentrations, inflow rate, number of ice-free days and throughflow fraction (Appendix C2). However, sediment volume (-3 to -50%) (parameterized by active sediment depth and sediment-to-lake area ratio), K_{OW} (10 to 106%), sediment deposition (5 to 76%) and burial (up to -23%), sediment degradation half-life (2 to 83%), organic carbon fraction (1 to 91%), and sediment volume fraction (2 to 96%) also affected sediment concentrations. The historical or buried contaminant burden may also contribute concentrations in the thin active sediment layer. However, these values are not taken into account in the two compartment lake model. Sediment processes and concentrations may be better described by a two compartment sediment model which can account for historical loadings and slow diffusion from lower sediment layers to the active layer.

Model uncertainty is controlled by the inherent uncertainty in the lake- and chemical-specific parameters incorporated into the model. The sensitivity analysis revealed that the most important terms were inflow concentration, water inflow rate, throughflow proportion, degradation rates, ice free days, and Henry's Law constant. Average inflow concentrations have large standard deviations, in many cases resulting from their temporal variation. Measurements of degradation rates and Henry's Law constants under arctic conditions are few to non-existent. The throughflow proportion is difficult to measure and varies with time. It is best obtained through model calibration. These factors culminate in considerable uncertainty in model predictions. The unsteady-state model reduces some of the variation by incorporating temporal dependencies of concentrations, inflow rates, degradation, and throughflow fraction into the model.

To summarize, the steady-state model accurately estimates Amituk Lake concentrations based on measured loadings and adequately describes lake processes contributing to contaminant fate. Lake concentrations are dictated primarily by the snowpack chemical burden. However, for compounds like HCB and Σ-chlordane with low inflow concentrations, the ice-off period during the summer is sufficiently long that lake concentrations are influenced by atmospheric concentrations. This research supports results of Freitas and coworkers (1994, 1997) by illustrating the response of lake concentrations to annual loading changes. The model proved to be quite robust to uncertainties in parameterization of lake characteristics and physico-chemical properties. Although several values were updated from the previous research effort, the main conclusions remain unchanged. Furthermore, the stability of the model allowed for estimation of system-specific degradation rates for several compounds, one of the least known parameters for arctic conditions. In general, contaminants enter the lake via snowmelt and are promptly exported from the lake, although the relative importance of air-water exchange and degradation as loading and loss mechanisms is greater than previously observed for arctic lakes.

The unsteady-state model is applied in the following section to further investigate lake mixing, annual variation, and the effects of over-winter processes on lake concentrations and extend estimates for predictive purposes.

5.2 Amituk Lake Unsteady-state Model Results and Discussion

The unsteady-state model considers annual cycles in hydrology, ice cover, inflowing chemical concentrations, and precipitation. In this section, lake mixing was again investigated. Model results were obtained for the 1993 and 1994 summer seasons and for the period from 1992 to 1994 and compared to measured values over the summer seasons and from year-to-year. The model was used to estimate the degradation rate of α- and γ-HCH. Finally, the model was used to predict future lake contaminant levels based on varying loading regimes.

5.2.1 Parameterization of Lake Mixing

Mixing in high arctic lakes is limited during snowmelt due to ice cover and density differences between inflow and lake water (Bergmann and Welch, 1985). This has been observed through water chemistry measurements at Char Lake (Schindler et al., 1974a) and Amituk Lake (Semkin, 1996; unpubl.). Variation of ice cover and inflowing stream discharges affect the extent of lake mixing, and with temporal variations in OC concentrations, the amount of chemical that enters the lake.

Insight into the mixing regime of Amituk Lake is provided by detailed lake and stream measurements taken in the summer of 1994. Conductivity measurements revealed that a stable layer of water forms under the ice that increases to about 9 m depth before ice-off (Semkin et al., unpubl.). The ionic chemistry (Ca^{2+}, Mg^{2+}, alkalinity, conductivity) of this layer reflects the snowmelt event, decreasing with the influx of meltwater that is dilute in these species (Semkin, 1996; unpubl.). Major ion concentrations at lake depths of 20 and 40 m remained constant during the snowmelt period, indicating that little mixing occurred between the top layer and the water column. After July 18, when ice cover disappeared, values at all depths were similar, indicating complete mixing (Semkin et al., unpubl.).

The frequency of OC concentration measurements in the inflow and outflow streams and in Amituk Lake, especially for the more abundant α-HCH, also provide lake mixing information. α-HCH concentrations were similar at 20 (Figure 5.10) and 40 m depths, but increased at 3 m depth during peak snowmelt, reflecting inputs from higher stream concentrations (Ch. 3, Semkin et al., unpubl.). The α-HCH concentration at 40 m depth on June 15, 1994 (Adjusted Julian Day (AJD) 1 or Julian Day 166), before snowmelt, was lower than for the rest of the water column before increasing the following week after snowmelt had begun. It is possible that the increase was caused by a portion of the inflowing water containing higher α-HCH concentrations reached lake bottom as an underflow. Peak stream discharge occurred on June 30 (AJD 16) after which 20 m α-HCH concentrations were higher (Semkin et al., unpubl.). Although the sub-ice layer is relatively stable, a high discharge event may inject meltwater past this layer to greater depths. Such an event would account for the increase in α-HCH concentrations at lake depths. Outflow α-HCH concentrations were high during peak snowmelt resulting from the throughflow of inflow water. Outflow concentrations remained high for an extended period from about June 29 to July 9 (AJD 15 to 25), possibly due to a lag in the outflow of 3 m water and the decreasing influence of inflowing water concentrations (Figure 5.10).

Enantiomer ratio analyses for α-HCH add to this information (Ch. 3). ERs at 3 m depth and in the outflow were essentially identical, reflecting stream inputs and minimal mixing in the water column. At 40 m, similarly to α-HCH concentrations, the ER was lower on June 15 but increased after the beginning of snowmelt, either from mixing in the water

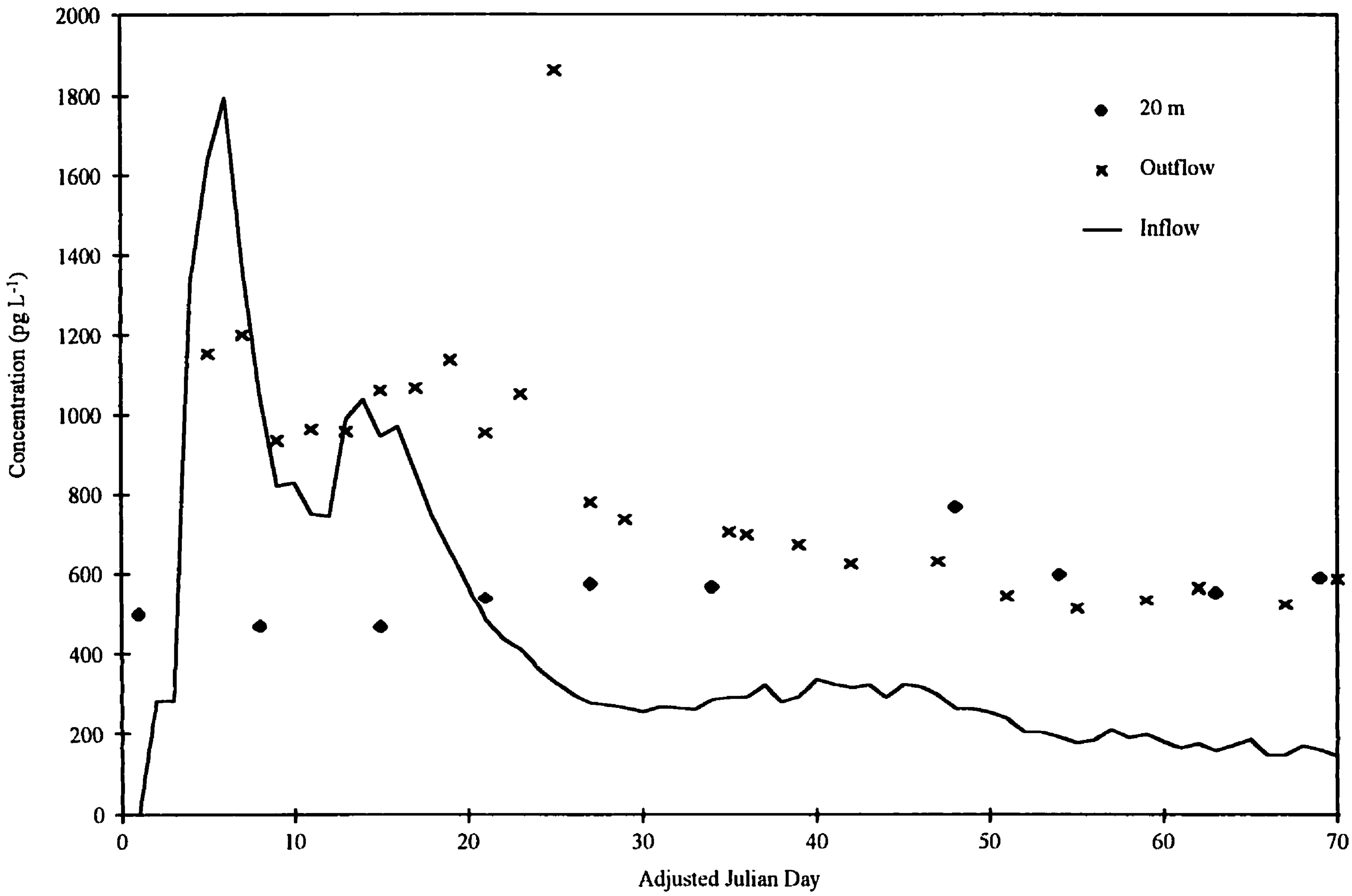

Figure 5.10: Summer 1994 outflow, 20 m and weighted inflow α-HCH concentrations (pg L^{-1}) at Amituk Lake

column induced by inflowing water or the direct influx of meltwater to 40 m depth. There was also a slight increase in ERs at 20 and 40 m depth after peak snowmelt, possibly a result of injection of meltwater through the sub-ice layer. Late in the summer ERs at 40 m remained lower than those at 20 m, possibly due to incomplete mixing to lake-bottom or degradation at the sediment-water interface.

The mixing parameter for the unsteady-state model was assigned values for each day of the summer period to account for the mixing of inflowing and sub-ice water with the water column, based on 1994 α-HCH concentrations and ERs and major ion concentrations. A value of 0.4 was assigned for June 15 (AJD 1) to account for influx to lake depths, and then increased June 19 to 21 (AJD 5 to 7) to 0.8 when inflowing stream discharges increased and inflow and outflow α-HCH ERs and concentrations were similar. From June 28 to July 4 (AJD 14 to 20), encompassing the peak inflow, the parameter was reduced to 0.1 to mimic an injection of meltwater to lake depths. After this, the mixing parameter was increased to 0.9 to minimize the effect of the top layer and inflowing streams on water column concentrations, then gradually decreased over the summer as lake mixing became more prevalent.

The values assigned to the mixing parameter allows the model to adequately predict lake concentrations in 1993 and 1994 (Figure 5.11). However, the model underestimates outflow concentrations and export fluxes. The underestimation occurs predominantly from June 29 to July 9 (AJD 15 to 25) during the time that the sub-ice layer forms and persists and feeds the outflow resulting in measured outflow concentrations well above lake and inflow values (Figure 5.10). The predicted outflow concentration responds to the rapid decrease in inflow concentrations for the more water soluble compounds, rather than the extended contribution of the sub-ice layer. The underestimation could be addressed with a two-compartment model that separates the upper layer from the remainder of the lake water. The following section evaluates the ability of the model to predict time-dependent summer lake concentrations.

5.2.2 Model Results - Summer Seasons

The unsteady-state model was used to estimate time-dependent lake concentrations for 10 OCs in Amituk Lake resulting from snowmelt and atmospheric loading contributions and within-lake processes for the summers of 1993 and 1994. The predicted water column concentrations were compared to measured values at 20 m depth that are considered to be representative of the lake (Semkin et al., unpubl.). Results are presented in Figure 5.11 for α- and γ-HCH, heptachlor epoxide and Σ-DDT. Results for the remaining OCs are depicted in Appendix C3.

The model was initialized with the volume weighted average lake concentration at the beginning of each summer. In some cases the first measurement was deemed an outlier and omitted. Model predictions were found to be sensitive to initial water concentrations.

The model is effective in predicting changing concentrations over the summer for α-HCH (Fig. 5.11 (a)), particularly in 1994 which is not surprising since the model was calibrated with these data. The model accounts for the increase in lake concentration after peak snowmelt. Although there is more variability in measured concentrations in 1993, the trend is matched by the model. The model is similarly effective in predicting 1993 and 1994 γ-HCH and Σ-DDT lake concentrations (Fig. 5.11 (b, d)), and concentrations of heptachlor epoxide (Fig. 5.11 (c)) using the degradation half-life to 50000 h.

Initial sediment concentration values were obtained from literature values (Muir et al., 1995, 1996b, Table 4.6) or assigned a value of 0.01 ng/g if unreported. Predicted 1993 and 1994 Amituk sediment concentrations for all OCs were unaffected by inflow loadings over the summer or by concentration changes due to cryoconcentration. A gradual decrease in sediment concentration was noted for each OC resulting from sediment transformation and/or sediment-to-water diffusion.

Initial sediment values assigned to the model from analysis of the top sediment core layer (0-1 cm) of median age 1980 include historical OCs that should be considered buried because of the low burial rate and mixed layer depth (Muir et al., 1995). This chemical inventory overly influences sediment processes. The estimation of sediment concentrations may be improved by updated concentration data from cores obtained in 1993. A two-

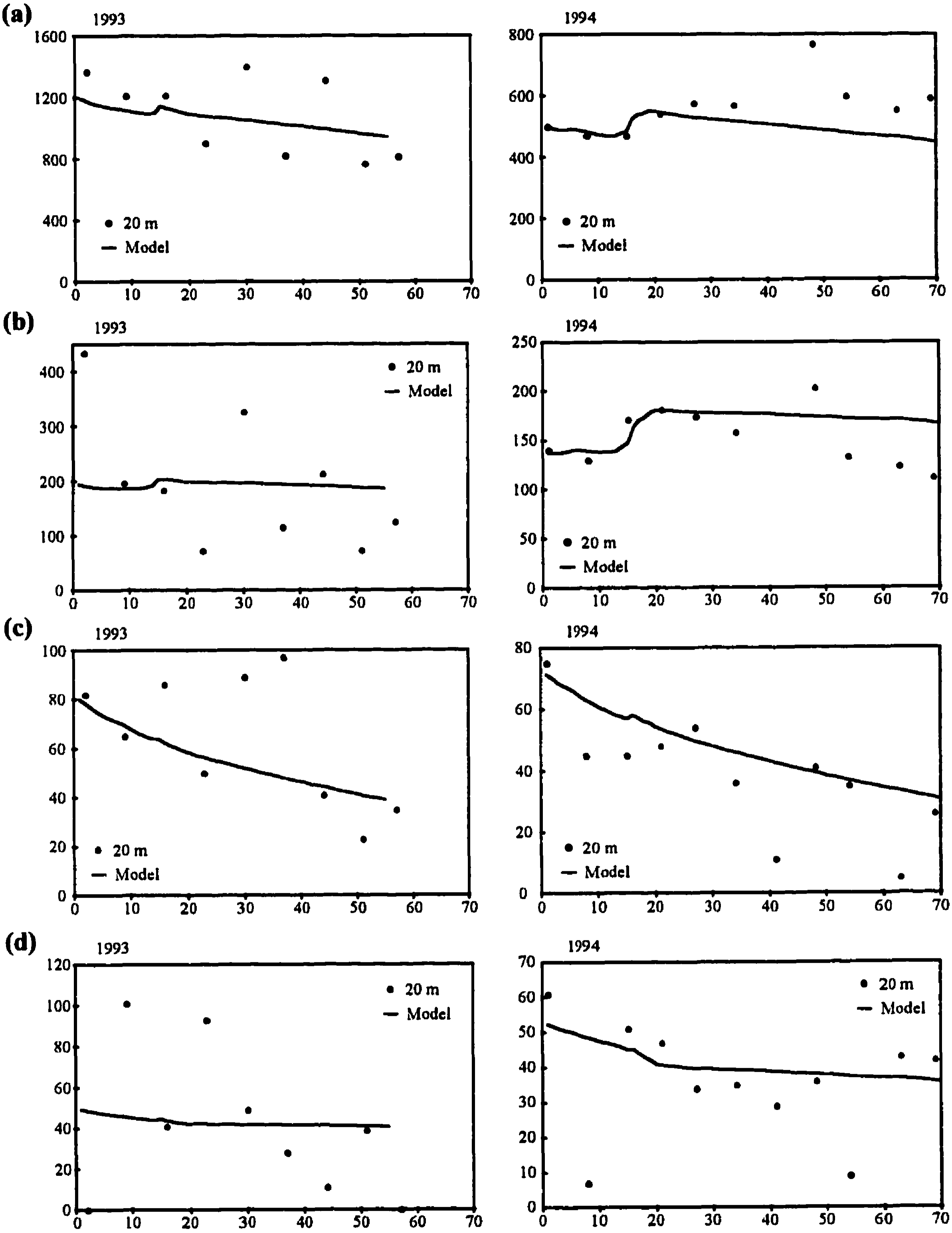

Figure 5.11: Measured (20 m) and modeled Amituk Lake concentrations (pg/L) by AJD for 1993 and 1994 for (a) α-HCH, (b) γ-HCH, (c) heptachlor epoxide and (d) Σ-DDT.

compartment sediment model separating the thin active layer (i.e. 0.5 cm or less) and the historical OC inventory may improve model predictions.

The unsteady-state model accounts for lake mixing, air-water exchange and transformation processes for the summer season at Amituk Lake. The influence of air-water exchange on water column concentrations is reduced from that estimated by the steady-state model because of the parameterization of the throughflow fraction to mimic influences of the sub-ice layer. Loadings to the lake via the inflow were approximately 7 to 60% higher, depending on the chemical, using time-dependent inflow concentrations estimates than for average inflow concentrations used by the steady-state model.

The steady-state model provides sufficient estimates of summer lake concentrations based on measured loadings. Trends in process rates were similar between the steady- and unsteady-state models. For example, the reversal in net air-water exchange flux from 1993 to 1994 was observed for α-HCH in both models and similar summer degradation fluxes were obtained by both models for all chemicals. The simplicity of the steady-state model likely renders it more useful for predicting summer lake concentrations for known loadings. However, the unsteady-state model is useful for examining changes in lake mixing and chemical loadings over the summer. Furthermore, only the unsteady-state model is able to account for over-winter lake processes as discussed in the following sections.

5.2.3 Model Results - Annual Variation

The unsteady-state model was then used to consider annual variations in chemical loadings that result from differences in air and snowpack concentrations and snowmelt events from year-to-year. The model was initialized with average summer 1992 concentrations and run through June 14, 1995 using snowmelt and precipitation events for each summer and two complete annual cycles of ice cover growth and decay.

Daily predicted chemical concentrations in Amituk Lake from August 23, 1992 (AJD 70) to June 14, 1995 (AJD 1095) and measured concentrations (Semkin et al., unpubl., 1992 values listed in App. of Freitas, 1994) are illustrated in Figures 5.12 and 5.13 for selected chemicals with the remainder depicted in Appendix C4. In general, the model effectively accounts for variations in lake concentrations between 1992 and 1994 for the chemicals studied and illustrates the influence of the dominant processes of snowmelt loading, cryoconcentration as ice thickens over winter, and year-round degradation.

Cryoconcentration had the effect of increasing lake concentrations by 5-10% over-winter for dieldrin and heptachlor epoxide (Figure 5.12 (a, c), β-HCH, HCB, Σ-chlordane, Σ-DDT, and Σ-PCB (App. C4). These compounds are more persistent than α- and γ-HCH and endosulfan I which did not exhibit cryoconcentration due to over-winter degradation of the latter. Welch and Bergmann (1985) reported cryoconcentration of ions in lake in Saqvaqjuac on the Hudson Bay coast.

At the onset of snowmelt in June, most lake concentrations decreased as meltwater diluted the water column and the effect of cryoconcentration was eliminated. This was most clearly seen for Σ-DDT and Σ-PCB in 1993 and HCB and Σ-chlordane in 1994, for which dilution was accentuated by lower loadings relative to the previous year. Endosulfan I (Figure 5.12 (b)) was the exception to the dilution pattern because it had no chemical inventory after winter. After dilution from ice melt and inflow, concentrations generally increased during peak snowmelt as meltwater mixed with the water column. The increase was more pronounced for compounds that preferentially eluted from the snowpack resulting in elevated loadings during peak melt and was not seen for Σ-DDT. The results illustrate the rapid response of lake concentrations to annual variations in chemical loadings.

Unlike the steady-state model, chemical transformation in the water column and sediments occur throughout the year in the unsteady-state model, resulting in approximately four times the amount of chemical degraded annually within the lake. Degradation was found to be particularly influential to year-over-year lake concentrations for α-HCH and γ-HCH (Figure 5.13 (a, b)), endosulfan I, and heptachlor epoxide (Figure 5.12 (b, c)). The degradation half-life of 6960 h calculated for α-HCH in Chapter 3 exceeded the effect of cryoconcentration and accounted for declines in lake inventories over winter from 1992 to 1993 and from 1993 to 1994 (Figure 5.13 (a)). For γ-HCH, the initial degradation half-life of 148 032 h (Harner et al., in press) was reduced to 11 000 h to simulate annual concentrations (Figure 5.13 (b)). Thus γ-HCH degradation in Amituk Lake has a rate approaching that of α-HCH and is much more rapid than that reported in the Eastern Arctic Ocean where γ-HCH degradation was much slower than for α-HCH (Harner et al., in press). This is reasonable

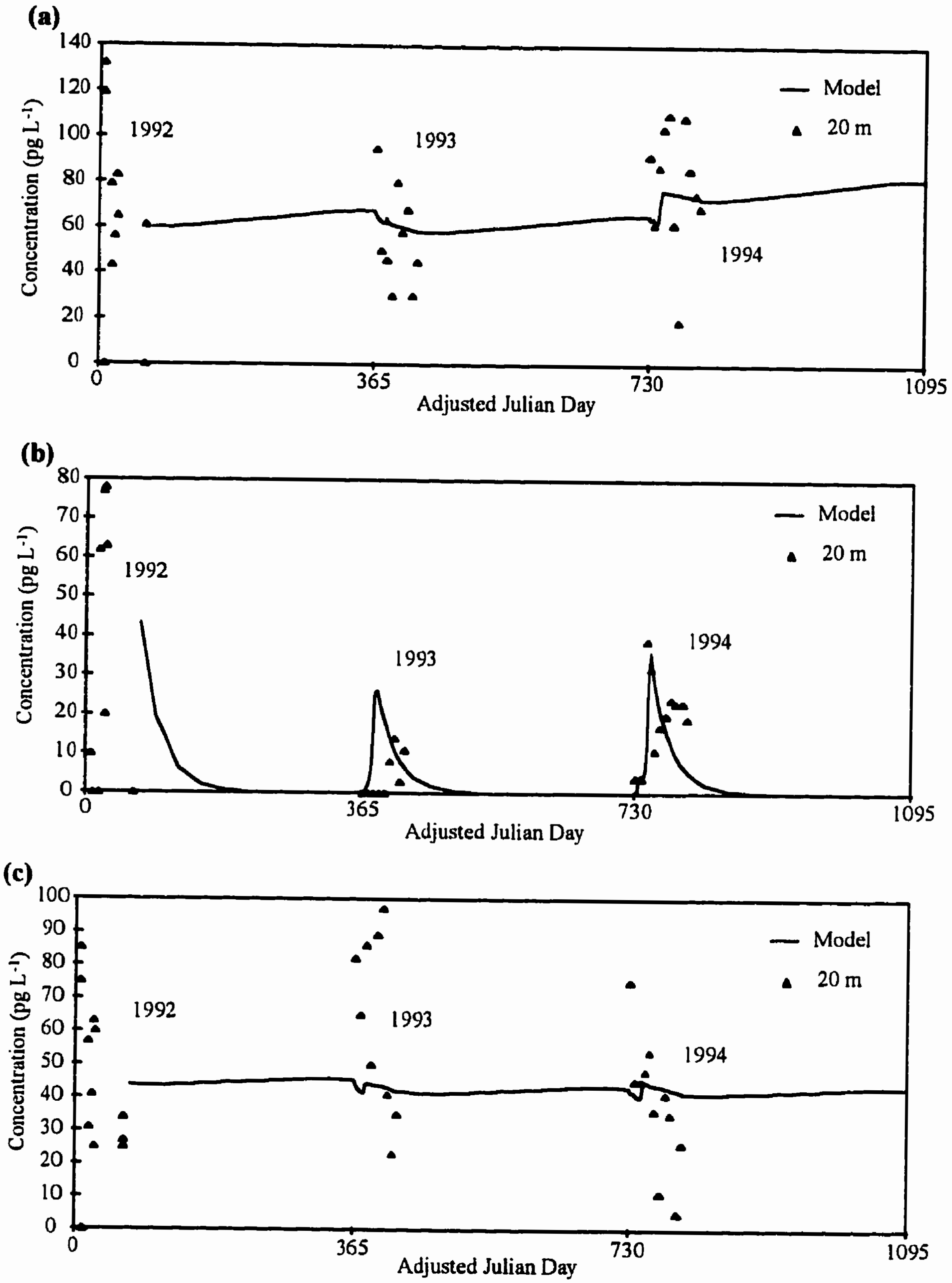

Figure 5.12: 1992 to 1994 modeled and measured concentrations in Amituk Lake for (a) dieldrin, (b) endosulfan I and (c) heptachlor epoxide

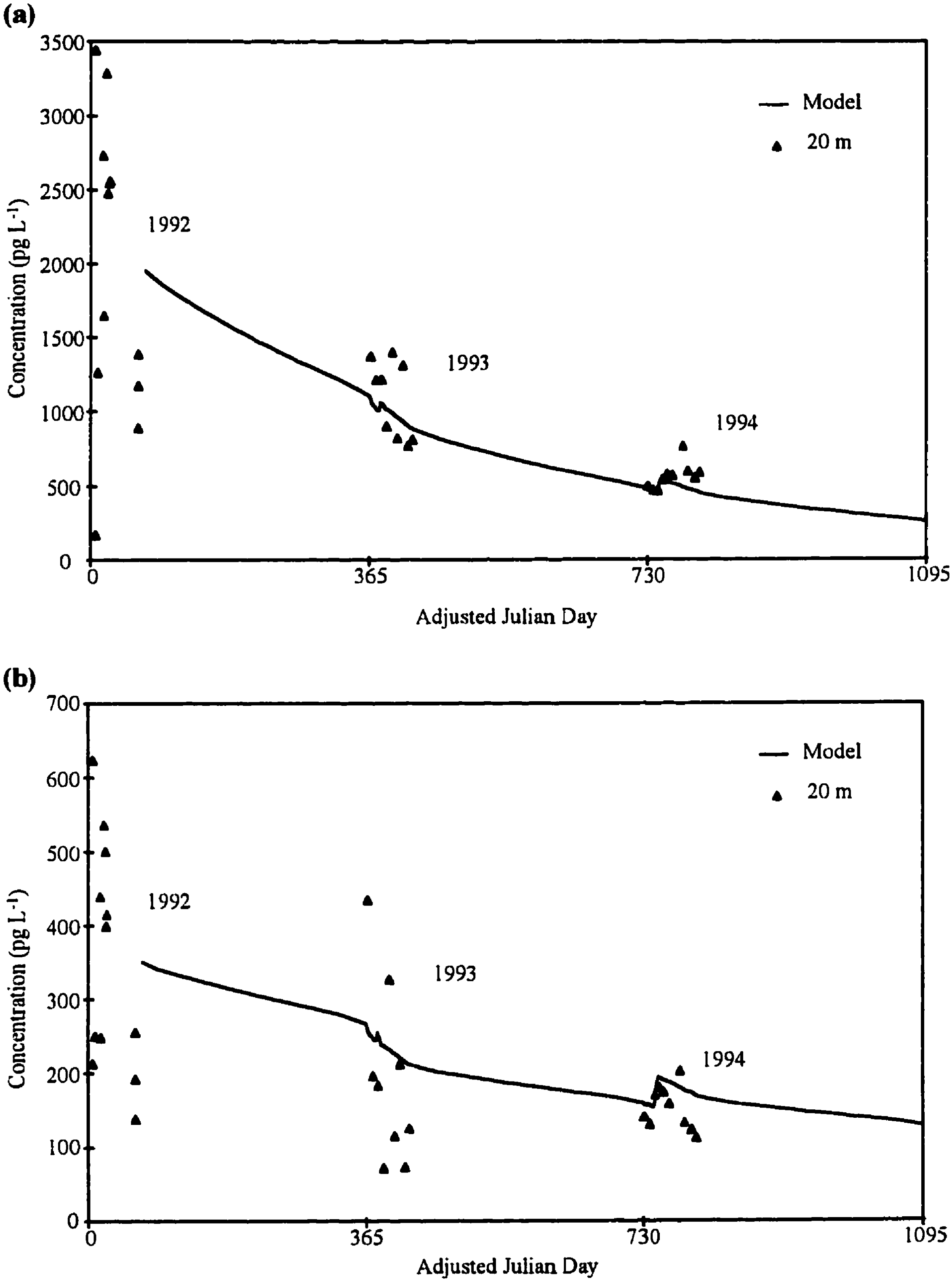

Figure 5.13: 1992 to 1994 modeled and measured concentrations in Amituk Lake for (a) α-HCH and (b) γ-HCH

since the solids-water interfacial area (the presumed site of degradation) is greater in the lake than in the ocean. The lake results are also more consistent with those of Buser and Müller (1995), who found γ-HCH to be the more rapidly degraded isomer in a sewage sludge, than the slow degradation noted in the Arctic Ocean. The half-life estimated for heptachlor epoxide for the steady-state model (50 000 h) allowed accurate prediction of annual lake concentrations (Figure 5.12 (c)) and is 30 times greater than the value listed in Table 4.3 obtained from literature (Mackay et al., 1997). Endosulfan I loaded to the lake each year was rapidly degraded over winter (Figure 5.12 (b)).

Export of chemical from the water column remained the dominant loss process for all chemicals, except for α-HCH, γ-HCH and endosulfan I where degradation was dominant. However, this conclusion is qualified by the underprediction of the outflow flux by the model. The predicted influence of air-water gas exchange on loadings and losses from the lake were greatly diminished by using the time-variable throughflow fraction as a means of simulating lake mixing. Sediment exchange and degradation processes were high relative to the steady-state model and sediment concentrations were sensitive to initial values which are relatively uncertain.

The unsteady-state model accounted for variations in seasonal loadings on an annual scale, supporting the findings of the steady-state model and of Freitas et al. (1994, 1997) that inflow loadings and export drive contaminant dynamics. The exercise of developing the unsteady-state model revealed the importance of the sub-ice layer to contaminant dynamics, particularly for export fluxes. The model proved most useful for estimating degradation rates, which were found to be considerably faster for α- and γ-HCH than those reported for Eastern Arctic Ocean water. The estimated rate for heptachlor epoxide was much slower than values reported for system-specific temperate conditions. Overall, the model captured annual and year-to-year patterns and confirmed the earlier conclusion that arctic lakes behave as chemical conduits rather than chemical sinks for most contaminants. The model clearly showed the rapid response of the water column to annual loading changes, as explored further below.

5.2.4 Lake Response to Loading Reductions

The ability of the model to account for variations in input values and provide sufficient estimates of lake concentrations suggests that processes governing contaminant fate within the lake have been adequately described. Thus the model can be used to predict contaminant levels in the lake in response to reduced or eliminated loadings, providing an indication of the ability of the lake to recover from elevated loadings.

To evaluate contaminant levels in Amituk Lake under reduced loadings, the model was initialized with June 1994 chemical concentrations and loadings, then executed over several years with loadings set to zero or halved every year from 1994 levels. Endosulfan I is not shown as concentrations in the lake rapidly approach zero after summer loading ends. The response of lake and sediment concentrations to halved and eliminated loadings for selected compounds are presented in Figure 5.14 while predicted lake concentrations under zero loadings are illustrated for each compound in Figure 5.15.

Lake concentrations responded quickly to reductions in lake loadings as indicated by previous results, declining more rapidly when loadings were eliminated. The difference is greatest for the first year after which loadings were halved and eliminated. This highlights the role of export of chemical from the lake with the dilute meltwaters. However, in terms of overall persistence, similar results were obtained under both loading regimes. For α-HCH (Figure 5.14 (a)), lake concentrations approach zero three years after loadings are eliminated and after 5 years under the reduced loadings regime. Dieldrin and Σ-PCB (Figure 5.14 (b, c)) were more persistent than α-HCH, approaching stable lake concentrations maintained by sediment contributions after 7 or 8 years.

Sediment concentrations decreased more slowly than water concentrations with little difference resulting from the two loading scenarios (Figure 5.14). α-HCH sediment concentrations declined rapidly due to degradation while dieldrin and Σ-PCB showed a gradual linear decrease. However, no indication of PCB degradation down core was observed for arctic lake sediments (Muir et al., 1996b) and the transformation half-life for DDT to DDD was 74 ± 45 years in Amituk Lake sediments (Muir et al., 1995), suggesting degradation effects may be less important to sediment concentrations than predicted.

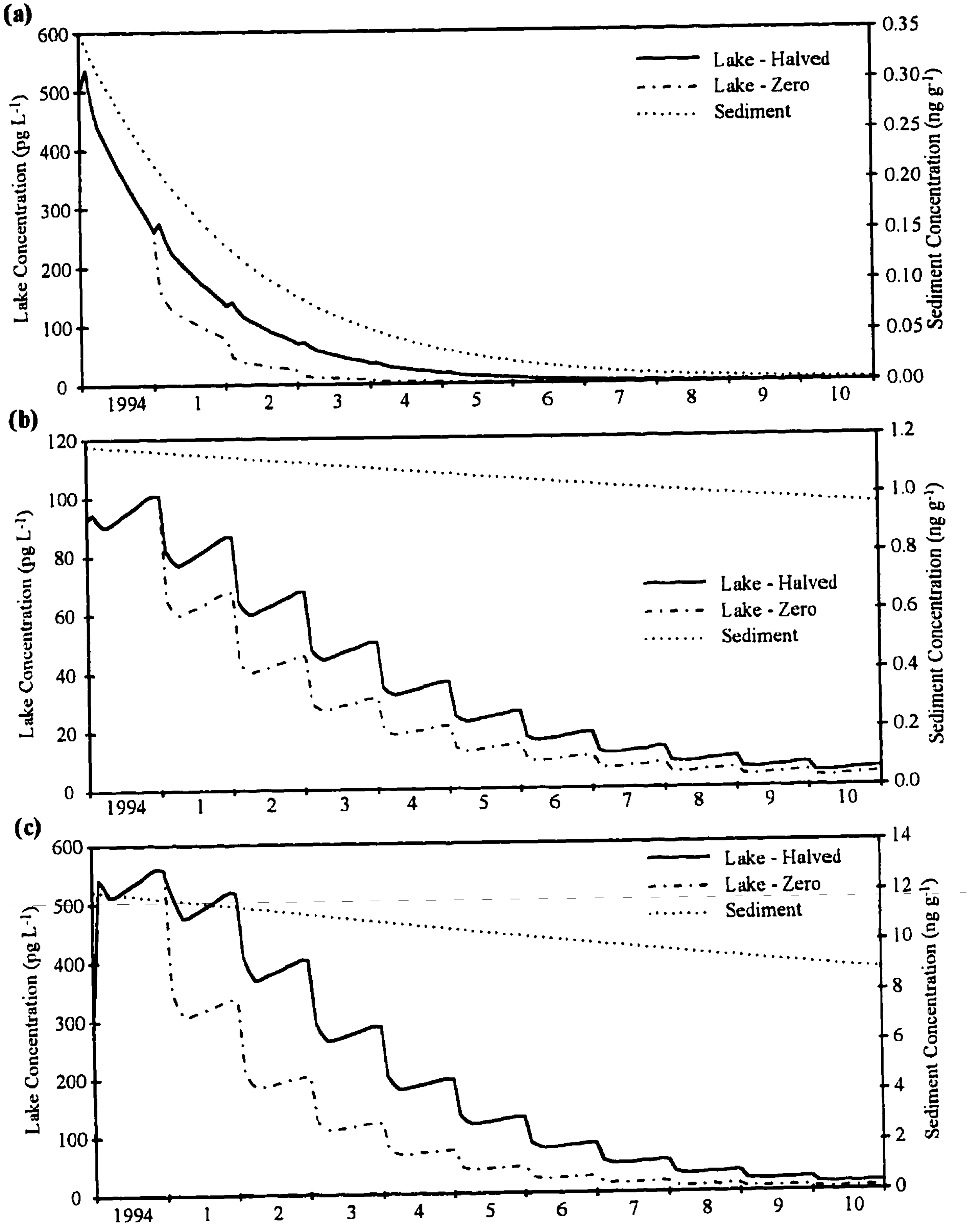

Figure 5.14: Predicted lake and sediment concentrations under reduced and eliminated loading regimes for (a) α-HCH, (b) dieldrin and (c) Σ-PCB for 10 years after 1994 loadings

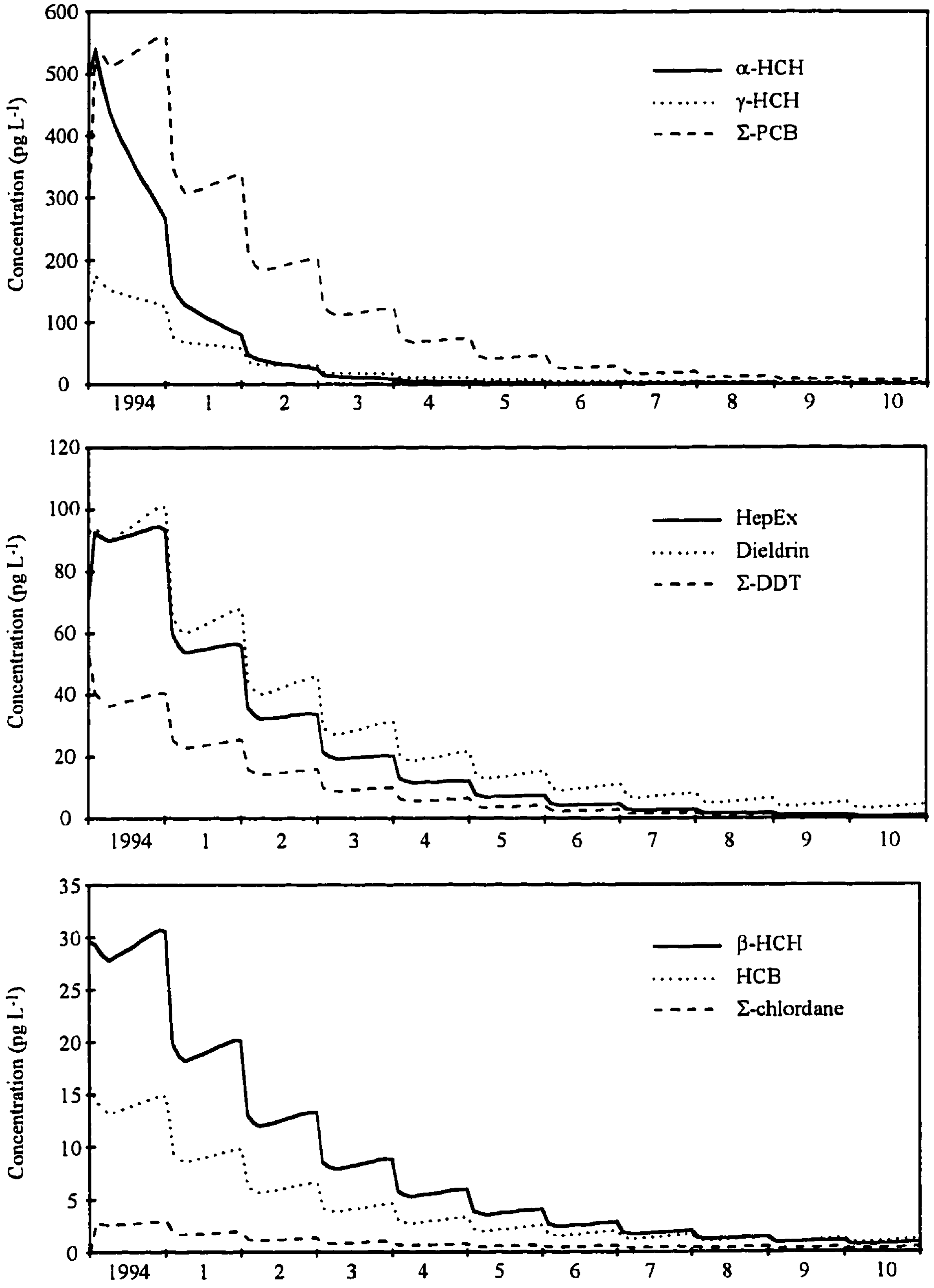

Figure 5.15: Predicted lake concentrations for 1994 loadings followed by zero loadings for ten years

Predicted concentrations for each chemical approached zero or a stable level maintained by the sediment inventory within 6 years of elimination of loadings (Figure 5.15). α- and γ-HCH were the least persistent as they were influence by both degradation and export with each snowmelt event. The remaining compounds were predominantly affected by export, as illustrated by the dramatic drop in concentrations with snowmelt inflow after over-winter cryoconcentration. Chemical concentrations and behaviour in the sediments become important as lake concentrations approach constant values. However, updated sediment information is required to estimate these levels.

5.3 Summary

The steady-state model estimates of OC concentrations in Amituk Lake were generally accurate within one standard deviation of average measured values. The relative importance of inflowing chemical loadings and export via the outflow support the conclusions of Freitas et al. (1994, 1997) that arctic lakes act as conduits for contaminants and respond rapidly to changes in loadings. This research strengthens these conclusions using 1993 and 1994 loadings, that again illustrated the rapid response of water column concentrations to inflow loadings. Air-water gas exchange was found to be an important process for HCB and Σ-chlordane and varied as loadings declined. This was evident in the reversal of the net flux from volatilization to absorption for α-HCH as inflow loadings and lake concentrations declined from 1993 to 1994. Model results also indicated that degradation is an important process in Amituk Lake, accounting for about 10% of losses for Σ-DDT and Σ-PCB to 90% for endosulfan I. Model estimates were improved by increasing and decreasing degradation half-lives for heptachlor epoxide and γ-HCH, respectively, relative to those reported in the literature. A sensitivity analysis indicated that the model estimates of lake concentrations were quite robust to uncertainty in physico-chemical properties and system-specific characteristics. Chemical concentrations in the inflow were most influential.

The unsteady-state model incorporates temporal-variation in lake mixing, ice cover, stream discharges and concentrations, and year-round degradation. Estimated summer lake concentrations compared well with measured values for 1993 and 1994, suggesting that annual loadings and over-winter processes were adequately described. Lake concentrations typically increased over winter due to cryoconcentration, then rapidly declined due to dilution from ice melt and meltwater inflow. After this, lake concentrations increased for compounds preferentially eluting from the snowpack (e.g. HCHs, endosulfan I). Examination of the mixing regime of Amituk Lake using the model revealed that the formation of a sub-ice layer of stream water caused a lag in the appearance of elevated OC concentrations in the outflow, indicating that a two-compartment treatment of the water column may more accurately describe lake dynamics. The throughflow parameter accounted for increases in lake concentrations by simulating the injection of meltwater below the sub-ice layer during peak melt. The model has proved most useful for estimating degradation rates, e.g. α-HCH, γ-HCH and heptachlor epoxide. The model was also useful for highlighting the rapid response of the lake to loading reductions with lake concentrations stabilizing within 6 years, after which water concentrations were maintained by the sediments that respond very slowly to loading changes.

6. Conclusions and Recommendations

6.1 Conclusions

The following conclusions have been drawn from the study of α-HCH degradation within arctic watersheds and modeling the fate of a suite of organochlorine chemicals in one of those systems, Amituk Lake.

α-HCH degradation study:

- Enantiomer ratios declined from a racemic value in snow to as low as 0.35 in headwater streams by the end of summer in 1994, substantiating the previous results of Falconer et al. (1995a) and indicating that microbial degradation may reduce contaminant loadings to arctic lakes from the snowpack.

- Warming stream temperatures and increasing chemical contact time with substrates supporting microbial populations, indicated by correlations of ERs with stream discharges and parameters indicating chemical weathering, were found to influence the extent of degradation. The biological productivity of the substrate was also positively correlated with enantioselective degradation.

- Approximately 7% of total α-HCH was estimated to be enantioselectively degraded prior to entering Amituk Lake, most of which was degraded when stream burdens and ERs were high during peak melt rather than late in the summer when ERs were low. This estimate is a lower limit of the amount biologically degraded due to the assumption that only one enantiomer degrades when in fact both do but with differing rates.

- Mixing of the sub-ice layer with the lake water column during the melt period was limited, as indicated by high α-HCH concentrations and ERs at 3 m depth and in the outflow that were characteristic of inflow contributions. Limited mixing of inflowing waters with elevated ERs and lake water accounted for the observed increase in lake ERs later in the summer after peak inflow.

- Over-winter degradation within Amituk Lake was indicated by the depleted ER and concentrations measured at 40 m depth prior to snowmelt and suggests that the sediment-water interface may be the site of degradation.

- The loss of α-HCH from the lake over the winter from August, 1993 to June 15, 1994 is attributed to microbial degradation (50%) and hydrolysis (2%), with a combined degradation rate of 0.80 y^{-1}. Most of this degradation was non-enantioselective.

- Lake ERs decrease with increasing water residence times in Amituk, Char and Meretta Lakes, supporting the occurrence of within lake enantioselective degradation.

OC modeling study of Amituk Lake:

- Steady-state and unsteady-state models estimated lake concentrations of 10 OCs and PCB homologs (steady-state model only) to within 1 to 1.5 standard deviations of measured values.

- The unsteady-state model estimates of lake concentrations reproduced measured values within a year and year-to-year from 1992 to 1994.

- Lake concentrations were accurately predicted by the steady-state model with inflow loadings and chemical export as the dominant fate processes, supporting conclusions drawn by Freitas and co-workers (1994; 1997) that arctic lakes act as conduits rather than sinks for chemicals.

- Steady-state model results indicated that degradation losses accounted for 10 to 90% of losses for α-HCH, endosulfan I, Σ-chlordane, Σ-DDT and Σ-PCB.

- Modeled lake concentrations responded rapidly to variations in loadings. Water concentrations are predicted to fall within 6 years in response to loading reductions, however sediment concentrations will remain elevated for a prolonged time period.

- Lake mixing and the formation of a sub-ice layer influenced the amount of chemical entering the lake. A time-dependent mixing parameter was assigned to approximate this phenomenon. Consequently, the unsteady-state model results indicated the chemical-dependent throughflow of 38 to 45% of chemical entering the lake.

- Estimated degradation half-lives of 11 000 h (rate of 0.55 y^{-1}) and 50 000 h (0.12 y^{-1}) for γ-HCH and heptachlor epoxide, respectively, accounted for yearly variation in measured lake concentrations.

6.2 Recommendations

The importance of degradation to contaminant fate, identified by field studies for α-HCH and substantiated by model results, indicates that further understanding of this phenomenon under arctic conditions is required. In addition, improvements to the whole lake model are recommended in order to improve estimates of chemical fate. Specifically, the following further research efforts are recommended:

1. Investigation and identification of the microbial population and substrates responsible for α-HCH degradation. Determining degradation rates under varying environmental conditions would be useful for estimates of contaminant fate.

2. The model indicates that knowledge of degradation is important in predicting contaminant fate for γ-HCH, endosulfan I, and heptachlor epoxide. Based on these results, and the importance of α-HCH degradation, it is recommended that degradation losses in arctic systems be investigated for OC compounds of concern.

3. The sub-ice layer that forms from inflowing water influences lake mixing and loadings, and thus contaminant fate processes. It is recommended that an additional water compartment be added to the lake model to account for the effects of this layer on water column concentrations and chemical export.

4. Historical inventories in lake sediments are included in reported sediment concentrations for arctic lakes, even in the top 1 cm sediment core slice. Separation of the sediment compartment into two layers, a thin active layer subject to lake processes and a deeper layer containing past chemical burdens, is recommended to more accurately describe the influence of sediments on lake concentrations and chemical persistence.

References

Addison, R.F. and Brodie, P.F. (1973) Occurrence of DDT residues in beluga whales (*Delphinapterus leucas*) from the Mackenzie Delta, N.W.T. J. Fish. Res. Board Can., 30, 1733-1736.

Addison, R.F. and Smith, T.G. (1974) Organochlorine residue levels in Arctic ringed seals: variation with age and sex. Oikos, 25, 335-337.

Alaee, M., Backus, S., Gregor, D. and Swyripa, M. (1995) Enantiomeric ratios of α-HCH in waters from Yukon and Mackenzie Rivers in Western Canadian Arctic. Paper presented at Second World Congress, Soc. for Environ. Toxicol. and Chem., Vancouver, B.C., Canada, 1995.

Alaee, M., Moore, L., Wilkinson, R.J., Spencer, C. and Stephens, G. (1997a) Enantiomeric ratios of α-hexachlorocyclohexane (HCH) in water from the Great Slave Lake, NWT. Organohalogen Compd., 31, 282-285.

Alaee, M. (1997b) A study of the sources and fate of organochlorine contaminants in Yukon River basin. In: Jensen, J. (Ed), Synopsis of Research Conducted Under the 1995/97 Northern Contaminants Program. Indian and Northern Affairs Canada, Environmental Studies No. 72, QS-8573-000-EF-A1, Cat. No., R71-19/74-1997E, 9-17.

Atkinson, R. (1987) A structure-activity relationship for the estimation of rate constants for the gas-phase reactions of OH radicals with organic compounds. Int. J. Chem. Kinet., 19, 799-828.

Atlas, E. and Giam, C.S. (1988) Ambient concentrations and precipitation scavenging of atmospheric organic pollutants. Water, Air, Soil Pollut., 39, 19-36.

Bachmann, A., Walet, P., Wijnen, P., de Bruin, W., Huntjens, L.M., Roelofsen, W. and Zehnder, A.J.B. (1988a) Biodegradation of alpha- and beta-hexachlorocyclohexane in a soil slurry under different redox conditions. Appl. Environ. Microbiol., 54, 143-149.

Bachmann, A., de Bruin, W., Jumelet, J.C., Rijnaarts, H.H.N. and Zehnder, A.J.B. (1988b) Aerobic biomineralization of alpha-hexachlorocyclohexane in contaminated soil. Appl. Environ. Microbiol., 54, 548-554.

Barrie, L.A., Hoff, R.M. and Daggupaty, S.M (1981) The influence of mid-latitudinal pollution sources on haze in the Canadian Arctic. Atmos. Environ., 15, 1407-1419.

Barrie, L.A. (1986) Arctic air pollution: an overview of current knowledge. Atmos. Environ., 20, 643-663.

Barrie, L.A., Gregor, D., Hargrave, B., Lake, R., Muir, D., Shearer, R., Tracey, B. and Bidleman, T. (1992) Arctic contaminants: sources, occurrence and pathways. Sci. Total Environ., 122, 1-74.

Barrie, L., Macdonald, R., Bidleman, T., Diamond, M., Gregor, D., Semkin, R., Strachan, W., Alaee, M., Backus, S., Bewers, M., Gobeil, C., Halsall, C., Hoff, J., Li, A., Lockhart, L., Mackay, D., Muir, D., Pudykiewicz, J., Reimer, K., Smith, J., Stern, G., Schroeder, W., Wagemann, R., Wania, F. and Yunker, M. (1997) Chapter 2. Sources, Occurrence and Pathways. In: Jensen, J., Adare, K. and Shearer, R. (Eds), Canadian Arctic Contaminants Assessment Report, Indian and Northern Affairs Canada, Ottawa, 1997.

Benezet, H.J. and Matsumura, F. (1973) Isomerization of γ-BHC to α-BHC in the environment. Nature, 243, 480-481.

Bergmann, M.A. and Welch, H.E. (1985) Spring meltwater mixing in small Arctic lakes. Can. J. Fish. Aquat. Sci., 42, 1789-1798.

Bidleman, T.F., Patton, G.W., Walla, M.D., Hargrave, B.T., Vass, W.P., Erickson, P., Fowler, B., Scott, V. and Gregor, D.J. (1989) Supply of chlorinated camphenes to Arctic Ocean fauna by atmospheric transport. Arctic, 42, 307-313.

Bidleman, T.F., Falconer, R.L and Walla, M.D. (1995a) Toxaphene and other organochlorine compounds in air and water at Resolute Bay, N.W.T, Canada. Sci. Total Environ., 160/161, 55-63.

Bidleman, T.F., Jantunen, L.M., Falconer, R.L. and Barrie, L.A. (1995b) Decline of hexachlorocyclohexane in the arctic atmosphere and reversal of air-sea gas exchange. Geophys. Res. Lett., 22, 219-222.

Bidleman, T.F., Jantunen, L.M.M., Wiberg, K., Harner, T., Brice, K.A., Su, K., Falconer, R.L., Leone, A.D., Aigner, E.J. and Parkhurst, W.J. (1998) Soil as a source of atmospheric heptachlor epoxide. Environ. Sci. Technol., 32, 1546-1548.

Bowes, G.W. and Jonkel, C.J. (1975) Presence and distribution of polychlorinated biphenyls (PCB) in Arctic and subarctic marine food chains. J. Fish. Res. Board Can., 32, 2111-2123.

Bright, D.A., Dushenko, W.T., Grundy, S.L. and Reimer, K.J. (1995) Evidence for short-range transport of polychlorinated biphenyls in the Canadian Arctic using congener signatures of PCBs in soils. Sci. Total Environ., 160/161, 251-263.

Brown, N.J. and Brown, A.W.A. (1970) Biological fate of DDT in a sub-Arctic environment. J. Wildl. Manage., 34, 929-940.

Brubaker, Jr., W.W. and Hites, R.A. (1998) OH reaction kinetics of gas-phase α- and γ-hexachlorocyclohexane and hexachlorobenzene. Environ. Sci. Technol., 32, 766-769.

Buser, H.-R. and Müller, M.D. (1995) Isomer and enantioselective degradation of hexachlorocyclohexane isomers in sewage sludge under aerobic conditions. Environ. Sci. Technol., 29, 664-672.

Calamari, D., Bacci, E., Focardi, S., Gaggi, C., Morosini, M. and Vighi, M. (1991) Role of plant biomass in the global environmental partitioning of chlorinated hydrocarbons. Environ. Sci. Technol., 25, 1489-1495.

Cohen, Y., Ed. (1986) Pollutants in a Multimedia Environment. Plenum Press, New York.

Clausen, J., Braestrup, L. and Berg, O. (1974) The content of polychlorinated hydrocarbons in Arctic mammals. Bull. Environ. Contamin. Toxicol., 12, 529-534.

de March, L. (1975) Nutrient budgets for a high Arctic lake (Char Lake, N.W.T.). Verh. Internat. Verein. Limnol., 19, 496-503.

de March, L. (1978) Permanent sedimentation of nitrogen, phosphorous, and organic carbon in a high Arctic lake. J. Fish. Res. Board Can., 35, 1089-1094.

Deo, P.G., Karanth, N.G. and Karanth, N.G. (1994) Biodegradation of hexachlorocyclohexane isomers in soil and food environment. Crit. Rev. Microbiol., 20, 57-78.

Dewailly, E., Nantel, A., Weber, J.-P. and Meyer, F. (1989) High levels of PCBs in breast milk of Inuit women from Arctic Quebec. Bull. Environ. Contamin. Toxicol., 43, 641-646.

Dewailly, E., Ayotte, P., Laliberte, C., Muir, D.C.G. and Norstrom, R.J. (1994) Human exposure to polychlorinated biphenyls through the aquatic food chain in the Arctic. Environ. Health Perspect., 101, 618-620.

Environment Canada (1990) The Climates of Canada. Ottawa, Canada.

Falconer, R.L. and Bidleman, T.F. (1994) Vapor pressures and predicted particle/gas distributions of polychlorinated biphenyl congeners as functions of temperature and ortho-chlorine substitution. Atmospheric Environ., 28, 547-554.

Falconer, R.L., Bidleman, T.F., Gregor, D.J., Semkin, R. and Teixeira, C. (1995a) Enantioselective breakdown of α-hexachlorocyclohexane in a small arctic lake and its watershed. Environ. Sci. Technol., 29, 1297-1302.

Falconer, R.L., Bidleman, T.F. and Gregor, D.J. (1995b) Air-water gas exchange and evidence for metabolism of hexachlorocyclohexanes in Resolute Bay, N.W.T. Sci. Total Environ., 160/161.

Faller, J., Hühnerfuss, H., König, W.A., Krebber, R. and Ludwig, P. (1991a) Do marine bacteria degrade α-hexachlorocyclohexane stereoselectively? Environ. Sci. Technol., 25, 676-678.

Faller, J., Hühnerfuss, H., König, W.A. and Ludwig, P. (1991b) Gas chromatographic separation of the enantiomers of marine organic pollutants. Distribution of α-HCH enantiomers in the North Sea. Mar. Pollut. Bull., 22, 82-86.

Fellin, P., Barrie, L.A., Dougherty, D., Toom, D., Muir, D., Grift, N., Lockhart, L. and Billeck, B. (1996) Air monitoring in the Arctic: results for selected persistent organic pollutants for 1992. Environ. Toxicol. Chem., 15, 253-261.

Finizio, A., Bidleman, T.F. and Szeto, S.Y. (1998) Emission of chiral pesticides from an agricultural soil in the Fraser Valley, British Columbia. Chemosphere, 36, 345-355.

Freitas, H. (1994) A preliminary mass balance model for describing the fate of organochlorines and mercury in Arctic lakes. M.A.Sc. thesis, University of Toronto, Toronto, Ontario, 124 pp + appendices.

Freitas, H., Diamond, M., Semkin, R. and Gregor, D. (1997) Contaminant fate in high Arctic lakes: development and application of a mass balance model. Sci. Total Environ., 201, 171-187.

Gregor, D.J., Peters, A.J., Teixeira, C., Jones, N., and Spencer, C. (1995) The historical residue trend of PCBs in the Agassiz Ice Cap, Ellesmere Island, Canada. Sci. Total Environ., 160/161, 117-126.

Halsall, C.J., Bailey, R., Stern, G.A., Barrie, L.A., Fellin, P., Muir, D.C.G., Rosenberg, B., Rovinsky, F.Ya., Kononov, E.Ya. and Pastukhov, B. (1998) Multi-year observations of organohalogen pesticides in the arctic atmosphere. Environ. Pollut., 102, 51-62.

Hambrey, M. (1994) Glacial Environments. UBC Press, Vancouver, p. 176.

Hargrave, B.T., Vass, W.P., Erickson, P.E. and Fowler, P.R. (1988) Atmospheric transport of organochlorines to the Arctic Ocean. Tellus, 40B, 480-493.

Hargrave, B.T., Barrie, L.A., Bidleman, T.F. and Welch, H.E. (1997) Seasonality in exchange of organochlorines between arctic air and seawater. Environ. Sci. Technol., 31, 3258-3266.

Haugen, J.-E., Wania, F., Ritter, N. and Schlabach, M. (1998) Hexachlorocyclohexanes in air in Southern Norway. Temporal variation, source allocation, and temperature dependence. Environ. Sci. Technol. 32, 217-224.

Harner, T., Kylin, H., Bidleman, T.F. and Strachan, W.M.J. (1999) Removal of α- and γ-hexachlorocyclohexane and enantiomers of α-hexachlorocyclohexane in the Eastern Arctic Ocean. Environ. Sci. Technol., in press.

Heron, R. (1985) Decay of a High Arctic Lake Ice Cover. Ph.D. thesis, McMaster University, Hamilton, Ontario, 189 pp.

Hinckley, D.A., Bidleman, T.F., Foreman, W.T. and Tuschall, J.R. (1990) Determination of vapor pressures for nonpolar and semipolar organic compounds from gas chromatographic retention data. J. Chem. Eng. Data, 35, 232-237.

Hinckley, D.A., Bidleman, T.F. and Rice, C.P. (1991) Atmospheric organochlorine pollutants and air-sea exchange of hexachlorocyclohexane in the Bering and Chukchi Seas. J. Geophys. Res., 96, 7201-7213.

Hobbie, J.E. (1973) Arctic limnology: a review. In: M.E. Britton (ed.), Alaskan Arctic Tundra, Tech. Paper No. 25. Arctic Inst. of N. America, pp. 127-168.

Hobbie, J.E. (1984) Polar limnology. In: F.B. Taub (ed.) Ecosystems of the World 23: Lakes and Reservoirs. Elsevier, Amsterdam, pp. 63-105.

Hoff, R.M. and Chan, K.W. (1986) Atmospheric concentrations of chlordane at Mould Bay, N.W.T., Canada. Chemosphere, 15, 449-452.

Holden, A.V. (1970) Monitoring organochlorine contamination of the marine environment by the analysis of residues in seals. In: M. Ruivo (Ed.) (1972) Marine Pollution and Sea Life. Fishing News (Books) Ltd., England, pp. 266-272.

Hov, O., Penkett, S.A., Isaksen, I.S.A. and Semb, A. (1984) Organic gases in the Norwegian Arctic. Geophys. Res. Lett., 11, 425-428.

Hühnerfuss, H., Faller, J., König, W.A. and Ludwig, P. (1992) Gas chromatographic separation of the enantiomers of marine pollutants. 4. Fate of hexachlorocyclohexane isomers in the Baltic and North Sea. Environ. Sci. Technol., 26, 2127-2133.

Hummert, K., Vetter, W. and Luckas, B. (1995) Levels of alpha-HCH, lindane, and enantiomeric ratios of alpha-HCH in marine mammals from the northern hemisphere. Chemosphere, 31, 3489-3500.

Inland Waters Directorate (1979) Analytical Methods Manual. Water Quality Branch, Environment Canada, Ottawa.

Iverson, T. (1984) On the atmospheric transport of pollution to the Arctic. Geophys. Res. Lett., 11, 457-460.

IPCS (International Programme on Chemical Safety) (1992) Environmental Health Criteria 123: Alpha- and Beta-hexachlorocyclohexanes. World Health Organization, Geneva.

Iwata, H., Tanabe, S., Sakai, N. and Tatsukawa, R. (1993) Distribution of persistent organochlorines in the ocean air and seawater and the role of ocean on their global transport and fate. Environ. Sci. Technol., 27, 1080-1098.

Iwata, H., Tanabe, S., Iida, T., Baba, N., Ludwig, J.P. and Tatsukawa, R. (1998) Enantioselective accumulation of α-hexachlorocyclohexane in northern fur seals and double-breasted cormorants: effects of biological and ecological factors in the higher trophic levels. Environ. Sci. Technol., 32, 2244-2249.

Jantunen, L.M. and Bidleman, T.F. (1995) Reversal of the air-water gas exchange direction of hexachlorocyclohexanes in the Bering and Chukchi Seas: 1993 versus 1988. Environ. Sci. Technol., 29, 1081-1089.

Jantunen, L.M. and Bidleman, T.F. (1996) Air-water gas exchange of hexachlorocyclohexanes (HCHs) and the enantiomers of α-HCH in arctic regions. J. Geophys. Res., 101, 28837-28846.

Jantunen, L.M. and Bidleman, T.F. (1997) Correction to "Air-water gas exchange of hexachlorocyclohexanes (HCHs) and the enantiomers of α-HCH in arctic regions." J. Geophys. Res., 102, 19279-19282.

Jantunen, L.M. and Bidleman, T.F. (1998) Organochlorine pesticides and enantiomers of chiral pesticides in Arctic Ocean water. Arch. Environ. Contam. Toxicol., in press.

Jensen, J., Adare, K. and Shearer, R. (Eds) (1997) Canadian Arctic Contaminants Assessment Report. Indian and Northern Affairs Canada, Ottawa.

Johri, A.K., Dua, M., Tuteja, D., Saxena, R. and Lal, R. (1996) Genetic manipulations of microorganisms for the degradation of hexachlorocyclohexane. FEMS Microbiol. Rev., 19, 69-84.

Joranger, E. and Ottar, B. (1984) Air pollution studies in the Norwegian Arctic. Geophys. Res. Lett., 11, 365-368.

Kalff, J. and Welch, H.E. (1974) Phytoplankton production in Char Lake, a natural polar lake, and in Meretta Lake, a polluted polar lake, Cornwallis Island, Northwest Territories. J. Fish. Res. Board Can., 31, 621-636.

Kawano, M., Inoue, T., Wada, T., Hidaka, H. and Tatsukawa, R. (1988) Bioconcentration and residue patterns of chlordane compounds in marine animals: invertebrates, fish, mammals, and seabirds. Environ. Sci. Technol., 22, 792-797.

Khalil, M.A.K. and Rasmussen, R.A. (1983) Gaseous tracers of Arctic haze. Environ. Sci. Technol., 17, 157-164.

Kinloch, D., Kuhnlein, H. and Muir, D.C.G. (1992) Inuit foods and diet: a preliminary assessment of benefits and risks. Sci. Total Environ., 122, 247-278.

Kinney, S.P. (1997) A physically-based hydrologic model of a high arctic watershed and evaluation using isotope tracers. M.Sc. thesis, University of Waterloo, Waterloo, Ontario, 96 pp. + appendices.

Kucklick, J.R., Hinckley, D.A. and Bidleman, T.F. (1991) Determination of Henry's Law constants for hexachlorocyclohexanes in distilled water and artificial seawater as a function of temperature. Marine Chemistry 34, 197-209.

Kwok, E.S. and Atkinson, R. (1995) Estimation of hydroxyl radical reaction rate constants for gas-phase organic compounds using a structure-reactivity relationship: an update. Atmos. Environ., 29, 1685-1695.

Li, Y.F., Bidleman, T.F., Barrie, L.A. and McConnell, L.L. (1998) Global hexachlorocyclohexane use trends and their impact on the arctic atmospheric environment. Geophys. Res. Lett., 25, 39-41.

Ludwig, P., Hühnerfuss, H., König, W.A. and Gunkel, W. (1992) Gas chromatographic separation of the enantiomers of marine pollutants. Part 3. Enantioselective degradation of α-hexachlorocyclohexane and γ-hexachlorocyclohexane by marine microorganisms. Mar. Chem. 38, 12-23.

Mackay, D. and Paterson, S. (1981) Calculating fugacity. Environ. Sci. Technol., 15, 1006-1014.

Mackay, D. and Paterson, S. (1982) Fugacity revisited. Environ. Sci. Technol., 16, 654A-660A.

Mackay, D., Paterson, S. and Joy, M. (1983) A quantitative water, air, sediment interaction (QWASI) fugacity model for describing the fate of chemicals in lakes. Chemosphere, 12, 981-997.

Mackay, D. and Diamond, M. (1989) Application of the QWASI (quantitative water air sediment interaction) fugacity model to the dynamics of organic and inorganic chemicals in lakes. Chemosphere, 18, 1343-1365.

Mackay, D. (1991) Multimedia Environmental Models: The Fugacity Approach. Lewis Publishers, Chelsea, Michigan.

Mackay, D., Shiu, W.-Y. and Ma, K.-C. (1992) Illustrated handbook of physical-chemical properties and environmental fate for organic chemicals. Volume I. Lewis Publishers, Boca Raton.

Mackay, D., Shiu, W.-Y. and Ma, K.-C. (1997) Illustrated handbook of physical-chemical properties and environmental fate for organic chemicals. Volume V. Lewis Publishers, Boca Raton.

Malaiyandi, M. and Shah, S.M. (1984) Evidence of photoisomerization of hexachlorocyclohexane isomers in the ecosphere. J. Environ. Sci. Health, A19, 887-910.

Mitchell, M. (1956) Visual range in the polar regions with particular reference Alaskan Arctic. J. Atmos. Terr. Phys., Special Supplement, 195-211.

Möller, K. and Hühnerfuss, H. (1993) On the diversity of enzymatic degradation pathways of α-hexachlorocyclohexane as determined by chiral gas chromatography. J. High Res. Chromatog., 16, 672-673.

Morgan, K.C. and Kalff, J. (1972) Bacterial dynamics in two high-arctic lakes. Freshwat. Biol., 2, 217-228.

Mössner, S., Spraker, T.R., Becker, P.R. and Ballschmiter, K. (1992) Ratios of enantiomers of alpha-HCH and determination of alpha-, beta-, and gamma-HCH isomers in brain and other tissues of neonatal northern fur seals (Callorhinus ursinus). Chemosphere, 24, 1171-1180.

Muir, D., Norstrom, R.J. and Wagemann, R. (1986) Chlorinated hydrocarbons and heavy metals in Arctic marine mammals, fish and polar beasts; preliminary results in 1983/84 samples. Proc. Int. Conf. on Arctic Water Pollution Research: Applications of Science and Technology.

Muir, D.C.G., Grift, N.P., Ford, C.A., Reiger, A.W., Hendzel, M.R. and Lockhart, W.L. (1989) Evidence for long range transport of toxaphene to remote arctic and subarctic waters from monitoring of fish tissues. In: Kurtz, D. (Ed.) Long Range Atmospheric Transport of Pesticides. Lewis Publishers, Chelsea, Michigan.

Muir, D.C.G., Ford, C.A., Grift, N.P., Metner, D.A. and Lockhart, W.L. (1990) Geographic variation of chlorinated hydrocarbons in burbot (*Lota lota*) from remote lakes and rivers in Canada. Arch. Environ. Contam. Toxicol., 19, 530-542.

Muir, D.C.G., Wagemann, R., Hargrave, B.T., Thomas, D.J., Peakall, D.B. and Norstrom, R.J. (1992) Arctic marine ecosystem contamination. Sci. Total Environ., 122, 75-134.

Muir, D.C.G., Grift, N.P., Lockhart, W.L., Wilkinson, P., Billeck, B.N. and Brunskill, G.J. (1995) Spatial trends and historical profiles of organochlorine pesticides in Arctic lake sediments. Sci. Total Environ., 160/161, 447-457.

Muir, D., Braune, B., DeMarch, B., Norstrom, R., Wagemann, M., Gamberg, M., Poole, K., Addison, R., Bright, D., Dodd, M., Duschenko, W., Eamer, J., Evans, M., Elkin, B., Grundy, S., Hargrave, B., Hebert, C., Johnstone, R., Kidd, K., Koenig, B., Lockhart, L., Payne, J., Peddle, J. and Reimer, K. (1996a) Chapter 3. Ecosystem uptake and effects. In: Jensen, J., Adare, K. and Shearer, R. (Eds), Canadian Arctic Contaminants Assessment Report, Indian and Northern Affairs Canada, Ottawa, 1997.

Muir, D.C.G., Omelchenko, A., Grift, N.P., Savoie, D.A., Lockhart, W.L., Wilkinson, P. and Brunskill, G.J. (1996b) Spatial trends and historical deposition of polychlorinated biphenyls in Canadian midlatitude and Arctic lake sediments. Environ. Sci. Technol., 30, 3609-3617.

Müller, M.D., Schlabach, M. and Oehme, M. (1992) Fast and precise determination of α-hexachlorocyclohexane enantiomers in environmental samples using chrial high-resolution gas chromatography. Environ. Sci. Technol., 26, 566-569.

Ngabe, B., Bidleman, T.F. and Falconer, R.L. (1993) Base hydrolysis of α- and γ-hexachlorocyclohexanes. Environ. Sci. Technol. 27, 1930-1933.

Norstrom, R.J. and Muir, D.C.G. (1994) Chlorinated hydrocarbon contaminants in arctic marine mammals. Sci. Total Environ., 154, 107-128.

Ockenden, W.A, Steinnes, E., Parker, C. and Jones, K.C. (1998a) Observations on persistent organic pollutants in plants: implications for their use as passive air samplers and for POP cycling. Environ. Sci. Technol., 32, 2721-2726.

Ockenden, W.A., Sweetman, A.J., Prest, H.F., Steinnes, E. and Jones, K.C. (1998b) Toward an understanding of the global atmospheric distribution of persistent organic pollutants: the use of semipermeamble membrane devices as time-integrated passive samplers. Environ. Sci. Technol., 32, 2795-2803.

Oehme, M. and Ottar, B. (1984) The long-range transport of polychlorinated hydrocarbons to the Arctic. Geophys. Res. Lett., 11, 1134-1136.

Ottar, B. (1981) The transfer of airborne pollutants to the Arctic region. Atmos. Environ., 15, 1439-1445.

Pacyna, J.M. and Oehme, M. (1988) Long-range transport of some organic compounds to the Norwegian Arctic. Atmos. Environ., 22, 243-257.

Paterson, S. and Mackay, D. (1985) The fugacity concept in environmental modelling. In: O. Hutzinger (Ed.) The Handbook of Environmental Chemistry, Volume 2/Part C, Springer-Verlag, Heidelberg, pp. 121-140.

Patton, G.W., Hinckley, D.A., Walla, M.D. and Bidleman, T.F. (1989) Airborne organochlorines in the Canadian High Arctic. Tellus, 41B, 243-255.

Patton, G.W., Walla, M.D., Bidleman, T.F. and Barrie, L.A. (1991) Polycyclic aromatic and organochlorine compounds in the atmosphere of Northern Ellesmere Island, Canada. J. Geophys. Res., 96, 10867-10877.

Pfaffenberger, B., Hühnerfuss, H., Kallenborn, R., Köhler-Günther, A., König, W.A. and Krüner, G. (1992) Chromatographic separation of the enantiomers of marine pollutants. Part 6: comparison of the enantioselective degradation of α-hexachlorocyclohexane in marine biota and water. Chemosphere, 25, 719-725.

Pfaffenberger, B., Hardt, I., Huhnerfuss, H., Konig, W.A., Rimkus, G., Glausch, A., Schurig, V. and Hahn, J. (1994) Enantioselective degradation of α-hexachlorocyclohexane and cyclodiene insecticides in Roe-deer liver samples from different regions of Germany. Chemosphere, 29, 1543-1554.

Rahn, K.A. and McCaffrey, R.J. (1979) Compositional differences between Arctic aerosol and snow. Nature, 280, 479-480.

Rahn, K.A. and McCaffrey, R.J. (1980) On the origin and transport of the winter Arctic aerosol. Ann. N.Y. Acad. Sci., 338, 486-503.

Rahn, K.A. and Heidam, N.Z. (1981) Progress in Arctic air chemistry, 1977-1980: a comparison of the first and second symposia. Atmos. Environ., 15, 1345-1348.

Rasmussen, R.A. and Khalil, M.A.K. (1984) Gaseous bromine in the Arctic and Arctic haze. Geophys. Res. Lett., 11, 433-436.

Ridal, J.J., Bidleman, T.F., Kerman, B., Fox, M.E. and Strachan, W.M.J. (1997) Enantiomers of α-hexachlorocyclohexane as tracers of air-water gas exchange in Lake Ontario. Environ. Sci. Technol., 31, 1940-1945.

Rigler, F.H. (1975) The Char Lake project: an introduction to limnology in the Canadian Arctic. In: T.W.M. Cameron and L.W. Billingsley (eds.) Energy Flow - Its Biological Dimensions. Royal Society of Canada, Ottawa, for the Canadian Committee for the International Biological Program, pp. 172-198.

Rittman (1994) In Situ Bioremediation. Noyes Publications, Park Ridge, N.J..

Sahu, S.K., Patnaik, K.K., Bhuyan, S., Sreedharan, B., Kurihara, N., Adhya, T.K. and Sethunathan, N. (1995) Mineralization of α-, γ-, and β- isomers of hexachlorocyclohexane by a soil bacterium under aerobic conditions. J. Agric. Food Chem., 43, 833-837.

Schindler, D.W., Welch, H.E., Kalff, J., Brunskill, G.J. and Kritsch, N. (1974a) Physical and chemical limnology of Char Lake, Cornwallis Island (75° N Lat.). J. Fish. Res. Board Can., 31, 585-607.

Schindler, D.W., Kalff, J., Welch, H.E., Brunskill, G.J., Kling, H. and Kritsch, N. (1974b) Eutrophication in the high arctic - Meretta Lake, Cornwallis Island (75° N Lat.). J. Fish. Res. Board Can., 31, 647-662.

Schindler, D.W., Kidd, K.A., Muir, D.C.G. and Lockhart, W.L. (1995) The effects of ecosystem characteristics on contaminant distribution in northern freshwater lakes. Sci. Total Environ., 160/161, 1-17.

Schroeder, W.H. and Lane, D.A. (1988) The fate of toxic airborne pollutants. Environ. Sci. Technol., 22, 240-246.

Schwarzenbach, R.P., Gschwend, P.M. and Imboden, D.M. (1993) Environmental Organic Chemistry. John Wiley and Sons, Inc., New York.

Semkin, R and Gregor, D. (1993) Processes and fluxes of contaminants in aquatic systems. In: J.L. Murray and R.G. Shearer (eds.), Synopsis of Research Conducted Under the 1992/93 Northern Contaminants Program, Environmental Studies No. 70. Department of Indian Affairs and Northern Development, Ottawa. Cat. No. R71-19/70-1993E, pp. 57-68.

Semkin, R. (1996) Processes and fluxes of contaminants in aquatic systems - 1994/95. In: J.L. Murray, R.G. Shearer and S.L. Han (eds.), Synopsis of Research Conducted Under the 1994/95 Northern Contaminants Program, Environmental Studies No. 73. Department of Indian Affairs and Northern Development, Ottawa. Cat. No. R71-19/73-1995E, pp. 105-118.

Shaw, G.E. (1975) The vertical distribution of tropospheric aerosols at Barrow, Alaska. Tellus, 27, 39-49.

Shaw, G.E. (1982) Atmospheric turbidity in the polar regions. J. Appl. Met., 21, 1080-1088.

Shearer, R. and Murray, J.L. (1997) Chapter 1. Introduction. In: Jensen, J., Adare, K., and Shearer, R. (Eds), Canadian Arctic Contaminants Assessment Report, Indian and Northern Affairs Canada, Ottawa.

Shiu, W.-Y., Wania, F., Hung, H. and Mackay, D. (1997) Temperature dependence of aqueous solubility of selected chlorobenzenes, polychlorinated biphenyls, and dibenzofuran. J. Chem. Eng. Data, 42, 293-297.

Steinwandter, H. (1976) Lindane metabolism in plants. II. Formation of α-hexachlorocyclohexane. Chemosphere, 5, 221-226.

Steinwandter, H. and Schlüter, H. (1978a) Experiments on lindane metabolism in plants. IV. A kinetic investigation. Bull. Environ. Contam. Toxicol., 20, 174-179.

Steinwandter, H. (1978b) Experiments on lindane metabolism in plants. III. Formation of β-HCH. Bull. Environ. Contamin. Toxicol., 20, 535-536.

Stern, G.A., Halsall, C.J., Barrie, L.A., Muir, D.C.G., Fellin, P., Rosenberg, B., Rovinsky, F.Ya., Kononov, E.Ya. and Pastukhov, B. (1997) Polychlorinated biphenyls in arctic air. 1. Temporal and spatial trends: 1992-1994. Environ. Sci. Technol., 31, 3619-3628.

Tanabe, S., Kumaran, P., Iwata, H., Tatsukawa, R. and Miyazaki, N. (1996) Enantiomeric ratios of α-hexachlorocyclohexane in blubber of small cetaceans. Mar. Pollut. Bull., 32, 27-31.

Thomas, D.J., Tracey, B., Marshall, H. and Norstrom, R.J. (1992) Arctic terrestrial ecosystem contamination. Sci. Total Environ., 122, 135-164.

Verta, M., Matilainen, T., Porvari, P., Niemi, M., Uusi-Rauva, A. and Bloom, N.S. (1994) Methylmercury sources in boreal lake ecosystems. In: C.J. Watras and J.W. Huckabee, Mercury pollution: integration and synthesis. Lewis Publishers, Boca Raton.

Voldner, E.C. and Li Y.-F. (1995) Global usage of selected persistent organochlorines. Sci. Total Environ., 160/161, 201-210.

Vonk, J.W. and Quirijns, J.K. (1979) Anaerobic formation of α-hexachlorocyclohexane from γ-hexachlorocyclohexane in soil and by *Escherichia coli*. Pesticide Biochemistry and Physiology, 12, 68-74.

Wania, F. (1997) Modelling the fate of non-polar organic chemicals in an ageing snowpack. Chemosphere, 35, 2345-2363.

Wania, F. and Mackay, D. (1993) Global fractionation and cold condensation of low volatility organochlorine compounds in polar regions. Ambio, 22, 10-18.

Wania, F. and Mackay, D. (1995) A global distribution model for persistent organic chemicals. Sci. Total Environ., 160/161, 211-232.

Wania, F. and Mackay, D. (1996) Tracking the Distribution of Persistent Organic Pollutants. Environ. Sci. Technol., 30, 390A-396A.

Welch, H.E. and Kalff, J. (1974) Benthic photosynthesis and respiration in Char Lake. J. Fish. Res. Board Can., 31, 609-620.

Welch, H.E. and Bergmann, M.A. (1985) Water circulation in small Arctic lakes in winter. Can. J. Fish. Aquat. Sci., 42, 506-520.

Welch, H. (1991) Comparisons between lakes and seas during the arctic winter. Arctic Alpine Res., 23, 11-23.

Whetstone, R.R., Davis, F.C. and Ballard, S.A. (1953) Interconversion of hexachlorocyclohexane isomers. J. Am. Chem. Soc., 75, 1768-1769.

Willett, K.L., Ulrich, E.M. and Hites, R.A. (1998) Differential toxicity and environmental fates of hexachlorocyclohexane isomers. Environ. Sci. Technol., 32, 2197-2207.

Woo, M.K. (1976) Hydrology of a small Canadian high Arctic basin during the snowmelt period. Catena, 3, 155-168.

Woo, M.K. (1980) Hydrology of a small lake in the Canadian high Arctic. Arctic Alpine Res., 12, 227-235.

Woo, M.K., Heron, R. and Steer, P. (1981) Catchment hydrology of a high Arctic lake. Cold Regions Sci. Technol., 5, 29-41.

Woo, M.K., Heron, R., Marsh, P. and Steer, P. (1983) Comparison of weather station snowfall with winter snow accumulation in high Arctic basins. Atmosphere-Ocean, 21, 312-325.

Woo, M.K. and Steer, P. (1982) Occurrence of surface flow on arctic slopes, southern Cornwallis Island. Can. J. Earth Sci., 19, 2368-2377.

Woo, M.K. and Steer, P. (1983) Slope hydrology as influenced by thawing of the active layer, Resolute, N.W.T.. Can. J. Earth Sci., 20, 978-986.

Appendices

Appendix A1 1994 Amituk Lake and Streams Measurements

Table A1.1: 1994 Enatiomeric Ratios and Concentrations of α-HCH in Amituk Lakes and Streams

Table A1.1: 1994 Enantiomeric Ratios and Concentrations of α-HCH in Amituk Lake and Streams

			(+)/(-) Enantiomer Ratio		Concentration	Temperature	Discharge
Site	Date	Type	BGB-172	Beta-DEX	(pg L^{-1})[1]	(°C)[1]	(m^3 s^{-1})[1]
Mud Creek	Jun. 5	s	1.01		-	-	-
	Jun. 7	s	1.01		-	-	-
	Jun. 23	w	0.72		307	3.0	0.5364
	Jul. 2	w	0.65	0.66	166	2.0	0.1748
	Jul. 6	w	0.79	0.81	192	10.0	0.0993
	Jul. 14	w	0.69		20	7.5	0.0151
	Jul. 27	w	0.69		62	6.0	0.0510
	Aug. 10	w	0.88		71	8.0	0.0068
Gorge Creek	Jun. 7	s	1.02		-	-	-
	Jun. 7	sm	0.96		-	-	-
	Jun. 24	w	1.00		2330	1.0	0.1772
	Jul. 1	w	0.95		927	0.0	2.4528
	Jul. 6	w	0.80	0.80	386	3.5	1.5855
	Jul. 15	w	0.50		273	3.0	0.0480
	Jul. 23	w	0.63		451	3.0	0.1759
	Aug. 9	w	0.36		89	4.0	0.0241
Cave Creek	Jun. 8	s	1.00		-	-	-
	Jun. 27	w	0.92		618	0.0	0.5730
	Jul. 2	w	0.91		958	0.0	0.5436
	Jul. 6	w	0.84		651	2.0	0.3677
	Jul. 15	w	0.60		440	1.5	0.0446
	Jul. 23	w	0.64	0.62	362	2.0	0.0836
	Aug. 9	w	0.65		293	1.5	0.0184
Lake - 3 m	Jun. 15	w	0.73		644	1.8	
	Jun. 22	w	0.80		794	1.7	
	Jun. 29	w	0.90		944	3.1	
	Jul. 5	w	0.88		857	2.2	
	Jul. 18	w	0.76	0.75	638	2.7	
	Jul. 25	w	0.77		583	2.4	
	Aug. 7	w	0.74		627	3.7	
Lake - 20 m	Jun. 15	w	0.74		499	2.4	
	Jun. 22	w	0.73		470	2.6	
	Jun. 29	w	0.73	0.73	469	2.6	
	Jul. 5	w	0.74		541	2.7	
	Jul. 18	w	0.76		569	2.7	
	Jul. 25	w	0.77		(143)	2.9	
	Aug. 7	w	0.76		598	3.7	
Lake - 40 m	Jun. 15	w	0.66		342	2.4	
	Jun. 22	w	0.71		626	2.5	
	Jun. 29	w	0.72		689	2.7	
	Jul. 5	w	0.73		727	2.8	
	Jul. 18	w	0.72		680	2.8	
	Jul. 25	w	0.74		693	2.9	
	Aug. 7	w	0.74		688	3.7	
Outflow	Jun. 25	w	0.83		964	3.0	1.5382
	Jul. 1	w	0.90		1069	1.5	3.5251
	Jul. 7	w	0.88		1053	4.0	2.5046
	Jul. 15	w	0.80		738	3.8	0.4831
	Jul. 23	w	0.76		674	3.0	0.3834
	Aug. 8	w	0.75		514	4.0	0.2843

s - snow; sm - snowmelt; w - water

[1] Semkin et al. (unpubl.)

Appendix A2 Linear Correlation Analysis Results - Mud and Cave Creeks

Table A2.1:	Correlation coefficients (r^2) for α-HCH ERs and concentrations, and stream discharge, temperature, and water chemistry parameters for Mud Creek in 1994
Table A2.2:	Correlation coefficients (r^2) for α-HCH ERs and concentrations, and stream discharge, temperature, and water chemistry parameters for Cave Creek in 1994

Table A2.1: Correlation coefficients (r^2) for α-HCH ERs and concentrations, and stream discharge, temperature, and water chemistry parameters for Mud Creek in 1994.

Parameter	ER	Conc.	Discharge	Temp.	SS	Cond.	Ca^{2+}	Mg^{2+}	Alkal.	NO_3-N	DOC
ER	1.00										
Concentration	0.00	1.00									
Discharge	0.06	***0.82***	1.00								
Temperature	0.43	0.19	0.40	1.00							
Suspend. Sed.	0.00	0.56	***0.85***	0.22	1.00						
Conductivity	0.20	***0.72***	0.58	0.24	0.26	1.00					
Ca^{2+}	0.24	***0.70***	***0.66***	0.43	0.33	***0.95***	1.00				
Mg^{2+}	***0.86***	***0.96***	0.16	0.20	0.46	0.57	0.31	1.00			
Alkalinity	0.21	***0.76***	***0.64***	0.27	0.29	***0.99***	***0.95***	***0.95***	1.00		
NO_3-N	0.11	0.48	0.17	0.05	0.06	0.19	0.20	0.09	0.20	1.00	
DOC	0.37	0.01	0.08	0.02	0.07	0.21	0.18	0.29	0.18	0.34	1.00

Bold italicized type - significant to $p < 0.05$

Table A2.2: Correlation coefficients (r^2) for α-HCH ERs and concentrations, and stream discharge, temperature, and water chemistry parameters for Cave Creek in 1994.

Parameter	ER	Conc.	Discharge	Temp.	SS	Cond.	Ca^{2+}	Mg^{2+}	Alkal.	NO_3-N	DOC
ER	1.00										
Concentration	***0.69***	1.00									
Discharge	***0.97***	***0.74***	1.00								
Temperature	0.52	0.44	0.58	1.00							
Suspend. Sed.	0.00	0.02	0.03	0.03	1.00						
Conductivity	0.54	0.61	0.46	0.05	0.09	1.00					
Ca^{2+}	***0.69***	***0.63***	0.61	0.10	0.05	***0.97***	1.00				
Mg^{2+}	0.36	0.57	0.31	0.01	0.06	***0.95***	***0.86***	1.00			
Alkalinity	***0.63***	***0.65***	0.55	0.09	0.09	***0.99***	***0.98***	***0.90***	1.00		
NO_3-N	0.14	0.44	0.17	0.56	0.00	0.04	0.03	0.04	0.06	1.00	
DOC	***0.67***	***0.69***	0.60	0.18	0.03	***0.68***	***0.69***	0.59	***0.70***	0.16	1.00

Bold italicized type - significant to $p < 0.05$

Appendix A3 Enantioselective Degradation of α-HCH in Amituk Streams

Table A3.1: Gorge Creek α-HCH concentration and ER estimates for amount degraded calculations

Julian Day	AJD	Stream Discharge ($m^3 s^{-1}$)	α-HCH Conc. ($pg L^{-1}$)	Fitted Conc. ($pg L^{-1}$)	Amount α-HCH (mg)	ER	Fitted ER	Amount Degraded (mg)
169	4	0.2392		3268	67.53		1.00	0.00
170	5	0.3033		3122	81.80		1.00	0.00
171	6	0.3799	2969	2951	96.87		1.00	0.00
172	7	0.3300		2763	78.78		1.00	0.00
173	8	0.2459	2481	2564	54.46		1.00	0.00
174	9	0.1893		2358	38.57		1.00	0.00
175	10	0.1772	2330	2151	32.93	1.00	1.00	0.00
176	11	0.2225		1947	37.43		1.00	0.00
177	12	0.4614	1609	1748	69.69		0.98	0.53
178	13	0.8656		1558	116.51		0.96	2.16
179	14	1.2828	1369	1378	152.77		0.94	4.51
180	15	1.1375		1211	119.02		0.92	4.83
181	16	3.7892		1057	346.13		0.90	17.89
182	17	2.4528	927	918	194.50	0.95	0.88	12.22
183	18	2.1900		793	150.06		0.86	11.10
184	19	3.2098		683	189.47		0.84	16.15
185	20	3.2889	603	588	167.11		0.82	16.12
186	21	1.5512		507	67.99		0.81	7.32
187	22	1.5855	386	440	60.31	0.80	0.79	7.18
188	23	1.5727		386	52.46		0.77	6.84
189	24	1.3949	471	344	41.46		0.75	5.87
190	25	1.1956		313	32.32		0.73	4.94
191	26	0.9810		292	24.72		0.72	4.06
192	27	0.5650		279	13.62		0.70	2.39
193	28	0.1489		274	3.53		0.69	0.66
194	29	0.1016		275	2.42		0.67	0.48
195	30	0.0543		282	1.32		0.65	0.28
196	31	0.0480	273	292	1.21	0.50	0.64	0.27
197	32	0.0337		305	0.89		0.62	0.21
198	33	0.0337		319	0.93		0.61	0.23
199	34	0.0240		334	0.69		0.60	0.18
200	35	0.0240	213	349	0.72		0.58	0.19
201	36	0.0306		363	0.96		0.57	0.26
202	37	0.0371		375	1.20		0.56	0.34
203	38	0.0436		385	1.45		0.54	0.43
204	39	0.1759	451	392	5.96	0.63	0.53	1.83
205	40	0.1626		396	5.57		0.52	1.77
206	41	0.2102		397	7.21		0.51	2.36
207	42	0.2791		394	9.50		0.50	3.20
208	43	0.2378	429	388	7.96		0.48	2.77
209	44	0.1955		378	6.38		0.47	2.28
210	45	0.2027		365	6.39		0.46	2.34
211	46	0.1384		350	4.18		0.45	1.57
212	47	0.0913	278	332	2.62		0.44	1.01
213	48	0.0758		312	2.04		0.43	0.81
214	49	0.0765		291	1.93		0.43	0.78
215	50	0.0791		270	1.84		0.42	0.76
216	51	0.1033	391	249	2.22		0.41	0.93
217	52	0.2132		228	4.20		0.40	1.80
218	53	0.1938		209	3.50		0.39	1.52
219	54	0.0811		192	1.35		0.39	0.60
220	55	0.0526		178	0.81		0.38	0.36
221	56	0.0241	89	167	0.35	0.36	0.37	0.16
222	57	0.0048		159	0.07		0.37	0.03
223	58	0.0032		156	0.04		0.36	0.02
224	59	0.0041	103	157	0.06		0.36	0.03
225	60	0.0263		161	0.37		0.35	0.18
226	61	0.0273		170	0.40		0.35	0.19
227	62	0.0149	160	181	0.23		0.34	0.11
228	63	0.1257		195	2.11		0.34	1.05
229	64	0.1021		209	1.85		0.33	0.92
230	65	0.0785		223	1.51		0.33	0.76
231	66	0.0661		235	1.34		0.33	0.68
232	67	0.1696	347	241	3.53		0.32	1.80
233	68	0.1971		239	4.07		0.32	2.09
234	69	0.1003		225	1.95		0.32	1.00
235	70	0.0874	144	194	1.47		0.32	0.76

Table A3.2: Mud Creek α-HCH concentration and ER estimates for amount degraded calculations

Julian Day	AJD	Stream Discharge ($m^3 s^{-1}$)	α-HCH Conc. (pg L^{-1})	Fitted Conc. (pg L^{-1})	Amount α-HCH (mg)	ER	Fitted ER	Amount Degraded (mg)
167	2	0.5149		140	6.24		0.84	0.53
168	3	0.4383	255	217	8.23		0.81	0.84
169	4	0.4052		271	9.50		0.79	1.12
170	5	0.3123	157	307	8.28		0.77	1.09
171	6	0.2792		327	7.90		0.75	1.13
172	7	0.3954	503	336	11.49		0.74	1.75
173	8	0.4659		336	13.51		0.72	2.17
174	9	0.5364	307	328	15.21	0.72	0.71	2.53
175	10	0.3908		316	10.66		0.71	1.83
176	11	0.4747	320	300	12.29		0.70	2.15
177	12	0.4153		281	10.09		0.70	1.78
178	13	0.3325	185	262	7.52		0.70	1.34
179	14	0.2830		242	5.91		0.70	1.05
180	15	0.2587		222	4.96		0.70	0.88
181	16	0.2545	189	203	4.46		0.70	0.79
182	17	0.2095		185	3.35		0.70	0.59
183	18	0.1748	166	168	2.54	0.65	0.70	0.44
184	19	0.2214		153	2.92		0.71	0.50
185	20	0.2010		138	2.40		0.71	0.41
186	21	0.0903		126	0.98		0.71	0.16
187	22	0.0993	192	114	0.98	0.79	0.72	0.16
188	23	0.1314		104	1.18		0.72	0.19
189	24	0.1497		95	1.23		0.72	0.20
190	25	0.1477	75	87	1.11		0.72	0.18
191	26	0.1417		79	0.97		0.72	0.16
192	27	0.0886		73	0.56		0.72	0.09
193	28	0.0284		67	0.16		0.72	0.03
194	29	0.0146		62	0.08		0.72	0.01
195	30	0.0151	20	57	0.07	0.69	0.72	0.01
196	31	0.0149		53	0.07		0.72	0.01
197	32	0.0160		49	0.07		0.72	0.01
198	33	0.0160		46	0.06		0.72	0.01
199	34	0.0094		43	0.03		0.71	0.01
200	35	0.0094		40	0.03		0.71	0.01
201	36	0.0161	34	38	0.05		0.71	0.01
202	37	0.0159		36	0.05		0.70	0.01
203	38	0.0273		35	0.08		0.70	0.01
204	39	0.0688		34	0.20		0.69	0.04
205	40	0.0281		33	0.08		0.69	0.01
206	41	0.0468		33	0.13		0.69	0.02
207	42	0.0655		34	0.19		0.68	0.04
208	43	0.0510	62	35	0.15	0.69	0.68	0.03
209	44	0.0665		36	0.21		0.68	0.04
210	45	0.0182		38	0.06		0.68	0.01
211	46	0.0163		41	0.06		0.68	0.01
212	47	0.0157		44	0.06		0.69	0.01
213	48	0.0154		47	0.06		0.69	0.01
214	49	0.0157		50	0.07		0.70	0.01
215	50	0.0160	38	54	0.07		0.71	0.01
216	51	0.0160		58	0.08		0.72	0.01
217	52	0.0862		61	0.45		0.74	0.07
218	53	0.0363		64	0.20		0.76	0.03
219	54	0.0276		66	0.16		0.78	0.02
220	55	0.0183		68	0.11		0.81	0.01
221	56	0.0089		69	0.05		0.84	0.00
222	57	0.0068	71	69	0.04	0.88	0.88	0.00
223	58	0.0061		67	0.04		0.87	0.00
224	59	0.0068		65	0.04		0.86	0.00
225	60	0.0120		61	0.06		0.85	0.01
226	61	0.0193		57	0.09		0.84	0.01
227	62	0.0147		51	0.07		0.83	0.01
228	63	0.0633		45	0.25		0.82	0.02
229	64	0.0329		39	0.11		0.81	0.01
230	65	0.0161	34	33	0.05		0.80	0.01
231	66	0.0467		28	0.11		0.79	0.01
232	67	0.1071		25	0.23		0.78	0.03
233	68	0.0476		26	0.11		0.77	0.01
234	69	0.0308		32	0.08		0.76	0.01
235	70	0.0126	44	44	0.05		0.75	0.01

Table A3.3: Cave Creek α-HCH concentration and ER estimates for amount degraded calculations

Julian Day	AJD	Stream Discharge ($m^3 s^{-1}$)	α-HCH Conc. (pg L^{-1})	Fitted Conc. (pg L^{-1})	Amount α-HCH (mg)	ER	Fitted ER	Amount Degraded (mg)
177	12	0.5368		331	15.36		0.96	0.33
178	13	0.5730	618	632	31.28	0.92	0.95	0.88
179	14	0.5454		827	38.95		0.93	1.37
180	15	0.3671		939	29.79		0.92	1.27
181	16	0.7546	1034	989	64.47		0.90	3.25
182	17	0.8696		992	74.54		0.89	4.37
183	18	0.5436	958	963	45.21	0.91	0.87	3.03
184	19	0.7724		911	60.80		0.86	4.61
185	20	0.6031	822	847	44.12		0.84	3.74
186	21	0.2357		776	15.81		0.83	1.49
187	22	0.3677	651	705	22.39	0.84	0.81	2.31
188	23	0.5549		636	30.51		0.80	3.44
189	24	0.4784	611	574	23.71		0.78	2.91
190	25	0.3933		518	17.61		0.77	2.33
191	26	0.3160		471	12.87		0.75	1.83
192	27	0.1583		433	5.92		0.74	0.90
193	28	0.0622		403	2.16		0.72	0.35
194	29	0.0310		380	1.02		0.71	0.17
195	30	0.0250		365	0.79		0.69	0.14
196	31	0.0446	440	355	1.37	0.60	0.68	0.26
197	32	0.0448		350	1.35		0.67	0.27
198	33	0.0322		349	0.97		0.65	0.20
199	34	0.0384		351	1.16		0.64	0.25
200	35	0.0379	258	354	1.16		0.63	0.26
201	36	0.0465		358	1.44		0.62	0.34
202	37	0.0965		362	3.02		0.61	0.73
203	38	0.0745		365	2.35		0.60	0.58
204	39	0.0836	362	368	2.66	0.64	0.59	0.68
205	40	0.0651		369	2.07		0.59	0.54
206	41	0.1215		369	3.87		0.58	1.03
207	42	0.1205		367	3.83		0.58	1.03
208	43	0.0731	393	365	2.30		0.57	0.63
209	44	0.0613		361	1.91		0.57	0.52
210	45	0.0574		357	1.77		0.57	0.49
211	46	0.0449		352	1.37		0.57	0.38
212	47	0.0397	376	346	1.19		0.57	0.33
213	48	0.0428		341	1.26		0.57	0.34
214	49	0.0401		337	1.17		0.58	0.31
215	50	0.0365		333	1.05		0.58	0.28
216	51	0.0688	302	329	1.96		0.59	0.50
217	52	0.1179		326	3.32		0.60	0.83
218	53	0.0639		324	1.79		0.61	0.43
219	54	0.0358		322	1.00		0.62	0.23
220	55	0.0221		321	0.61		0.64	0.14
221	56	0.0184	293	318	0.51	0.65	0.65	0.11
222	57	0.0213		315	0.58		0.65	0.12
223	58	0.0138		311	0.37		0.65	0.08
224	59	0.0184	352	304	0.48		0.65	0.10
225	60	0.0297		295	0.76		0.65	0.16
226	61	0.0290		282	0.71		0.65	0.15
227	62	0.0307	239	266	0.71		0.65	0.15
228	63	0.0649		246	1.38		0.65	0.29
229	64	0.0469		223	0.90		0.65	0.19
230	65	0.0349		197	0.59		0.65	0.13
231	66	0.0443		169	0.65		0.65	0.14
232	67	0.0819	150	142	1.01		0.65	0.21
233	68	0.0689		119	0.71		0.65	0.15
234	69	0.0302		103	0.27		0.65	0.06
235	70	0.0415	98	100	0.36		0.65	0.08

α-HCH ER Prediction Equations

β - Adjusted Julian Day (AJD), beginning June 15.

Gorge Creek

ERs assumed to be 1.00 to AJD 11

Equation: $1.267525-0.02561901*\beta+0.0001722659*\beta^2$

Mud Creek

ERs set to decline by 0.01 from AJD 57 to AJD 70

Equation: $0.9189734-0.04238664*\beta+0.002775096*\beta^2-7.141303e^{-5}*\beta^3+6.239961e^{-7}*\beta^4$

Cave Creek

ERs set to 0.65 from AJD 57 to AJD 70

Equation: $1.051255-0.001481846*\beta-0.0006363414*\beta^2+9.577858e^{-6}*\beta^3$

Derivation of Equation (1) of Chapter 3

The amount of α-HCH enantioselectively degraded (N_{deg}) is given by:

$$N_{\text{deg}} = [\, X_{\alpha\text{-HCH}} / (\text{ER} + 1)\,] - [\, \text{ER} * X_{\alpha\text{-HCH}} / (\text{ER} + 1)\,]$$

where $X_{\alpha\text{-HCH}}$ is the total amount of α-HCH in the stream and ER is the (+)/(-) enantiomer ratio. It is assumed that only the (+) enantiomer degrades.

The amount of α-HCH in the stream ($X_{\alpha\text{-HCH}}$) is calculated by from measured discharges and estimated concentrations (Tables A3.1 to A3.3)

To obtain the amount enantioselectively degraded (N_{deg}), two equations are solved:

$$\text{ER} = X_{(+)\text{-}\alpha\text{-HCH}} / X_{(-)\text{-}\alpha\text{-HCH}} \qquad \text{A}$$

$$X_{\alpha\text{-HCH}} = X_{(+)\text{-}\alpha\text{-HCH}} + X_{(-)\text{-}\alpha\text{-HCH}} \qquad \text{B}$$

where $X_{(+)\text{-}\alpha\text{-HCH}}$ and $X_{(-)\text{-}\alpha\text{-HCH}}$ are the amounts of (+)-α-HCH and (-)-α-HCH, respectively. Rearranging A to:

$$X_{(+)\text{-}\alpha\text{-HCH}} = \text{ER} * X_{(-)\text{-}\alpha\text{-HCH}} \qquad \text{C}$$

and substituting into B gives:

$$X_{\alpha\text{-HCH}} = X_{(-)\text{-}\alpha\text{-HCH}} * (\text{ER} + 1) \quad \text{or}$$

$$X_{(-)\text{-}\alpha\text{-HCH}} = X_{\alpha\text{-HCH}} / (\text{ER} + 1), \qquad \text{D}$$

the amount of (-)-α-HCH in the stream water and substituting D into C gives:

$$X_{(+)\text{-}\alpha\text{-HCH}} = \text{ER} * X_{\alpha\text{-HCH}} / (\text{ER} + 1) \qquad \text{E}$$

the amount of (+)-α-HCH in the stream water. The amount enantioselectively degraded (N_{deg}) is thus the difference between D and E:

$$N_{\text{deg}} = X_{(-)\text{-}\alpha\text{-HCH}} - X_{(+)\text{-}\alpha\text{-HCH}} \quad \text{or}$$

$$N_{\text{deg}} = [\, X_{\alpha\text{-HCH}} / (\text{ER} + 1)\,] - [\, \text{ER} * X_{\alpha\text{-HCH}} / (\text{ER} + 1)\,]$$

Sample Calculations of Expected Amituk Lake ER

End of summer 1993 α-HCH inventory: 6977 mg
Estimated ER (1992 value of Falconer et al., 1995a): 0.77

Assume 305 days of degradation over-winter.

From Eqs. E and D above, the amounts of each enantiomer at the end of summer 1993:

(+)-α-HCH: 3035 mg
(-)-α-HCH: 3942 mg

Assume $3k_{\alpha-} = k_{\alpha+}$, i.e. for $k_{\alpha} = 0.849\ y^{-1}$, $k_{\alpha+} = 0.637\ y^{-1}$ and $k\alpha- = 0.212\ y^{-1}$

Using Eq. (2) of Chpt. 3 (pg. 37):

For (+)-α-HCH:
Co = 3035 mg
t = 305/365 = 0.8356 y
$k_{\alpha+} = 0.637\ y^{-1}$
$k_h = 0.022\ y^{-1}$

Thus:
$C = C_o * \exp[-(k_{\alpha+}+k_h)t]$
$C = 3035 * \exp[-(0.659*0.8356)]$
C = 1750 mg = (+)-α-HCH

For (-)-α-HCH:
Co = 3942 mg
t = 305/365 = 0.8356 y
$k_{\alpha+} = 0.212\ y^{-1}$
$k_h = 0.022\ y^{-1}$

Thus:
$C = C_o * \exp[-(k_{\alpha-}+k_h)t]$
$C = 3942 * \exp[-(0.234*0.8356)]$
C = 3242 mg = (-)-α-HCH

The expected lake ER at the beginning of the following melt would be:

ER = (+)-α-HCH / (-)-α-HCH
ER = 1750 / 3242
ER = 0.54

if the rate of degradation of (+)-α-HCH was 3 times that of (-)-α-HCH. Since the ER was about 0.74 at the beginning of melt in 1993, the rates differ only slightly or most degradation was non-enantioselective.

Appendix A4 July 1997 ER, Concentration and Temperature Measurements

Table A4.1: α-HCH ERs and concentrations from lakes and streams sampled in July, 1997

Table A4.1: α-HCH ERs and concentrations from lakes and streams sampled in July, 1997

		(+)/(-) Enantiomer Ratio		Concentration	Temperature
Site/Date	Location	BGB-172	Beta-DEX 120	(pg L^{-1})	(°C)
Mud Creek					
Jul. 17	1	0.78	0.78	475	5.0
	2	0.76	0.76	420	3.0
	3	0.81	0.81	600	8.3
	4	0.87	0.86	620	2.0
Jul. 29	1	0.76	0.76	207	4.5
	2	0.66	0.67	173	4.0
	3	0.77	0.73	344	4.3
	4	0.78	0.77	454	4.3
Gorge Creek					
Jul. 17	1	0.86	0.89	733	1.5
	2	0.86	0.88	624	2.3
	3	0.82	0.82	568	3.0
	4	0.84	0.87	565	3.3
Jul. 29	1	0.64	0.63	534	2.5
	2	0.77	0.76	579	2.5
	3	0.56	0.56	336	4.5
	4	0.64	0.64	432	4.0
Char Lake					
Jul. 10	Inlet 1	0.70	0.68	414	4.5
	Inlet 2	0.88	0.88	602	0.5
	Inlet 3	0.77	0.78	474	1.0
	Inlet 4	0.64	0.63	733	2.0
	10 m	0.65	0.66	1021	2.5
	Outflow	-	-	-	1.5
Jul. 19	Inlet 1	0.71	0.61	64	7.8
	Inlet 2	0.75	0.81	300	2.5
	Inlet 3	0.72	0.72	437	4.3
	Inlet 4	0.47	0.47	640	7.8
	10 m	0.62	0.65	977	3.5
	Outflow	0.72	0.73	641	2.5
Jul. 27	Inlet 1	0.58	0.59	70	4.0
	Inlet 2	0.76	0.75	279	1.8
	Inlet 3	0.74	0.76	461	3.5
	Inlet 4	0.38	0.36	619	4.5
	10 m	0.69	0.67	839	-
	Outflow	0.69	0.68	843	3.8
Meretta Lake					
Jul. 11	Inlet 1	0.42	0.44	429	9.5
	Inlet 2	0.73	0.80	828	9.0
	5 m	0.84	0.88	1264	3.5
	Outflow	0.84	0.85	758	3.0
Jul. 19	Inlet 1	0.43	0.46	332	8.5
	Inlet 2	0.81	0.79	669	8.5
	5 m	0.90	0.89	1205	-
	Outflow	0.82	0.82	603	5.0
Jul. 27	Inlet 1	0.54	0.50	336	3.8
	Inlet 2	0.81	0.80	721	4.5
	5 m	-	-	-	-
	Outflow	0.84	0.84	680	3.3
Wetland	Inflow	0.85	0.87	433	10.0
	Centre	0.69	0.69	285	11.3
	Outflow	0.63	0.65	175	11.8

Appendix B1 Program Listing for the Amituk Lake Steady State Model in Borland C++ v.4.5

```
#include <stdio.h>
#include <math.h>
#include <stdlib.h>

/* 1994 Amituk Lake Steady State Model based on H.Freitas model in Visual Basic.  1993 & 1994 data,
        updated properties, concentrations, and lake characteristics. */

/* External Variable Declarations */

        double Aw, LkMD, ASD, Gwi, Gwo, AnnPre, SedDep, SedRes, SedBur, SedLkArea, TFfrac;
        double IPCn, WCPCn, AerCn, pSusP, pAerP, pSedS, FOCwcp, FOCseds, FOCress, FOCip;
        double Ta, Tw, Vaerdep, ScRat, VFsed, Days, R, MW, VPL, LKow, H, tw, ts, Cair, Cin, kw, ka;
        double ks, Vw, Vs, VFaer, VFip, VFwcp, Grn, Gdd, Gwd, Gawi, Gip, Gawo, Gop, As, Gsed;
        double Grsp, Gbr, Zw, TaK, Za, TwK, Zq, Kow, Koc, Zip, Zwcp, Zsed, Zrsp, ZwB, ZaB, ZsB;
        double ZinB, kow, Dwa, Daw, Dwd, Ddd, Drn, Dwi, Dpi, Dwo, Dpo, Dwt, Dbr, Dst, Drsp, Ddep;
        double Dsw, Dws, Qin, Qa, Qw, Qs, CiB, Cip, Cip2, Cwc, CwcB, Cwcp, Cwcp2, Co, Cop, Cpino;
        double CsedB, Csed, Cpw, Csedt, CaB, Caer, CaerC, CaB2, Crnp, Crnds, Rbr, Rrsp, Rdep, Rsw;
        double Rws, Raw, Rwa, Rwd, Rdd, Rrn, Rwi, Rpi, Rwo, Rpo, Rwt, Rst;
        float chemprop[9][10], pcbchemprop[9][8], chemconc[2][10], pcbconc[2][8];
        int i, j, k, l, m, n;
        FILE *fotpt;
        FILE *fphyschem;
        FILE *fconc;
        char *fname[40];

main()
{

/* Function Declarations */

        void proparray(void), concarray(void), props(void), inconcs(void), volumes(void), volfracts(void);
        void gvalues(void), zvalues(void), dvalues(void),aquiv(void), concs(void), fluxes(void), print(void);

/* Initializing Amituk Lake Characteristics */

        Aw = 378395.9;              /* Water Surface Area (m2) */
        LkMD = 19.4;                /* Lake Mean Depth (m) */
        ASD = 0.03;                 /* Active Sediment Depth (m) */
        AnnPre = 0.1314;            /* Annual Precipitation (m/yr) */
        SedDep = 45.4;              /* Sediment Deposition Rate (g/m2/yr) */
        SedRes = 0.0;               /* Sediment Resuspension Rate (g/m2/yr) */
        SedBur = 121.;              /* Sediment Burial Rate (g/m2/yr) */
        SedLkArea = 0.3752;         /* Sediment/Lake Area Ratio */
        TFfrac = 0.5;               /* Through-flow Fraction */
        IPCn = 7.42;                /* Inflow Particle Concentration (mg/L) */
        WCPCn = 1.47;               /* Water Column Particle Concentration (mg/L) */
        AerCn = 0.2;                /* Aerosol Concentration (ug/m3) */
        pSusP = 2000.;              /* Density of Suspended Particles (kg/m3) */
        pAerP = 1500.;              /* Density of Aerosol Particles (kg/m3) */
        pSedS = 2000.;              /* Density of Sediment Solids (kg/m3) */
        FOCwcp = 0.05;              /* OC Fraction of Water Column Particles */
        FOCseds = 0.012;            /* OC Fraction of Suspended Sediment Particles */
        FOCress = 0.012;            /* OC Fraction of Resuspended Sed. Particles */
        FOCip = 0.05;               /* OC Fraction of Inflow Suspended Particles */
        Ta = 4.;                    /* Summer Air Temperature (deg C) */
```

```
        Tw = 1.8;                               /* Summer Water Temperature (deg C) */
        Vaerdep = 1.8;                          /* Aerosol Deposition Velocity (m/h) */
        ScRat = 200000.;                        /* Scavenging Ratio */
        VFsed = 0.50;                           /* Volume Fraction of Sediment */
        Days = 92;                              /* Days without ice cover */
/* Additional Variables to Initialize */
        R = 8.314;                              /* Gas Constant (Pa.m3/mol.K) */
/* Amituk Lake Steady State Model */
        printf ("\n\nThis is the Amituk Lake Steady State Model\n\n");
        printf ("For which year would you like to obtain results?\n\n");
        printf ("1 - 1993\t2 - 1994\n\n");
        printf ("Enter the number of your choice\n\n");
        scanf ("%i", &i);
        if (i == 1){
                Gwi = 5358131.;                 /* 1993 Water Inflow Rate (m3/yr) */
                Gwo = 5358131.;                 /* 1993 Water Outflow Rate (m3/yr) */
                }
        else{
                Gwi = 5322568.;                 /* 1993 Water Inflow Rate (m3/yr) */
                Gwo = 5322568.;                 /* 1993 Water Outflow Rate (m3/yr) */
                }
        printf ("\nChoose which Chemical you are interested in:\n\n");
        printf ("1 - a-HCH\t2 - b-HCH\t3 - g-HCH\n");
        printf ("4 - HCB\t\t5 - Dieldrin\t6 - Endosulfan I\n");
        printf ("7 - Heptachlor Epoxide\t\t8 - S-Chlordanes\n");
        printf ("9 - S-DDT\t10 - PCBs\n\n");
        printf ("Enter the number of your choice\n\n");
        scanf ("%i", &j);
        if (j == 10) {
                printf ("\nWould you like to run Sum-PCBs or homolog groups?\n\n");
                printf ("1 - Sum-PCBs\t2 - Homologs\n\n");
                printf ("Enter the number of your choice\n\n");
                scanf ("%i", &k);
                }
        if (j == 10 && k == 2){
                printf ("\nWhich PCB homolog group would you like to run?\n\n");
                printf ("1 - Mono\t2 - Di\t\t3 - Tri\t\t4 - Tetra\n");
                printf ("5 - Penta\t6 - Hexa\t7 - Hepta\t8 - Octa\n\n");
                printf ("Enter the number of your choice\n\n");
                scanf ("%i", &n);
                *fname = "pcbpchem.txt";
                fphyschem = fopen(*fname, "r");
                if (fphyschem == NULL){
                        printf ("Error opening file %s.\n", *fname);
                        exit(0);
                        }
                }
        else {
                *fname = "physchem.txt";
                fphyschem = fopen(*fname, "r");
                if (fphyschem == NULL){
```

```
                        printf ("Error opening file %s.\n", *fname);
                        exit(0);
                        }
                }
        proparray();
        concarray();
        props();
        inconcs();

        *fname = "ssoutput.dat";
        fotpt = fopen(*fname, "w");
        if (fotpt == NULL){
                printf ("Error opening file %s.\n", *fname);
                exit(0);
                }
        else {
                printf ("\n\nThe file %s has been created.\n\n", *fname);
                }

        volumes();
        volfracts();
        gvalues();
        zvalues();
        dvalues();
        aquiv();
        concs();
        fluxes();
        print();

        fclose(fotpt);
        printf("\nEnd of Program\n");
        printf("\nData files can be handled in Excel");
}
/*------------------------------------------------------------------------*/

        /* Chemical Property and Concentration Functions */

void proparray(void)

        /* This function reads physchem properties into an array from a file */
        /* Each row is a different property, each column is a different chemical */

{
        if (j == 10 && k == 2) {                        /* For PCB homolog runs */
                for (m = 0; m < 9; m++){
                        for (l = 0; l < 8; l++){
                                fscanf(fphyschem,"%f\t", &pcbchemprop[m][l]);
                                }
                        fscanf(fphyschem,"\n");
                        }
                }
        else {                                          /* For all other chemicals */
                for (m = 0; m < 9; m++){
                        for (l = 0; l < 10; l++){
                                fscanf(fphyschem,"%f\t", &chemprop[m][l]);
                                }
                        fscanf(fphyschem,"\n");
```

```
                        }
                }
        fclose(fphyschem);
        return;
}
void concarray(void)
        /* This function reads concentrations into an array from a file.  Row 0 is air concentration, row */
        /* 1 is water concentrations, and each column is a different chemical*/
{
        if (j == 10 && k == 2) {                        /* For PCB homolog runs */
                if (i == 1) *fname = "cbconc93.txt";
                else *fname = "cbconc94.txt";
                fconc = fopen(*fname, "r");
                if (fconc == NULL){
                        printf ("Error opening file %s.\n", *fname);
                        exit(0);
                        }
                for (l = 0; l < 8; l++){
                        fscanf(fconc,"%f\t", &pcbconc[0][l]);
                        }
                        fscanf(fconc,"\n");
                for (l = 0; l < 8; l++){
                        fscanf(fconc,"%f\t", &pcbconc[1][l]);
                        }
                }
        else {                                          /* For all other chemicals */
                if (i == 1) *fname = "conc93.txt";
                else *fname = "conc94.txt";
                fconc = fopen(*fname, "r");
                if (fconc == NULL){
                        printf ("Error opening file %s.\n", *fname);
                        exit(0);
                        }
                for (l = 0; l < 10; l++){
                        fscanf(fconc,"%f\t", &chemconc[0][l]);
                        }
                        fscanf(fconc,"\n");
                for (l = 0; l < 10; l++){
                        fscanf(fconc,"%f\t", &chemconc[1][l]);
                        }
                }
        fclose(fconc);
        return;
}
void props(void)
        /* This function initializes phys-chem property variables according to choide of chemical */
{
        if (j == 10 && k == 2) {
                MW = pcbchemprop[0][n-1];               /* Molecular Weight (g/mol) */
                VPL = pcbchemprop[1][n-1];              /* Liquid Vapour Pressure (Pa) */
                LKow = pcbchemprop[2][n-1];             /* Log Kow */
```

```
                H = pcbchemprop[3][n-1];                /* Henry's Law Constant (Pa mol/m3) */
                tw = pcbchemprop[4][n-1];               /* Degr. Half-life in Water (h) */
                ts = pcbchemprop[5][n-1];               /* Degr. Half-life in Sediment (h) */
                kw = pcbchemprop[6][n-1];               /* Water MTC (m/h) */
                ka = pcbchemprop[7][n-1];               /* Air MTC (m/h) */
                ks = pcbchemprop[8][n-1];               /* sediment MTC (m/h) */
                }
        else {
                MW = chemprop[0][j-1];                  /* Molecular Weight (g/mol) */
                VPL = chemprop[1][j-1];                 /* Liquid Vapour Pressure (Pa) */
                LKow = chemprop[2][j-1];                /* Log Kow */
                H = chemprop[3][j-1];                   /* Henry's Law Constant (Pa mol/m3) */
                tw = chemprop[4][j-1];                  /* Degr. Half-life in Water (h) */
                ts = chemprop[5][j-1];                  /* Degr. Half-life in Sediment (h) */
                kw = chemprop[6][j-1];                  /* Water MTC (m/h) */
                ka = chemprop[7][j-1];                  /* Air MTC (m/h) */
                ks = chemprop[8][j-1];                  /* sediment MTC (m/h) */
                }
        return;
}
void inconcs(void)
        /* This function initializes input concentration variables according to choice of chemical */
{
        if (j == 10 && k == 2) {
                Cair = pcbconc[0][n-1];                 /* PCB air conc. (pg/m3) */
                Cin = pcbconc[1][n-1];                  /* Inflow PCB water conc. (pg/L) */
                }
        else {
                Cair = chemconc[0][j-1];                /* Air concentration. (pg/m3) */
                Cin = chemconc[1][j-1];                 /* Inflow water conc. (pg/L) */
                }
        return;
}
/*-----------------------------------------------------------------*/
        /* Model Calculation Functions */
void volumes(void)
        /* calculates lake water and sediment volumes */
{
        Vw = Aw * LkMD;                                 /* Lake Water Volume (m3) */
        Vs = Aw * ASD * SedLkArea;                      /* Active Lake Sediment Volume (m3) */
        return;
}
void volfracts(void)
        /* calculates volume fractions of particles in bulk phase */
{
        VFaer = AerCn / (pAerP * pow(10,9));            /* vol. fract. of aerosols */
        VFip = IPCn / (pSusP * 1000);                   /* vol. fract. of inflow particles*/
        VFwcp = WCPCn / (pSusP * 1000);                 /* vol. fract. of water col. particles*/
        return;
```

```
}
void gvalues(void)
        /* calculates the G-values, rate of physical processes */
{
        /* Air G-Values */
        Grn = (AnnPre/2)*(Aw/(24*Days))*(1-TFfrac);     /* Adj. rain rate (m3/h) */
        Gdd = Vaerdep * Aw * VFaer * (1-TFfrac);        /* Dry Depos. rate (m3/h) */
        Gwd = Grn * VFaer * ScRat;                      /* Wet Depos. rate (m3/h) */
        /* Water G-Values */
        Gawi = (Gwi * (1-TFfrac)) / (24*Days);          /* Adj. water inflow rate (m3/h) */
        Gip = Gawi * VFip;                              /* Particle inflow rate (m3/h) */
        Gawo = (Gwo * (1-TFfrac)) / (24*Days);          /* Adj. water outflow rate (m3/h) */
        Gop = Gawo * VFwcp;                             /* Particle outflow rate (m3/h) */
        /* Sediment G-Values */
        As = Aw * SedLkArea;                            /* Sediment Area (m2) */
        Gsed = (SedDep*Aw) / (24*Days*pSusP*1000);      /* Sed. Depostion rate (m3/h) */
        Grsp = (SedRes*As) / (24*Days*pSedS*1000);      /* Sed. Resuspens. rate (m3/h) */
        Gbr = (SedBur*As) / (24*Days*pSedS*1000);       /* Sed. Burial rate (m3/h) */
        return;
}
void zvalues(void)
        /* Calculates Z-values in Aquivalence form */
{
        TaK = Ta + 273.16;                              /* Air Temp. in Kelvin */
        TwK = Tw + 273.16;                              /* Water Temp. in Kelvin */
        Zw = 1.;                                        /* Water Z-value */
        Za = H / (R*TaK);                               /* Air Z-value */
        Zq = (6000000. / VPL) * Za;                     /* Aerosol Z-value */
        Kow = pow(10,LKow);                             /* Octanol-water partition coefficient */
        Koc = 0.41 * Kow;                               /* Org. Carb.-water part. coefficient */
        Zip = (Koc*FOCip*pSusP*Zw)/1000;                /* Infl. Part. Z-value */
        Zwcp = (Koc*FOCwcp*pSusP*Zw)/1000;              /* Water Col. Part. Z-value */
        Zsed = (Koc*FOCseds*pSedS*Zw)/1000;             /* Sediment Z-value */
/*      Zsed = (10000*pSedS*Zw)/1000;                   /* Kp - chemical dependent */
        Zrsp = Zsed;
        /* Bulk Z-Values */
        ZwB = Zw*(1-VFwcp) + Zwcp*VFwcp;                /* Bulk Water Z-value */
        ZinB = Zw*(1-VFip) + Zip*VFip;                  /* Bulk Inflow Z-value */
        ZaB = Za*(1-VFaer) + Zq*VFaer;                  /* Bulk Air Z-value */
        ZsB = Zw*(1-VFsed) + Zsed*VFsed;                /* Bulk Sediment Z-value */
        return;
}
void dvalues(vcid)
        /* Calculates D-values (m3/h)*/
{
        kow = 1/(1/kw+R*TwK/(H*ka));                    /* Overall waterside MTC */
```

```
        /* Air D-values */

        Dwa = kow*Aw*Zw;                        /* Volatilization */
        Daw = kow*Aw*Zw;                        /* Adsorption */
        Dwd = Gwd*Zq;                           /* Wet Deposition */
        Ddd = Gdd*Zq;                           /* Dry Deposition */
        Drn = Grn*Zw;                           /* Rain Dissolution */

        /* Water D-values */

        Dwi = Gawi*Zw;                          /* Water Inflow */
        Dpi = Gip*Zip;                          /* Particle Inflow */
        Dwo = Gawo*Zw;                          /* Water Outflow */
        Dpo = Gop*Zwcp;                         /* Particle Outflow */
        Dwt = Vw*ZwB*0.693/tw;                  /* Water Degradation */

        /* Sediment D-values */

        Dbr = Gbr*Zsed;                         /* Sediment Burial */
        Dst = Vs*ZsB*0.693/ts;                  /* Sediment Transformation */
        Drsp = Grsp*Zrsp;                       /* Sediment Resuspension */
        Ddep = Gsed*Zwcp;                       /* Sediment Deposition */
        Dsw = As*Zw*ks;                         /* Sediment - Water Diffusion */
        Dws = As*Zw*ks;                         /* Water-Sediment Diffusion */
        return;
}
void aquiv(void)
        /* Calculates Aquivalences (mol/m3)(Mass Balance Equations)(Equilibrium Criterion) */
{
        Qin = Cin / (ZinB*MW*pow(10,9));                /* Inflow Aquivalence */
        Qa = Cair / (Za*MW*pow(10,12));                 /* Air Aquivalence */
        Qw = (Qa*(Drn+Ddd+Dwd+Daw)+Qin*(Dwi+Dpi))/(Dwt+Dwa+Dwo+Ddep+Dws-
             (((Ddep+Dws)*(Drsp+Dsw))/(Dsw+Dbr+Drsp+Dst)));  /* Water Aquivalence */
        Qs = Qw*(Ddep+Dws)/(Drsp+Dsw+Dbr+Dst);         /* Sediment Aquivalence */
        return;
}
void concs(void)
        /* Calculates Concentrations in Various Compartments */
{
        /* Inflow */

        CiB = Qin*ZinB*MW*pow(10,9);            /* Bulk Inflow Conc. (pg/L) */
        Cip = Qin*Zip*MW*VFip*pow(10,9);        /* Conc. in Particle (pg/L) */
        Cip2 = Qin*Zip*MW*pow(10,9)/pSusP;      /* Conc. in Particle (pg/g) */

        /* Lake Water Column */

        Cwc = Qw*Zw*MW*pow(10,9);               /* Water Column Conc. (pg/L) */
        CwcB = Qw*ZwB*MW*pow(10,9);             /* Bulk Water Conc. (pg/L) */
        Cwcp = Qw*Zwcp*MW*VFwcp*pow(10,9);      /* Conc. in Particle (pg/L) */
        Cwcp2 = Qw*Zwcp*MW*pow(10,9)/pSusP;     /* Conc. in Particle (pg/g) */

        /* Outflow */

        Co = (Qin*Zw*TFfrac + Qw*Zw*(1-TFfrac))*MW*pow(10,9);  /* Outflow Water Conc.(pg/L) */
        Cop = (Qin*Zip*TFfrac*VFip + Qw*Zwcp*(1-TFfrac)*VFwcp)*MW*pow(10,9); /*CinP(pg/L)*/
        Cpino = TFfrac*IPCn+(1-TFfrac)*WCPCn;   /* Conc. of Particles in Outflow (mg/L) */
```

```
        /* Sediment */

        CsedB = Qs*ZsB*MW*pow(10,6)/pSedS;            /* Bulk Sediment Conc. (ng/g) */
        Csed = Qs*Zsed*MW*pow(10,6)/pSedS;            /* Dry Sediment Conc. (ng/g) */
        Cpw = Qs*Zw*MW*pow(10,6)/pSedS;               /* Sed. Pore Water Conc. (ng/L sed.) */
        Csedt = (Csed*VFsed) + Cpw*(1-VFsed);         /* Total Sediment Conc. (ng/g) */

        /* Air */

        CaB = Qa*ZaB*MW*pow(10,12);                   /* Bulk Air Conc. (pg/m3) */
        Caer = Qa*Zq*MW*pow(10,12);                   /* Conc. on Aerosols (pg/m3 parts) */
        CaerC = Caer*VFaer;                           /* Conc. in air from Aerosols (pg/m3) */
        CaB2 = CaerC + Cair*(1-VFaer);                /* Alternate Calc. bulk air conc. (pg/m3) */

        /* Rain */

        Crnp = Qa*VFaer*ScRat*Zq*MW*pow(10,9);        /* Conc. from Part. in rain (pg/L) */
        Crnds = Qa*Zw*MW*pow(10,9);                   /* Conc. from dissn in rain (pg/L) */
        return;
}
void fluxes(void)
        /* Calculates annual fluxes in mg/year */
{
        Rbr = Dbr*Qs*MW*24*Days*1000;                 /* Sediment Burial Flux */
        Rrsp = Drsp*Qs*MW*24*Days*1000;               /* Sed. Resuspension Flux */
        Rdep = Ddep*Qs*MW*24*Days*1000;               /* Sed. Deposition Flux */
        Rst = Dst*Qs*MW*24*Days*1000;                 /* Sed. Transformation Flux */
        Rsw = Dsw*Qs*MW*24*Days*1000;                 /* Sed.-Water Diffusion Flux */
        Rws = Dws*Qw*MW*24*Days*1000;                 /* Water-Sed. Diffusion Flux */
        Raw = Daw*Qa*MW*24*Days*1000;                 /* Adsorption Flux */
        Rwa = Dwa*Qw*MW*24*Days*1000;                 /* Volatilization Flux */
        Rwd = Dwd*Qa*MW*24*Days*1000/(1-TFfrac);      /* Wet Part. Deposition Flux */
        Rdd = Ddd*Qa*MW*24*Days*1000/(1-TFfrac);      /* Dry Part. Deposition Flux */
        Rrn = Drn*Qa*MW*24*Days*1000/(1-TFfrac);      /* Rain Deposition Flux */
        Rwi = Dwi*Qin*MW*24*Days*1000/(1-TFfrac);     /* Water Inflow Flux */
        Rpi = Dpi*Qin*MW*24*Days*1000/(1-TFfrac);     /* Particle Inflow Flux */
        Rwo = (Dwo*Qw*24*Days+Gwi*TFfrac*Zw*Qin)*MW*1000;        // Water Outflow Flux
        Rpo = (Dpo*Qw*24*Days+Gwi*VFip*TFfrac*Zip*Qin)*MW*1000;  // Particle Outflow Flux
        Rwt = Dwt*Qw*MW*24*Days*1000;                 /* Water Transformation Flux */
        return;
}
void print(void)
        /* Prints the concentrations and fluxes for the steady state model */
{
        fprintf(fotpt,"\nAmituk Lake Steady State Model - Output\n\n");
        fprintf(fotpt,"Chemical Concentrations in Environmental Compartments\n\n");
        fprintf(fotpt,"Inflow:\nWater Inflow(Bulk) (pg/L) = \t%e\n", CiB);
        fprintf(fotpt,"Particle Assoc. Chemical (pg/L) = \t%e\n", Cip);
        fprintf(fotpt,"Particle Assoc. Chemical (pg/g) = \t%e\n", Cip2);
        fprintf(fotpt,"Water Column:\nWater Column (pg/L) = \t%e\n", Cwc);
        fprintf(fotpt,"Bulk Water Column (pg/L) = \t%e\n", CwcB);
        fprintf(fotpt,"Particle Assoc. Chemical (pg/L) = \t%e\n", Cwcp);
        fprintf(fotpt,"Particle Assoc. Chemical (pg/g) = \t%e\n", Cwcp2);
        fprintf(fotpt,"Outflow:\nWater Outflow (pg/L) = \t%e\n", Co);
        fprintf(fotpt,"Particle Assoc. Chemical (pg/L) = \t%e\n", Cop);
```

```
        fprintf(fotpt,"Particle Outflow Conc. (mg/L) = \t%e\n", Cpino);
        fprintf(fotpt,"Sediment:\nBulk Sediment (ng/g) = \t%e\n", CsedB);
        fprintf(fotpt,"Dry Sediment (ng/g) = \t%e\n", Csed);
        fprintf(fotpt,"Pore Water (ng/L) = \t%e\n", Cpw);
        fprintf(fotpt,"Total Sediments (ng/g) = \t%e\n", Csedt);
        fprintf(fotpt,"Air:\nBulk Air (pg/m3) = \t%e\n", CaB);
        fprintf(fotpt,"Aerosol-adsorbed (pg/m3 parts.) = \t%e\n", Caer);
        fprintf(fotpt,"Aerosol-assoc. conc. in air (pg/m3 air) = \t%e\n", CaerC);
        fprintf(fotpt,"Total Air (pg/m3) = \t%e\n", CaB2);
        fprintf(fotpt,"Rain:\nParticle Assoc. Chemical (pg/L) = \t%e\n", Crnp);
        fprintf(fotpt,"Dissolved Chemical (pg/L) = \t%e\n", Crnds);
        fprintf(fotpt,"\n\nChemical Fluxes in mg/year\n\n");
        fprintf(fotpt,"Sediment Burial = \t%e\n", Rbr);
        fprintf(fotpt,"Sediment Resuspension = \t%e\n", Rrsp);
        fprintf(fotpt,"Sediment Deposition = \t%e\n", Rdep);
        fprintf(fotpt,"Sediment-Water Diffusion = \t%e\n", Rsw);
        fprintf(fotpt,"Water-Sediment Diffusion = \t%e\n", Rws);
        fprintf(fotpt,"Absorption = \t%e\n", Raw);
        fprintf(fotpt,"Volatilization = \t%e\n", Rwa);
        fprintf(fotpt,"Wet Particle Deposition = \t%e\n", Rwd);
        fprintf(fotpt,"Dry Particle Deposition = \t%e\n", Rdd);
        fprintf(fotpt,"Rain Dissolution = \t%e\n", Rrn);
        fprintf(fotpt,"Water Inflow = \t%e\n", Rwi);
        fprintf(fotpt,"Particle Inflow = \t%e\n", Rpi);
        fprintf(fotpt,"Water Outflow = \t%e\n", Rwo);
        fprintf(fotpt,"Particle Outflow = \t%e\n", Rpo);
        fprintf(fotpt,"Water Transformation = \t%e\n", Rwt);
        fprintf(fotpt,"Sediment Transformation = \t%e\n", Rst);
        return;
}
```

Appendix B2 Steady-state Model Input Files

Chemical Concentration Input Files for Steady-state Model Use

Physical-Chemical Properties Input Files for Initial Model Use

Chemical Concentration Input Files for Steady-state Model Use

File "conc93.txt"

	(a-HCH)	(b-HCH)	(g-HCH)	(HCB)	(Dieldrin)	(Endo I)	(HepEx)	(S-Chlord)	(S-DDT)	(S-PCB)
(Cair)	49.93	0.41	6.25	44.45	1.67	4.36	1.58	3.66	0.37	39.52
(Cinfl)	1469.63	37.88	376.02	32.43	71.01	137.05	60.98	89.52	44.45	575.64

File "conc94.txt"

	(a-HCH)	(b-HCH)	(g-HCH)	(HCB)	(Dieldrin)	(Endo I)	(HepEx)	(S-Chlord)	(S-DDT)	(S-PCB)
(Cair)	41.77	0.09	7.04	39.83	1.4	4.38	1.5	3.29	0.76	32.08
(Cinfl)	601.97	29.20	212.48	6.83	95.48	88.61	47.42	5.53	18.95	899.23

File "cbconc93.txt"

	(Mono)	(Di)	(Tri)	(Tetra)	(Penta)	(Hexa)	(Hepta)	(Octa)
(Cair)	3.71	1.25	15.43	6.32	5.90	3.42	2.92	0.44
(Cinfl)	164.48	110.24	102.00	136.96	27.98	15.05	1.74	2.44

File "cbconc94.txt"

	(Mono)	(Di)	(Tri)	(Tetra)	(Penta)	(Hexa)	(Hepta)	(Octa)
(Cair)	3.26	1.10	12.28	4.76	3.87	2.86	3.23	0.60
(Cinfl)	589.62	11.50	29.38	134.12	73.97	30.12	22.42	2.03

Physical-chemical Properties Input Files for Initial Model Use

File "physchem.txt"

	(a-HCH)	(b-HCH)	(g-HCH)	(HCB)	(Dieldrin)	(Endo I)	(HepEx)	(S-Chlord)	(S-DDT)	(S-PCB)
(MW)	290.85	290.85	290.85	284.79	380.93	406.95	389.2	409.8	330.2	302.3
(VPL)	0.02188	0.0264	0.005864	0.01215	0.0006127	0.0003923	0.054	0.000307	0.0000779	0.00985
(LKow)	3.81	3.8	3.7	5.5	5.2	3.62	5	6	6.05	6.1
(H)	0.1235	0.116	0.07554	6.53	0.036	0.23	2.8	0.35	0.02	1.261
(tw)	41160	110000	148032	110000	192720	440	1680	70000	175200	110000
(ts)	41160	110000	148032	110000	192720	440	1680	70000	175200	110000
(kw)	0.025	0.025	0.025	0.025	0.025	0.025	0.025	0.025	0.025	0.025
(ka)	2.5	2.5	2.5	2.5	2.5	2.5	2.5	2.5	2.5	2.5
(ks)	0.0001	0.0001	0.0001	0.0001	0.0001	0.0001	0.0001	0.0001	0.0001	0.0001

File "pcbpchem.txt"

	(Mono)	(Di)	(Tri)	(Tetra)	(Penta)	(Hexa)	(Hepta)	(Octa)
(MW)	188.7	223.1	257.5	292	326.4	360.9	395.3	429.8
(VPL)	0.128	0.012	0.00284	0.000593	0.000123	0.0000338	0.00000919	0.00000293
(LKow)	4.5	5.1	5.7	5.9	6.3	7	6.9	7.3
(H)	5.502	1.844	2.064	0.882	0.577	1.752	0.282	0.229
(tw)	11000	11000	34000	110000	110000	110000	110000	110000
(ts)	34000	34000	110000	110000	110000	110000	110000	110000
(kw)	0.025	0.025	0.025	0.025	0.025	0.025	0.025	0.025
(ka)	2.5	2.5	2.5	2.5	2.5	2.5	2.5	2.5
(ks)	0.0001	0.0001	0.0001	0.0001	0.0001	0.0001	0.0001	0.0001

Appendix B3 Program Listing for the Amituk Lake Unsteady-state Model in Borland C++ v.4.5

```
#include <stdio.h>
#include <math.h>
#include <stdlib.h>

// Amituk Lake Unsteady State Model based on H. Freitas arctic lake model
// in Visual Basic; Modified.

        double LA,LkMD,ASD,SedLkArea,pSusP,pAerP,pSedS,SedDep,SedRes,SedBur,TFfrac,IPCn;
        double WCPCn,AerCn,FOCwcp,FOCseds,FOCress,FOCip,Ta,Tw,Vaerdep,ScRat,VFsed,Pi,pW,pIce;
        double R,H,MW,VPL,LKow,tw,ts,Cair,CIsed,CIlk,kw,ka,ks,Vw,Vs,LR,ITto,IRto,Vwt,YRbr,YRrsp;
        double YRdep,YRst,YRsw,YRws,YRaw,YRwa,YRwd,YRdd,YRrn,YRwi,YRpi,YRwo,YRpo,YRwt;
        double Zw,TaK,Za,TwK,Zq,Kow,Koc,Zip,Zwcp,Zsed,Zrsp,ZwB,ZinB,ZaB,ZsB,VFaer,VFip,VFwcp;
        double RITD,ITt,RIRD,IRt,RITG,RIRG,Aw,mean,var,normrain,Fgrg,Cgrg,Fmud,Cmud,Fcve,Ccve;
        double Feast,Ceast,Fout,Gin,Cin,Grn,Gdd,Gwd,AnnPre,Gwi,Gip,Gwo,Gop,As,Gsed,Grsp,Gbr,kow;
        double
Dwa,Daw,Dwd,Ddd,Drn,Dwi,Dpi,Dwo,Dpo,Dwt,Dbr,Dst,Drsp,Ddep,Dsw,Dws,SDa,SDi,SDs;
        double SDw,SDws,SDos,Qin,Qa,Qst,Qwt,Qwto,Qsto,CiB,Cwc,Csed,Rbr,Rrsp,Rdep,Rst,Rsw,Rws;
        double Raw,Rwa,Rwd,Rdd,Rrn,Rwi,Rpi,Rwo,Rpo,Rwt,Cip,Cip2,CwcB,Cwcp,Cwcp2,Cop,Cpino;
        double CsedB,Cpw,Csedt,CaB,Caer,CaerC,CaB2,Crnp,Crnds,Vwto,Cof,X,Y,Xt,Yt;
        float chemprop[9][10], disch93[55][5], disch94[70][5], airconc[2][10];
        float CIlke[2][10], CIsedt[2][10], Cplshch[70][3], Cminhch[70][3];

        int yr,pd,i,j,k,finyr,m,l,A;
        FILE *fotpt;
        FILE *faircns;
        FILE *finitcns;
        FILE *fdchrg93;
        FILE *fdchrg94;
        FILE *fphyschem;
        char *fname[40];
        char *fnme[40];

main()
{

// Function Declarations
        void proparray(void),props(void),conc94(void),conc93(void),dischg93(void);
        void dischg94(void),volumes(void),initial(void),zvalues(void),initcn(void);
        void volfracts(void),icecov(void),areas(void),rainfall(void),flows(void);
        void asconc(void),inflowgc(void),gvalues(void),dvalues(void),aquiv(void);
        void conc(void),fluxdy(void),printdy(void),printyr(void),aircn(void),TFfract(void);

// Initializing Amituk Lake Characteristics
        LA = 378395.9;                  // Lake Surface Area (m2)
        LkMD = 19.4;                    // Lake Mean Depth (m)
        ASD = 0.03;                     // Active Sediment Depth (m)
        SedLkArea = 0.3752;             // Sediment/Lake Area Ratio
        AnnPre = 0.1314;                // Annual Precipitation (m/yr)
        pSusP = 2000.;                  // Density of Suspended Particles (kg/m3)
        pAerP = 1500.;                  // Density of Aerosol Particles (kg/m3)
        pSedS = 2000.;                  // Density of Sediment Solids (kg/m3)
        SedDep = 45.4;                  // Sediment Deposition Rate (g/m2/yr)
        SedRes = 0.0;                   // Sediment Resuspension Rate (g/m2/yr)
        SedBur = 121.;                  // Sediment Burial Rate (g/m2/yr)
```

```
        IPCn = 7.42;                           // Inflow Particle Concentration (mg/L)
        WCPCn = 1.47;                          // Water Column Particle Concentration (mg/L)
        AerCn = 0.2;                           // Aerosol Concentration (ug/m3)
        FOCwcp = 0.05;                         // OC Fraction of Water Column Particles
        FOCseds = 0.012;                       // OC Fraction of Suspended Sediment Particles
        FOCress = 0.012;                       // OC Fraction of Resuspended Sed. Particles
        FOCip = 0.05;                          // OC Fraction of Inflow Suspended Particles
        Ta = 4.;                               // Summer Air Temperature (deg C)
        Tw = 1.8;                              // Summer Water Temperature (deg C)
        Vaerdep = 1.8;                         // Aerosol Deposition Velocity (m/h)
        ScRat = 200000.;                       // Scavenging Ratio
        VFsed = 0.50;                          // Volume Fraction of Sediment
// Initializing Additional Variables
        Pi = 3.141592654;                      // Pi
        pW = 1000.;                            // Density of Water (kg/m3)
        pIce = 917.;                           // Density of Ice (kg/m3)(Schindler et al., 1974.
        R = 8.314;                             // Gas Constant (Pa.m3/mol.K)
// Amituk Lake Unsteady State Model (Single Species)
        printf ("\n\nThis is the Amituk Lake Unsteady State Model\n\n");
        printf ("\nChoose which Chemical you are interested in:\n\n");
        printf ("1 - a-HCH\t2 - b-HCH\t3 - g-HCH\n");
        printf ("4 - HCB\t\t5 - Dieldrin\t6 - Endosulfan I\n");
        printf ("7 - Heptachlor Epoxide\t\t8 - S-Chlordanes\n");
        printf ("9 - S-DDT\t10 - PCBs\n\n");
        printf ("Enter the number of your choice\n\n");
        scanf ("%i", &i);

        *fnme = "physchem.txt";
        fphyschem = fopen(*fnme, "r");
        if (fphyschem == NULL){
                printf ("Error opening file %s.\n", *fnme);
                exit(0);
                }

        proparray();
        props();
        aircn();
        dischg93();
        dischg94();
        initcn();

        printf("\n\nThe model begins on June 15, 1993");
        printf("\nMeasured Values are available for 1993 and 1994");
        printf("\nHow many years would you like the Unsteady State Model to Run?");
        printf("\nEnter a number between 1 and 50.\n\n");
        scanf("%i", &finyr);

        yr = 2.;                               // Yr 1 = 1993, Yr 0 = 1992(winter), Yr 2 = 1994

        *fname = "ssoutput.dat";
        fotpt = fopen(*fname, "w");
        if (fotpt == NULL){
                printf ("Error opening file %s.\n", *fname);
                exit(0);
                }
```

```
        else {
                printf ("\n\nThe file %s has been created.\n\n", *fname);
                }
        for (yr = 2; yr <= finyr; yr++){
                if (yr == 0){A = 71.;}
                if (yr >= 1){A = 1.;}
                fprintf(fotpt,"\nDaily Concentrations and Fluxes for Year:  %i", yr);
                fprintf(fotpt,"\nAJDay\tCin\tCwc\tCof\tCsed");
                fprintf(fotpt,"\n\t(pg/L)\t(pg/L)\t(pg/L)\t(ng/g)");

                if (yr <= 1){Cair = airconc[0][i-1];}
                if (yr == 2){Cair = airconc[1][i-1];}
                if (yr > 2){Cair = 0.;}

                volumes();
                volfracts();
                zvalues();
                initial();
                for (pd = A; pd <= 365; pd++){
                        TFfract();
                        icecov();
                        rainfall();
                        asconc();
                        flows();
                        inflowgc();
                        gvalues();
                        dvalues();
                        aquiv();
                        conc();
                        fluxdy();
                        printdy();
                        }
                CIlk = Cwc;                     // Re-init. Lake conc. for next year (pg/L)
                CIsed = Csed;                   // Re-init. sed. conc. for next year (ng/g)
                printyr();
                }
        fclose(fotpt);
        printf("\nEnd of Program\n");
        printf("\nData files can be handled in Excel");
}
//-----------------------------------------------------------------------------
        // Chemical Property and Stream Discharge Functions

void proparray(void)
        // This function reads physchem properties into an array from a file
        // Each row is a different property, each column is a different chemical
{
        for (m = 0; m < 9; m++){
                for (l = 0; l < 10; l++){
                        fscanf(fphyschem,"%f\t", &chemprop[m][l]);
                        }
                fscanf(fphyschem,"\n");
                }
        fclose(fphyschem);
        return;
```

```
}
void props(void)
        // This function initializes phys-chem property variables according
        // to choice of chemical
{
        MW = chemprop[0][i-1];                  // Molecular Weight (g/mol)
        VPL = chemprop[1][i-1];                 // Liquid Vapour Pressure (Pa)
        LKow = chemprop[2][i-1];                // Log Kow
        H = chemprop[3][i-1];                   // Henry's Law Constant (Pa mol/m3)
        tw = chemprop[4][i-1];                  // Degr. Half-life in Water (h)
        ts = chemprop[5][i-1];                  // Degr. Half-life in Sediment (h)
        kw = chemprop[6][i-1];                  // Water MTC (m/h)
        ka = chemprop[7][i-1];                  // Air MTC (m/h)
        ks = chemprop[8][i-1];                  // sediment MTC (m/h)
        return;
}
void conc94(void)
        // 1994 Daily Stream Concentrations
{
        switch (i) {
                case 1: // alphaHCH
                        Cgrg = 3429.111+78.34662*pd-37.51604*pow(pd,2)+2.158319*pow(pd,3)-
                                0.05243451*pow(pd,4)+5.880126*pow(10,-4)*pow(pd,5)-2.503327
                                *pow(10,-6)*pow(pd,6);
                        Cmud = 21.3932+96.04544*pd-10.06446*pow(pd,2)+0.414678*pow(pd,3)-
                                0.008350995*pow(pd,4)+8.234703*pow(10,-5)*pow(pd,5)-3.188925
                                *pow(10,-7)*pow(pd,6);
                        Ccve = -27006.54+5832.477*pd-485.4507*pow(pd,2)+21.05235*pow(pd,3)-
                                0.5215588*pow(pd,4)+7.449579*pow(10,-3)*pow(pd,5)-5.715073
                                *pow(10,-5)*pow(pd,6)+1.824351*pow(10,-7)*pow(pd,7);
                        Ceast = 1479.254-154.8519*pd+6.622915*pow(pd,2)-0.1394947*pow(pd.3)
                                +0.001453774*pow(pd,4)-6.036062*pow(10,-6)*pow(pd,5);
                        break;
                case 2: // betaHCH
                        Cgrg = -3.9075075*pow(10,-8)*pow(pd,6)+7.868093*pow(10,-6)*pow(pd.5)-
                                0.0005202783*pow(pd,4)+0.008233154*pow(pd,3)+0.4111639
                                *pow(pd,2) -16.05759*pd+172.93;
                        Cmud = 1.3352149*pow(10,-6)*pow(pd,5)-0.0002709598*pow(pd,4)
                                +0.01983006*pow(pd,3)-0.6169923*pow(pd,2)+6.771727*pd+10.5708;
                        Ccve = -0.00150985*pow(pd,3)+0.227359*pow(pd,2)-11.25953*pd+197.4742;
                        Ceast = -6.976347*pow(10,-4)*pow(pd,3)+0.1006644*pow(pd,2)-4.521*pd
                                +63.0714;
                        break;
                case 3: // gammaHCH
                        Cgrg = -6.629619*pow(10,-7)*pow(pd,6)+0.0001579849*pow(pd,5)-0.01431017
                                *pow(pd,4)+0.6023107*pow(pd,3)-10.990592*pow(pd,2)+35.28608
                                *pd+927.9241;
                        Cmud = -9.81679*pow(10,-7)*pow(pd,6)+2.69236*pow(10,-5)*pow(pd,5)-
                                0.0028692*pow(pd,4)+0.145837*pow(pd.3)-3.33416*pow(pd.2)
                                +17.198*pd+299.194;
                        Ccve = 1.861372*pow(10,-5)*pow(pd,5)-0.00394123*pow(pd,4)+0.30851*
                                pow(pd,3)-10.70853*pow(pd,2)+146.7682*pd-231.7753;
                        Ceast = 553.419697*exp(-0.096561*pd);
```

```
            break;
    case 4:  // HCB
            Cgrg = 8.6851418*pow(10,-7)*pow(pd,5)-0.0001713929*pow(pd,4)
                   +0.01226843*pow(pd,3)-0.3752661*pow(pd,2)+3.917663*pd+12.33376;
            Cmud = -0.04614*pd+3.54011;
            Ccve = -5.983673*pow(10,-4)*pow(pd,3)+0.0878194*pow(pd,2)-4.102486*pd
                   +60.6442;
            Ceast = 1.703876*pow(10,-5)*pow(pd,4)-0.00273528*pow(pd,3)+0.1499
                   *pow(pd,2)-3.2424*pd+22.633;
            break;
    case 5:  // Dieldrin
            Cgrg = 0.0001098784*pow(pd,4)-0.02065141*pow(pd,3)+1.378255*pow(pd,2)-
                   38.776645*pd+456.8238;
            Cmud = -0.019091*pow(pd,2)+0.237029*pd+105.2659;
            Ccve = -7.803781*pow(10,-4)*pow(pd,3)+0.145041*pow(pd,2)-
                   9.281129*pd+258.1953;
            Ceast = -2.2068*pow(10,-6)*pow(pd,5)+0.00033109*pow(pd,4)-0.0150539
                   *pow(pd,3)+0.137694*pow(pd,2)+2.998*pd+62.866;
            break;
    case 6:  // Endosulfan I
            Cgrg = -3.0987521*pow(10,-7)*pow(pd,6)+7.7085217*pow(10,-5)*pow(pd,5)-
                   0.007406667*pow(pd,4)+0.3388097*pow(pd,3)-
                   7.100474*pow(pd,2)+42.741413*pd+334.2262;
            Cmud = 2.97542077*pow(10,-6)*pow(pd,5)-0.0005813746*pow(pd,4)+
                   0.03981796*pow(pd,3)-1.0803415*pow(pd,2)+7.358122*pd+84.9854;
            Ccve = -0.00617683*pow(pd,3)+0.9163*pow(pd,2)-43.86664*pd+698.5637;
            Ceast = 3.415896*pow(10,-5)*pow(pd,4)-0.0063327*pow(pd,3)+0.4162058
                   *pow(pd,2)-11.959*pd+154.0845;
            break;
    case 7:  // Heptachlor Epoxide
            Cgrg = 2.0179789*pow(10,-6)*pow(pd,5)-0.0003271262*pow(pd,4)+0.01641153
                   *pow(pd,3)-0.1414209*pow(pd,2)-8.854356*pd+192.4627;
            Cmud = 3.0559343*pow(10,-6)*pow(pd,5)-0.0005838257*pow(pd,4)+0.04017943
                   *pow(pd,3)-1.1941725*pow(pd,2)+13.60316*pd+7.93921;
            Ccve = -8.04877*pow(10,-4)*pow(pd,3)+0.1092465*pow(pd,2)-4.88659*pd
                   +111.32;
            Ceast = 51.2827*exp(-0.015286*pd);
            break;
    case 8:  // Sum-Chlordane
            Cgrg = -0.0001109286*pow(pd,3)+0.017785029*pow(pd,2)-0.027765*pd
                   +22.6389;
            Cmud = -0.6555*log(pd)+2.61;
            Ccve = 200.645535*exp(-0.145723*pd);
            Ceast = -2.4729*log(pd)+9.727;
            break;
    case 9:  // Sum-DDT
            Cgrg = 1.241828*pow(10,-5)*pow(pd,4)-0.002348653*pow(pd,3)+0.1605792
                   *pow(pd,2)-5.059741*pd+79.9212;
            Cmud = 2.0453584*pow(10,-6)*pow(pd,5)-0.0003055438*pow(pd,4)+0.01424696
                   *pow(pd,3)-0.2123156*pow(pd,2)+0.9290444*pd+9.109;
            Ccve = -5.48864*pow(10,-4)*pow(pd,3)+0.07571*pow(pd,2)-3.20562*pd
                   +48.2295;
            Ceast = 2.86017673*pow(10,-8)*pow(pd,6)-7.6004411*pow(10,-6)*pow(pd,5)
                   +7.8615512*pow(10,-4)*pow(pd,4)-0.03919646*pow(pd,3)+0.9401147
```

```
                                  *pow(pd,2)-9.36685*pd+33.8458;
                          break;
                  case 10:  // Sum-PCB
                          Cgrg = 0.0006654862*pow(pd,4)-0.088126437*pow(pd,3)+2.867389*pow(pd,2)-
                                  6.1102366*pd+982.5631;
                          Cmud = -0.0004371045*pow(pd,4)+0.05031*pow(pd,3)-1.344081*pow(pd,2)-
                                  9.014963*pd+1206.268;
                          Ccve = 0.00099659*pow(pd,4)-0.184758*pow(pd,3)+12.0005*pow(pd,2)-
                                  324.3799*pd+3501.813;
                          Ceast = 2.0985*pd+408.96;
                          break;
                  default:  printf ("ERROR - Illegal Entry - Re-run Program\n");
                          abort();
                  }
          return;
}
void conc93(void)
          // 1993 Daily Stream Concentrations
{
          switch (i) {
                  case 1:   // alphaHCH
                          Cgrg = 49631.*pow(pd,-1.2091);
                          Cmud = 4908.4*exp(-0.1604*pd);
                          Ccve = 5598.4*exp(-0.0655*pd);
                          Ceast = -363.51*log(pd)+1489.;
                          break;
                  case 2:   // betaHCH
                          Cgrg = -39.303*log(pd)+157.3973;
                          Cmud = -13.007*log(pd)+66.401;
                          Ccve = 129.73*pow(pd,-0.5421);
                          Ceast = 2.5022*pow(pd,0.768);
                          break;
                  case 3:   // gammaHCH
                          Cgrg = 42991.*pow(pd,-1.7187);
                          Cmud = 590.26*exp(-0.1019*pd);
                          Ccve = 76408.*pow(pd,-1.9551);
                          Ceast = -39.789*log(pd)+171.74;
                          break;
                  case 4:   // HCB
                          Cgrg = -6.299*log(pd)+54.6467;
                          Cmud = -0.1521*pd+34.537;
                          Ccve = 1319.3*pow(pd,-1.3478);
                          Ceast = -0.2286*pd+14.943;
                          break;
                  case 5:   // Dieldrin
                          Cgrg = 600.1*pow(pd,-0.7394);
                          Cmud = -1.9003*pd+109.48;
                          Ccve = 977.1*pow(pd,-0.8008);
                          Ceast = -10.198*log(pd)+70.016;
                          break;
                  case 6:   // Endosulfan I
                          Cgrg = 658.96*exp(-0.0926*pd);
                          Cmud = -68.106*log(pd)+282.01;
```

```
                        Ccve = 36843.*pow(pd,-1.8655);
                        Ceast = 0.005292*pow(pd,3)-0.47713*pow(pd,2)+10.6551*pd+3.9;
                        break;
                case 7: // Heptachlor Epoxide
                        Cgrg = 337.52*pow(pd,-0.5486);
                        Cmud = -0.3336*pd+46.665;
                        Ccve = -1.267*pd+101.61;
                        Ceast = 80.224*exp(-0.0190*pd);
                        break;
                case 8: // Sum-Chlordane
                        Cgrg = 318.9706*exp(-0.04925*pd);
                        Cmud = 0.96365*pd+10.29595;
                        Ccve = -1.15917*pd+74.5089;
                        Ceast = -0.15306*pd+30.9796;
                        break;
                case 9: // Sum-DDT
                        Cgrg = 17.894*log(pd)-1.0163;
                        Cmud = 1.1971*pd+8.6078;
                        Ccve = 69.7;
                        Ceast = -1.2398*pd+53.58;
                        break;
                case 10: // Sum-PCB
                        Cgrg = 194.41*log(pd)-32.208;
                        Cmud = 17.346*pd+303.55;
                        Ccve = 1256.2*exp(-0.0642*pd);
                        Ceast = 12.805*pd+340.02;
                        break;
                default: printf ("ERROR - Illegal Entry - Re-run Program\n");
                        abort();
                }
        return;
}
void dischg94(void)
// Opens 1994 stream discharge file and assigns values to an array
{
        *fnme = "disc94.txt";
        fdchrg94 = fopen(*fnme, "r");
        if (fdchrg94 == NULL){
                printf ("Error opening file %s.\n", *fnme);
                exit(0);
                }
        for (j = 0; j < 70; j++){
                for (k = 0; k < 5; k++){
                        fscanf(fdchrg94,"%f\t", &disch94[j][k]);
                        }
                fscanf(fdchrg94,"\n");
                }
        fclose(fdchrg94);
        return;
}
void dischg93(void)
        // Opens 1993 stream discharge file and assigns values to an array
```

```
{
        *fnme = "disc93.txt";
        fdchrg93 = fopen(*fnme, "r");
        if (fdchrg93 == NULL){
                printf ("Error opening file %s.\n", *fnme);
                exit(0);
                }
        for (j = 0; j < 55; j++){
                for (k = 0; k < 5; k++){
                        fscanf(fdchrg93,"%f\t", &disch93[j][k]);
                        }
                fscanf(fdchrg93,"\n");
                }
        fclose(fdchrg93);
        return;
}
void aircn(void)
        // Enters air concentrations from a file into an array for chosen year
{
        *fnme = "ussaircn.txt";
        faircns = fopen(*fnme, "r");
        if (faircns == NULL){
                printf ("Error opening file %s.\n", *fnme);
                exit(0);
                }
        for (j = 0; j < 2; j++){
                for (k = 0; k < 10; k++){
                        fscanf(faircns,"%f\t", &airconc[j][k]);
                        }
                fscanf(faircns,"\n");
                }
        fclose(faircns);
        return;
}
void initcn(void)
        //  Enters initial sediment and lake concentrations into arrays
{
        *fnme = "ussinit.txt";
        finitcns = fopen(*fnme, "r");
        if (finitcns == NULL){
                printf ("Error opening file %s.\n", *fnme);
                exit(0);
                }
        for (k = 0; k < 10; k++){
                fscanf(finitcns,"%f\t", &Cllke[0][k]);
                }
        fscanf(finitcns,"\n");
        for (k = 0; k < 10; k++){
                fscanf(finitcns,"%f\t", &Clsedt[1][k]);
                }
        fclose(finitcns);
        Clsed = Clsedt[1][i-1];                 // 1992 from Muir et al., 1995
```

```
        Cllk = Cllke[0][i-1];              // 1993 mid-June from Semkin, unpubl. (or June 1992)
        return;
}
void asconc(void)
        // Calculates daily concentrations
{
        if (yr == 1){conc93();}
        else{conc94();}
        return;
}
void TFfract(void)
        // Water throughflow without mixing during melt
{
        if (pd == 1){TFfrac = 0.4;}
        if (pd == 2){TFfrac = 0.4;}
        if (pd == 3){TFfrac = 0.4;}
        if (pd == 4){TFfrac = 0.4;}
        if (pd == 5){TFfrac = 0.5;}
        if (pd == 6){TFfrac = 0.6;}
        if (pd == 7){TFfrac = 0.8;}
        if (pd == 8){TFfrac = 0.8;}
        if (pd == 9){TFfrac = 0.8;}
        if (pd == 10){TFfrac = 0.8;}
        if (pd == 11){TFfrac = 0.8;}
        if (pd == 12){TFfrac = 0.8;}
        if (pd == 13){TFfrac = 0.7;}
        if (pd == 14){TFfrac = 0.4;}
        if (pd == 15){TFfrac = 0.1;}
        if (pd == 16){TFfrac = 0.1;}
        if (pd == 17){TFfrac = 0.1;}
        if (pd == 18){TFfrac = 0.1;}
        if (pd == 19){TFfrac = 0.1;}
        if (pd == 20){TFfrac = 0.1;}
        if (pd == 21){TFfrac = 0.9;}
        if (pd == 22){TFfrac = 0.88;}
        if (pd == 23){TFfrac = 0.86;}
        if (pd == 24){TFfrac = 0.84;}
        if (pd == 25){TFfrac = 0.82;}
        if (pd > 25){TFfrac = TFfrac-0.015;}
        if (pd > 70){TFfrac = 0.;}
        return;
}
//-----------------------------------------------------------------------
        // Model Calculation Functions
void volumes(void)
        // Calculates lake water and sediment volumes
{
        Vw = LA * LkMD;                    // Lake Water Volume (m3)
        Vs = LA * ASD * SedLkArea;         // Active Lake Sediment Volume (m3)
        return;
}
void volfracts(void)
```

```
        // Calculates volume fractions of particles in bulk phase
{
        VFaer = AerCn / (pAerP * pow(10,9));     // vol. fract. of aerosols
        VFip = IPCn / (pSusP * 1000);            // vol. fract. of inflow particles
        VFwcp = WCPCn / (pSusP * 1000);          // vol. fract. of water col. particles
        return;
}
void zvalues(void)
        // Calculates Z-values in Aquivalence form
{
        TaK = Ta + 273.16;                       // Air Temp. in Kelvin
        TwK = Tw + 273.16;                       // Water Temp. in Kelvin

        Zw = 1.;                                 // Water Z-value
        Za = H / (R*TaK);                        // Air Z-value
        Zq = (6000000. / VPL) * Za;              // Aerosol Z-value

        Kow = pow(10, LKow);                     // Octanol-water partition coefficient
        Koc = 0.41 * Kow;                        // Org. Carb.-water part. coefficient

        Zip = (Koc*FOCip*pSusP*Zw)/1000;                 // Infl. Part. Z-value
        Zwcp = (Koc*FOCwcp*pSusP*Zw)/1000;               // Water Col. Part. Z-value
        Zsed = (Koc*FOCseds*pSedS*Zw)/1000;              // Sediment Z-value
        Zrsp = Zsed;
// Bulk Z-Values
        ZwB = Zw*(1-VFwcp) + Zwcp*VFwcp;                 // Bulk Water Z-value
        ZinB = Zw*(1-VFip) + Zip*VFip;                   // Bulk Inflow Z-value
        ZaB = Za*(1-VFaer) + Zq*VFaer;                   // Bulk Air Z-valuc
        ZsB = Zw*(1-VFsed) + Zsed*VFsed;                 // Bulk Sediment Z-value
        return;
}
void initial(void)
        // Provides initial values for variables involved in time-step calcs.
{
        LR = sqrt(LA/Pi);                        // Lake Radius (m)
        if (yr == 0){
                ITto = 0.;
                IRto = 0.;
                }
        else {
                ITto = 2.2;                      // 1994 Ice Thickness on June 15
                IRto = LR;                       // Ice Radius = Lake Radius on June 15
                }
        Qsto = CIsed*pSedS/(Zsed*MW*pow(10,6));          // Init.Sed.Aquiv.(mol/m3)
        Qwto = CIlk/(Zw*MW*pow(10,9));                   // Init.LkWater.Aquiv.(mol/m3)

        YRbr = 0.;
        YRrsp = 0.;
        YRdep = 0.;
        YRst = 0.;
        YRsw = 0.;
        YRws = 0.;
        YRaw = 0.;
        YRwa = 0.;
```

```
        YRwd = 0.;
        YRdd = 0.;
        YRrn = 0.;
        YRwi = 0.;
        YRpi = 0.;
        YRwo = 0.;
        YRpo = 0.;
        YRwt = 0.;
        X = 0.;
        Y = 0.;
        return;
}
void icecov(void)
{
        Vwto =  Vw-((Pi*pow(IRto,2)*ITto*pW)/pIce);       // Frozen Lake Volume (m3) (June 15)
        if (pd <= 31){                                     // Ice Decay June 15 to Jul. 15
                RITD = -2.2 / (31);
                ITt = ITto + RITD;
                RIRD = -LR / (31);
                IRt = IRto + RIRD;
                Aw = LA - (Pi*pow(IRt,2));
                }
        if (pd > 31 && pd <= 92){                                    // Ice Off Jul. 16 to Sept. 14
                RITD = 0.;
                ITt = 0.;
                RIRD = 0.;
                IRt = 0.;
                Aw = LA - (Pi*pow(IRt,2));
                }
        if (pd > 92 && pd <= 326){                         // Ice Growth Sept. 15 to May 6
                RITG = 2.2 / (234);
                ITt = ITto + RITG;
                RIRG = 0.;
                IRt = LR;
                Aw = 0.;
                }
        if (pd > 326 && pd <= 365){                        //  Max. Ice Thickness May 7 to Jun. 14
                RITG = 0.;
                ITt = ITto + RITG;
                RIRG = 0.;
                IRt = LR;
                Aw = 0.;
                }
        Vwt = Vw-((Pi*pow(IRt,2)*ITt*pW)/pIce);            // Lake Volume (m3)
        ITto = ITt;                                        // Re-initializes ice dimensions
        IRto = IRt;
        return;
}
void rainfall(void)
        // Calculates normal distribution of summer rainfall
{
        mean = 50.;                                        // Rainfall begins June 15 - pd 1 and peaks
```

```
        var = mean/4;                                   // on Aug. 3 -pd 50, ends Sept. 23 - pd 101
        normrain = (1/(var*pow(2.*Pi,0.5)))*exp(-1.*pow(pd-mean,2.)/(2.*pow(var,2.)));
        if (pd > 101) normrain = 0.;
        return;
}
void flows(void)
        // Assigns daily discharges and concentrations. Inflow discharge multiplied by 1.106 to acccount for
the
        // 10.6% of inflow that is unguaged (Semkin, unpubl. 1993 data)
{
        if (yr == 1){
                if (pd <= 55){
                        Fgrg = disch93[pd-1][0]*1.106;
                        Fmud = disch93[pd-1][1]*1.106;
                        Fcve = disch93[pd-1][2]*1.106;
                        Feast = disch93[pd-1][3]*1.106;
                        Fout = disch93[pd-1][4];
                        }
                if (pd > 55){
                        Fgrg = 0.;
                        Cgrg = 0.;
                        Fmud = 0.;
                        Cmud = 0.;
                        Fcve = 0.;
                        Ccve = 0.;
                        Feast = 0.;
                        Ceast = 0.;
                        Fout = 0.;
                        }
                }
        else{
                if (pd <= 70){
                        Fgrg = disch94[pd-1][0]*1.106;
                        Fmud = disch94[pd-1][1]*1.106;
                        Fcve = disch94[pd-1][2]*1.106;
                        Feast = disch94[pd-1][3]*1.106;
                        Fout = disch94[pd-1][4];
                        }
                if (pd > 70){
                        Fgrg = 0.;
                        Cgrg = 0.;
                        Fmud = 0.;
                        Cmud = 0.;
                        Fcve = 0.;
                        Ccve = 0.;
                        Feast = 0.;
                        Ceast = 0.;
                        Fout = 0.;
                        }
                }
        return;
}
void inflowgc(void)
```

```
        // Calculates inflow G-value and inflow concentration
{
        Gin = (Fgrg+Fmud+Fcve+Feast);
        if (Cgrg < 0){Cgrg = 0.;}
        if (Cmud < 0){Cmud = 0.;}
        if (Ccve < 0){Ccve = 0.;}
        if (Ceast < 0){Ceast = 0.;}
        if (Gin == 0){
                Cin = 0.;
                }
        else{
                Cin = ((Cgrg*Fgrg)+(Cmud*Fmud)+(Ccve*Fcve)+(Ceast*Feast))/Gin;
                }
        return;
}
void gvalues(void)
        // calculates the G-values, rate of physical processes
{
// Air G-Values
        Grn = (AnnPre/2)*(normrain)*(Aw/(101))*(1-TFfrac);      // Rain rate (m3/d)
        Gdd = Vaerdep*24*Aw*VFaer*(1-TFfrac);                   // Dry Depos. rate (m3/d)
        Gwd = Grn * VFaer * ScRat;                              // Wet Depos. rate (m3/d)
// Water G-Values
        Gwi = Gin*60*60*24*(1-TFfrac);                  // Adj. water inflow rate (m3/d)
        Gip = Gwi * VFip;                               // Particle inflow rate (m3/d)
        Gwo = Fout*60*60*24*(1-TFfrac);                 // Adj. water outflow rate (m3/d)
        Gop = Gwo * VFwcp;                              // Particle outflow rate (m3/d)

        X = Gwi*1000*Cin/pow(10,9);                     // Amount of chemical entering lake (mg/d)
        Y = Gin*60*60*24*TFfrac*1000*Cin/pow(10,9);     // Amt passing over (mg/d)

// Sediment G-Values
        As = LA * SedLkArea;                            // Sediment Area (m2)
        Gsed = (SedDep*LA) / (101*pSusP*1000);          // Sed. Depostion rate (m3/d)
        Grsp = (SedRes*As) / (101*pSedS*1000);          // Sed. Resuspens. rate (m3/d)
        Gbr = (SedBur*As) / (101*pSedS*1000);           // Sed. Burial rate (m3/d)
        if (pd > 101){
                Gsed = 0.;                              // Processes negligible after ice formation
                Grsp = 0.;
                Gbr = 0.;
                }
        return;
}
void dvalues(void)
        // Calculates D-values (m3/d)
{
        kow = 1/(1/kw+R*TwK/(H*ka));            // Overall waterside MTC
// Air D-values
        Dwa = kow*Aw*Zw;                        // Volatilization
        Daw = kow*Aw*Zw;                        // Adsorption
        Dwd = Gwd*Zq;                           // Wet Deposition
        Ddd = Gdd*Zq;                           // Dry Deposition
        Drn = Grn*Zw;                           // Rain Dissolution

// Water D-values
```

```
        Dwi = Gwi*Zw;                              // Water Inflow
        Dpi = Gip*Zip;                             // Particle Inflow
        Dwo = Gwo*Zw;                              // Water Outflow
        Dpo = Gop*Zwcp;                            // Particle Outflow
        Dwt = Vwt*ZwB*0.693*24/tw;                 // Water Degradation

// Sediment D-values
        Dbr = Gbr*Zsed;                            // Sediment Burial
        Dst = Vs*ZsB*0.693*24/ts;                  // Sediment Transformation
        Drsp = Grsp*Zrsp;                          // Sediment Resuspension
        Ddep = Gsed*Zwcp;                          // Sediment Deposition
        Dsw = As*Zw*ks;                            // Sediment - Water Diffusion
        Dws = As*Zw*ks;                            // Water-Sediment Diffusion
        return;
}
void aquiv(void)
        // Calculates Aquivalences (Mass Balance Equations)(Equilibrium Criterion)
{
// Sum of D-values used in water Aquivalence Equation
        SDa = Drn + Ddd + Dwd + Daw;               // Sum of air to lakewater D-values
        SDi = Dwi + Dpi;                                   // Sum of inflow D-values
        SDs = Dsw + Drsp;                          // Sum of sed. to lakewater D-values
        SDw = Dwa+Dws+Dwt+Ddep+Dpo+Dwo;                    // Sum of lakewater loss D-values

// Sum of D-values used in sediment Aquivalence Equation
        SDws = Ddep + Dws;                                 // Sum of water to sed. D-values
        SDos = Dst + Dsw + Dbr + Drsp;                     // Sum of out of sediment D-values

// Aquivalences
        Qin = Cin / (ZinB*MW*pow(10,9));                   // Inflow Aquivalence (mol/m3)
        Qa = Cair / (Za*MW*pow(10,12));                    // Air Aquivalence (mol/m3)
        Qst = ((((Qwto*SDws)-(Qsto*SDos))*1)/(Zsed*Vs)) + Qsto;  // Sediment Aquivalence (mol/m3)
        Qwt = (((Qa*SDa+Qin*SDi+Qsto*SDs-Qwto*SDw)*1)/(Zw*Vwt))+(Qwto*Vwto/Vwt);
                                                           // Water Aquivalence (mol/m3)
        Vwto = Vwt;
        Qwto = Qwt;
        Qsto = Qst;
        return;
}
void conc(void)
        // Calculates concentrations in varios media
{
// Inflow
        CiB = Qin*ZinB*MW*pow(10,9);                       // Bulk Inflow Conc. (pg/L)
        Cip = Qin*Zip*MW*VFip*pow(10,9);                   // Conc. in Particle (pg/L)
        Cip2 = Qin*Zip*MW*pow(10,9)/pSusP;                 // Conc. in Particle (pg/g)

// Lake Water Column
        Cwc = Qwt*Zw*MW*pow(10,9);                         // Water Column Conc. (pg/L)
        CwcB = Qwt*ZwB*MW*pow(10,9);                       // Bulk Water Conc. (pg/L)
        Cwcp = Qwt*Zwcp*MW*VFwcp*pow(10,9);                // Conc. in Particle (pg/L)
        Cwcp2 = Qwt*Zwcp*MW*pow(10,9)/pSusP;               // Conc. in Particle (pg/g)

// Outflow
        Cof = (Qin*Zw*TFfrac + Qwt*Zw*(1-TFfrac))*MW*pow(10,9);        // Outflow Water Conc.(pg/L)
        if (Qin == 0){Cof = 0.;}                                       // No outflow occurs.
```

```
        Cop = (Qin*Zip*TFfrac*VFip + Qwt*Zwcp*(1-TFfrac)*VFwcp)*MW*pow(10,9);
                                                        // Conc. in Part.(pg/L)
        Cpino = TFfrac*IPCn+(1-TFfrac)*WCPCn;          // Conc. of Particles in Outflow (mg/L)
// Sediment
        CsedB = Qst*ZsB*MW*pow(10,6)/pSedS;            // Bulk Sediment Conc. (ng/g)
        Csed = Qst*Zsed*MW*pow(10,6)/pSedS;            // Dry Sediment Conc. (ng/g)
        Cpw = Qst*Zw*MW*pow(10,6)/pSedS;               // Sed. Pore Water Conc. (ng/L sed.)
        Csedt = (Csed*VFsed) + Cpw*(1-VFsed);          // Total Sediment Conc. (ng/g)
// Air
        CaB = Qa*ZaB*MW*pow(10,12);               // Bulk Air Conc. (pg/m3)
        Caer = Qa*Zq*MW*pow(10,12);               // Conc. on Aerosols (pg/m3 parts)
        CaerC = Caer*VFaer;                       // Conc. in air from Aerosols (pg/m3)
        CaB2 = CaerC + Cair*(1-VFaer);            // Alternate Calc. bulk air conc. (pg/m3)
// Rain
        Crnp = Qa*VFaer*ScRat*Zq*MW*pow(10,9);    // Conc. from Part. in rain (pg/L)
        Crnds = Qa*Zw*MW*pow(10,9);               // Conc. from dissn in rain (pg/L)
        return;
}
void fluxdy(void)
        // Calculates daily fluxes (mg/d)
{
        Rbr = Dbr*Qst*MW*1000;                    // Sediment Burial Flux
        Rrsp = Drsp*Qst*MW*1000;                  // Sed. Resuspension Flux
        Rdep = Ddep*Qwt*MW*1000;                  // Sed. Deposition Flux
        Rst = Dst*Qst*MW*1000;                    // Sed. Transformation Flux
        Rsw = Dsw*Qst*MW*1000;                    // Sed.-Water Diffusion Flux
        Rws = Dws*Qwt*MW*1000;                    // Water-Sed. Diffusion Flux
        Raw = Daw*Qa*MW*1000;                     // Adsorption Flux
        Rwa = Dwa*Qwt*MW*1000;                    // Volatilization Flux
        Rwd = Dwd*Qa*MW*1000/(1-TFfrac);          // Wet Part. Deposition Flux
        Rdd = Ddd*Qa*MW*1000/(1-TFfrac);          // Dry Part. Deposition Flux
        Rrn = Drn*Qa*MW*1000/(1-TFfrac);          // Rain Deposition Flux
        Rwi = Dwi*Qin*MW*1000/(1-TFfrac);         // Water Inflow Flux
        Rpi = Dpi*Qin*MW*1000/(1-TFfrac);         // Particle Inflow Flux
        Rwo = (Dwo*Qwt+Gin*TFfrac*3600*24*Zw*Qin)*MW*1000;       // Water Outflow Flux
        Rpo = (Dpo*Qwt+Gin*VFip*TFfrac*3600*24*Zip*Qin)*MW*1000; // Particle Outflow Flux
        Rwt = Dwt*Qwt*MW*1000;                    // Water Transformation Flux
// Sum of fluxes for Yearly flux (mg/year)
        YRbr = YRbr + Rbr;
        YRrsp = YRrsp + Rrsp;
        YRdep = YRdep + Rdep;
        YRst = YRst + Rst;
        YRsw = YRsw + Rsw;
        YRws = YRws + Rws;
        YRaw = YRaw + Raw;
        YRwa = YRwa + Rwa;
        YRwd = YRwd + Rwd;
        YRdd = YRdd + Rdd;
        YRrn = YRrn + Rrn;
        YRwi = YRwi + Rwi;
        YRpi = YRpi + Rpi;
        YRwo = YRwo + Rwo;
```

```
        YRpo = YRpo + Rpo;
        YRwt = YRwt + Rwt;
        Xt = Xt + X;
        Yt = Yt + Y;

        return;
}
void printdy(void)
        // Prints daily concentrations and fluxes
{
        fprintf(fotpt,"\n%i\t%e\t%e\t%e\t%e\t%e\t%e", pd,Cin,Cwc,Cof,Csed);
        return;
}
void printyr(void)
        // Prints the concentrations and fluxes for the steady state model
{
        fprintf(fotpt,"\n\nAmituk Lake Unsteady State Model - Year %i", yr);
        fprintf(fotpt,"\n\nChemical Fluxes in mg/year\n\n");
        fprintf(fotpt,"Sediment Burial = \t%e\n", YRbr);
        fprintf(fotpt,"Sediment Resuspension = \t%e\n", YRrsp);
        fprintf(fotpt,"Sediment Deposition = \t%e\n", YRdep);
        fprintf(fotpt,"Sediment-Water Diffusion = \t%e\n", YRsw);
        fprintf(fotpt,"Water-Sediment Diffusion = \t%e\n", YRws);
        fprintf(fotpt,"Absorption = \t%e\n", YRaw);
        fprintf(fotpt,"Volatilization = \t%e\n", YRwa);
        fprintf(fotpt,"Wet Particle Deposition = \t%e\n", YRwd);
        fprintf(fotpt,"Dry Particle Deposition = \t%e\n", YRdd);
        fprintf(fotpt,"Rain Dissolution = \t%e\n", YRrn);
        fprintf(fotpt,"Water Inflow = \t%e\n", YRwi);
        fprintf(fotpt,"Particle Inflow = \t%e\n", YRpi);
        fprintf(fotpt,"Water Outflow = \t%e\n", YRwo);
        fprintf(fotpt,"Particle Outflow = \t%e\n", YRpo);
        fprintf(fotpt,"Water Transformation = \t%e\n", YRwt);
        fprintf(fotpt,"Sediment Transformation = \t%e\n", YRst);
        fprintf(fotpt,"\n\t%e\n", Xt);
        fprintf(fotpt,"\t%e\n", Yt);
        return;
}
```

Appendix B4 Unsteady-state Model Input Files

Files for Initial Unsteady-state Runs, 1993 and 1994

Unsteady-state Model Stream Discharge Files - 1993 and 1994

Files for Initial Unsteady-State Runs, 1993 and 1994

(Using Mean Concentrations)

For file "ussaircn.txt"

	(a-HCH)	(b-HCH)	(g-HCH)	(HCB)	(Dieldrin)	(Endo I)	(HepEx)	(S-Chlord)	(S-DDT)	(S-PCB)
(Cair93)	49.93	0.41	6.25	44.45	1.67	4.36	1.58	3.66	0.37	39.52
(Cair94)	41.77	0.09	7.04	39.83	1.4	4.38	1.5	3.29	0.76	32.08

Notes:

1. Air concentrations from Halsall et al., 199?; pers. comm..

For file "ussinit.txt" *(Initializes sediment and lake concentrations for pd 1 of year 1)*

	(a-HCH)	(b-HCH)	(g-HCH)	(HCB)	(Dieldrin)	(Endo I)	(HepEx)	(S-Chlord)	(S-DDT)	(S-PCB)
(Cllk)	1370.4	82.2	434.1	22.8	95.1	3.9	82.2	8.5	101.4	119.8
(Clsed)	0.35	0.01	0.55	1.14	1.18	0.01	0.1	1.65	1.67	12.2

Notes:

1. Lake concentrations (pg/L) from Semkin, unpubl. on June 16, 1993 (June 23, 1993 if June 16 is 0.0 pg/L; Avg. at 20 m if many 0's).
2. Sediment concentrations (ng/g) from Muir et al., 1995.
3. Σ-PCB June 23, 1993 chosen as June 16 value considered an outlier (1782.3 pg/L).
4. Endosulfan I value in sediment not reported but assumed to be 0.01 ng/g for modelling.

Unsteady-state model stream discharge files - 1993 and 1994

For file "disc93.txt"

(ADJ)	(Gorge)	(Mud)	(Cave)	(East)	(Outflow)
1	0.0000	0.0000	0.0000	0.0000	0.0000
2	0.0000	0.0000	0.0000	0.0000	0.0000
3	0.0000	0.0000	0.0000	0.0000	0.0000
4	0.0000	0.2150	0.0000	0.0000	0.0817
5	0.0385	0.2575	0.0000	0.0000	0.0275
6	0.0328	0.4750	0.0000	0.0000	0.0713
7	0.1779	0.6244	0.0000	0.0000	0.0858
8	0.2422	0.6990	0.0000	0.0000	0.1915
9	0.3064	0.7737	0.0000	0.0620	1.1046
10	0.3425	0.6791	0.5400	0.1067	2.9437
11	0.3786	0.5845	0.4673	0.1514	2.0456
12	0.7072	0.3716	0.3945	0.1528	1.9426
13	2.1151	0.7362	0.5861	0.2849	4.7038
14	1.5226	0.3002	0.4388	0.1832	3.1334
15	2.8473	0.2861	0.4238	0.0815	2.2468
16	2.3415	0.2889	0.5425	0.1220	5.5721
17	1.8356	0 2916	0.6611	0.1625	4.5452
18	1.4058	0.2194	0.4600	0.1187	3.3771
19	0.8297	0.1038	0.3174	0.0576	2.0839
20	0.9912	0 1028	0.2917	0.1490	2.2816
21	1.1092	0.1525	0.3853	0.0517	2.2666
22	0.8904	0.1048	0.2648	0.1566	2.2022
23	0.7636	0.0924	0.2708	0.1089	1.3313
24	0.6367	0.0799	0.2767	0.0612	1.3374
25	0.5030	0.0731	0.2446	0.0628	1.2128
26	0.3692	0.0663	0.2125	0.0307	1.0882
27	0.2471	0.0608	0.1482	0.0330	0.7984
28	0.2109	0.0433	0.1217	0.0256	0.7009
29	0.1747	0.0258	0.0952	0.0181	0.5944
30	0.2126	0.0355	0.1229	0.0323	0.5316
31	0.2505	0.0452	0.1507	0.0407	0.6741
32	0.4300	0.0725	0.1785	0.0763	0.9143
33	0 2345	0.0554	0.1383	0.0376	0.9425
34	0.2689	0.0774	0.1112	0.0329	0.7127
35	0.2179	0.0643	0.0847	0.0274	0.6535
36	0.1766	0.0462	0.0866	0.0262	0.6452
37	0.1565	0.0495	0.0742	0.0341	0.5192
38	0.1211	0.0491	0.0769	0.0221	0.5124
39	0.1134	0.0477	0.0704	0.0189	0.5060
40	0.1057	0.0463	0.0638	0.0157	0.4260
41	0.0979	0.0448	0.1010	0.0385	0.4814
42	0.1337	0.0875	0.1133	0.0356	0.5508
43	0.1583	0.0797	0.0966	0.0327	0.5977
44	0.1135	0.0464	0.0799	0.0299	0.5142
45	0.0837	0.0461	0.0665	0.0122	0.4999
46	0.0841	0.0282	0.1019	0.0224	0.4856
47	0.0946	0.0500	0.1108	0.0370	0.4817
48	0.0923	0.0607	0.0904	0.0360	0.5084
49	0.0900	0.0713	0.0804	0.0309	0.5077
50	0.0589	0.0359	0.0565	0.0107	0.4552
51	0.0831	0.0358	0.0454	0.0134	0.4093
52	0.0687	0.0153	0.0279	0.0065	0.3018
53	0.0444	0.0145	0.0284	0.0036	0.2662
54	0.0723	0.0109	0.0290	0.0000	0.2209
55	0.0106	0.0072	0.0296	0.0000	0.1779

For file "disc94.txt"

(ADJ)	(Gorge)	(Mud)	(Cave)	(East)	(Outflow)
1	0.0000	0.0000	0.0000	0.0000	0.0000
2	0.0000	0.5149	0.0000	0.0587	0.0000
3	0.0000	0.4383	0.0000	0.0306	0.1018
4	0.2392	0.4052	0.0000	0.0840	0.1332
5	0.3033	0.3124	0.0000	0.0393	0.2452
6	0.3799	0.2792	0.0000	0.0245	0.8354
7	0.3300	0.3954	0.0000	0.0587	1.0344
8	0.2459	0.4659	0.0000	0.0814	0.8522
9	0.1893	0.5364	0.0000	0.0784	1.1331
10	0.1772	0.3908	0.0000	0.0910	1.4277
11	0.2225	0.4747	0.0000	0.1519	1.5382
12	0.4614	0.4153	0.5368	0.1299	1.8527
13	0.8656	0.3325	0.5730	0.0670	1.7599
14	1.2828	0.2830	0.5454	0.1268	2.0878
15	1.1375	0.2587	0.3671	0.1623	2.1352
16	3.7892	0.2545	0.7546	0.1881	2.3733
17	2.4528	0.2095	0.8696	0.2099	3.5251
18	2.1900	0.1748	0.5436	0.2369	3.3160
19	3.2098	0.2214	0.7724	0.3392	3.9308
20	3.2889	0.2010	0.6031	0.3187	4.4215
21	1.5512	0.0903	0.2357	0.1826	2.8776
22	1.5855	0.0993	0.3677	0.1879	2.2450
23	1.5727	0.1314	0.5549	0 1343	2.5046
24	1.3949	0.1497	0.4784	0.1079	2.4712
25	1.1956	0.1477	0.3933	0.0800	2.1619
26	0.9810	0.1417	0.3160	0.0556	1.8467
27	0.5650	0.0886	0.1584	0.0336	1.1493
28	0.1489	0.0284	0.0622	0.0120	0.7556
29	0.1016	0.0147	0.0310	0.0075	0.4831
30	0.0543	0.0151	0.0250	0.0058	0.3642
31	0.0480	0.0149	0.0446	0.0079	0.3059
32	0.0337	0.0160	0.0448	0.0077	0.2911
33	0.0337	0.0160	0.0322	0.0063	0 2296
34	0.0240	0.0094	0.0384	0.0060	0.1822
35	0.0240	0.0094	0.0379	0.0061	0.1600
36	0.0306	0.0161	0.0465	0.0052	0.1308
37	0.0371	0.0160	0.0965	0.0058	0.1680
38	0.0436	0.0273	0.0745	0.0201	0.2393
39	0.1759	0.0688	0.0836	0.0291	0.3834
40	0.1626	0.0281	0 0651	0.0144	0.4088
41	0.2102	0.0468	0.1215	0.0317	0.4461
42	0.2791	0.0655	0.1205	0.0424	0.5979
43	0.2378	0.0510	0.0731	0.0197	0.6192
44	0.1955	0.0665	0.0613	0.0215	0.5523
45	0.2027	0.0183	0.0574	0.0213	0 5171
46	0.1384	0.0163	0.0449	0.0076	0.4278
47	0.0913	0.0157	0.0397	0.0057	0.3408
48	0.0758	0.0154	0.0428	0.0193	0.3062
49	0.0765	0.0157	0.0401	0.0101	0.2728
50	0.0791	0.0160	0.0365	0.0055	0.2302
51	0.1033	0.0160	0.0688	0.0254	0.2606
52	0.2132	0.0862	0.1179	0.0415	0.4077
53	0.1938	0.0363	0.0639	0.0204	0.4881
54	0.0811	0.0276	0.0358	0.0069	0.3988
55	0.0526	0.0183	0.0221	0.0069	0.2843
	0.0241	0.0089	0.0184	0.0067	0.2006
	0.0048	0.0068	0.0213	0.0056	0.1322
	0.0032	0.0061	0.0138	0.0052	0.0781
	0.0041	0.0068	0.0184	0.0051	0.0470
	0.0263	0.0120	0.0297	0.0098	0.0876
	0.0273	0.0193	0.0290	0.0104	0.0926
	0.0149	0.0147	0.0307	0.0067	0.1142
	0.1257	0.0633	0.0649	0.0288	0.1914
	0.1021	0.0329	0.0469	0.0147	0.2837
	0.0785	0.0161	0.0349	0.0066	0.2621
	0.0661	0.0467	0.0443	0.0168	0.2946
	0.1696	0.1071	0.0819	0.0364	0.3952
	0.1971	0.0476	0.0689	0.0261	0.5165
	0.1003	0.0308	0.0302	0.0063	0.4151
	0.0874	0.0126	0.0415	0.0065	0.2816

Appendix B5 1993 OC Measurements in Amituk Streams

Table B5.1: 1993 measured discharge and chemical concentrations for Gorge Creek

Table B5.2: 1993 measured discharge and chemical concentrations for Mud Creek

Table B5.3: 1993 measured discharge and chemical concentrations for Cave Creek

Table B5.4: 1993 measured discharge and chemical concentrations for East Creek

Table B5.5: 1993 measured discharge and chemical concentrations for Amituk Lake Outflow

Table B5.1: 1993 measured discharge and chemical concentrations for Gorge Creek (Semkin et al., unpubl.)

Date	AJD	Meas. Stream Q (m3/s)	HCB pg/L	Dieldrin pg/L	Heptach. Epoxide pg/L	Sum Chlord. pg/L	Endosulf. I pg/L	Alpha-HCH pg/L	Beta-HCH pg/L	Gamma-HCH pg/L	SUM DDT pg/L	SUM PCB pg/L
190693	5	0.0385										
200693	6	0.0328	48.8	170.6	128.6	187	442.9	5429.1	108.6	1818.4	42.9	297.9
210693	7	0.1779										
230693	9	0.3064										
250693	11	0.3786										
260693	12	0.7072	34.5	84.9	82.9	162.5	202.9	2663.4	27.1	772.7	23.1	477.5
270693	13	2.1151										
280693	14	1.5226										
290693	15	2.8473										
10793	17	1.8356										
20793	18	1.4058										
30793	19	0.8297	28.8	67.8	65.7	193.6	88.6	1543.4	29.1	235.5	55.8	1073.7
40793	20	0.9912										
50793	21	1.1092										
60793	22	0.8904										
80793	24	0.6367										
100793	26	0.3692	31.2	55.5	62	119.3	64.8	780.8	42.3	139.3	49.3	618.7
110793	27	0.2471										
130793	29	0.1747										
150793	31	0.2505										
160793	32	0.43										
170793	33	0.2345	41.9	46.4	47.2	41.6	33.3	792.2	30.6	117.9	73.9	621.7
180793	34	0.2689										
190793	35	0.2179										
200793	36	0.1766										
210793	37	0.1565										
220793	38	0.1211										
250793	41	0.0979										
260793	42	0.1337										
270793	43	0.1583										
280793	44	0.1135										
290793	45	0.0837										
300793	46	0.0841										
310793	47	0.0946										
10893	48	0.0923										
20893	49	0.09										
30893	50	0.0589										
40893	51	0.0831										
50893	52	0.0687										
60893	53	0.0444										
70893	54	0.0723										
80893	55	0.0106										

Table B5.2: 1993 measured discharge and chemical concentrations for Mud Creek (Semkin et al., unpubl.)

Date	AJD	Meas. Stream Q (m3/s)	HCB pg/L	Dieldrin pg/L	Heptach. Epoxide pg/L	Sum Chlord. pg/L	Endosulf. I pg/L	Alpha-HCH pg/L	Beta-HCH pg/L	Gamma-HCH pg/L	SUM DDT pg/L	SUM PCB pg/L
180693	4	0.215										
190693	5	0.2575										
200693	6	0.475										
210693	7	0.62435										
230693	9	0.7737	30.8	93.7	44.4	35.4	138.9	1747.8	66.7	309.6	0	346.5
250693	11	0.5845										
260693	12	0.3716	5.7	15.7	5.5	2.1	16.4	104.7	8.5	23.1	0	228.8
270693	13	0.7362										
280693	14	0.3002										
290693	15	0.2861										
10793	17	0.2916										
20793	18	0.2194										
30793	19	0.1038	37.4	70.6	45.7	19.3	82.9	492	21.2	69.8	20	1437.9
40793	20	0.1028										
50793	21	0.1525										
60793	22	0.1048										
80793	24	0.0799										
100793	26	0.0663	27.2	61.4	29.7	50.7	40.5	308.6	13.9	33.6	125.2	356.8
110793	27	0.0608										
130793	29	0.0258										
150793	31	0.0452										
160793	32	0.0725										
170793	33	0.0554										
180793	34	0.0774										
190793	35	0.0643										
200793	36	0.0462										
210793	37	0.0495										
220793	38	0.0491										
250793	41	0.0448										
260793	42	0.0875										
270793	43	0.0797										
280793	44	0.0464										
290793	45	0.0461										
300793	46	0.0282										
310793	47	0.05										
10893	48	0.0607										
20893	49	0.0713	136	16.5	32.5	54.8	28.6	1	29.5	4.6	35.5	1142.6
30893	50	0.0359										
40893	51	0.0358										
50893	52	0.0153										
60893	53	0.0145										
70893	54	0.0109										
80893	55	0.0072										

Table B5.3: 1993 measured discharge and chemical concentrations for Cave Creek (Semkin et al., unpubl.)

Date	AJD	Meas. Stream Q (m3/s)	HCB pg/L	Dieldrin pg/L	Heptach. Epoxide pg/L	Sum Chlord. pg/L	Endosulf. I pg/L	Alpha-HCH pg/L	Beta-HCH pg/L	Gamma-HCH pg/L	SUM DDT pg/L	SUM PCB pg/L
240693	10	0.54										
260693	12	0.3945	45.9	130.6	85.7	67.9	477.1	2672	42.9	589.8	61.7	499.5
270693	13	0.5861										
280693	14	0.4388										
290693	15	0.4238										
10793	17	0.6611										
20793	18	0.46										
30793	19	0.3174	0	34	24.7	61.1	101.2	0	21.3	40	70.8	901.7
40793	20	0.2917										
50793	21	0.3853										
60793	22	0.2648										
80793	24	0.2767										
100793	26	0.21245	16.7	75.9	68.5	19.9	79.5	943	17.3	132.7	76.7	91.7
110793	27	0.1482										
130793	29	0.0952										
160793	32	0.1785										
170793	33	0.1383										
180793	34	0.1112										
190793	35	0.0847										
200793	36	0.0866										
210793	37	0.0742										
220793	38	0.0769										
240793	40	0.0638										
250793	41	0.101										
260793	42	0.1133										
280793	44	0.0799										
290793	45	0.0665	7.7	44.9	43	30.9	36.2	304.5	20.5	44.4	0	86.8
300793	46	0.1019										
310793	47	0.1108										
10893	48	0.0904										
20893	49	0.0804										
30893	50	0.0565										
40893	51	0.0454										
50893	52	0.0279										
80893	55	0.0296										

Table B5.4: 1993 measured discharge and chemical concentrations for East Creek (Semkin et al., unpubl.)

Date	AJD	Meas. Stream Q (m3/s)	HCB pg/L	Dieldrin pg/L	Heptach. Epoxide pg/L	Sum Chlord. pg/L	Endosulf. I pg/L	Alpha-HCH pg/L	Beta-HCH pg/L	Gamma-HCH pg/L	SUM DDT pg/L	SUM PCB pg/L
180693												
230693	9	0.062										
250693	11	0.1514										
260693	12	0.1528	11.3	52	61.1	4.9	72.2	633.9	8.5	92.9	36.1	139.1
270693	13	0.2849										
290693	15	0.0815										
10793	17	0.1625										
20793	18	0.1187										
30793	19	0.0576	0	35.8	62	73.9	70.4	475.9	107	42.3	49.3	1196.3
40793	20	0.149										
50793	21	0.0517										
60793	22	0.1566										
80793	24	0.0612										
90793	25	0.0628										
100793	26	0.0307	24.5	26.3	45.9	6.3	51.4	105.9	15.1	14.7	0	446.6
110793	27	0.033										
130793	29	0.0181										
140793	30	0.0323										
150793	31	0.0407										
160793	32	0.0763										
170793	33	0.0376										
180793	34	0.0329										
190793	35	0.0274										
200793	36	0.0262										
210793	37	0.0341										
220793	38	0.0221										
240793	40	0.0157										
250793	41	0.0385										
280793	44	0.0299										
290793	45	0.0122										
300793	46	0.0224										
310793	47	0.037	0	38.1	33	22.9	0	182.7	43.4	38.2	0	909.8
10893	48	0.036										
20893	49	0.0309										
30893	50	0.0107										
40893	51	0.0134										
50893	52	0.0065										
60893	53	0.0036										

Table B5.5: 1993 measured discharge and chemical concentrations for Amituk Lake Outflow (Semkin et al., unpubl.)

Date	AJD	Meas. Stream Q (m3/s)	HCB pg/L	Dieldrin pg/L	Heptach. Epoxide pg/L	Sum Chlord. pg/L	Endosulf. I pg/L	Alpha-HCH pg/L	Beta-HCH pg/L	Gamma-HCH pg/L	SUM DDT pg/L	SUM PCB pg/L
180693	4	0.0817										
190693	5	0.0275										
200693	6	0.0713										
210693	7	0.0858										
220693	8	0.1915										
230693	9	1.1046										
240693	10	2.9437	39.6	84	84.8	65.9	121.2	1309.7	27.3	265	51.5	378.3
250693	11	2.0456										
260693	12	1.9426										
270693	13	4.7038										
280693	14	3.1334										
290693	15	2.2468										
300693	16	5.5721	25.6	61.2	84.5	67	93	2234.4	33.8	336.5	86.7	587.5
10793	17	4.5452										
20793	18	3.3771										
30793	19	2.0839										
40793	20	2.2816										
50793	21	2.2666										
60793	22	2.2022										
70793	23	1.3313	25.6	61.2	53.5	80	70.4	1583.7	28.2	347.7	36.6	205.4
80793	24	1.3374										
100793	26	1.0882										
110793	27	0.7984										
120793	28	0.7009										
130793	29	0.5944										
140793	30	0.5316										
150793	31	0.6741	92.1	0.1	49.9	5.5	37.5	961.2	57.9	85.8	0	308.1
160793	32	0.9143										
170793	33	0.9425	0	0.1	45.4	34.1	60	1056.8	85.8	72.6	33.6	387.9
180793	34	0.7127										
190793	35	0.6535										
200793	36	0.6452										
210793	37	0.5192										
220793	38	0.5124										
230793	39	0.506										
240793	40	0.426										
250793	41	0.4814										
260793	42	0.5508										
270793	43	0.5977										
280793	44	0.5142										
300793	46	0.4856										
310793	47	0.4817										
10893	48	0.5084										
20893	49	0.5077										
30893	50	0.4552										
40893	51	0.4093	138.9	0.1	63.9	64.2	0	1565.3	121.7	101.9	64.5	1057.6
50893	52	0.3018										
60893	53	0.2662										
70893	54	0.2209										
120893	59	0.1349	27.6	23.9	57.5	46	0	973.2	84.9	149.2	8.1	308.7

Appendix B6 1994 OC Measurements in Amituk Streams

Table B6.1: 1994 measured discharge and chemical concentrations for Gorge Creek

Table B6.2: 1994 measured discharge and chemical concentrations for Mud Creek

Table B6.3: 1994 measured discharge and chemical concentrations for Cave Creek

Table B6.4: 1994 measured discharge and chemical concentrations for East Creek

Table B6.5: 1994 measured discharge and chemical concentrations for Amituk Lake Outflow

Table B6.1: 1994 measured discharge and chemical concentrations for Gorge Creek (Semkin et al., unpubl.)

Date	AJD	Meas. Stream Q (m3/s)	HCB pg/L	Dieldrin pg/L	Heptach. Epoxide pg/L	Sum Chlord. pg/L	Endosulf. I pg/L	Alpha-HCH pg/L	Beta-HCH pg/L	Gamma-HCH pg/L	SUM DDT pg/L	SUM PCB pg/L
180694	4	0.2392										
190694	5	0.3033										
200694	6	0.3799	28	255	130	15	408	2969	89	863	42	1057
210694	7	0.3300										
220694	8	0.2459	20	198	122	5	321	2481	71	724	58	1020
230694	9	0.1893										
240694	10	0.1772	25	220	121	14	381	2330	77	753	45	1219
250694	11	0.2225										
260694	12	0.4614	21	190	88	27	283	1609	35	486	47	1126
270694	13	0.8656										
280694	14	1.2828	28	142	66	24	194	1369	30	410	52	1078
290694	15	1.1375										
300694	16	3.7892										
10794	17	2.4528	15	108	40	9	157	927	23	340	9	1357
20794	18	2.1900										
30794	19	3.2098										
40794	20	3.2889	12	93	48	0	103	603	21	259	7	1456
50794	21	1.5512		0								
60794	22	1.5855		83	44	0	58	386	20	153	34	1706
70794	23	1.5727										
80794	24	1.3949	12	87	39	8	64	471	26	226	26	1617
90794	25	1.1956										
100794	26	0.9810										
110794	27	0.56496										
120794	28	0.1489										
130794	29	0.10160										
140794	30	0.0543										
150794	31	0.048	9	58	20	0	29	273	31	66	8	1167
160794	32	0.0337										
170794	33	0.03370										
180794	34	0.02400										
190794	35	0.0240	0	82	33	5	24	213	23	88	43	1373
200794	36	0.03055										
210794	37	0.0371										
220794	38	0.0436										
230794	39	0.1759	0	66	29	6	26	451	29	174	7	1467
240794	40	0.1626										
250794	41	0.2102										
260794	42	0.2791										
270794	43	0.2378	5	86	40	2	30	429	27	139	7	1093
280794	44	0.1955										
290794	45	0.2027										
300794	46	0.1384										
310794	47	0.0913	9	62	22	5	20	278	24	74	22	1526
10894	48	0.0758										
20894	49	0.0765										
30894	50	0.0791										
40894	51	0.1033	4	81	41	3	32	391	26	121	8	1242
50894	52	0.2132										
60894	53	0.1938										
70894	54	0.0811										
80894	55	0.05260										
90894	56	0.0241	0	64	21	0	24	89	20	22	13	639
100894	57	0.0048										
110894	58	0.0032										
120894	59	0.0041	0	40	34	0	14	103	24	10	7	264
130894	60	0.0263										
140894	61	0.0273										
150894	62	0.0149	0	58	29	1	11	160	17	18	6	156
160894	63	0.1257										
170894	64	0.10208										
180894	65	0.0785										
190894	66	0.0661										
200894	67	0.1696	0	33	28	0	12	347	23	132	4	847
210894	68	0.1971										
220894	69	0.1003										
230894	70	0.0874	0	64	48	0	15	144	23	50	7	178

Table B6.2: 1994 measured discharge and chemical concentrations for Mud Creek (Semkin et al., unpubl.)

Date	AJD	Meas. Stream Q (m3/s)	HCB pg/L	Dieldrin pg/L	Heptach. Epoxide pg/L	Sum Chlord. pg/L	Endosulf. I pg/L	Alpha-HCH pg/L	Beta-HCH pg/L	Gamma-HCH pg/L	SUM DDT pg/L	SUM PCB pg/L
120694												
160694	2	0.5149										
170694	3	0.4383	5	101	41	2	83	255	26	324	8	1406
180694	4	0.4052										
190694	5	0.3123	6	114	50	1	116	157	25	295	15	1248
200694	6	0.2792										
210694	7	0.3954	3	103	49	2	122	503	40	367	8	521
220694	8	0.46593										
230694	9	0.5364	3	100	64	0	68	307	37	211	7	1230
240694	10	0.3908										
250694	11	0.4747	12	117	56	0	79	320	44	286	9	1101
260694	12	0.4153										
270694	13	0.3325	2	102	73	4	53	185	20	169	13	735
280694	14	0.2830										
290694	15	0.2587										
300694	16	0.2545	0	85	36	1	58	189	16	153	6	686
10794	17	0.2095										
20794	18	0.1748	0	110	42	0	40	166	20	125	6	730
30794	19	0.2214										
40794	20	0.2010										
50794	21	0.0903										
60794	22	0.0993	5	104	39	1	47	192	27	116	6	1302
70794	23	0.1314										
80794	24	0.1497										
90794	25	0.1477	2	120	32	0	17	75	12	20	54	1103
100794	26	0.1417										
110794	27	0.0886										
120794	28	0.0284										
130794	29	0.0146										
140794	30	0.0151	0	5	27	0	6	20	4	0	21	762
140794	31	0.0149										
160794	32	0.0160										
170794	33	0.01595										
180794	34	0.00940										
190794	35	0.00940										
200794	36	0.0161	1	71	28	0	8	34	5	0	40	414
210794	37	0.0159										
220794	38	0.0273										
230794	39	0.0688										
240794	40	0.02810										
250794	41	0.04680										
260794	42	0.06550										
270794	43	0.05100	3	83	34	0	13	62	8	0	35	396
280794	44	0.06650										
290794	45	0.0182										
300794	46	0.0163										
310794	47	0.0157										
10894	48	0.0154										
20894	49	0.0157										
30894	50	0.0160	5	75	34	0	37	38	9	0	57	1528
40894	51	0.0160										
50894	52	0.08620										
60894	53	0.03630										
70894	54	0.02760										
80894	55	0.01825										
90894	56	0.00890										
100894	57	0.00680	0	40	14	0	16	71	7	0	1	724
110894	58	0.00610										
120894	59	0.00680										
130894	60	0.01200										
140894	61	0.01930										
150894	62	0.01470										
160894	63	0.06330										
170894	64	0.03290										
180894	65	0.01610	0	63	10	0	9	34	3	0	9	1211
190894	66	0.04670										
200894	67	0.10710										
210894	68	0.04760										
220894	69	0.03080										
230894	70	0.01260	0	18	7	0	6	44	1	0	21	621

Table B6.3: 1994 measured discharge and chemical concentrations for Cave Creek (Semkin et al., unpubl.)

Date	AJD	Meas. Stream Q (m3/s)	HCB pg/L	Dieldrin pg/L	Heptach. Epoxide pg/L	Sum Chlord. pg/L	Endosulf. I pg/L	Alpha-HCH pg/L	Beta-HCH pg/L	Gamma-HCH pg/L	SUM DDT pg/L	SUM PCB pg/L
260694	12	0.5368										
270694	13	0.5730	19	157	61	52	253	618	101	424	17	1040
280694	14	0.5454										
290694	15	0.3671										
300694	16	0.7546	22	144	65	26	231	1034	58	411	16	601
10794	17	0.8696										
20794	18	0.5436	11	158	64	13	201	958	54	389	9	473
30794	19	0.7724										
40794	20	0.6031	5	101	43	10	121	822	22	322	15	451
50794	21	0.2357										
60794	22	0.3677	8	117	41	6	94	651	65	238	6	507
70794	23	0.5549										
80794	24	0.4784	0	109	40	6	70	611	51	232	7	486
90794	25	0.3933										
100794	26	0.3160										
110794	27	0.1583										
120794	28	0.0622										
130794	29	0.0310										
140794	30	0.0250										
150794	31	0.0446	0	80	47	2	37	440	18	113	5	364
160794	32	0.0448										
170794	33	0.0322										
180794	34	0.0384										
190794	35	0.0379	0	76	38	2	22	258	17	40	4	454
200794	36	0.0465										
210794	37	0.0965										
220794	38	0.0745										
230794	39	0.0836	0	73	35	1	22	362	15	95	10	497
240794	40	0.0651										
250794	41	0.1215										
260794	42	0.1205										
270794	43	0.0731	0	79	68	2	26	393	15	110	4	523
280794	44	0.0613										
290794	45	0.0574										
300794	46	0.0449										
310794	47	0.0397	2	63	20	0	27	376	44	100	30	294
10894	48	0.0428										
20894	49	0.0401										
30894	50	0.0365										
40894	51	0.0688	0	53	31	0	18	302	16	64	7	402
50894	52	0.1179										
60894	53	0.0639										
70894	54	0.0358										
80894	55	0.0221										
90894	56	0.0184	0	46	35	0	21	293	14	61	11	256
100894	57	0.0213										
110894	58	0.0138										
120894	59	0.0184	0	63	55	7	38	352	13	66	30	328
130894	60	0.0297										
140894	61	0.0290										
150894	62	0.0307	0	49	29	0	21	239	11	39	11	285
160894	63	0.0649										
170894	64	0.0469										
180894	65	0.0349										
190894	66	0.0443										
200894	67	0.0819	0	57	32	0	12	150	9	61	8	162
210894	68	0.0689										
220894	69	0.0302										
230894	70	0.0415	0	51	29	0	6	98	8	25	6	117

Table B6.4: 1994 measured discharge and chemical concentrations for East Creek (Semkin et al., unpubl.)

Date	AJD	Meas. Stream Q (m3/s)	HCB pg/L	Dieldrin pg/L	Heptach. Epoxide pg/L	Sum Chlord. pg/L	Endosulf. I pg/L	Alpha-HCH pg/L	Beta-HCH pg/L	Gamma-HCH pg/L	SUM DDT pg/L	SUM PCB pg/L
160694	2	0.0587										
170694	3	0.0306										
180694	4	0.0840	16	83	41	6	120	938	62	399	9	330
190694	5	0.0393										
200694	6	0.0245										
210694	7	0.0587	4	91	33	4	92	777	19	394	4	567
220694	8	0.0814	1	70	32	4	87	557	24	329	0	341
230694	9	0.0784										
240694	10	0.0910			59	14	38	417	28	259		
250694	11	0.1519										
260694	12	0.1299	0	92	36	5	53	325	27	126	4	414
270694	13	0.0670										
280694	14	0.1268	0	122	47	3	67	301	21	199	8	603
290694	15	0.1623										
300694	16	0.1881										
10794	17	0.2099	0	85	29	3	40	202	11	106	8	267
20794	18	0.2369										
30794	19	0.3392	0	113	65	2	43	179	15	88	11	593
40794	20	0.3187										
50794	21	0.1826										
60794	22	0.1879	0	111	42	1	47	81	0	22	12	257
70794	23	0.1343										
80794	24	0.1078										
90794	25	0.0800	0	116	64	34	47	107	64	34	14	1265
100794	26	0.0556										
110794	27	0.0336										
120794	28	0.0120										
130794	29	0.0075	0	61	26	0	7	27	0		17	449
140794	30	0.0058										
150794	31	0.0079										
160794	32	0.0077										
170794	33	0.0063										
180794	34	0.0060										
190794	35	0.0061										
200794	36	0.0052	0	61	34	0	4	35	0		10	606
210794	37	0.0058										
220794	38	0.0201										
230794	39	0.0291										
240794	40	0.0144										
250794	41	0.0317										
260794	42	0.0424	0	68	98	1	43	93	0	18	2	566
270794	43	0.0197										
280794	44	0.0215										
290794	45	0.0213										
300794	46	0.0076										
310794	47	0.0057										
10894	48	0.0193										
20894	49	0.0101										
30894	50	0.0055	0	58	20	0	14	46	0		3	529
40894	51	0.0254										
50894	52	0.0415										
60894	53	0.0204										
70894	54	0.0069										
80894	55	0.0069										
90894	56	0.0067										
100894	57	0.0056										
110894	58	0.0052										
120894	59	0.0051										
130894	60	0.0098										
140894	61	0.0104										
150894	62	0.0067										
160894	63	0.0288										
170894	64	0.0147										
180894	65	0.0066	0	50	34	13	8	34	0		4	940
190894	66	0.0168										
200894	67	0.0364										
210894	68	0.0261										
220894	69	0.0063										
230894	70	0.0065	0	27	9	0	3	6	3		7	487

Table B6.5: 1994 measured discharge and chemical concentrations for Amituk Lake Outflow (Semkin et al., unpubl.)

Date	AJD	Meas. Stream Q (m3/s)	HCB pg/L	Dieldrin pg/L	Heptach. Epoxide pg/L	Sum Chlord. pg/L	Endosulf. I pg/L	Alpha-HCH pg/L	Beta-HCH pg/L	Gamma-HCH pg/L	SUM DDT pg/L	SUM PCB pg/L
170694	3	0.1018										
180694	4	0.1332										
190694	5	0.2452	24	145	65	0	164	1155	43	350	9	518
200694	6	0.8354										
210694	7	1.0344	8	164	68	0	206	1202	39	444	9	531
220694	8	0.8522										
230694	9	1.1331	6	131	73	0	0	936	25	301	12	532
240694	10	1.4277										
250694	11	1.5382	0	133	60	0	103	964	27	296	6	427
260694	12	1.8527										
270694	13	1.7599	0	120	48	0	111	959	26	281	18	819
280694	14	2.0878										
290694	15	2.1352	0	139	47	0	161	1062	30	381	12	553
300694	16	2.3733										
10794	17	3.5251	13	118	53	0	136	1069	22	386	13	606
20794	18	3.3160										
30794	19	3.9308	37	143	92	0	136	1138	30	380	12	519
40794	20	4.4215										
50794	21	2.8776	13	114	77	0	89	956	27	286	14	586
60794	22	2.2450										
70794	23	2.5046	8	122	69	0	81	1053	26	325	17	613
80794	24	2.4712										
90794	25	2.1619	6	213	83	0	166	1863	66	521	10	413
100794	26	1.8467										
110794	27	1.1493	0	96	17	13	54	782	20	211	5	825
120794	28	0.7556										
130794	29	0.4831	5	100	39	0	46	738	16	199	6	481
140794	30	0.3642										
150794	31	0.3059										
160794	32	0.2911										
170794	33	0.2296										
180794	34	0.1822										
190794	35	0.1600	8	94	46	0	39	707	21	198	8	301
200794	36	0.1308	6	102	39	0	24	700	18	190	11	444
210794	37	0.1680										
220794	38	0.2393										
230794	39	0.3834	6	96	39	0	20	674	33	149	9	338
240794	40	0.4088										
250794	41	0.4461										
260794	42	0.5979	3	103	48	0	24	626	25	182	5	460
270794	43	0.6192										
280794	44	0.5523										
290794	45	0.5171										
300794	46	0.4278										
310794	47	0.3408	4	81	53	0	38	632	25	152	6	352
10894	48	0.3062										
20894	49	0.2728										
30894	50	0.2302										
40894	51	0.2606	0	58	40	0	14	547	21	134	3	452
50894	52	0.4077										
60894	53	0.4881										
70894	54	0.3988										
80894	55	0.2843	3	68	30	0	13	514	18	134	6	339
90894	56	0.2006										
100894	57	0.1322										
110894	58	0.0781										
120894	59	0.0470	2	74	35	0	14	536	22	151	13	443
130894	60	0.0876										
140894	61	0.0926										
150894	62	0.1142	0	81	38	0	24	566	20	149	6	240
160894	63	0.1914										
170894	64	0.2837										
180894	65	0.2621										
190894	66	0.2946										
200894	67	0.3952	5	87	33	0	14	524	19	152	4	536
210894	68	0.5165										
220894	69	0.4150										
230894	70	0.2816	0	75	37	0	22	588	19	155	7	365

Appendix B7 Fitted Inflow Stream Concentration Equations

1993 Inflow Stream Concentration Equations

1994 Inflow Stream Concentration Equations

1993 Inflow Stream Concentration Equations

Gorge Creek

α-HCH: $49631\beta^{-1.2091}$
β-HCH: $-39.303\mathrm{LN}(\beta)+157.3973$
γ-HCH: $42991\beta^{-1.7187}$
HCB: $-6.299\mathrm{LN}(\beta)+54.6467$
Dieldrin: $600.1\beta^{-0.7394}$
Endo I: $658.96\mathrm{EXP}(-0.0926\beta)$
HepEx: $337.52\beta^{-0.5486}$
Σ-Chlor: $318.9706\mathrm{EXP}(-0.04925\beta)$
Σ-DDT: $17.894\mathrm{LN}(\beta)-1.0163$
(-1 pt.)Σ-PCB: $194.41\mathrm{LN}(\beta)-32.208$

Mud Creek

α-HCH: $4908.4\mathrm{EXP}(-0.1604\beta)$
β-HCH: $-13.007\mathrm{LN}(\beta)+66.401$
(-1 pt.)γ-HCH: $590.26\mathrm{EXP}(-0.1019\beta)$
(-2 pt.)HCB: $-0.1521\beta+34.537$
(-1 pt.)Dieldrin: $-1.9003\beta+109.48$
(-1 pt.)Endo I: $-68.106\mathrm{LN}(\beta)+282.01$
(-1 pt.)HepEx: $-0.3336\beta+46.665$
(-1 pt.)Σ-Chlor: $0.96365\beta+10.29595$
Σ-DDT: $1.1971\beta+8.6078$
Σ-PCB: $17.346\beta+303.55$

Cave Creek

(-1 pt.)α-HCH: $5598.4\mathrm{EXP}(-0.0655\beta)$
β-HCH: $129.73\beta^{-0.5421}$
(-1 pt.)γ-HCH: $76408\beta^{-1.9551}$
(-1 pt.)HCB: $1319.3\beta^{-1.3478}$
(-1 pt.)Dieldrin: $977.1\beta^{-0.8008}$
Endo I: $36843\beta^{-1.8655}$
HepEx: $-1.267\beta+101.61$
(-1 pt.)Σ-Chlor: $-1.15917\beta+74.5089$
(-1 pt.)Σ-DDT: 69.7
Σ-PCB: $1256.2\mathrm{EXP}(-0.0642\beta)$

East Creek

α-HCH: $-363.51\mathrm{LN}(\beta)+1489$
β-HCH: $2.5022\beta^{0.768}$
γ-HCH: $-39.789\mathrm{LN}(\beta)+171.74$
HCB: $-0.2286\beta+14.943$
Dieldrin: $-10.198\mathrm{LN}(\beta)+70.016$
Endo I: $0.005292\beta^3-0.47713\beta^2+10.6551\beta+3.9$
HepEx: $80.224\mathrm{EXP}(-0.0190\beta)$
Σ-Chlor: $-0.15306\beta+30.9796$
Σ-DDT: $-1.2398\beta+53.58$
Σ-PCB: $12.805\beta+340.02$

1994 Inflow Stream Concentration Equations

Gorge Creek

α-HCH: $3429.111+78.34662\beta-37.51604\beta^2+2.158319\beta^3-0.05243451\beta^4+5.880126\text{x}10^{-4}\beta^5-2.503327\text{x}10^{-6}\beta^6$
β-HCH: $-3.9075075\text{x}10^{-8}\beta^6+7.868093\text{x}10^{-6}\beta^5-0.0005202783\beta^4+0.008233154\beta^3+0.4111639\beta^2-16.05759\beta+172.93$
γ-HCH: $-6.629619\text{x}10^{-7}\beta^6+0.0001579849\beta^5-0.01431017\beta^4+0.6023107\beta^3-10.990592\beta^2+35.28608\beta+927.9241$
HCB: $8.6851418\text{x}10^{-7}\beta^5-0.0001713929\beta^4+0.01226843\beta^3-0.3752661\beta^2+3.917663\beta+12.33376$
Dieldrin: $0.0001098784\beta^4-0.02065141\beta^3+1.378255\beta^2-38.776645\beta+456.8238$
Endo I: $-3.0987521\text{x}10^{-7}\beta^6+7.7085217\text{x}10^{-5}\beta^5-0.007406667\beta^4+0.3388097\beta^3-7.100474\beta^2+42.741413\beta+334.2262$
HepEx: $2.0179789\text{x}10^{-6}\beta^5-0.0003271262\beta^4+0.01641153\beta^3-0.1414209\beta^2-8.854356\beta+192.4627$
Σ-Chlor: $-1.109286\text{x}10^{-4}\beta^3+0.017785029\beta^2-1.027765\beta+22.6389$
Σ-DDT: $1.241828\text{x}10^{-5}\beta^4-0.002348653\beta^3+0.1605792\beta^2-5.059741\beta+79.9212$
Σ-PCB: $0.0006654862\beta^4-0.088126437\beta^3+2.867389\beta^2-6.1102366\beta+982.5631$

Mud Creek

α-HCH: $21.3932+96.04544\beta-10.06446\beta^2+0.414678\beta^3-0.008350995\beta^4+8.234703\text{x}10^{-5}\beta^5-3.188925\text{x}10^{-7}\beta^6$
β-HCH: $1.3352149\text{x}10^{-6}\beta^5-0.0002709598\beta^4+0.01983006\beta^3-0.6169923\beta^2+6.771727\beta+10.5708$
γ-HCH: $-9.81679\text{x}10^{-7}\beta^6+2.69236\text{x}10^{-5}\beta^5-0.0028692\beta^4+0.145837\beta^3-3.33416\beta^2+17.198\beta+299.194$
(-1 pt.) HCB: $-0.04614\beta+3.54011$
(-1 pt.) Dieldrin: $-0.019091\beta^2+0.237029\beta+105.2659$
Endo I: $2.97542077\text{x}10^{-6}\beta^5-0.0005813746\beta^4+0.03981796\beta^3-1.0803415\beta^2+7.358122\beta+84.9854$
HepEx: $3.0559343\text{x}10^{-6}\beta^5-0.0005838257\beta^4+0.04017943\beta^3-1.1941725\beta^2+13.60316\beta+7.93921$
Σ-Chlor: $-0.6555\ \text{LN}(\beta)+2.61$
Σ-DDT: $2.0453584\text{x}10^{-6}\beta^5-0.0003055438\beta^4+0.01424696\beta^3-0.2123156\beta^2+0.9290444\beta+9.109$
Σ-PCB: $-0.0004371045\beta^4+0.05031\beta^3-1.344081\beta^2-9.014963\beta+1206.268$

Cave Creek

(-1 pt.) α-HCH: $-27006.54+5832.477\beta-485.4507\beta^2+21.05235\beta^3-0.5215588\beta^4+7.449579\mathrm{x}10^{-3}\beta^5-5.715073\mathrm{x}10^{-5}\beta^6+1.824351\mathrm{x}10^{-7}\beta^7$
(-1 pt.) β-HCH: $-0.00150985\beta^3+0.227359\beta^2-11.25953\beta+197.4742$
γ-HCH: $1.861372\mathrm{x}10^{-5}\beta^5-0.00394123\beta^4+0.30851\beta^3-10.70853\beta^2+146.7682\beta-231.7753$
HCB: $-5.983673\mathrm{x}10^{-4}\beta^3+0.0878194\beta^2-4.102486\beta+60.6442$
Dieldrin: $-7.803781\mathrm{x}10^{-4}\beta^3+0.145041\beta^2-9.281129\beta+258.1953$
Endo I: $-0.00617683\beta^3+0.9163\beta^2-43.86664\beta+698.5637$
HepEx: $-8.04877\mathrm{x}10^{-4}\beta^3+0.1092465\beta^2-4.88659\beta+111.32$
Σ-Chlor: $200.645535\mathrm{EXP}(-0.145723\beta)$
(-2 pt.) Σ-DDT: $-5.48864\mathrm{x}10^{-4}\beta^3+0.07571\beta^2-3.20562\beta+48.2295$
Σ-PCB: $0.00099659\beta^4-0.184758\beta^3+12.0005\beta^2-324.3799\beta+3501.813$

East Creek

α-HCH: $1479.254-154.8519\beta+6.622915\beta^2-0.1394947\beta^3+0.001453774\beta^4-6.036062\mathrm{x}10^{-6}\beta^5$
(-1 pt.) β-HCH: $-6.976347\mathrm{x}10^{-4}\beta^3+0.1006644\beta^2-4.521\beta+63.0714$
γ-HCH: $553.419697\mathrm{EXP}(-0.096561\beta)$
HCB: $1.703876\mathrm{x}10^{-5}\beta^4-0.00273528\beta^3+0.1499\beta^2-3.2424\beta+22.633$
Dieldrin: $-2.2068\mathrm{x}10^{-6}\beta^5+0.00033109\beta^4-0.0150539\beta^3+0.137694\beta^2+2.998\beta+62.866$
Endo I: $3.415896\mathrm{x}10^{-5}\beta^4-0.0063327\beta^3+0.4162058\beta^2-11.959\beta+154.0845$
(-1 pt.) HepEx: $51.2827\mathrm{EXP}(-0.015286\beta)$
Σ-Chlor: $-2.4729\mathrm{LN}(\beta)+9.727$
Σ-DDT: $2.86017673\mathrm{x}10^{-8}\beta^6-7.6004411\mathrm{x}10^{-6}\beta^5+7.8615512\mathrm{x}10^{-4}\beta^4-0.03919646\beta^3+0.9401147\beta^2-9.36685\beta+33.8458$
(-2 pt.) Σ-PCB: $2.0985\beta+408.96$

Notes: Number of excluded outliers in parentheses.

Appendix B8 Measured Concentrations of Selected Compounds at Amituk Lake

1993 Measured Lake Concentrations

1994 Measured Lake Concentrations

1993 Measured Lake Concentrations (Semkin, unpubl.)

			α-HCH		β-HCH		γ-HCH		HCB		Dieldrin	
Date	Julian Day	AJD	3 m	20 m	3 m	20 m	3 m	20 m	3 m	20 m	3 m	20 m
160694	167	2		1370		82		434		0		95
230694	174	9		1212		14		196		23		50
300694	181	16		1214		13		183		17		46
70794	188	23	1695	902	25	55	301	72	31	73	60	30
140794	195	30	1178	1401	26	124	173	326	28	30	55	80
210792	202	37	1353	820	33	20	171	115	25	3	52	58
280794	209	44	1034	1310	47	17	196	212	20	7	38	68
40894	216	51	906	767	22	11	172	73	25	25	53	30
100894	222	57	820	811	25	32	133	125	21	16	46	45

			Endosulfan I		Heptachlor Epoxide		Σ-Chlordanes		Σ-DDT		Σ-PCB	
Date	Julian Day	AJD	3 m	20 m	3 m	20 m	3 m	20 m	3 m	20 m	3 m	20 m
160694	167	2		0		82		153		0		1782
230694	174	9		0		65		135		101		120
300694	181	16		0		86		129		41		192
70794	188	23	76	0	70	50	102	131	27	93	467	285
140794	195	30	36	0	67	89	122	108	44	49	548	465
210792	202	37	58	8	58	97	83	103	53	28	294	325
280794	209	44	36	14	58	41	71	139	53	11	627	409
40894	216	51	11	3	73	23	78	170	23	39	238	259
100894	222	57	55	11	55	35	65	47	36	0	326	385

1994 Measured Lake Concentrations (Semkin, unpubl.)

				α-HCH			β-HCH			γ-HCH			HCB			Dieldrin	
Date	Julian Day	AJD	3 m	20 m	40 m	3 m	20 m	40 m	3 m	20 m	40 m	3 m	20 m	40 m	3 m	20 m	40 m
150694	166	1	644	499	342	49	27	24	180	140	50	16	39	0	95	92	110
220694	173	8	794	470	626	23	26	28	234	130	148	5	13	0	90	62	106
290694	180	15	944	469	689	37	25	23	334	171	186	15	7	11	111	87	99
50794	186	21	857	541	727	59	24	34	257	181	187	4	1	1	105	104	102
110794	192	27	684	576	768	20	29	28	177	174	214	0	6	0	66	110	78
180792	199	34	638	569	680	39	57	38	174	158	165	0	2	0	99	62	93
250794	206	41	583		693	19		21	126		165	5	0	4	70	19	57
10894	213	48	561	769	652	21	33	39	148	203	168	0	14	0	75	109	66
70894	219	54	627	598	688	22	21	28	167	133	181	12	0	0	74	86	60
160894	228	63	579	553	734	32	44	23	141	123	199	14	0	14	66	75	70
220894	234	69	487	591	505	20	17	56	135	112	117	0	1	0	83	69	50

				Endosulfan I			Heptachlor Epoxide			Σ-Chlordanes			Σ-DDT			Σ-PCB	
Date	Julian Day	AJD	3 m	20 m	40 m	3 m	20 m	40 m	3 m	20 m	40 m	3 m	20 m	40 m	3 m	20 m	40 m
150694	166	1	0	4	11	71	75	53	71	75	53	7	61	57	888	752	430
220694	173	8	61	4	6	32	45	51	32	47	51	17	7	8	210	336	283
290694	180	15	125	39	30	37	45	35	37	55	35	15	51	23	405	313	285
50794	186	21	85	32	19	49	48	47	49	48	47	8	47	38	260	237	219
110794	192	27	36	11	10	34	54	65	34	54	65	3	34	32	177	506	355
180792	199	34	27	17	24	48	36	49	54	40	49	10	35	41	291	340	265
250794	206	41	22	20	11	31	11	53	32	11	53	8	29	41	278	143	198
10894	213	48	23	24	31	31	41	43	50	56	45	5	36	36	445	454	357
70894	219	54	36	23	24	54	35	45	54	35	45	4	9	35	320	246	170
160894	228	63	24	23	28	33	5	57	67	12	57	9	43	31	868	700	169
220894	234	69	22	19	27	40	26	21	43	49	49	4	42	40	384	369	505

Appendix C1 Steady-state Model Process Fluxes

1993 Steady-state Model Process Fluxes for Amituk Lake - OCs

1994 Steady-state Model Process Fluxes for Amituk Lake - OCs

1993 Steady-state Model Process Fluxes for Amituk Lake - PCBs

1994 Steady-state Model Process Fluxes for Amituk Lake - PCBs

1993 Steady-state Model Process Fluxes for Amituk Lake - Organochlorine Compounds

Process	Flux (mg/year)									
	α-HCH	β-HCH	γ-HCH	HCB	Dieldrin	Endo I	HepEx	Σ-Chlord	Σ-DDT	Σ-PCB
Sediment Burial =	0.65	0.02	0.15	0.54	1.14	0.05	0.00	0.39	4.66	37.55
Sediment Resuspension =	0.00	0.00	0.00	0.00	0.00	0.00	0.00	0.00	0.00	0.00
Sediment Deposition =	2.73	0.08	0.64	2.24	4.73	0.19	0.02	1.62	19.43	156.47
Sediment-Water Diffusion =	37.62	1.11	11.43	0.63	2.66	4.06	0.02	1.44	1.54	11.06
Water-Sediment Diffusion =	41.40	1.11	11.35	0.67	2.17	4.01	0.44	2.60	1.20	11.76
Absorption =	104.56	0.86	13.12	72.79	3.51	9.09	2.96	9.83	0.78	78.86
Volatilization =	148.22	3.74	24.91	98.46	2.27	26.61	32.32	189.28	0.70	409.76
Wet Particle Deposition =	0.01	0.00	0.00	0.01	0.01	0.04	0.00	0.00	0.02	0.02
Dry Particle Deposition =	0.00	0.00	0.00	0.00	0.00	0.01	0.00	0.00	0.01	0.00
Rain Dissolution =	23.16	0.20	4.74	0.39	2.66	1.09	0.03	0.11	1.06	1.80
Water Inflow =	7866.77	202.77	2013.24	165.79	371.53	733.87	321.84	845.83	203.45	2588.65
Particle Inflow =	7.73	0.19	1.53	7.97	8.96	0.47	4.90	12.87	34.72	495.71
Water Outflow =	7471.32	196.38	1976.55	139.73	371.15	709.56	198.92	645.40	204.14	2299.66
Particle Outflow =	4.55	0.12	0.91	4.53	5.36	0.28	2.56	7.10	20.82	286.00
Water Transformation =	360.46	3.62	27.48	2.19	4.05	7.45	95.10	23.39	2.53	39.77
Sediment Transformation =	6.13	0.07	0.40	1.86	2.24	0.09	0.92	3.70	10.10	129.52

1994 Steady-state Model Process Fluxes for Amituk Lake - Organochlorine Compounds

Process	Flux (mg/year) α-HCH	β-HCH	γ-HCH	HCB	Dieldrin	Endo I	HepEx	Σ-Chlord	Σ-DDT	Σ-PCB
Sediment Burial =	0.28	0.01	0.09	0.28	1.51	0.03	0.00	0.14	2.07	57.14
Sediment Resuspension =	0.00	0.00	0.00	0.00	0.00	0.00	0.00	0.00	0.00	0.00
Sediment Deposition =	1.15	0.06	0.37	1.18	6.30	0.12	0.01	0.60	8.62	238.09
Sediment-Water Diffusion =	15.86	0.85	6.55	0.33	3.54	2.66	0.01	0.53	0.68	16.83
Water-Sediment Diffusion =	17.45	0.85	6.51	0.35	2.89	2.63	0.35	0.96	0.53	17.90
Absorption =	87.47	0.19	14.77	65.23	2.94	9.13	2.81	8.98	1.60	64.01
Volatilization =	62.49	2.86	14.28	51.60	3.03	17.44	25.11	69.98	0.31	623.51
Wet Particle Deposition =	0.01	0.00	0.00	0.01	0.01	0.04	0.00	0.00	0.04	0.01
Dry Particle Deposition =	0.00	0.00	0.00	0.00	0.00	0.01	0.00	0.00	0.01	0.00
Rain Dissolution =	19.38	0.04	5.34	0.35	2.23	1.09	0.03	0.10	2.18	1.46
Water Inflow =	3200.89	155.27	1130.08	34.68	496.24	471.34	248.62	301.04	86.16	4016.99
Particle Inflow =	3.14	0.15	0.86	1.67	11.96	0.30	3.78	4.58	14.70	769.23
Water Outflow =	3082.29	149.86	1117.60	46.93	493.37	458.77	153.63	232.23	88.24	3528.10
Particle Outflow =	1.86	0.09	0.51	1.12	7.15	0.18	1.98	2.54	8.88	442.27
Water Transformation =	151.98	2.77	15.76	1.15	5.40	4.89	73.88	8.65	1.12	60.52
Sediment Transformation =	2.58	0.05	0.23	0.97	2.98	0.06	0.72	1.37	4.48	197.09

1993 Steady-state Model Process Fluxes for Amituk Lake - PCB Homologs

Process	Mono	Di	Tri	Tetra	Penta	Hexa	Hepta	Octa
				Flux (mg/year)				
Sediment Burial =	0.10	0.28	2.47	6.26	3.46	4.79	1.27	1.24
Sediment Resuspension =	0.00	0.00	0.00	0.00	0.00	0.00	0.00	0.00
Sediment Deposition =	0.43	1.17	10.28	26.08	14.41	19.97	5.30	5.16
Sediment-Water Diffusion =	1.20	0.83	1.83	2.92	0.64	0.18	0.06	0.02
Water-Sediment Diffusion =	1.80	1.75	1.93	3.10	0.68	0.19	0.06	0.02
Absorption =	6.30	2.44	29.80	12.81	12.12	6.69	6.07	0.92
Volatilization =	232.95	87.21	106.58	76.76	11.23	9.00	0.51	0.16
Wet Particle Deposition =	0.00	0.00	0.02	0.04	0.19	0.40	1.26	0.60
Dry Particle Deposition =	0.00	0.00	0.01	0.01	0.06	0.12	0.38	0.18
Rain Dissolution =	0.04	0.04	0.43	0.41	0.59	0.11	0.59	0.11
Water Inflow =	877.09	579.58	507.82	654.74	115.01	31.99	4.22	3.24
Particle Inflow =	4.22	11.10	38.71	79.11	34.91	48.65	5.10	9.83
Water Outflow =	592.56	439.64	418.98	592.39	116.02	32.20	7.53	3.72
Particle Outflow =	2.26	6.12	21.85	45.90	20.97	29.21	3.85	6.18
Water Transformation =	58.76	57.33	20.66	10.34	2.36	0.80	0.26	0.13
Sediment Transformation =	1.14	3.13	8.51	21.59	11.93	16.53	4.39	4.27

1994 Steady-state Model Process Fluxes for Amituk Lake - PCB Homologs

Process	Mono	Di	Tri	Tetra	Penta	Hexa	Hepta	Octa
				Flux (mg/year)				
Sediment Burial =	0.36	0.03	0.83	6.07	8.14	8.73	7.28	1.14
Sediment Resuspension =	0.00	0.00	0.00	0.00	0.00	0.00	0.00	0.00
Sediment Deposition =	1.50	0.13	3.47	25.29	33.93	36.37	30.35	4.75
Sediment-Water Diffusion =	4.23	0.09	0.62	2.83	1.51	0.32	0.34	0.02
Water-Sediment Diffusion =	6.36	0.19	0.65	3.01	1.61	0.35	0.36	0.02
Absorption =	5.53	2.14	23.71	9.65	7.95	5.59	6.72	1.25
Volatilization =	822.56	9.63	36.00	74.43	26.44	16.39	2.95	0.15
Wet Particle Deposition =	0.00	0.00	0.02	0.03	0.13	0.34	1.40	0.81
Dry Particle Deposition =	0.00	0.00	0.01	0.01	0.04	0.10	0.42	0.25
Rain Dissolution =	0.03	0.03	0.34	0.31	0.38	0.09	0.66	0.15
Water Inflow =	3123.28	60.06	145.30	636.91	302.04	63.59	54.04	2.68
Particle Inflow =	15.02	1.15	11.08	76.95	91.67	96.73	65.29	8.13
Water Outflow =	2101.89	46.46	128.04	573.74	287.86	61.13	57.83	3.26
Particle Outflow =	8.03	0.64	6.38	44.59	54.06	57.20	40.02	5.22
Water Transformation =	207.49	6.33	6.98	10.03	5.57	1.46	1.46	0.12
Sediment Transformation =	4.04	0.35	2.88	20.94	28.09	30.11	25.12	3.93

Appendix C2 Sediment Sensitivity Analysis Results

Table C2.1:	Percent difference in sediment OC concentrations resulting from variation of physico-chemical and lake characteristic parameters listed in Tables 4.2 and 4.3
Table C2.2:	Percent difference in sediment PCB concentrations resulting from variation of physico-chemical and lake characteristic parameters listed in Tables 4.2 and 4.4

Table C2.1: Percent difference in sediment OC concentrations resulting from variation of physico-chemical and lake characteristic parameters listed in Tables 4.2 and 4.3

	Percentage Change from Base Case									
Parameter	α-HCH	β-HCH	γ-HCH	HCB	Dieldrin	Endo I	HepEx	Σ-Chlor	Σ-DDT	Σ-PCB
Henry's Law constant	-3.8	-3.5	-2.6	-38.5	-1.4	-0.9	-13.7	-9.0	-1.6	-18.7
Octanol-water Partition Coeff.	85.3	99.1	101.3	95.8	106.4	10.7	53.5	78.6	79.5	80.8
Water MTC	0	0	0	1.9	0	0	-1	0.2	0	-0.6
Air MTC	1.4	-3.3	0.1	7.5	0	2.9	-12	19.9	2.4	-16.7
Sediment MTC	4.6	0.3	-0.3	0.9	-5.5	79	44.4	2.3	-1.7	0.3
Water Half-life	4.7	1.8	1.4	0.7	1.1	81.5	40.1	2.4	1.1	1.2
Sediment Half-life	7.5	2.9	1.7	44.5	23.2	83.1	96	67.1	45.7	57.7
Air Concentration	5.7	0.3	3	78.3	1.6	4	2.2	32.6	5.1	2.6
Inflow Water Concentration	94.3	99.7	97	21.7	98.4	96	97.8	67.4	94.9	97.4
Active Sediment Depth	-12.2	-5.3	-3.3	-38.1	-27.4	-47.6	-49.5	-44.5	-38.6	-42.3
Water Inflow Rate	3.8	3.7	1.1	-10.1	1.8	79.3	61.2	-4.9	5.4	22
Annual Precipitation	0.6	0	0.5	0.2	0.4	0.2	0	1.3	2.1	0
Sediment Deposition	6.8	6.6	5.3	76	62.2	4.5	52.5	75.2	72.9	76.4
Sediment Burial	-1.5	-1.6	-1.3	-15.2	-16	-0.1	-0.4	-12.9	-22.5	-17.5
Sediment/Lake Area Ratio	-3.5	-3.4	-2.7	-39.2	-32.4	-2.3	-26.6	-46.4	-46.8	-47.1
Sediment Organic Carbon Fraction	73.6	86.7	91.1	11.5	27.7	6.0	0.9	2.5	4.3	2.9
Ice-free Days	-9.2	-8.9	-4.5	-27.1	-26.8	-46.8	-57.4	-33.1	-37.6	-52.4
Sediment Volume Fraction	7.2	2.8	1.7	44.5	23.1	76.1	95.6	67.0	45.7	57.7
Throughflow Fraction	-6.8	-6.6	-2.5	8.2	-3.7	-45.6	-42.4	5.8	-10.5	-25.7

Note: Each parameter was increased by 100% except for Sediment Volume Fraction (50% decrease) and Throughflow Fraction (50% increase).

Table C2.2: Percent difference in sediment PCB concentrations resulting from variation of physico-chemical and lake characteristic parameters listed in Tables 4.2 and 4.4

	Percentage Change from Base Case							
Parameter	Mono	Di	Tri	Tetra	Penta	Hexa	Hepta	Octa
Henry's Law constant	-26.1	-20.6	-24.4	-16	-11.1	-14.6	-4.4	-2.7
Octanol-water Partition Coeff.	66.7	73.8	91.6	85.3	69.3	37.3	34.7	17.3
Water MTC	0	0	0	0	0	0	0	0
Air MTC	-25.9	-15.7	-7.9	-13.8	-7.6	-9.3	5.2	14.6
Sediment MTC	16.6	18.1	0.7	0.5	0.2	0	0	0
Water Half-life	7.1	10.7	3.5	1.4	1.4	0.9	1.1	0.8
Sediment Half-life	30.6	58.9	50.2	54.7	60	62.8	62.7	63.2
Air Concentration	0.4	6.6	23.4	2.7	4	6.8	11.8	25.6
Inflow Water Concentration	99.6	93.4	76.6	97.3	96	93.2	88.2	74.4
Active Sediment Depth	-31.9	-42.6	-40.1	-41.4	-42.8	-43.6	-43.5	-43.6
Water Inflow Rate	48.6	28.8	14.5	16.3	17.6	44.1	29.3	37.9
Annual Precipitation	0	0.1	0.2	0	0.1	0.2	1.5	6.6
Sediment Deposition	26.1	57.5	79.4	78.1	67.4	37.6	34.9	17.7
Sediment Burial	-4	-6.2	-16.2	-17	-17.9	-18.3	-18.3	-18.3
Sediment/Lake Area Ratio	-13.3	-29.6	-42.8	-45.4	-48.3	-49.8	-49.7	-49.9
Sediment Organic Carbon Fraction	32.5	10.7	7.4	4.6	1.7	0.2	0.3	0.1
Ice-free Days	-46.2	-47.8	-45	-49.2	-47.8	-50	-41.4	-52.4
Sediment Volume Fraction	30.4	58.7	50.2	54.7	59.9	62.8	62.7	63.2
Throughflow Fraction	-39.4	-28.9	-15.4	-21.3	-22.1	-35.8	-28.8	-32.5

Note: Each parameter was increased by 100% except for Sediment Volume Fraction (50% decrease) and Throughflow Fraction (50% increase)

Appendix C3 Unsteady-state Model Predictions of Summer Lake Concentrations

(a) β-HCH

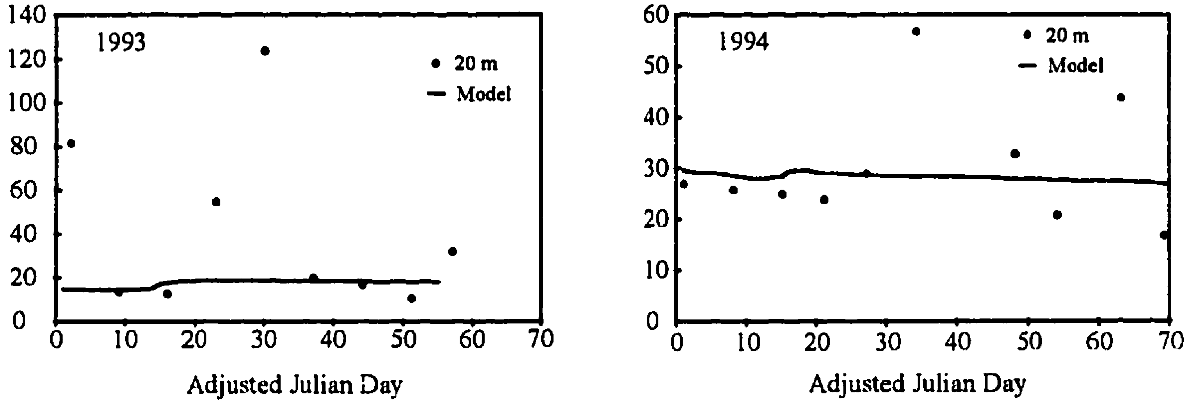

(b) HCB

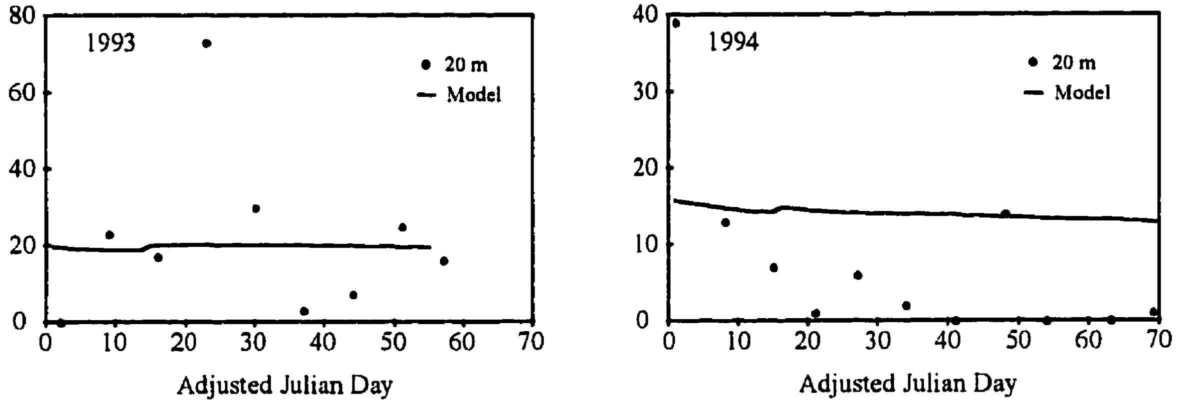

(c) Dieldrin

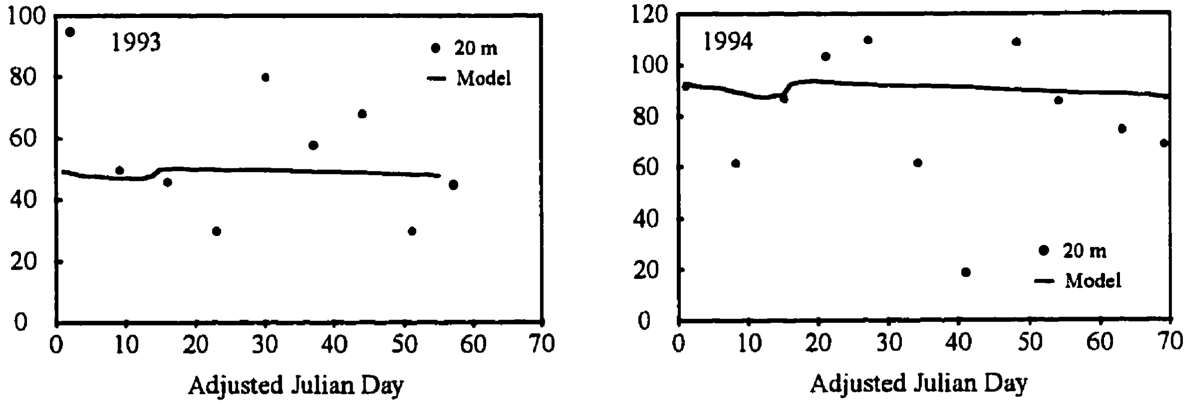

(d) Endosulfan I

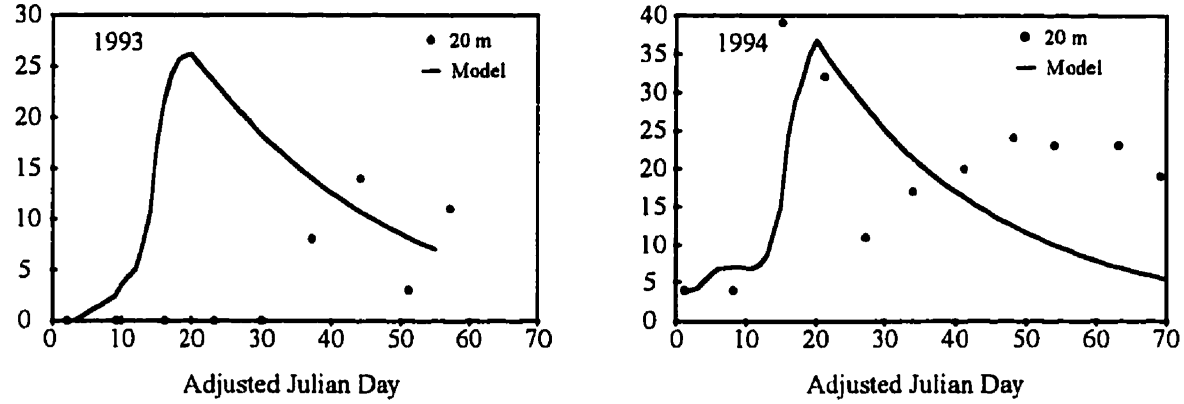

(e) Σ-chlordane

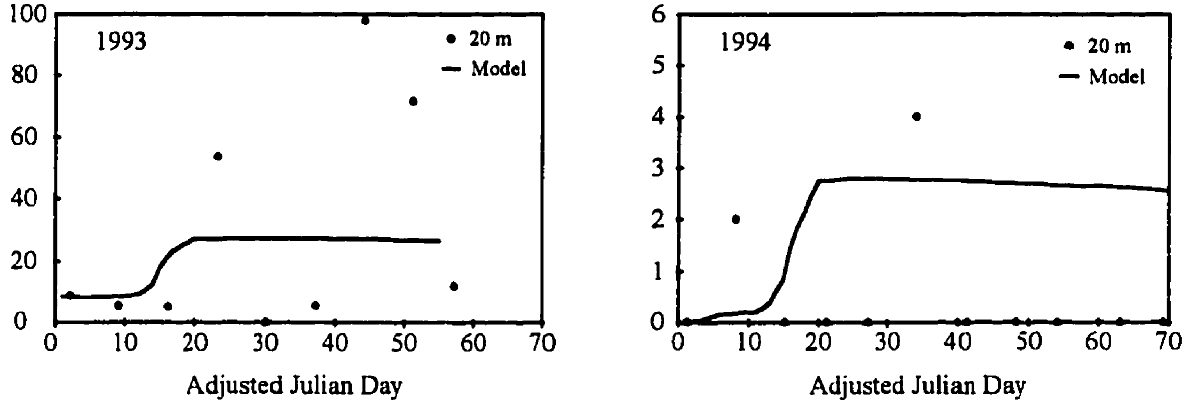

(f) Σ-PCB

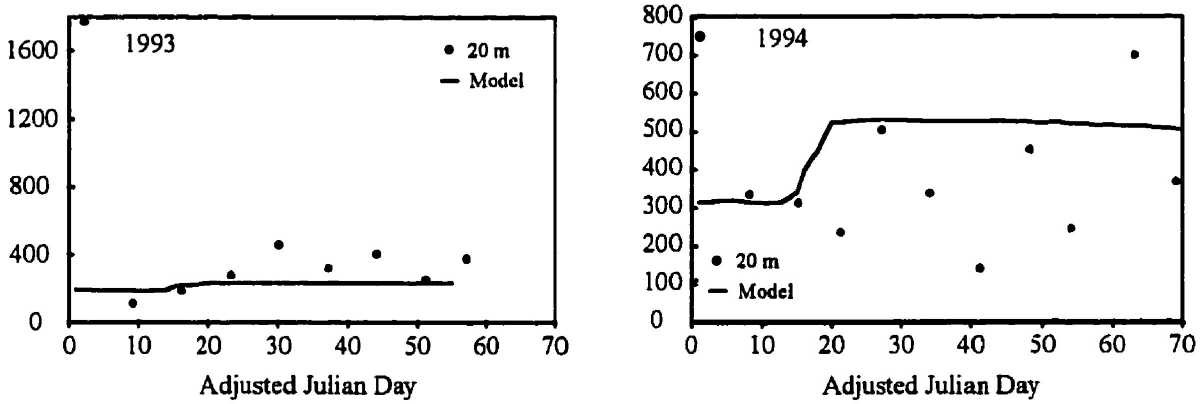

Appendix C4 Modeled and Measured OC Concentrations in Amituk Lake from 1992 to 1994

(a) β-HCH

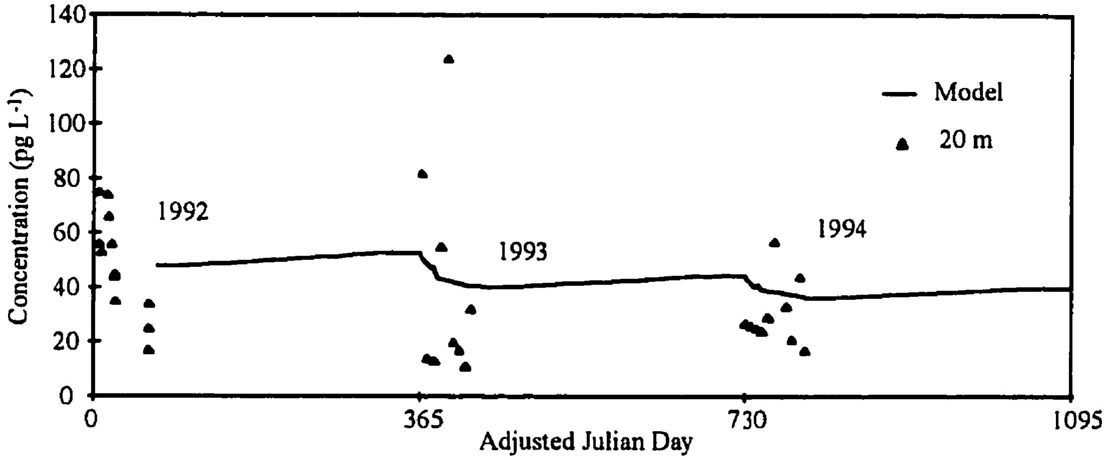

(b) HCB

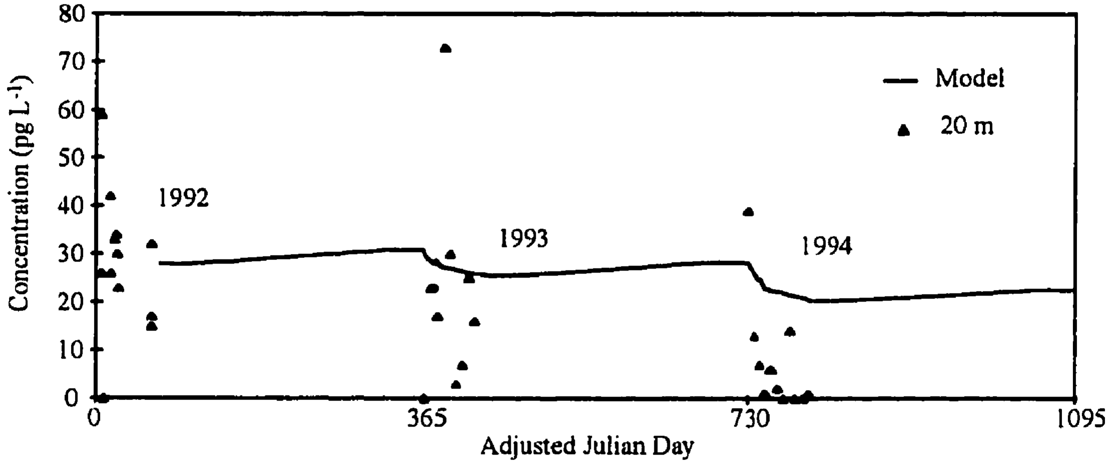

(c) Σ-chlordane

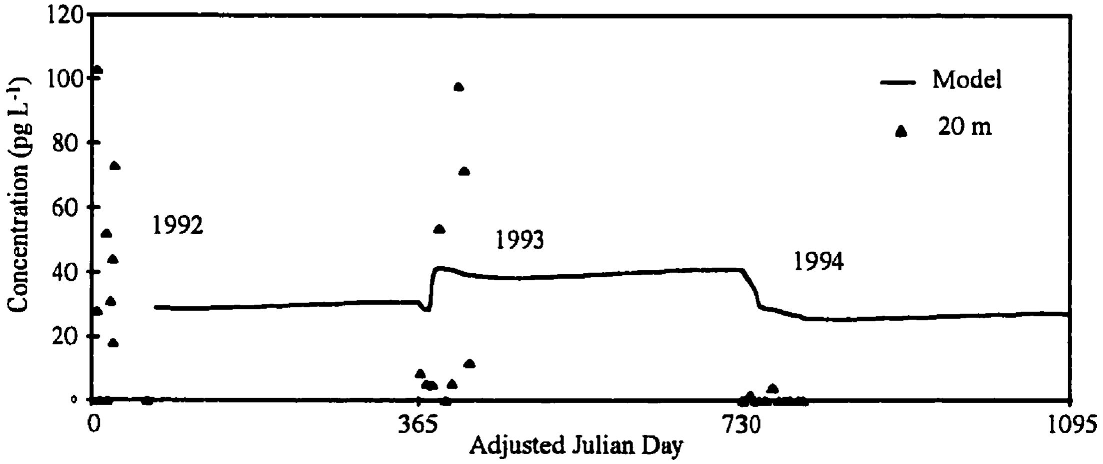

(d) Σ-DDT

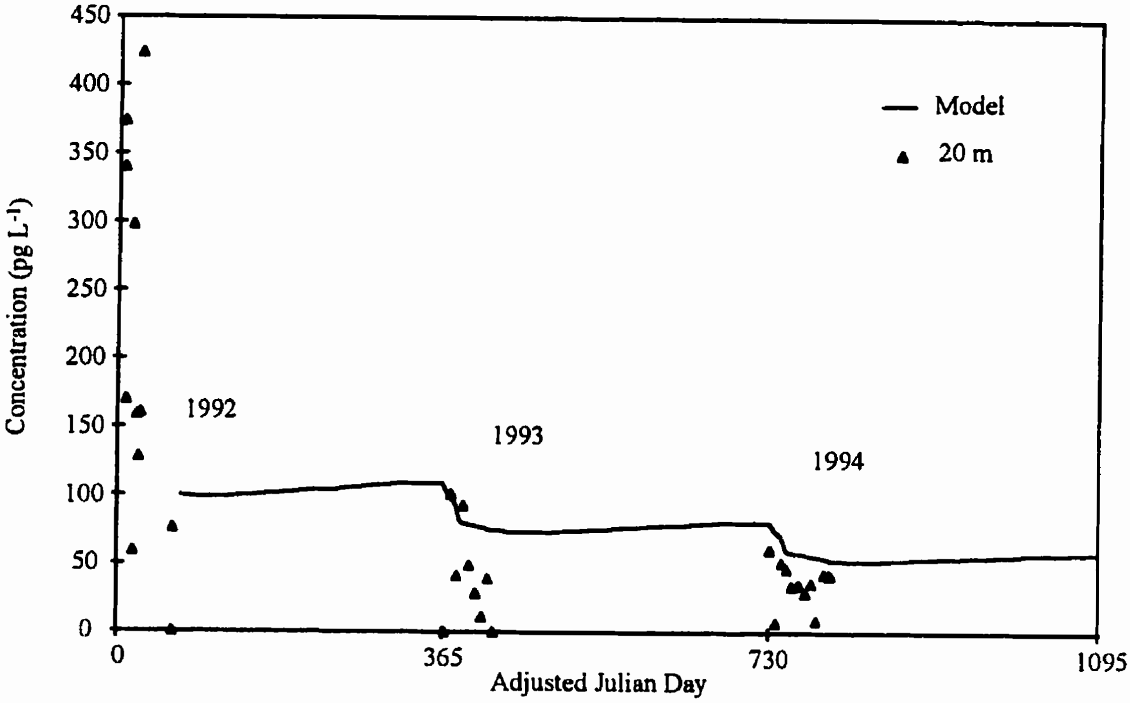
Concentration (pg L-1)
450
400
350
300
250
200
150
100
50
0
Model
20 m
1992
1993
1994
0
365
730
1095
Adjusted Julian Day

(e) Σ-PCB

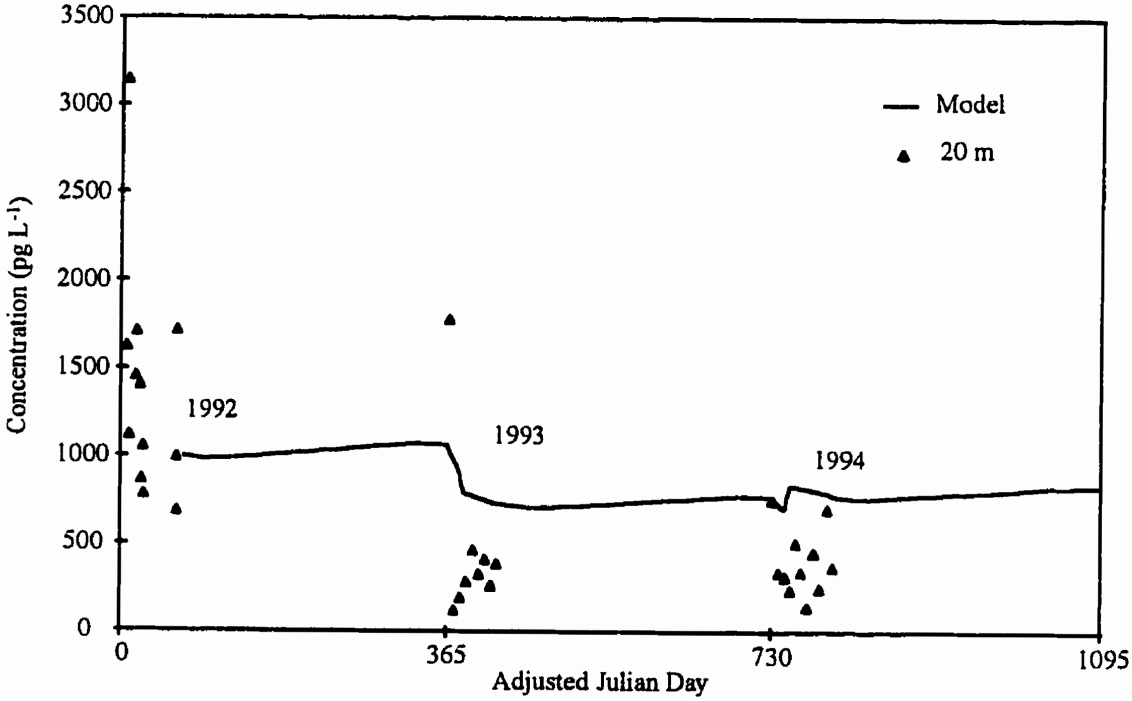
Concentration (pg L-1)
3500
3000
2500
2000
1500
1000
500
0
Model
20 m
1992
1993
1994
0
365
730
1095
Adjusted Julian Day